Perfusion Imaging and Tissue Biomarkers for Colorectal Cancer

Esme Hill

St Catherine's College, Oxford

Supervisors:

Professor Ricky Sharma

Professor Mike Partridge

A thesis submitted for the degree of *Doctor of Philosophy*

Hilary Term 2015

Abstract

Background: Systemic chemotherapy and radiotherapy play an important role in the treatment of colorectal cancer. Tumour perfusion and oxygenation is known to influence radiosensitivity and chemosensitivity. In this thesis, I propose that the evaluation of changes in tumour perfusion using perfusion CT (pCT) and dynamic contrast-enhanced (Dce) MRI can guide the rational sequencing of drugs and radiation.

Methods: Dce-MRI and pCT scans were incorporated into a clinical trial of hypofractionated pelvic radiotherapy and nelfinavir in 10 patients with rectal cancer. Toxicity and tissue biomarkers (tumour cell density, microvessel density, CAIX, HIF1-α, phospho-Akt and phospho-PRAS40) were evaluated. pCT liver scans were incorporated into an imaging study in patients with colorectal liver metastases randomised to receive either oxaliplatin/ 5FU chemotherapy or oxaliplatin/ 5FU chemotherapy plus selective internal radiotherapy.

Results: After 7 days of nelfinavir concurrent with hypo-fractionated pelvic radiotherapy, there was a mean 42% increase in median K^{trans} (P=0.03, paired t test) on Dce-MRI and a median 30% increase in mean blood flow on pCT (P=0.028, Wilcoxon Rank Sum), although no statistically significant changes in perfusion parameters were demonstrated after 7 days of nelfinavir prior to radiotherapy. The feasibility of evaluating tumour cell density in rectal biopsies before and after radiotherapy and a radiosensitising drug as an early endpoint of response was demonstrated. In patients with colorectal liver metastases who received oxaliplatin and modified de Gramont chemotherapy alone, after 4 cycles of chemotherapy, a 28% decrease in the mean hepatic arterial fraction was observed (P=0.018, paired t test). Between pCT scans 2 days before SIRT and 39-47 days following SIRT and continued 2-weekly chemotherapy, there was a mean 62% (P=0.009) reduction in Blood Flow and 61% (P=0.006) reduction in Blood Volume (paired t test).

Conclusions

This research does not support the hypothesis that nelfinavir before radiotherapy improves blood flow to human rectal cancer. Increases in rectal tumour perfusion during radiotherapy and concurrent nelfinavir are likely to be primarily explained by the acute biological effects of radiation. Four or more cycles of oxaliplatin and modified de Gramont chemotherapy may result in changes in tumour perfusion of colorectal liver metastases which would be detrimental to subsequent radiotherapy. Selective internal radiotherapy resulted in substantial reductions in tumour perfusion 39-47 days after the treatment. Perfusion imaging can be used to detect changes in tumour perfusion in response to radiotherapy and systemic therapy which have implications for the sequencing of therapies.

Acknowledgments

I would like to begin by thanking my supervisors Professor Ricky Sharma and Professor Mike Partridge for their support in the conduct of this research and in the development of this thesis. Professor Sharma provided me with the opportunity and encouragement to undertake this project at the outset; he has been a great source of ideas and provided constructive feedback on all of my work. Professor Partridge has been an immense source of moral support, giving me the encouragement and confidence to develop my own ideas, as well as providing technical advice on the physics aspect of the project and detailed feedback on my written work.

There are many other people (too many to mention each by name) who have contributed to different aspects of this research; I am grateful for each and every contribution. I would particularly like to thank Mark Anderson, Consultant Radiologist, for his guidance and contribution to image analysis in this project. Many thanks to Julia Schnabel, Monica Enescu and Amalia Cifor for their input into the image registration and pharmacokinetic modelling of the Dce-MRI data; I am admiring of their expertise and have very much enjoyed collaboration with them. Thank you to our collaborators Nick West, Professor Philip Quirke and Emmer Tinkler-Hindall for their advice and practical assistance with respect to 'Tumour Cell Density' analysis in rectal tumour biopsies, as well as their provision of historical data. I would like to thank Lai-Mun Wang for her expertise and for the considerable time that she spent assisting me with the pathological analysis of tissue specimens in this project; I have learnt a great deal from our time spent at the double-headed microscope! Thank you also to the SONATINA and FOXFIRE trial teams for their support in the conduct of this research.

I would also like to acknowledge funding from the Oxfordshire Health Services Research Committee for a fellowship grant during the first year of my *DPhil* study. I subsequently received funding from the Oxford Cancer Imaging Centre to complete this project. I would not have been able to conduct this research without their support.

I would like to thank my family for their ceaseless support during the period of my study. Thank you to my husband, Martin for his understanding and patience, to my daughter Charlotte, for the endless distractions and to my parents, for their willingness to provide practical support.

Finally, I would like to thank the patients who participated in this research, whom I had the privilege of looking after during and after trial participation and got to know as individuals. I dedicate this thesis to them.

Contents

List of Figures

List of Tables

List of Abbreviations

AIF	**Arterial Input Function**
AJCC	**American Joint Committee on Cancer**
AlkP	**Alkaline phosphatase**
AP	**Arterial Perfusion**
BF	**Blood Flow**
BV	**Blood Volume**
CAIX	**Carbonic Anhydrase IX**
CAPOX	**Capecitabine and Oxaliplatin**
CBV	**Cerebral Blood Volume**
CEA	**Carcino-embryonic Antigen**
Cis	**Cisplatin**
CR	**Complete Response**
CRM	**Circumferential Resection Margin**
CT	**Computed Tomography**
CT CAP	**Computed Tomography Chest Abdomen Pelvis**
CTCAE	**Common Toxicity Criteria for Adverse Events**

Dce-MRI	**Dynamic contrast-enhanced Magnetic Resonance Imaging**
DFS	**Disease Free Survival**
DL	**Dose Level**
DNA-PK	**DNA-phosphokinase**
DSB	**Double Strand Breaks**
EASL	**European Association for the Study of the Liver**
EGFR	**Epidermal Growth Factor Receptor**
EMVI	**Extramural Vascular Invasion**
FGF	**Fibroblast Growth Factors**
5-FU	**5-Fluorouracil**
FOLFIRI	**5-Fluorouracil, Leucovorin, Irinotecan**
FOLFOX	**5-Fluorouracil, Leucovorin, Oxaliplatin**
FUDR HAC	**Floxuridine Hepatic Arterial Chemotherapy**
G	**Grade**
GCP	**Good Clinical Practice**
Gem	**Gemcitabine**
GTV	**Gross Tumour Volume**
Gy	**Gray**
HAART	**Highly Active Anti-retroviral Therapy**
HAF	**Hepatic Arterial Fraction**
HIF-1	**Hypoxia Inducible Factor-1**
HPI	**Hepatic Perfusion Index**
HR	**Hazard Ratio**
HU	**Hounsfield Units**
IRTK	**Image Registration Toolkit**
LCCRT	**Long Course Chemo-radiotherapy**
LV	**Leucovorin**
MC	**Motion Correction**

MMR	**Mismatch Repair**
MRI	**Magnetic Resonance Imaging**
mrTRG	**Tumour Regression Grade on MRI**
MVD	**Microvessel Density**
n	**Number**
NFV	**Nelfinavir**
NICE	**National Institute of Clinical Excellence**
OAR	**Organs at Risk**
OER	**Oxygen Enhancement Ratio**
OS	**Overall Survival**
mTOR	**Mammalian Target of Rapamycin**
MTT	**Mean Transit Time**
pCR	**Pathological Complete Response**
pCT	**Perfusion Computed Tomography**
PE	**Peak Enhancement**
PET	**Positron Emission Tomography**
PIP-3	**Phosphatidylinositol-triphosphate**
PI3-K	**Phosphoinositide-3-Kinase**
PR	**Partial Response**
PRAS-40	**Proline Rich Akt Substrate of 40 Kilo-daltons**
PS	**Permeability Surface Area Product**
PTEN	**Phosphatase and Tensin Homologue Gene**
PTV	**Planning Target Volume**
QOL	**Quality of Life**
RE	**Radio-embolization**
RECIST	**Response Evaluation Criteria in Solid Tumours**
RFA	**Radiofrequency Ablation**
ROI	**Region of Interest**

RT	**Radiotherapy**
SCRT	**Short Course Radiotherapy**
SD	**Stable Disease**
SIRT	**Selective Internal Radiotherapy**
SPECT	**Single Photon Emission CT**
SSB	**Single Strand Breaks**
SUV	**Standardised Uptake Value**
TCD	**Tumour Cell Density**
^{99}Tc-MAA	**Technetium-99 macro-aggregated albumin**
TMG	**Trial Management Group**
TNM	**Tumour, Node, Metastasis**
TRG	**Tumour Regression Grade**
TTP	**Time to Progression**
TTP	**Time to peak attenuation**
UICC	**Union for International Cancer Control**
VEGF	**Vascular Endothelial Growth Factor**
VOI	**Volume of Interest**

1 Background

1A General Introduction

A1 Colorectal Cancer

Colorectal cancer is a common disease and the fourth most frequently occurring cancer in the UK. Over 40,000 new cases of colorectal cancer are diagnosed each year in the UK, accounting for 13% of new cancer cases[i].The rectum represents the most common site of primary cancer of the large bowel, with 27 % of primary bowel cancers being sited there. More than 90% of bowel cancers are adenocarcinomas.

Patients with colorectal cancer are routinely staged using the American Joint Committee on Cancer (AJCC)/Union for International Cancer Control (UICC) tumour, node, metastasis (TNM) system[1], which classifies tumours according to the extent of the primary tumour in relation to the layers of the bowel wall (T), regional lymph node involvement with cancer cells (N) and whether the cancer has metastasised elsewhere in the body (M). Patients can be allocated a clinical TNM stage (cTcNcM or TNM) based on radiological and clinical tests or a pathological TNM stage (pTpNpM) based on histopathological examination of a resected tumour specimen. T*is* tumours are the earliest local stage of bowel tumours, before invasion of the basement membrane of the bowel mucosa; T1 tumours are those which have invaded the basement membrane of the bowel mucosa; T2 tumours are those which have penetrated the muscularis mucosa (muscle layer of the bowel wall) but not beyond it; T3 tumours are those which have penetrated through the muscularis mucosa and penetrated the serosa or peri-rectal fat and rectal tumours are sub-classified according to the depth of extra-mural invasion: T3a: <1mm, T3b 2-

[i] Cancer Research UK website; accessed Jan 2014
URL:http://www.cancerresearchuk.org/cancerinfo/cancerstats/types/bowel/incidence

5mm T3c> 5-8mm, T3d>8mm; T4 tumours are those which have grown through all layers of the bowel wall and may be involving the peritoneum or other organs.

Figure 1 Diagram illustrating examples of each of the 4 local tumour (T) stages of bowel cancer in relation to a cross-section of bowel wall

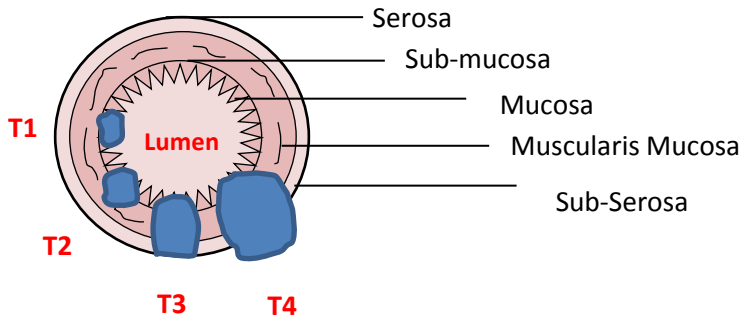

There are 3 categories of nodal (N) stage: N0, which means there is no evidence of regional lymph node cancer spread; N1, which means that 1-3 regional lymph nodes are involved by cancer and N2, which means that 4 or more regional lymph nodes are involved by cancer. Colorectal cancers are classified into one of two M stages dependent on the absence (M0) or presence (M1) of metastatic spread. Tumours are classified into 1 of 5 stages according to the TNM groupings.

Table 1 Summary of Stages of colorectal cancer according to T, N and M sub-groupings.

Stage	T	N	M
0	Tis	0	0
I	1 or 2	0	0
IIA	T3	0	0
IIB	T4	0	0
IIIA	T1 or 2	1	0
IIIB	T3	1	0
IIIC	Any	2	0
IV	Any	Any	1

Surgery is the primary curative treatment for Stage I to III colorectal cancers and pathological TNM stage is an important predictor of prognosis [1-7].Approximately 9% of patients with cancers

of the colon or rectum in the UK have metastatic disease at the time of presentation and this group of patients have a particularly poor outlook, with an overall 5 year survival of only 6%[ii].

A significant proportion of patients initially treated with curative intent for Stage I to III colorectal cancers subsequently relapse with metastatic disease, with the liver being the most common site of metastasis. The median survival of patients with metastatic colorectal cancer is less than 9 months without treatment[8] and 1.5 to 2.5 years with treatment[9]. However, in a subset of patients with liver only metastatic colorectal cancer, in whom surgical resection can be achieved, the 5 year survival rates average 30-40% [10-19], with 20% of patients achieving long-term cure [20]. Of all patients with metastatic colorectal cancer, as many as 30% may have liver-only metastases[21] and approximately 50% of the recurrences after resection of the primary tumour are localised to the liver[8, 19, 22]. However only 10-20% of liver metastases are immediately amenable to surgery [23].

A2 Pelvic Radiotherapy for Rectal Cancer

Although surgery is the primary curative treatment for rectal cancer, patients are at risk of developing loco-regional pelvic relapse after surgery alone and over half of all patients with operable or potentially operable rectal cancer are currently considered for preoperative radiotherapy as a routine part of their optimum management. Biologically effective doses of >30 Gy radiation to the pelvis have been demonstrated to reduce the risk of local tumour recurrence[24, 25] and can downstage locally advanced tumours to facilitate curative resection and potentially allow sphincter preservation for low tumours. There are two widely accepted pre-operative radiotherapy schedules: short course radiotherapy (SCRT), consisting of 25 Gy delivered in 5 daily fractions in one week, followed by surgery within 5-7 days and a long-course of pre-operative chemo-radiotherapy to a total dose of radiotherapy 45-50.4 Gy, delivered in 1.8 Gy

[ii] Cancer Research UK Website, accessed Dec 2014
URL: http://www.cancerresearchuk.org/about-cancer/type/bowel-cancer/treatment/statistics-and-outlook-for-bowel-cancer

fractions over 5-6 weeks, with concomitant fluoropyrimidine chemotherapy [LCCRT], and delayed surgery at 6-12 weeks.

SCRT followed by immediate surgery has been offered to patients with resectable rectal cancer in Europe[26] since it has been shown to halve the risk of local recurrence[27, 28].LCCRT and delayed surgery has been recommended for patients with borderline resectable, unresectable or low rectal tumours since it has been shown to lead to tumour downsizing, tumour regression by histological grade and pathological complete responses, which correlate with improved outcome for patients[29-31]. Although SCRT followed by immediate surgery is not usually advocated for patients with borderline operable or inoperable tumours, the biologically effective dose of SCRT is of a similar magnitude to 45 Gy in 25 fractions[32] and the CR07 study of SCRT followed by immediate surgery suggested that a significant T-stage downstaging effect [p=0.0001] occurred in the SCRT group despite the short time interval (i.e. days) between the last fraction of RT and surgery[28]. Further published series have suggested a downstaging effect from SCRT when surgery is delayed [33, 34].

Table 2 Summary of stratification of rectal tumours for risk of local recurrence and recommendations for use of radiotherapy (adapted from NICE Clinical Guideline 131)

Risk of local recurrence	**Characteristics of Rectal Tumour**	**Recommended Management**
Low	cT1 or cT2 or cT3a and no lymph node involvement	Do not offer SCRT or LCCRT unless as part of a clinical trial
Moderate	Any cT3b or greater • Potential surgical margin is not threatened or • Any suspicious node not threatening the surgical margin or • The presence of vascular invasion	Consider SCRT If tumour borderline between moderate and high risk, consider LCCRT
High	• A threatened margin (tumour <1mm mesorectal fascia) • Low tumours encroaching onto the inter-sphincteric plane or with levator involvement	Offer LCCRT

There has recently been a move away from routinely offering SCRT for all patients with resectable rectal cancers, particularly because of the risks of late radiation effects [35, 36]. Currently in the UK, a risk adapted approach to selecting patients for pre-operative SCRT or LCCRT is advocated by the National Institute of Health and Care Excellence (NICE)[37].

Although the combination of a long course of radiotherapy and chemotherapy (with capecitabine or infusional 5-fluorouracil) is generally well tolerated, some patients are not fit for concomitant chemotherapy with radiotherapy and those patients are treated with a long course of radiotherapy alone or SCRT.

Patients with rectal cancer and synchronous inoperable metastatic disease may be offered initial palliative radiotherapy to the rectal tumour for control of local tumour symptoms, such as pain and bleeding or systemic chemotherapy alone[37]. The initial management of primary rectal tumours in the presence of potentially operable synchronous metastatic disease is more contentious and there is no consensus on the optimum management for these patients[38]. Strategies for treating this patient sub-group are summarised in table 3 and include LCCRT followed by systemic chemotherapy or systemic chemotherapy followed by LCCRT. The potential value of systemic therapy without radiation in this group of patients has also been shown in a study in which all 32 patients who completed 6 weeks of oxaliplatin and infusional fluorouracil (FOLFOX) with bevacizumab [Cycles 1-4] showed tumour regression and proceeded to R0 resection, and pathological complete response (pCR) was documented in 25% of the resected cases [39]. Similarly, a previous study of RT followed by capecitabine and oxaliplatin (CAPOX) plus bevacizumab showed that radical resection of primary and radical resection and/or radiofrequency ablation (RFA) of all metastatic disease was possible in 72% cases. These investigators also reported a pCR rate of 26% in resected rectal specimens [40].The strategy of SCRT followed by systemic combination chemotherapy has recently been adopted as an alternative strategy for patients with resectable metastatic rectal cancer, on the grounds that

systemic chemotherapy during the interval between SCRT and surgery allows delivery of full dose systemic treatment which may potentially add to the down-sizing effect of SCRT.

Table 3 Advantages and disadvantages of therapeutic pre-operative strategies for management of locally advanced rectal cancer with synchronous, potentially operable metastases

Strategies	Advantages	Disadvantages
LCCRT pelvis followed by systemic chemotherapy	Maximises potential for downstaging of primary tumour	Risk of metastatic progression during LCCRT
Systemic chemotherapy alone (+/- biological agents)	Rapid treatment of metastatic disease May avoid need for RT	May require prolonged treatment (> 3months) for downsizing May not achieve rapid palliation
SCRT pelvis followed by systemic chemotherapy	Rapid delivery of local RT and palliation Chemotherapy may enhance downsizing effect of SCRT	Uncertain whether this strategy is as effective at downstaging borderline/inoperable tumours as LCCRT
Systemic chemotherapy followed by LCCRT pelvis	Rapid treatment of metastatic disease	Risk of metastatic disease progression during LCCRT Initial chemotherapy may compromise efficacy of subsequent LCCRT

Despite radiotherapy playing an important role in the treatment of many patients with rectal cancer, outcomes are not optimal for all patients. There is therefore scientific interest in understanding the mechanisms underlying resistance to radiotherapy in rectal cancer and developing treatments which may improve tumour sensitivity to radiation, with a view to improving resection rates as well as reducing local recurrence rates and sphincter preservation rates.

A3 Chemotherapy for Colorectal Liver Metastases

Systemic chemotherapy has an established role in current treatment strategies for patients with metastatic colorectal cancer, including those with liver metastases. Until the last decade of the twentieth century, chemotherapeutic options were limited to different schedules of the anti-metabolite 5-Fluorouracil (5-FU). The highest response rates were observed when 5-FU was

combined with folinic acid (leucovorin) [41, 42] delivered as a bimonthly schedule, consisting of a 2 hour high dose leucovorin (LV) infusion followed by a 5FU bolus of 400mg/m^2 and a 22 hour infusion of 5-FU (given on the 1st and 2nd day of each 2-week cycle), known as the de Gramont regimen [43]. Studies have since demonstrated superior benefits for treating untreated metastatic colorectal cancer with a combination of 5FU/LV and oxaliplatin or irinotecan in comparison to 5FU/LV alone [44-47]. Oxaliplatin in combination with 5FU/LV has been adopted internationally as a standard of care for the first line therapy of patients with metastatic colorectal cancer, which has been demonstrated in large scale trials to consistently result in response rates of 50-60%, progression free survival of 8-9 months and overall survival of 16-18 months [48].

A number of non-randomised studies in patients deemed to have initially inoperable liver metastases have demonstrated that neoadjuvant combination chemotherapy can render 11-33% of cases amenable to potentially curative resection [49-55] and result in 5 year survival rates of 30-40%. It is uncertain which chemotherapy regimen is optimal; 5FU/LV[53] Oxaliplatin/5FU/LV(FOLFOX)[51, 54], Irinotecan/5FU/LV(FOLFIRI) [55] and Oxaliplatin/Irinotecan/5FU/LV[49, 50] have all been demonstrated to convert patients with initially unresectable liver metastases to suitability for resection, with the highest response rates for combinations of 5FU/LV with Oxaliplatin and/or Irinotecan. In a randomised comparison of FOLFOX and FOLFIRI in patients with metastatic colorectal cancer, significantly higher rates of metastectomy were demonstrated in patients having FOLFOX rather than FOLFIRI first line, with a fewer number of treatment cycles required before surgery[56]. A criticism of these studies is the lack of standardised definition of “initially unresectable” metastases. Nevertheless, a correlation between tumour response and resection rate across clinical studies[57] has been demonstrated and patients with unresectable liver predominant colorectal liver metastases have become the focus of research evaluating neoadjuvant treatments in combination with systemic chemotherapy (such as the anti-EGFR antibody, cetuximab and the anti-VEGF antibody, bevacizumab) with

optimism that this will enhance response rates and thus improve rates of curative resection in this disease. Current NICE guidelines support the use of cetuximab in patients with potentially operable colorectal liver metastases and wild type *KRAS* in the first line setting[58]. Preliminary data from Phase III trials of chemotherapy and biologically targeted agents have not consistently shown statistically significant increases in response rates with cetuximab[9, 59] or bevacizumab[60, 61], with only modest increases in the frequency of down-staging to resectability with either drug over chemotherapy alone[60, 62-64].

A limitation of delivering neoadjuvant chemotherapy prior to resection of liver metastases is the development of pathological liver steatosis and dysfunction, which may occur with oxaliplatin-based or irinotecan-based chemotherapy [65-68] and that worsens with cumulative dosing. A problem after resection of liver metastases is the risk of disease relapse in the liver post-surgery, usually not at the resection site. Of those patients with liver-dominant or liver-only metastases, where the hepatic disease is unlikely to become resectable even with neoadjuvant systemic therapy, there is still a robust rationale for maximising efforts on local control of the liver disease, since patients with metastatic colorectal cancer frequently die of liver failure[69].

A4 Selective Internal Radiotherapy for liver metastases

Multiple loco-regional strategies are under investigation to improve the outcome for patients with unresectable colorectal liver metastases, including radio-frequency ablation, microwave ablation, hepatic arterial chemotherapy, cryotherapy and radio-embolization (RE), also known as selective internal radiotherapy (SIRT). SIRT is a treatment that has been developed over the past 2 decades to treat multiple sites of tumour within the liver, using biocompatible microspheres loaded with the radioactive isotope Yttrium-90, either in the form of resin microspheres (SIR-Spheres®, Sirtex Medical Ltd, Sydney, Australia) or glass microspheres (TheraSpheres®, BTG plc.,London). Yttrium-90 emits pure beta radiation (electrons with a mean energy of 0.93 MeV),

which has a mean depth of penetration of 2.5 mm and maximum depth of 11 mm in water/tissue; Yttrium-90 has a physical half-life of 64.1 hours. The SIRT technique involves trans-femoral catheterisation of the hepatic artery using fluoroscopic guidance and direct arterial injection of between 40 and 80 million radiolabelled (^{90}Y) resin microspheres; it exploits the fact that hepatic tumours derive up to 90% of their blood supply from the hepatic artery rather than the portal venous system[70]. The microspheres have a mean diameter of about 30-35 μm (whereas the diameter of liver arterioles are 2.5 -75 μm and diameter of end-arterioles are 8 μm) so they preferentially lodge in the abnormal microvasculature of tumours rather than passing into the capillary and venous system, delivering a high dose of radiation to the tumour whilst relatively sparing the normal parenchyma, such that it can be regarded as a form of intra-arterial brachytherapy[71].

Over the past 2 decades there has been considerable clinical experience of using SIR-spheres to treat patients with metastatic colorectal cancer globally. Whilst, there are studies which suggest that that Yttrium-90 SIRT alone is a beneficial treatment in the salvage setting (i.e. in patients with chemo-refractory disease) [72-79], response rates are only modest (range 5-41%). The highest response rates have been demonstrated in Phase I/II trials of SIRT in combination with chemotherapy as first or second line therapy for metastatic colorectal cancer (response rates up to 91%) [80-84](see table 4) raising hopes that SIRT in this setting could translate into improved hepatic resection rates and overall survival. The Phase II randomised study of systemic 5-FU and Leucovorin (LV) plus SIRT versus 5-FU/LV alone conducted by Van Hazel et al [81] in 21 previously *untreated* patients, was a key step forward to demonstrate safety and proof-of-principle for combining SIRT with chemotherapy, and paved the way for subsequent studies using oxaliplatin or irinotecan in combination with 5-FU.

Table 4 Summary of prospective trials of SIRT in patients with colorectal liver metastases.

TTP= time to progression; DFS= disease-free survival; OS =overall survival; y=years; m=months; FUDR HAC=floxuridine hepatic arterial chemotherapy

Reference	Trial Design	Number	Treatment	Clinical benefits		
				Response rate	TTP/DFS	Median OS
First line						
Gray [80]	Phase III	74	SIR-spheres + FUDR HAC FUDR HAC	44% p=0.001 18%	15.9 m 9.7 m	39% at 2y 29% at 2y
Van Hazel et al[81]	Phase II	21	SIR-spheres +5FU/LV 5FU/LV	91% p=0.001 0%	18.6m TTP 3.6m TTP	29.4m 12.4m
Sharma et al[82]	Phase I	20	SIR-FOLFOX 4	90%	9.2m 12.4m (liver-only mets)	-
Second line						
Lim et al [83]	Phase II	30	SIR-spheres +5FU/LV (in 70%)	33%	5.3m PFS	-
Van Hazel [84]	Phase I	25	SIR-spheres + Irinotecan	48%	6m TTP	12.2m
Chemo-refractory disease						
Hendlisz[85]	Phase III	44	SIR-spheres + 5FU SIR-spheres	10% 0%	5.5m p=0.003 2.1m	10.3m p=0.8 7.3m
Cosimelli[73]	Phase II	50	SIR-spheres	24%	4m	12.6m
Sofocleous[75]	Phase I	19	SIR-spheres	5%	2m 5.1m (liver)	14.9m

In a Phase I-II trial of SIRT in combination with FOLFOX chemotherapy for patients with unresectable colorectal liver metastases in the first line setting, Sharma et al[86] treated 20 patients with oxaliplatin at escalating doses of 30-85mg/m^2 and full dose LV/5-FU for Cycle 1-3 and full dose FOLFOX 4 for cycles 4-12. The primary endpoint of the study was toxicity and the dose limiting toxicity was demonstrated to be grade 3/4 neutropenia (12 patients) with a maximum tolerated dose of oxaliplatin 60mg/m^2 for cycles 1-3. The combination treatment was generally well tolerated and 18 of the 20 patients (90%) demonstrated a partial RECIST (Response

Evaluation Criteria In Solid Tumours) response to treatment; two (10%) had stable disease. Two (10%) of the patients responded to therapy sufficiently enough to enable them to undergo a partial hepatic resection. The median progression-free survival was 9.3 months overall, and 14.2 months in the seven patients with liver-only metastases, suggesting that the addition of SIRT might be most beneficial in this patient group. The overall median time to progression in the liver was 12.3 months.

This phase I-II study has paved the way for larger scale randomised phase III trials of oxaliplatin and 5-FU with or without SIRT in the first line therapy of patients with liver-dominant metastatic colorectal cancer. Two studies have recently closed to recruitment: the international SIRFLOX study, which is a randomised comparison study of FOLFOX6 plus SIR-spheres versus FOLFOX6 alone as first line treatment in patients with non-resectable liver metastases from primary colorectal cancer; and the UK National Cancer Research Network FOXFIRE trial, an open label randomised trial of 5-FU, Oxaliplatin and Folinic acid +/- interventional Radio-Embolization as first line treatment for patients with unresectable liver only or liver-predominant metastatic colorectal cancer. A third, the FOXFIRE Global study is also an international randomised trial of FOLFOX6 plus SIR-spheres versus FOLFOX6 (with or without the addition of bevacizumab), which recruited 364 patients and is in the follow-up phase until 31st October 2016. In combination, these three trials will recruit in excess of 1020 patients in total; data from the three trials will be pooled to analyse the primary endpoint of overall survival after 2 years of follow-up, as well as secondary endpoints including progression free-survival, resection rate, response rate and quality of life. The FOXFIRE trial will also analyse health economics. Unless a significant amount of post-trial cross-over occurs in the subject group, it is hoped that the results of these large trials will definitively answer the question whether the addition of SIRT to first line chemotherapy provides survival benefit over giving chemotherapy alone.

A5 Tumour perfusion and its importance for treatment outcomes

There is growing recognition that the tumour microenvironment plays an important part in cancer development, progression and responsiveness to anti-cancer therapies. One of the biological factors which can influence the efficacy of radiation treatment and chemotherapy for tumours is tumour perfusion, which by definition is the blood flow per unit volume of tissue resulting in delivery of nutrients and elimination of waste. All living tissues are dependent on blood vessels for delivery of oxygen, nutrients and elimination of waste products and in normal tissues, angiogenesis (the process by which new blood vessels are formed from pre-existing vasculature) is a tightly regulated balance between stimulatory and inhibitory signals. Tumour growth and survival is dependent on the ability to establish a secure blood supply and one of the hallmarks of cancer is the ability to sustain angiogenesis [87, 88]. Importantly, cancers acquire the ability to develop their own blood supply during tumour progression by gaining the ability to tip the balance between stimulatory and inhibitory factors for angiogenesis in favour of stimulation, which has been termed the 'angiogenic switch'[89] (see figure 2). The angiogenic pathway is controlled by a number of proteins, including vascular endothelial growth factors (VEGFs) and fibroblast growth factors (FGFs) which are regulated by gene transcription.

Figure 2 Diagrammatic representation of the angiogenic switch, illustrating that the balance between the regulatory proteins which stimulate and inhibit angiogenesis determine whether angiogenesis proceeds.

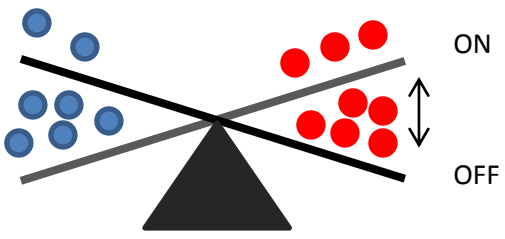

Pro-angiogenic factors
VEGF-A
VEGF-B, -C
FGF1 and 2

Anti-angiogenic factors
Thrombospondin-1, -2
Interferon
Angiostatin
Endostatin

(Adapted from *Cell,* 88, Hanahan and Folkman. Patterns and Emerging mechanisms of the Angiogenic Switch during Tumorigenesis, p353-364, Copyright 1996, with permission from Elsevier):

http://www.sciencedirect.com/science/article/pii/S0092867400801087

In contrast to the capillaries of normal tissues, tumour capillaries are structurally abnormal and often dilated, fragile, tortuous and elongated. The distribution of vessels may be heterogeneous, with some regions having a very low vessel density and others extensive neovascularisation[90]. The tumour vessels are also functionally abnormal. They frequently have gaps in the endothelium due to lack of complete unison of the plasma membranes of adjacent cells, with reduced pericyte coverage and smooth muscle cells; this characteristic makes the capillaries leaky. VEGF also contributes to the hyper-permeability of tumour capillaries by binding to endothelial receptors, which permits plasma proteins, such as fibrin and albumin to diffuse into the extra-vascular extracellular space. The leakiness of tumours can also lead to accumulation of fluid in the tumour parenchyma and in combination with defective lymphatic drainage of tumours caused by proliferating tumour cells, this can result in high interstitial pressure[91]. Structural and functional abnormalities in combination with regions of low vascular density can create resistance to flow and reduce regional tumour perfusion. The capillary network in tumours is typically chaotic and there may be shunting of blood, with spatial and temporal variations in tumour blood flow [90, 91].The greatest tumour vessel density in many tumours, including colorectal cancers, typically occurs at the tumour periphery and as the tumour grows the centre becomes increasingly hypovascular. Poor vascularity occurs in more than half of human tumours, irrespective of histology and grade [92]. Considerable variation in tumour vascularisation and perfusion can exist between tumours and experimental data shows that in general, inter-tumour variation exceeds intra-tumoural variation [93, 94].

Aberrant vascularity and perfusion in tumour tissues is a significant factor contributing to hypoxia, which is defined as a partial pressure of oxygen below physiological requirements. Hypoxia occurs in approximately 50-60% solid tumours[95] and it develops as a result of an imbalance between oxygen delivery to the tumour by tumour blood vessels and oxygen consumption by proliferating tumour cells (see figure 3). Perfusion-limited delivery of oxygen to tumour cells caused by vascular stasis or blockage is typically transient and hence this type of

hypoxia is called ‘acute hypoxia’. Hypoxia can also result from increased distances between vessels and tumour cells in regions of low vessel density, since the diffusion distance of oxygen is approximately 150-200 µm and cells which are more than a radius of 150 µm away from a blood vessel will suffer from increasing degrees of hypoxia and eventually anoxia [96]. Regions of tumour beyond the diffusion distance of oxygen become necrotic. Diffusion-limited hypoxia is termed ‘chronic hypoxia’.

Figure 3 Illustration of the oxygen gradients in tissue resulting from cellular distance from vessels carrying oxygenated blood and cellular switch from oxidative to glycolytic metabolism in hypoxic conditions (adapted with permission from “Jordan and Sonveaux. Targeting tumour perfusion and oxygenation to improve the outcome of anti-cancer therapy. *Frontiers in Pharmacology,* Copyright 2012” under Creative Commons License: http://creativecommons.org/licenses/by-nc/3.0/legalcode).

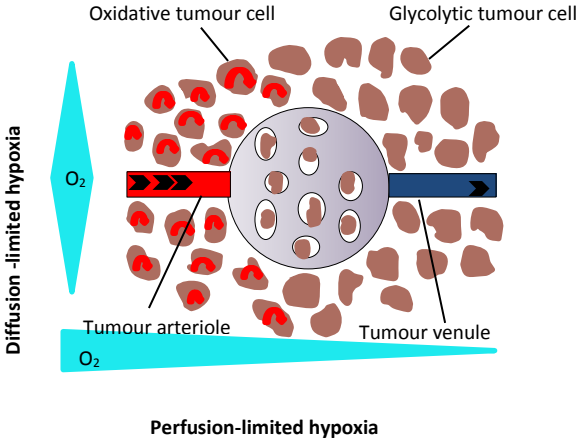

Hypoxia (partial pressures of oxygen in tissue <10 mm Hg) has been demonstrated to limit the efficacy of radiotherapy across a range of tumour types[97-100] and oxygenated tumour cells are approximately three times more susceptible to radiation damage compared to hypoxic or anoxic cells, referred to as the oxygen enhancement ratio (OER)[101, 102]. The relationship between hypoxia and radiation resistance is explained by the fact that oxygen is required to “fix” (make permanent) DNA damage caused by radiation induced free radical formation (see figure 4); in the absence of available oxygen, thiol containing compounds are reduced, which can restore the DNA to its initial form. Hypoxia (0.2 to 1 mm Hg oxygen) can also result in cell arrest, typically in G1/S phase and leads to an accumulation of quiescent cells[91]. Hypoxia can also result in clonal

selection of a more aggressive phenotype and genetic instability. For example, it has been demonstrated that hypoxia can select for survival of cells which have lost the tumour suppressor gene, p53, and reduce tumour cell death by apoptosis [103]. In many cancer types, there is clinical data showing an association between hypoxia and metastatic spread as well as prognosis, independent of treatment modality [104-106].

Figure 4 Diagram illustrating the 'oxygen fixation hypothesis'. The figure originally presented here cannot be made freely available via ORA because of copyright. The figure was sourced from "Chapter 6, Hall and Giaccia. *Radiobiology for the Radiologist*. Walters Kluwer, Lipincott Williams and Wilkins, 2011").

Hypoxia results in activation of hypoxia response pathways, the best characterised being that mediated through the Hypoxia- Inducible-Factor-1 (HIF-1). HIF-1 is a heterodimer, consisting of an alpha sub-unit and a beta sub-unit; the beta-unit is constitutively expressed, whereas the alpha sub-unit is degraded in normoxic conditions and stabilised in hypoxic conditions[107]. HIF1-alpha acts as a transcription factor to produce a range of effects, including the activation of genes involved in glycolysis and glucose transport (GLUT-1), angiogenesis (VEGF), cell growth/survival, invasion/metastasis and regulation of pH (Carbonic Anhydrase IX- CAIX). HIF1-alpha also can be regulated by mechanisms independent of hypoxia, for example it can be activated by the phosphoinositide-3-kinase (PI3-K)-AKT pathway.

Poor tumour perfusion can also cause resistance to chemotherapy drugs, directly as a result of impairment of intra-tumoural delivery of chemotherapy drugs; indirectly, the resultant hypoxia can reduce the penetration and efficacy of treatment through changes in transcellular pH gradients, cell cycle effects (limiting the activity of cell-cycle specific drugs) and decreased drug action due to HIF1-alpha function. It has been demonstrated pre-clinically that colon cancer cell lines are resistant to oxaliplatin due to a combination of such factors [108].

As angiogenesis is important in tumour biology, treatments are under development to target tumour blood vessel formation specifically and several anti-angiogenic agents have entered clinical practice. Jain et al[109] initially proposed the theory that anti-angiogenic agents could "normalise" tumour vasculature, improve tumour perfusion and delivery of chemotherapy. However, clinical studies of the impact of VEGF inhibitors on drug-penetration in a range of tumour types have demonstrated conflicting evidence, with studies in lung cancer[110] and rectal cancer respectively[111] showing rapid reductions in tumour perfusion as a result of the VEGF-A inhibitor, bevacizumab. There is also evidence that tumours can become resistant to angiogenic therapy[112, 113] and it can promote development of more aggressive cancer cells[114], possibly as a result of increased hypoxia[115]. It has been proposed that treatments targeting angiogenesis could be improved by optimising the sequencing of anti-angiogenic drugs with systemic chemotherapy[116].

In this thesis, it is argued that characterising the effect of anti-cancer therapies on tumour perfusion (whether radiotherapy, chemotherapy or targeted agents) is important for guiding rational sequencing of therapy and that robust methods for evaluating tumour perfusion are required.

A6 Imaging of Colorectal Cancer

In clinical practice, imaging is the most commonly used method for making management decisions, assessing tumour responsiveness to anticancer therapy and is also fundamental to

radiotherapy planning. Traditionally, computed tomography and MRI assessment of tumour morphology (shape and size) and stage (extent of spread) are used in this setting.

i) Computed Tomography

Computed Tomography (CT) is the most widely used imaging technique for patients with cancer. CT imaging of the pelvis has limitations for local staging of rectal cancers[117] and MRI is preferred, when not contra-indicated. CT of the Chest, Abdomen and Pelvis (with contrast) is also a routine test for evaluating the presence of metastatic disease in patients with diagnosed colorectal cancers. CT imaging to evaluate tumours is generally improved by the use of intravenous contrast administration, which is usually in the form of an iodinated contrast agent. Iodine has a high atomic number and hence tissues which preferentially concentrate the contrast will attenuate X-Rays more than other tissues, resulting in a brighter appearance on CT i.e. a higher CT number. Since the vasculature of tumours is abnormal and often highly permeable, tumours tend to take up or retain contrast material preferentially in comparison to surrounding normal tissue, which can be detected as contrast enhancement on CT imaging, although the enhancement properties and timing of different tumours varies somewhat. Contrast enhancement can be influenced by factors such as the patient's cardiac output, weight, fluid status and also the mode and timing of delivery of the contrast injection. There are 5 phases of enhancement with CT; early phase, when the contrast is still in the arteries before tissue enhancement (15-20s after contrast), late arterial, when tissues which receive an arterial blood supply will show optimal enhancement (30-35s), portal, when the liver enhances through blood supply via the portal vein (70s), equilibrium (180s), and delayed, when there is only enhancement of tissues with delayed washout (5-10 minutes). On a non-enhanced CT liver tumours are not usually visible because the contrast between the tumour and the liver parenchyma is too low.

Since normal liver tissue obtains most of its blood flow from the portal venous system, the majority of it enhances during the portal phase of imaging. Colorectal liver metastases, which

derive the majority of their blood supply from the hepatic artery can be relatively “hypo-vascular” and can be detected as foci of decreased attenuation, often with a rim of peripheral enhancement which may be detected during the arterial phase[118]. Hepatocellular carcinomas and hypervascular metastases may show significant enhancement during the arterial phase which tends to be diffuse. CT is the standard imaging modality for assessing response to systemic therapy in patients with metastatic colorectal cancer. Response of liver metastases is evaluated by bi-dimensional measurement of target lesions on sequential scans, according to RECIST guidelines[119, 120]; in the case of hepatocellular carcinomas a response assessment system which takes into account tumour necrosis has been advocated as an alternative by the ‘European Association for the Study of the Liver’ (EASL)[121].

Triple-phase liver CT (incorporating arterial phase, portal phase and delayed phase sequences) is also an important investigation for planning the delivery of SIRT, since arterial phase imaging provides detailed information on the hepatic arterial anatomy to help define vessels which may require coil embolization. CT imaging is used to compute the proportional volume of the liver affected by metastatic disease (used in the calculation of the activity of spheres required) and the proportional doses required to be delivered via the left and right hepatic arteries.

ii) Magnetic Resonance Imaging (MRI)

MRI is an imaging technique which uses strong magnetic fields and radio-waves to create images of the body, without the need for ionising radiation. In T1 weighted MRI images (using short time to echo and short time to repetition of radiofrequency pulses), short T1 tissues are bright and long T1 tissues are dark. Since fat has a short T1, it will appear bright, whereas water, which has a long T1, is dark. Conversely, in T2W images (using radiofrequency pulses with a long time to echo and long time to repetition); tissues with long T2 are bright.

In rectal cancer, pelvic T2W MRI (without the use of any contrast agent) has become the gold standard test for the loco-regional pre-operative staging of rectal cancer, providing superior soft-

tissue contrast over CT. The MERCURY trial demonstrated that MRI provides an accurate representation of the extent of the primary rectal tumour, particularly the proximity of the tumour and nodes to the mesorectal fascia (planned circumferential resection margin [CRM]), with a specificity of 92% to predict involvement of the CRM[122]. Involvement of the circumferential margin is associated with a high risk of local recurrence and poor survival after Total Mesorectal Excision [123]. Using these data, Patel et al[123] devised a scoring system for evaluating rectal tumour response to pre-operative chemo-radiotherapy on T2-weighted pelvic MRI, based along the lines of the pathological regression grading system, which estimates the proportion of tumour replaced by fibrotic stroma(which has a low signal on MRI).

Table 5 Summary of tumour regression grade scoring system for rectal cancer on MRI scans (mrTRG)

Tumour Regression Grade Score on MRI (mrTRG)	**MRI features**
mrTRG-1	- the absence of any tumour signal
mrTRG-2	- small amounts of residual tumor visible but with a predominant fibrotic low signal intensity
mrTRG-3	- mixed areas of low signal fibrosis and intermediate signal intensity present but without predominance of tumor
mrTRG-4	- predominantly tumour signal intensity remains with minimal fibrotic low signal intensity
mrTRG-5	- no fibrosis evident, tumor signal visible only

In a sub-study of the MERCURY trial, it was demonstrated that pelvic MRI 6-8 weeks after neoadjuvant radiotherapy can be used to define 'good' and 'poor' prognosis groups in which 'good responders' (mrTRG of 1-3) had a 72% 5 year OS and 64% DFS compared to a 27% OS (p=0.001) and 31% DFS (p=0.007). Post-treatment prediction of CRM status on MRI (mrCRM) was

also predictive of local recurrence on multivariate analysis. Notably, this was the first prospective study to show that radiological assessment of tumour response is associated with long-term outcomes. mrTRG on MRI 6-8 weeks after radiotherapy thus appears to be a promising early surrogate endpoint for long term treatment effectiveness. Although in this study, the reproducibility of mrTRG scans was assessed and all scans centrally reviewed by an expert radiologist, data relating to inter-observer agreement of mrTRG was not reported; it is therefore unclear how valuable this assessment might be in clinical practice.

iii) Perfusion Imaging of Colorectal Cancer

Whilst standard CT and MRI scans provide good structural and anatomical information about tumours, they do not provide information about physiological function nor do they characterise the effect of anti-cancer treatment on the tumour microenvironment. Changes in tumour shape and size after a period of treatment do not necessarily correlate with tumour response to therapy. A specific limitation of CT in assessing response of liver metastases to SIRT using RECIST criteria is that the tumours can increase in size initially as a result of treatment related oedema and necrosis [124]. Furthermore, as tumour response evaluation is usually performed after 8-12 weeks of chemotherapy or 6-12 weeks post completion of radiotherapy, patients may be subjected to toxicities of that treatment for that period of time whether or not the treatment works for them, with little opportunity to adapt the treatment other than on the basis of clinical assessment. Functional imaging of specific aspects of the tumour microenvironment could not only be useful in assessing the biological effect of biologically targeted agents in individual tumours, it could also be used to select optimal treatment dose based on biological effect, to guide rational sequencing of anti-cancer therapy and to adapt individual patient treatment on the basis of biological response to therapy[125].

This research project focuses on the development and application of functional imaging tests which have been developed to characterise tumour vascularity and perfusion in human tumours,

namely perfusion CT (pCT) and dynamic–contrast enhanced MRI (Dce-MRI). In section 1C, the principles and techniques underlying pCT are described and the literature relating to pCT in the assessment of rectal cancer is appraised, specifically with respect to its use in evaluating the effect of radiotherapy (RT) +/- radiosensitising agents. In section 1D, the principles and techniques underlying Dce-MRI are described; the literature relating to Dce-MRI in the assessment of rectal cancer is appraised. Finally, in section 1E, the literature with respect to perfusion imaging of colorectal liver metastases is reviewed, specifically relating to the evaluation of chemotherapy and SIRT. In this project, the general hypothesis that perfusion imaging with pCT and Dce-MRI can be used to assess the biological effect of radiosensitising drugs and to guide rational sequencing of systemic drugs and radiotherapy is tested.

1B Radio-sensitisation of Colorectal Cancer and Tissue Biomarkers of Response

B1 Radio-sensitisation

Steel and Peckham published a model for the ways in which drugs interact with radiotherapy in a seminal paper in 1979[126]. Radio-sensitisers are drugs that have the ability to potentiate the effects of ionising radiation on tumours[126]. The majority of drugs currently used as radiosensitisers in clinical practice were discovered empirically before their radiosensitising properties were demonstrated in the laboratory setting. At the cellular level, the addition of a radiosensitising drug to ionising radiation increases the proportion of cells killed and delays cell growth (*intrinsic* radio-sensitisation), but this is also influenced by the rate at which DNA damage is repaired and by tumour cell repopulation [127]. Traditionally, intrinsic radio-sensitisation is evaluated by clonogenic survival assays (measuring cell viability) and isobolographic plots of cell survival, comparing radiation effects with and without the drug under study. Using this method drugs can be characterised as having an antagonistic effect on cell kill, an additive effect or a super-additive (synergistic) effect, where the resulting effect is greater than that anticipated from

the addition of the two independent treatment effects[127]. *In vivo*, the combination of drug and radiation should improve local tumour control and/or eradicate microscopic metastases without exceeding the radiation tolerance of normal tissues to be a successful radio-sensitizer.

The interaction between radio-sensitizer and ionising radiation may not necessarily be selective for tumour cells and modifications of dose may be required to limit normal tissue toxicity. The concept of therapeutic gain underpins radiosensitisation in clinical practice, whereby the addition of a drug to radiotherapy should increase the tumour response over each therapy alone, when assessed at the same level of normal tissue side effects (see figure 5). It is generally recognised that few clinical trials are currently designed in a way that allows the interaction between chemotherapy and radiotherapy to be evaluated scientifically[127].

Figure 5 Illustration of the concept of the therapeutic ratio, which can be improved through use of radiosensitisers. For a given radiation dose, there will be a given tumour response and a given rate of toxicity. A radiosenisitiser will ideally enhance the radiation response at a given radiation dose, whilst enhancing the rate of radiation toxicity to a lesser degree, thus increasing the gap between the tumour radiation response and normal tissue toxicity curves, thus improving the therapeutic ratio (adapted by permission from Macmillan Publishers Ltd, Nature Reviews Clinical Oncology, Seiwert et al, The concurrent chemoradiation paradigm- general principles, Copyright 2007; http://www.nature.com/nrclinonc/journal/v4/n2/full/ncponc0714.html)

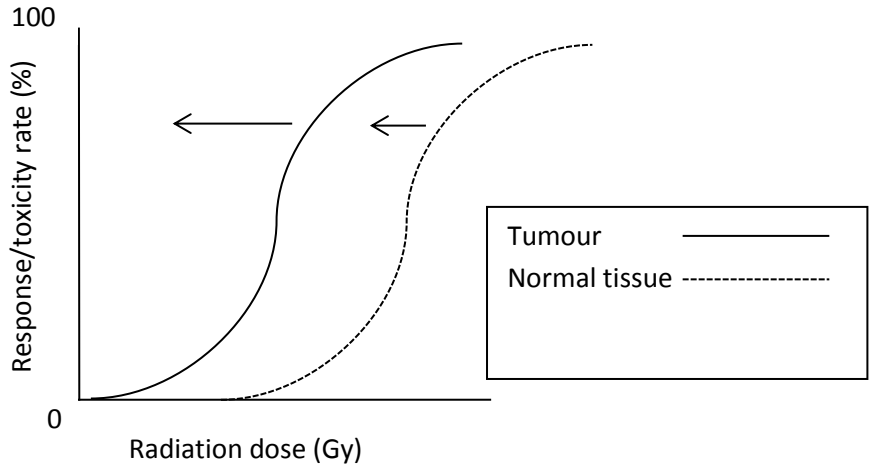

Radiation and chemotherapy can improve tumour control through direct interaction between the two, for example chemotherapy may kill cells in a radio-resistant phase of the cell cycle or convert single stranded DNA breaks into double stranded DNA breaks. Alternatively, both modalities may enhance tumour control through indirect methods, for example, chemotherapy may debulk a tumour and make it more readily treatable with radiotherapy, co-operate spatially by treating disease outside the radiation field or produce independent cell kill[128].

The model for radio-sensitisation initially proposed by Steel has been updated in the modern era due to the availability of molecularly targeted agents and drugs that can influence tumour stromal interactions. Bentzen et al. proposed a new framework for considering 5 exploitable mechanisms by which drugs can interact with radiotherapy, which incorporates biological co-operation in addition to cytotoxic enhancement, temporal modulation, spatial co-operation and normal tissue protection [129]. In this model, biological co-operation refers to selective targeting of distinct cell populations with different treatment mechanisms to achieve cell kill and/or tumour control. For example, vascular targeting agents such as combretastatin can be used to complement the biological effect of radiation, since vascular targeting agents characteristically lead to shutdown of tumour vasculature and tumour necrosis in the centre of tumours (which are hypoxic and relatively radio-resistant) whilst radiation is effective in the better-oxygenated cells of the tumour rim, where the vascular targeting agents are ineffective[130].

Harrington et al.[131] have recently developed and published guidelines setting out the core and optimum criteria to guide testing of the combination of targeted drugs and radiation in early phase clinical trials. These guidelines recommend that clinical studies of targeted agents and radiation should be underpinned by robust pre-clinical research which includes evidence of target identification/validation, pharmacokinetic studies to define therapeutic drug concentrations in human tissue and proof that target knockdown by the drug is associated with enhanced radiation sensitivity both *in vitro* and *in vivo*.

It is recognised that there are challenges associated with designing phase I trials of targeted drugs combined with radiation to assess toxicity; notably studies can be difficult to perform in end-stage or palliative patients yet conduct in radical patients can pose high risks if drug toxicity results in interruption of radiotherapy and frequently the standard radiation schedule for such patients involves concomitant cytotoxic chemotherapy, necessitating the evaluation of triple therapy. The traditional phase I trial design based on the initial recruitment of 3 patients in successive cohorts treated with escalating drug doses to evaluate dose limiting toxicities (typically defined as grade 3 toxicity) can be problematic in phase I trials of drugs and radiation, since radiation not infrequently results in acute grade 3 toxicities; it is recommended that careful consideration is required when defining which adverse events constitute dose limiting toxicities. A further challenge highlighted in phase I studies of drugs and radiation is the potential requirement for protracted follow-up of acute and late toxicities in comparison to studies of drugs alone, since acute radiation related toxicities can take time to resolve and late radiation don't become apparent typically more than 6-12 months after the end of treatment.

A recognised limitation of most *in vivo* models for testing radiosensitising drugs is that they don't incorporate appropriate methods to analyse normal tissue toxicity, although validated assays for the pre-clinical evaluation of normal tissue toxicity exist, for example the intestinal cell crypt assay [132, 133] or the ventral tongue mucosal assay[134].The principle underlying these methods is that following radiation exposure, proliferating cells undergo apoptosis or cell cycle arrest and are replaced by replicating stem cells which migrate to replace the lost epithelium (in the case of the intestine, from the intestinal crypts to the villi). In the case of the intestinal cell crypt assay, the number of surviving crypts in pathological specimens can be used as a marker of the survival of intestinal crypt stem cells[135]. Harrington et al [131] recommend use of one of these assays in pre-clinical research of radiosensitisers, in order to identify which drugs increase the sensitisation enhancement ratio of tumour relative to normal tissue and are therefore acceptable to be taken forward to clinical trials.

B2 Radiosensitisers in Colorectal Cancer

i) Cytotoxic chemotherapy agents

All of the principal chemotherapy drugs currently used in the treatment of colorectal cancer: 5-FU[136, 137], capecitabine[138], oxaliplatin[44, 139-148], and irinotecan[149-154] have been demonstrated to be intrinsic radiosensitisers by previous pre-clinical research. Proposed mechanisms of radio-sensitisation for each drug are summarised in table 6.

Table 6 Summary of drugs in use in colorectal cancer and their mechanisms of action as radiosensitisers. Abbreviations: DSBs- Double strand Breaks; SSBs-Single Strand Breaks; DNA-PK- DNA phosphokinase

Drug	DNA Damage	DNA Repair	Cell Cycle Effects	Apoptosis	Tumour Vasculature
5-FU/Capecitabine	Induction of DNA DSBs	Inhibition of DSB repair	Elimination of S phase cells		
Oxaliplatin	Formation of DNA adducts	Inhibition of DSB repair	Arrest in G2/M and S phases	P-53 independent cell kill	
Irinotecan	Converts SSbs to DSBs	Inhibition of topoisomerase I	Arrest in G2 Elimination of S-phase cells		
Cetuximab		Suppression of DNA-PK activity	Accumulation in G1 and G2	Increase in bax and decrease in bcl-2	Inhibition of VEGF release
Bevacizumab					Normalisation of vasculature

In this research, oxaliplatin and 5-FU are utilised as radiosensitising chemotherapy in combination with SIRT in patients with unresectable liver-predominant colorectal liver metastases. Of note, oxaliplatin has been evaluated in combination with 5-FU and radiation *in vitro*, where experiments revealed synergism in comparison to either radiation or the drugs alone[140]. A limitation of using combinations of cytotoxic drugs as radiosensitisers in the clinical setting is the

potential to enhance systemic toxicity, thereby potentially compromising the therapeutic ratio of treatment.

Table 7 Summary of phase III trials combining oxaliplatin and fluoropyrimidines with pre-operative pelvic radiotherapy

Trials	Number of patients	Inclusion criteria	Randomisation	Endpoints	
				Primary	Secondary
STAR 01 Aschele et al, 2011 [155]	747	Resectable rectal cancer <12cm anal verge Radiological evidence of perirectal fat or LN involvement	Arm A: RT 50.4Gy in 28#+ 5FU 225mg/m2/day Arm B: RT 50.4Gy in 28# + 5FU +0xaliplatin 60mg/m2 weekly x 6	OS(not reported here)	Tumour response pCR 16% Arm A vs 15% Arm B (p=0.982) Path M1 disease: 3% Arm A vs0.5% Arm B Toxicity: G3/4 diarrhoea 8% Arm A vs 24% Arm B (p<0.01)
PRODIGE-2 ACCORD 12/405 Trial Gerard et al, 2009 [156]	598	Resectable Rectal Cancer T3/4N0-2M0 T2 low	Arm A: RT 45Gy in 25# + Cape 800mg/m2 BD Arm B: RT 50Gy in 25# + Cape 800mg/m2 M-F + Oxaliplatin 50mg/m2/weekly x5	Resection Rate:	OS and DFS(unreported) Tumour response: 98% Arm A vs 98.6%Arm B pCR 13.8%Arm A vs 18.8% Arm B (p=0.11) Sphincter preservation rate: 75% Arm A vs 78% Arm B Pre-op G3/4 Toxicity 11% Arm A vs25% Arm B (p<0.01)
CAO/ARO/AIO-04 German Rectal Cancer Trial Rodel et al 2012 [157]	1265	Rectal Cancer T3-4N0 T1-4 N1-2	Arm A: RT 50.4Gy in 28# + 5FU (1000mg/m2) D1-5 and 29-33 +4 cycles adjuvant 5FU Arm B: RT 50.4Gy in 28# +Ox50mg/m2 D1, 8, 22 and 29 and 5FU 250mg/m2 D1-14 and 29-35 and 8 cycles of Ox/5FU	DFS	Toxicity: G3/4 20% Arm A vs 23% Arm B pCR: 13%Arm A vs 13% Arm B (p=0.038) (not a planned protocol endpoint)
NSABP-R04 Trial O'Connell 2014 [158]	1606	Resectable Rectal Cancer T3-4N0 T1-4N1-2	Arm 1: RT 5-6 weeks + Cont 5FU Arm 2: RT 5-6 weeks + Cont 5FU Ox(50mg/m2) weekly x 5 Arm 3: RT 5-6 weeks + Cape BD M-F during RT Arm 4: RT 5-6 weeks + Cape BD M-F during RT +Ox(50mg/m2) weekly x 5	Loco-regional Disease control(at 3y) OS and DFS QOL	Complete clinical response rate pCR rate: 17.8% (Arms 1 + 3) vs 19.5% A(Arms 2 + 4) (p=0.40) Sphincter preservation rate: 61%(Arms 1+3) vs 57.8% (Arms 2 + 4) (p=0.24) G3/4 Diarrhoea: 6.9% (Arms 1 +3) vs 16.5% (Arms 2 +4) (p=<0.001)
PETACC-6 Trial EORTC (Schmoll et al 2014) [159]	1090 expected	Resectable Rectal Cancer T3/4 and/ or N1-2 M0 <12cm anal verge	Arm 1: RT 5-6 weeks + Cape BD M-F during RT and post-op for 6 cycles q3 Arm 2: RT 5-6 weeks + Cape BD M-F during RT And Ox weekly for 5-6 weeks and post-op CAPOX for 6 cycles 3 weekly	DFS (3y) Loco-regional Failure Distant failure Pathological downstaging pCR rate Tumour Regression Grade R0 resection rate Sphincter preserving surgery rate Pre-operative complication rate Toxicity	OS(5 years) 74.5% Arm 1 vs 73.9% Arm 2 (p=0.78)

ABBREVIATIONS: RT=radiotherapy; LN=lymph node; M-F=monday to friday; D=day; Cape=capecitabine; Ox-oxaliplatin; OS overall survival; pCR=pathological complete response rate; DFS=disease free survival; QOL=quality of life

Phase I and II clinical trials in patients with rectal cancer have demonstrated that the incorporation of oxaliplatin into concurrent preoperative 5-FU based chemo-radiotherapy for rectal cancer is feasible [160-190], with promising pCR rates (ranging between 12 and 33%), and levels of toxicity considered to be acceptable. These are reviewed in detail in my review article on oxaliplatin as a radio-sensitizer[44]. However, results from phase III trials comparing neoadjuvant oxaliplatin-containing chemo-radiotherapy with standard 5-FU/capecitabine chemo-radiotherapy for rectal cancer (table 7) have not demonstrated any statistically significant increase in pCR rates or sphincter preservation rates from the addition of oxaliplatin to 5-FU or capecitabine pre-

operative radiation but have demonstrated statistically significant increased rates of grade 3 toxicity, particularly diarrhoea[155, 158, 193]. There is currently insufficient evidence to support the use of concurrent oxaliplatin and 5-FU with pre-operative radiotherapy for rectal cancer and other radiosensitisers warrant evaluation, particularly for patients with high risk rectal cancer.

In the different context of patients with liver-predominant metastatic colorectal cancer, the pre-clinical data demonstrating oxaliplatin as a radio-sensitizer in combination with promising phase I/II trial data supports further clinical evaluation of oxaliplatin's clinical potential to improve tumour response and outcomes in the phase III trial setting; since SIRT relatively spares normal tissue and it has mostly non-overlapping toxicities with chemotherapy, the combination of the two therapies should theoretically result in therapeutic gain, improving overall disease control and time to disease progression, whilst minimising unacceptable toxicity.

ii) Biologically targeted agents as radiosensitisers

There is increasing interest in the use of drugs which target molecular abnormalities which are expressed in tumour cells[194] rather than being directly cytotoxic, as a means of selectively enhancing radiation response in tumour tissue, whilst relatively sparing normal tissue effects. This class of agents offers the possibility of targeting the specific hallmarks of cancer such as growth factor self-sufficiency and angiogenesis which are relevant to tumour radiobiology. The biologically targeted agents cetuximab (which is an EGFR inhibitor) and bevacizumab (which is a VEGF-inhibitor) which are commonly used in the systemic treatment of metastatic colorectal cancer have also been considered as potential radiosensitisers in colorectal cancer. Although there is pre-clinical evidence that cetuximab is a potent radio-sensitizer *in vitro*[195], *in vivo*[196, 197]and in clinical trials of patients with cancer of the head and neck[198], the addition of cetuximab to pre-operative chemo radiation for rectal cancer (in combination with capecitabine, capecitabine and oxaliplatin or capecitabine and irinotecan) has resulted in disappointing pCR response rates, with an average of 9.1% (range 0-20%)[199-209], suggesting the addition of

cetuximab to chemo radiation has a sub-additive effect, tumour response appearing to be independent of *KRAS* status.

Although agents which inhibit VEGF and angiogenesis can reduce tumour blood flow and increase hypoxia, thus theoretically increasing chemo and radio-resistance, there is some pre-clinical evidence to suggest that drugs such as bevacizumab can enhance tumour radiation response[210-213] and even improve tumour oxygenation[210, 213, 214]. An explanation for this observation is that VEGF inhibition leads to a transient normalisation of the abnormal tumour vasculature reduced hydrostatic pressures and improved delivery of drugs and oxygen [215, 216]. It has been suggested that the time period during which vascular normalisation occurs is approximately 6 days [111, 212, 216], before vascularity begins to regress and perfusion diminishes. This is a potential limitation of using VEGF-inhibitors as radiosensitisers in combination with fractionated radiotherapy in the clinical setting and the timing of VEGF-inhibitors is likely to be crucial in determining the efficacy of such combinations.

Figure 6 Representation of the RAS-PI3K-Akt pathway, downstream of EGFR activation. Binding of ligand (EGF or TGFα) leads to dimerization of the EGF receptor and phosphorylation of tyrosine residues in its intracellular domain. This leads to activation of multiple pathways (only the RAS-RAF-Mek and PI3K-Akt-mTOR pathways shown here).

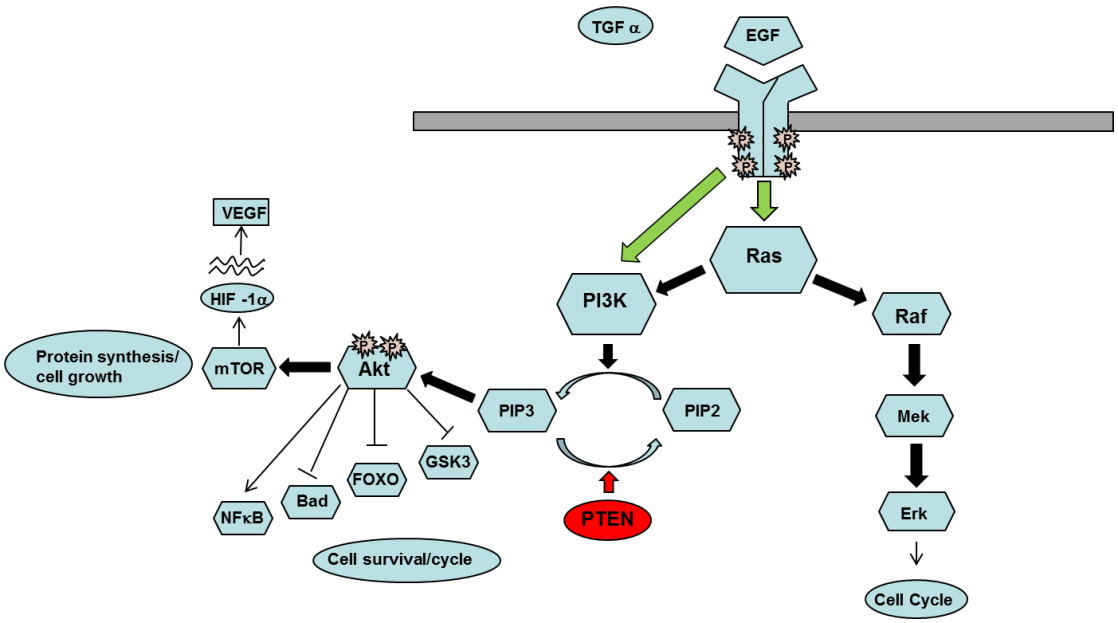

A number of other molecularly targeted agents are under investigation pre-clinically or clinically as potential radiosensitisers, for example inhibitors of DNA damage repair, cell cycle checkpoint kinase inhibitors and drugs which target tumour metabolism[217]. Agents which target tumour cell signalling pathways show particular promise. The phosphatidylinositol 3-Kinase (PI3-K)-Akt signalling pathway, which is activated in many human cancer cells [218], is associated with resistance to radiation [219-222]. PI3-kinases are a group of enzymes responsible for the phosphorylation of phosphatidylinositol. Phosphatidylinositol-triphosphate (PIP-3) is a second messenger generated by PI3-kinases, which activates the serine/threonine kinase Akt, leading to its phosphorylation (on two residues, Ser473 and Thr308). Akt itself regulates protein synthesis and cell growth by phosphorylation of mammalian target of rapamycin (mTOR). This pathway thus plays a key role in regulating cell proliferation, survival and growth but is also involved in the regulation of HIF-1 alpha and VEGF. The PI3-K-AKt pathway cannot only be activated as a result of EGFR overexpression/mutation but also Akt overexpression, *RAS* mutation, *PI3K* amplification/mutation and loss of the Phosphatase and Tensin Homologue (*PTEN*) gene[223] (see figure 6); since many colorectal cancers either express EGFR or harbour mutations of *RAS*, inhibitors of this pathway are a rational choice for further evaluation as clinical radiosensitisers in this tumour type. Agents which inhibit PI3-K have been demonstrated to increase radiation sensitivity both *in vitro* and *in vivo* in cells/tumours which have constitutive activation of the PI3-K-Akt pathway [220, 222,224]. Down-regulation of Akt with siRNA also causes radio-sensitisation of such cells[225]. In this thesis, I focus specifically on nelfinavir, an inhibitor of Akt, as a radio-sensitizer in patients with rectal cancer.

B3 Nelfinavir

i) Pre-clinical data

Nelfinavir is a non-peptidic protease inhibitor, which belongs to a class of drugs which have been used as anti-retroviral agents in therapeutic schedules for patients with Human

Immunodeficiency Virus (HIV) infection over the past two decades. Saquinavir was the first HIV protease inhibitor demonstrated to cause radio-sensitisation of cancer cells *in vitro* [226]. Subsequently, Gupta et al[227] tested five first generation HIV protease inhibitors (amprenavir, nelfinavir, saquinavir, ritonavir and indinavir) and demonstrated that the first three drugs inhibited Akt phosphorylation at Ser473 in cell lines with constitutive activation of AktSer473 but did not affect tumour cell growth kinetics, at serum concentrations typically achieved in patients with HIV. In clonogenic survival assays *in vitro*, nelfinavir and amprenavir in combination with radiation were demonstrated to produce synergistic effects compared with either the drugs or radiation alone. Of note, radio-sensitisation of cells in culture to nelfinavir has been demonstrated to be independent of *KRAS* status [227], which is of importance, since approximately 40% colorectal tumours have a *KRAS* mutation.

In mice transplanted with human tumour xenografts (SQ20B) with constitutionally activated Akt, 5 days of treatment with nelfinavir resulted in downregulation of Akt-473, also at serum concentrations achieved in HIV patients. *In vivo* clonogenic survival assays and tumour growth delay experiments in the tumour xenografts demonstrated a statistically significant synergistic effect between nelfinavir and radiation, without any increase in normal tissue toxicity (as determined by the epidermal skin thickness of the mice). The magnitude of the effect of nelfinavir and radiation on tumour growth delay observed was greater than that which was anticipated from intrinsic radio-sensitisation alone, which led to the hypothesis that nelfinavir may have an effect on the tumour environment, namely on tumour hypoxia and angiogenesis[228].

A series of experiments demonstrated that nelfinavir reduced VEGF expression (via activation of a transcription factor) in normoxic conditions and reduced HIF-1 alpha induction in hypoxic conditions both *in vitro* and *in vivo*, in mice transplanted with human tumour xenografts. In the *in vivo* experiments, treatment with nelfinavir resulted in a reduction in angiogenesis (as determined by a matrigel plug assay) and a reduction in hypoxia (as determined by

immunohistochemically staining for EF5, a 2-nitroimidazole which binds to regions of hypoxia)[228]. The functional mechanism underlying these changes was defined in a subsequent series of experiments, in which mice bearing tumours were treated with agents inhibiting different targets in the EGFR-RAS-PI3-K-Akt signalling pathway (iressa, an inhibitor of EGFR tyrosine kinase signalling, a farnesyl-transferase inhibitor L-778, 123 which inhibits wild-type *H-RAS* and mutated *N-RAS*, a PI3-K inhibitor, PI-103, and the Akt inhibitor nelfinavir) [229]. In nude mice bearing SQ20B tumour xenografts, 10 days of treatment with each of the EGFR-RAS-PI3K-Akt inhibitors resulted in a reduction in hypoxia (measured by luciferase expression on bioluminescent imaging and EF5 immunohistochemistry) in comparison to an increase in hypoxia in untreated controls and mice with HT1080 tumours (not expressing EGFR) treated with iressa. Three-dimensional power-Doppler ultrasound demonstrated significantly greater vascular flow in treated mice with SQ20B tumours compared to untreated controls and the rate of vascular flow increased at least 2-fold after 14 days of nelfinavir treatment. This research established an association between reduced hypoxia and improved tumour perfusion after tumour signalling inhibition using nelfinavir. Furthermore, *ex vivo* microscopy demonstrated an increase in perfused vessel density (evaluated using fluorescently tagged endothelial antibody CD31-RP), an increase in extravascular diffusion evaluated using injected Hoechst dye) as well as increased regularity and reduced vessel tortuosity in SQ20B tumours of treated versus control mice. Changes persisted between 5 and 14 days after treatment began (after which time experiments were terminated) suggesting inhibition of the EGFR-RAS-PI3-K-Akt signalling pathway results in durable improvements in vascular function, a potential advantage over anti-angiogenic drugs.

ii) Clinical data

Nelfinavir has come to the fore as PI3-K inhibitor for investigation as a radio-sensitizer in early phase clinical trials because the side effect profile of the drug is well characterised, having been used in many thousands of patients with HIV over the past two decades (summary of product characteristics accessed at https://www.medicines.org.uk/emc/medicine January 2014). It is well

tolerated in such patients, with low levels of toxicity and early treatment-related discontinuations [230].The main acute toxicities of treatment are gastrointestinal; diarrhoea (occurring>10%) typically occurs early after commencement of therapy but is usually mild or moderate and easily managed. Other common toxicities include rash, derangement of liver enzymes (approximately 2%) and low grade neutropenia. HIV-positive patients on nelfinavir who have received concomitant radiotherapy for a variety of malignancies appear to have tolerated the combination well. In a report by Oehler-Jänne et al., treatment with chemo radiation of HIV-negative patients and HIV-positive patients undergoing retro-viral therapy (HAART) was compared and there was no difference in acute nor late toxicity between the groups[231].

A limited number of clinical studies have investigated the safety and efficacy of nelfinavir in combination with chemo radiotherapy [232-235] (see table 8) in patients with a range of cancer types. In the first of these studies to be published[232], a phase-I dose escalation study (with 2 levels of gemcitabine), nelfinavir was administered continuously over 7 weeks with chemo-radiation involving cisplatin and gemcitabine plus 50.4 Gy in 28 daily fractions in 12 patients with locally advanced pancreatic cancer. At a dose of 1250 mg bd (equivalent to doses used in HIV therapy), nelfinavir reduced Ser473-phospho-Akt levels in the peripheral blood leukocytes of all evaluable patients (n=8) and the combination of nelfinavir with chemo radiation was tolerated with acceptable toxicity at both dose levels of gemcitabine; the incidence of adverse events was in keeping with those expected from standard chemo-radiation therapy for this disease, with none of the observed toxicities thought to be related to nelfinavir treatment. In a phase I study in patients with unresectable stage IIIA/B non-small cell lung cancer, nelfinavir was given at 2 dose levels (625 mg bd and 1250 mg bd) for 7 to 14 days before and concomitantly with a radical dose of radiation and concurrent cisplatin/etoposide chemotherapy and nelfinavir 1250mg bd was defined as the maximum tolerated dose.[233] A similarly designed phase I trial was conducted in patients with glioblastoma multiforme, where nelfinavir was also given for 7-10 days before radical brain radiotherapy and concurrent temozolamide; 3 dose-limiting episodes of

hepatotoxicity and 1 dose-limiting episode of GI toxicity was observed at the higher dose of nelfinavir (1250 mg bd), which was concluded to be the maximum tolerated dose[234].

Table 8 Summary of published studies having evaluated nelfinavir in combination with chemo-radiation in the treatment of human tumours.

Study	Tumour type	No. of patients	Treatment Regime	G3/4 toxicities observed	Dose Limiting Toxicities	Response rates
Brunner et al.[232]	Pancreatic adenocarcinoma (Unresectable or borderline resectable)	12	NFV 1250 mg bd 3 d before and concurrent with : 59.4Gy pancreas DL1 Cis 30 mg/m² Gem 200 mg/m² D1,8,22, 29 (n=5) DL2 Cis 30 mg/m² Gem 300 mg/m² D1,8,22,29 (n=5)	G3 leukopenia (4) G3 neutropenia (3) G3 Thrombocytopenia (2) G3 Nausea/vomiting (2) G3(1) G4 (1) Transaminase G3 Bilirubin (2) G3 AlkP (1) G3(2) G4 (1) Infection	G3 upper GI (1) at DL1 G3 nausea and vomiting (1) at DL2	5/10 PR CT 6/10 resection 5/9 CR ,2/9 NC and 2/9 PR PET
Rengen et al. [233]	Non-Small Cell Lung Cancer (Unresectable Stage IIIA/IIIB)	16	NFV 7-14 d before and concurrent with: 66.6 Gy in 38# involved field + Cis 50 mg/m² D1, 8, 29, 36 Etop50 mg/m² D1-5 , 29-36 DL1: NFV 625 mg bd (n=5) DL2 : NFV 1250 mg bd (n=8)	G3 oesophagitis (4) G3 pulmonary toxicity (1) G3 leukopenia (3) G3 anaemia (2) G3 thrombocytopenia (2) G3 upper GI (3) G3 hypotension (3) G3 fatigue (2) G4 leukopenia (6) G4 thrombocytopenia (1)	None	4/12 CR, 7/12 PR , 1/12 SD on CT 5/9 CR, 4/9 PR PET
Buijsen et al.[236]	Locally advanced rectal adenocarcinoma	12	50.4Gy in 28 # pelvis and Capecitabine 825mg/m² concurrent with NFV: DL1 NFV 750 mg bd (n=5) DL2 NFV1250 mg bd (n=3) DL3 NFV 1000 mg bd (n=3)	G3 transaminase (2) G3 cholangitis (1) G3 ileus G3 diarrhoea (2) G4 post-op wound complication (1)	G3 diarrhoea (2) at DL2 G3 transaminase (2) G3 cholangitis (1) G3 ileus G4 post-op wound complication (1) At DL3	pCR 3/11 (27%) Good TRG 4/11
Alonso – Basanta et al.[234]	Glioblastoma (post-op)	21	NFV 7-10 days before and concurrent with: 60 Gy in 30# GTV and Temozolomide 75 mg/m2 od DL1 NFV 625 mg bd (n=3) DL2 NFV 1250 mg bd (n=18)	diarrhoea (1) transaminase (8) Bilirubin (1) AlkP (1) Lymphopenia (2)	G3 hepatotoxicity (3) G3 diarrhoea (1) at DL2	Median PFS 7.2 m Median OS 13.7 m

Abbreviations: NFV= Nelfinavir; DL=Dose Level; Cis=Cisplatin; Gem=Gemcitabine; G=Grade; PR=Partial; Response; CR= Complete Response; NC=No Change; Etop= Etoposide; pCR= Pathological Complete Response; TRG= Tumour Regression Grade; PFS= Progression Free Survival; OS=Overall Survival

Only one published Phase I study has evaluated nelfinavir in combination with chemo-radiotherapy (capecitabine) in patients with rectal cancer [235, 236]. In contrast to the previous studies, this study investigated 3 dose levels of nelfinavir (750 mg bd, 1000 mg bd and 1250 mg

bd) and demonstrated dose limiting toxicities (GI or hepatotoxicity in all but one case) in the higher two dose levels, finding 750 mg bd to be the maximum tolerated dose of nelfinavir in combination with capecitabine. Evaluation of nelfinavir concentrations during therapy in this study revealed higher than expected concentration ratios of nelfinavir in 4/6 patients who developed dose limiting toxicity, requiring dose adjustments. The authors hypothesised that this may have been the result of a drug interaction between nelfinavir and capecitabine, since the latter is an inhibitor of CYP2C9, which is involved in nelfinavir metabolism.

Efficacy data were promising across the studies, with more than 50% of patients evaluated by 18-Fluoro-Deoxy-Glucose (FDG)-Positron Emission Tomography (PET) demonstrating a complete metabolic response in both the pancreatic and lung studies and more than 60% of patients with pancreatic cancer having completed the therapy proceeding to resection. The pCR rate of 27% in the rectal study was at the high end of the range of pCR rates reported in other studies of capecitabine chemo-radiation for locally advanced rectal cancer. However, the small number of patients and lack of controls in these studies of nelfinavir and chemo-radiation make it impossible to draw definite conclusions about the efficacy of the treatment combination in comparison to standard therapy.

Although the published data demonstrate the feasibility and toxicity of combining nelfinavir with chemo- amongst a range of tumour types, there is no published clinical trial data relating to the combination of nelfinavir with radiation alone, without the confounding effect of radiosensitising chemotherapy and the studies did not incorporate any biomarkers of radio-sensitisation. It is not possible to draw conclusions about the radiosensitising efficacy of nelfinavir. Furthermore, published data are lacking in relation to whether the changes in perfusion observed in pre-clinical studies with nelfinavir can be replicated in human subjects with cancer. Arguably, the greatest benefit from radiosensitisers with potential to reduce tumour hypoxia is in combination with hypo-fractionated radiotherapy regimens rather than prolonged fractionated courses of radiation

since reoxygenation which occurs as an effect of fractionated radiation may be limited in the shorter time-course. In this thesis, I evaluate the combination of nelfinavir before and during a course of hypo fractionated radiotherapy in patients with metastatic rectal cancer, requiring radiation either to palliate local tumour symptoms or to downstage the primary tumour prior to delayed resection. Specifically I test the hypotheses that this treatment combination is tolerated with acceptable toxicity, that nelfinavir improves tumour perfusion in patients with rectal cancer and evaluate potential tissue biomarkers of response.

B4. Tissue biomarkers in rectal cancer

In clinical practice, pathological assessment of tumours is fundamental to characterising the origin and behaviour of tumours prior to selecting cancer therapy. Current clinical guidelines recommend histological confirmation of rectal adenocarcinoma on diagnostic biopsy prior to offering therapy[iii]. The Dukes' classification and Tumour Node Metastasis (TNM) status, tumour grade and presence of lympho-vascular invasion are pathological descriptors of resected colorectal cancers which have been demonstrated to be prognostic for patient outcome and are widely used in clinical practice to guide clinical decision making, for example in selection for adjuvant chemotherapy[237].However, it is recognised that tumours, even those belonging to the same anatomical site and histological subtype, are biologically heterogeneous and there is growing emphasis on the characterisation of prognostic as well as predictive tissue biomarkers to allow personalisation of cancer therapy. For example, gene expression profiling of colorectal tumours for the *KRAS* mutation is now routine in many centres, as *KRAS* mutation has been demonstrated to predict lack of responsiveness to the monoclonal antibody, cetuximab [238]. Recently, recommendations have been made for colonic tumours to be profiled for mismatch repair (MMR) genes, as the loss of MMR expression is associated with lack of benefit from adjuvant chemotherapy in stage II colonic cancers[239]. With respect to the current

[iii] (CG131 Colorectal cancer: NICE Guideline, 2011
URL: https://www.nice.org.uk/guidance/CG131/NICEGuidance accessed Jan 2014).

management of rectal cancer, the decision whether to offer pre-operative chemo-radiotherapy or radiotherapy is still primarily based on the anatomical extent of the tumour on pelvic MRI without reference to biological sub-types or characteristics based on pathological analysis. Outside of clinical trials, capecitabine or 5-FU are the radiosensitisers used in the standard treatment of rectal cancer, irrespective of individual tumour characteristics.

Researchers have investigated numerous potential tissue biomarkers that may predict tumour response to pre-operative chemo-radiotherapy for rectal cancer [240-242], but no tissue biomarker has been sufficiently validated to enter routine clinical practice. There is a need to define biomarkers that not only predict response to radiation but those tumour sub-types that are likely to benefit from different types of radiosensitisers, for example those which can overcome tumour hypoxia or sensitise tumours with constitutionally activated PI3-K-Akt signalling, which are inherently radio resistant.

Histological biomarkers may also have potential to act as surrogate endpoints for treatment effectiveness in clinical trials. A major barrier to the advancement of radiosensitisers for cancers of the gastrointestinal tract has been uncertainty regarding the primary endpoint to be used to do power calculations for large-scale clinical trials. For neo-adjuvant therapy prior to surgery, the rate of pathological complete response (pCR) rate has been widely used as an endpoint to compare the efficacy of oxaliplatin and other potential radiosensitisers in concurrent chemo-radiotherapy regimes, particularly for rectal cancer. Its advantages as a comparative measure of efficacy are that it can be assessed at a short time interval after treatment[243] and it has been demonstrated to be an independent predictor of local recurrence, DFS, distant metastasis and OS[243]. However, pCR may be variably defined by pathologists[244] and is influenced by the time interval between chemo-radiotherapy and surgery. The Dvorak tumour regression grading system[245] and 'Royal College of Pathologists dataset guidelines for colorectal cancer reporting'[246] provide pathological classification systems which have also been used to compare

tumour response to pre-operative chemo-radiotherapy. However, classification of tumour regression grade (TRG) may also be somewhat subjective, with poor inter-observer reproducibility particularly in discrimination between no regression and minimal regression, is non-linear and lacks clear association with outcomes [247]. There is a need for a more robust and reproducible pathological endpoint for comparison of the relative efficacy of different pre-operative radiotherapy schedules and particularly for evaluation of novel radiosensitising drugs in early phase clinical trials.

i) Tumour cell density analysis

Solid epithelial tumours including colorectal adenocarcinomas are comprised of two compartments: the tumour parenchyma (carcinoma cells) and the tumour stroma (which consists of fibroblasts, inflammatory cells, extracellular matrix, lymphatics and blood vessels),on which they are dependent for nutritional support[248]. Tumours differ in their stromal composition, for example pancreatic tumours typically have a dense desmoplastic stroma, which is believed to be influential in restricting perfusion and drug delivery [249, 250]. Studies have suggested that the proportion of tumour cells in colorectal cancer may be important as a prognostic factor. In two retrospective studies of colonic tumours, Mesker et al demonstrated that the carcinoma-stromal ratio of haematoxylin and eosin stained colon cancer sections was an independent prognostic factor for survival in stage I and II colon cancer compared to lymph node status and tumour stage[251, 252], with a high proportion of stroma predicting for worse survival [252]. These findings have subsequently been validated prospectively in the context of stage II and III colon cancers from patients who participated in the VICTOR trial, in which the 5 year overall survival was 69% in tumours with a high stroma percentage(>50%) versus 83.4% in those with a low stroma percentage (<50%)[253]. The methodology for assessment of the proportion of tumour stroma in these studies was based on qualitative assessment of proportion of stroma versus tumour cells at the invasive margin of tumours with good inter-observer agreement for

categorisation between high and low scores rather than an objective quantitative method for measurement of the relative cellular components.

Using a novel histological technique based on quantitative tumour cell density (TCD) analysis to assess the relative proportion of tumour and stroma in a retrospective series of 145 colorectal tumours, West et al demonstrated that tumours with a low proportion of tumour cells (≤47%) were significantly associated with a lower cancer-specific survival than tumours with a high proportion of tumour cells (> 47%)(HR 2.087, P=0.024)[254]. On sub-group analysis the prognostic effect remained significant for colonic tumours but not for rectal tumours. There is no clear explanation for this discrepancy but it cannot be attributed to the effect of pre-operative therapy on outcome, as all patients were treatment-naïve irrespective of tumour location. It may be related to the small numbers in the rectal sub-group.

The technique for quantitative TCD analysis involves digital analysis and is described in detail in chapter 2[254]. The advantages of this technique over previously described methods are that it provides accurate quantitative measurement of different cellular components, with high reproducibility and that digital analysis is flexible, allowing annotation of scored points and data storage. It has been demonstrated that the proportion of tumour cells on TCD correlates closely with the proportion of stroma[254]. In contrast to the method described by Mesker et al. in which the invasive front of the tumour was selected for evaluation of the tumour- stroma proportion, in the series reported by West et al. the luminal surface of the tumour was selected for TCD analysis to allow future analysis regarding whether findings might be extrapolated to biopsy material.

Currently, published data are lacking to suggest that TCD in untreated rectal cancers is associated with prognosis or response to radiation. However, West et al have applied the technique for TCD analysis to several series of rectal cancers and demonstrated that it has value for comparing the relative efficacy of different pre-operative radiotherapy schedules [255]. In a retrospective study, TCD was evaluated in resected rectal cancers from patients having undergone surgery alone (i.e.

controls), patients having received 25 Gy in 5# with early resection, patients having received 50 Gy in 25# with single agent capecitabine and patients having received 45 Gy in 25# with capecitabine and oxaliplatin. Analysis demonstrated a statistically significant lower median TCD in tumours treated with each of the 3 pre-operative radiotherapy schedules in comparison to untreated controls. Furthermore, there were significant differences in the median TCD between the different groups, with the lowest median TCD being demonstrated in the group having received 45 Gy and dual agent radiosensitising chemotherapy, followed by 50 Gy and single agent chemotherapy(both groups proceeded to surgery 6 weeks post radiotherapy) then 25 Gy in 5#. The higher TCD observed in this latter group in comparison to tumours treated with long course-chemo radiotherapy regimes and delayed surgery (typically 8-10 weeks post radiotherapy) is likely to be at least in part a function of the earlier time point for TCD evaluation as there is unpublished data to suggest that TCD initially decreases with increasing time after radiotherapy, although eventually starts to increase with prolonged time to surgery (personal communication Nicholas West), which is likely to be due to tumour cell repopulation. Data from this study published in abstract form has been partly validated in the context of pre-treatment biopsies and post-treatment resection specimens from a separate series of patients treated with 45 Gy and CAPOX chemotherapy in Eindhoven (unpublished data- personal communication Nicholas West). Prospective validation is ongoing in the context of ongoing clinical trials, including the national Phase III randomised controlled trial ARISTOTLE, which compares 45 Gy in 25# with capecitabine and 45 Gy in 25# with irinotecan and capecitabine.

The feasibility of applying the technique for quantitative TCD to pre-treatment rectal biopsies has already been established by our collaborators Dr Nicholas West and Professor Phil Quirke at the University of Leeds (unpublished data). TCD has not previously been evaluated in rectal tumour biopsies after radiotherapy and this research tested the feasibility of evaluating TCD in rectal tumour biopsies after treatment with pelvic radiotherapy and its potential as an early endpoint for evaluating the efficacy of the novel radio-sensitizer, nelfinavir combined with pelvic

radiotherapy in the context of an early phase clinical trial. As a measure of tumour cell kill at an early time point in response to radiotherapy, it is explored whether changes in TCD may have value in discriminating significant differences in individual treatment response.

ii) Tissue markers associated with tumour perfusion and hypoxia

Tissue markers which characterise tumour vascularity or oxygenation are of particular interest, since they may help predict which tumours will be relatively resistant to radiotherapy (poor prognosis) and/or benefit from vascular/ oxygen modifying agents or radiotherapy dose intensification. A number of such markers have previously been evaluated in a range of tumour types, including colorectal cancer.

a)Micro-vessel Density

The density of micro-vessels (MVD), evaluated using immunohistochemical staining for endothelial cell markers has been examined as prognostic marker in a range of tumour types[256-260] and is considered to be a surrogate marker for angiogenesis. Since tumour micro-vessels are not uniformly distributed, the methods which have been developed to measure micro vessel density account for this. For example, the first method, published by Weidner is based on selecting 'hot spots' of high vascularity and averaging the mean number of micro-vessels per mm^2[257]; the Chalkley White method involves use of a graticule with 25 random points superimposed over the 3 areas of highest vascularity, to count the maximum number of points falling on a micro vessel in each area and deriving a mean point count; vascular grading involves subjective categorisation whilst image analysis involves automated recognition of the proportion of tissue infiltrated by immunohistochemically stained micro-vessels[261]. Each of these techniques has its limitations but the Chalkley method is the method currently recommended in consensus guidelines[261, 262], having the advantage over other methods in terms of reproducibility and speed of analysis.

A number of immunohistochemical markers present on vessels have been used to evaluate MVD. CD34 is a pan-endothelial marker, expressed on new and pre-existing vessels, which has high sensitivity but low specificity for tumour vessels, also being expressed on haemopoetic cells; CD31 is also an endothelial marker, which has higher specificity for blood vessels than CD34. CD105a, or endoglin, is a transmembrane glycoprotein marker, which is expressed in proliferating or 'activated' endothelial cells and more specific for tumour vessels than either of the other markers[263, 264] and is considered to be a better marker of neo-angiogenesis. Studies have shown that, specifically in patients with rectal cancer not having received pre-operative therapy, high MVD is an independent predictor for recurrence and survival[265, 266].

Two studies have evaluated MVD in patients as a potential biomarker of response to radiotherapy in rectal cancer[267, 268]. In a retrospective study of 101 patients with rectal cancer, treated with either LCCRT, SCRT or surgery without pre-operative radiotherapy, it was demonstrated that there was a significantly lower mean MVD in resected tumours treated with LCCRT than tumours treated with SCRT or no pre-operative therapy. The authors concluded that long course RT decreased angiogenesis in patients with rectal cancer but further assessment was needed to determine the changes required during a short course of RT. Although the MVD after SCRT was higher than that observed in the group receiving LCCRT, the proportion of moderate/poorly differentiated tumours was significantly higher than either the group receiving LCCRT or no RT and since MVD has previously been associated with tumour grade/differentiation it is not possible to make a direct comparison between MVD in the SCRT group and the other groups. Despite the findings of this study, MVD has not yet been prospectively validated as a biomarker for response to RT in rectal cancer and a separate study showed no association between MVD and response to RT[267]. Only one study has evaluated MVD (using CD34 antibody) in rectal tumours before and after RT[269]. In this study of 34 patients, biopsy samples were taken from the centre of tumours before radiotherapy and after radiotherapy (1 week after SCRT) or 6 weeks after long-course CRT;

there was a trend towards a reduction in MVD in the SCRT group but a statistically significant decrease in the LCCRT group.

b)Carbonic Anhydrase IX

Carbonic Anhydrase IX (CAIX) is a transmembrane zinc metalloproteinase, which plays a role in acid-base, electrolyte, water and oxygen balance and catalyses the reversible conversion of carbon dioxide and water to bicarbonate and hydrogen ions[270]. It is hypoxia inducible and its immunohistochemical expression has been demonstrated to be correlated with levels of hypoxia in human tumours[271]. CAIX is widely expressed in the cell membranes of many tumours, particularly renal cell carcinomas, particularly those linked with the Von-Hippel-Landau (VHL) mutation and loss of the VHL tumour suppressor gene[272]. CAIX expression in normal or benign tumour cells is rare[273]. Double staining of squamous cell cancers of the head and neck for CAIX and MVD has demonstrated that the median distance from the edge of CAIX expression to the nearest vessel is 80 µm, correlating with a pO2 level of 1%; high levels of CAIX expression are found in peri-necrotic areas, with the necrotic edge of CAIX expression equating to a 0.1% pO2 level[274]. However, a study of 101 patients with rectal cancer not receiving any neoadjuvant treatment demonstrated no association between CAIX expression and either MVD or survival. In this study, 73% rectal tumours had positive CAIX expression and an association between CAIX expression and lower Dukes' stage[266] was observed.

In contrast, a separate retrospective study of CAIX expression in 166 resected rectal tumours, from 37 patients treated with LCRT (29 of whom received concurrent capecitabine or 5FU), 75 treated with SCRT and 54 patients having received no pre-operative therapy,[275] found that the intensity of CAIX expression in resected tumour specimens was an independent prognosticator of disease free survival on multivariate analysis (which accounted for treatment received) and an independent prognosticator of disease specific survival in a Cox model, with a hazard ratio of 9.23 (95% CI 2.26- 37.64) for dying of disease with moderate-intense CAIX expression, as compared

with CAIX negative/weakly positive cases. A lower proportion of tumours had positive CAIX expression compared to the first study, 49% pre-treatment biopsies and 44% resected tumours. When the tumours having been treated with LCRT were categorised according to whether chemo was given concurrently, there was a statistically significant difference in staining intensity between the groups, those having received RT alone demonstrating more intense CAIX staining, which the authors speculated may be due to better tumour reoxygenation as a result of using a concomitant radio-sensitizer. However, compared to untreated controls, a higher proportion of tumours receiving either SCRT or LCCRT had a high proportion of negative/weakly expressing tumours. There were only 8 patients in the group receiving LCRT without chemo, who had a dramatically higher proportion of moderate/strong CAIX expressing tumours than the control group(87% vs 30%), which may suggest this small proportion of tumours were not representative. No studies have prospectively validated CAIX expression, as a predictor of response to pelvic radiotherapy in rectal tumours, nor prospectively evaluated CAIX expression in tumours before and after radiotherapy, with or without radiosensitising drugs.

c)HIF-1α

HIF1α, as a regulatory protein involved in the response to hypoxia, has also been demonstrated to be associated with prognosis in a range of tumour types[276-278], including rectal cancer[279, 280]; low HIF-1 alpha expression has also been positively associated with a high MVD[281]. HIF-1α (which has a half-life of less than 5 minutes[282]) is less sensitive a marker of hypoxia than CAIX (which has a half-life of 2-3 days) but provides a more accurate representation of transient changes in oxygenation[283] or acute hypoxia[284]. Only one study has evaluated HIF-1α expression in rectal tumours after radiotherapy as a predictor of disease outcome[281]. In a similarly designed study to their study of CAIX expression in rectal tumours, nuclear HIF-1α expression was evaluated in 168 resected rectal tumours and 79 diagnostic biopsies; 75 of the patients were treated with SCRT, 39 with LCRT and 54 no RT. Compared to tumours receiving no pre-op RT, a significantly higher proportion of tumours in the SCRT and LCRT groups had absent

HIF-1α expression (68% and 62% compared to 46%, p=0.046).Negative HIF-1α expression after LCRT was significantly associated with a better disease-specific survival in univariate but not multivariate analyses; there were a higher proportion of positively expressing tumours in the patients having a poor response to RT (Dvorak 0-1) than better response groups. Seventy percent of HIF-1α pre-treatment biopsies demonstrated positive HIF-1α expression, whilst 60% of post-treatment resection specimens were negative for HIF-1α, suggesting that RT may downregulate HIF-1α expression; the effect of LCRT and SCRT on HIF-1α expression was not considered separately. A separate study evaluated sequential changes in nuclear HIF-1α expression in rectal tumour biopsies 2, 4 and 6 weeks into LCCRT, with the benefit of being able to evaluate the effect of LCCRT on HIF-1α expression; this study showed decreasing expression of HIF-1α on sequential biopsies, but no association between HIF-1α expression and TRG, with the limitation that biopsies may not be representative of the whole tumour[285].

In summary, as for CAIX expression, HIF-1α expression during or after RT has not been validated as a predictive or prognostic marker in a prospective study and at present there is insufficient evidence to utilise these hypoxia markers or MVD in risk stratification of patients with rectal cancer in clinical practice. Their evaluation in future prospective trials of patients receiving pelvic radiotherapy and novel radiosensitisers may provide valuable information on the effects of such treatment on vascularity and hypoxia.

iii) Biomarkers of the EGFR-RAS-PI3-K-Akt signalling pathway

a)*KRAS*

Since it has been demonstrated that activation of the EGFR-RAS-PI3K-Akt signalling pathway is associated with tumour radio resistance, molecular or genetic markers associated with activation are of scientific interest as biomarkers of response to RT in clinical practice. It is also of particular interest to identify and develop biomarkers which allow personalised selection of radiosensitisers, potentially targeting molecular pathways to overcome inherent radio resistance. *KRAS* mutations

are present in approximately 30-40% of all colorectal tumours and the most common mutations occur in codons 12 and 13 (85%)[286-288]. There is some evidence to suggest that mutations in different codons are linked to activation of different signalling pathways[289, 290] and specifically, patients with tumours harbouring G12V mutations have a worse prognosis than G12D mutations[291]. A number of studies have investigated the effect of *KRAS* mutation on response to neoadjuvant LCCRT in rectal cancer but the findings have been conflicting[206, 209, 240, 292-299].

A meta-analysis of 8 trials including 696 patients demonstrated that *KRAS* mutation was present in 33.2% of patients with rectal cancer. *KRAS* mutation was not associated with decreased rates of pCR, tumour down-staging or an increase in cancer-related mortality[301]. A criticism of this overview is that 4 of the studies used study treatments containing cetuximab, response to which is known to be associated with lack of *KRAS* mutation; therefore it is not possible to separate the effect of *KRAS* mutation status on response to RT and response to cetuximab. Nevertheless, in 5 of the 7 trials identified that did not use cetuximab, the presence of a *KRAS* mutation did not predict response to RT or TRG. To date the available evidence suggests that *KRAS* mutation cannot be used to select patients for chemo-radiotherapy (with or without cetuximab) in rectal cancer.

Table 9 Summary of published studies evaluating *KRAS* mutation as a biomarker of response to radiotherapy for rectal cancer

Study	Treatment schedule	Number of patients	Percentage of patients with *KRAS* mutation	Association with response	Association with disease free and overall survival
Gaedecke et al. [292]	Pre-op CRT with 5FU +/- Oxaliplatin	94	48%	*KRAS* mutation not correlated with response; G12V mutations associated with higher response (TRG) than G13D (p=0.12)	No association with DFS/OS
Davies et al.[293]	Pre-op CRT with 5FU	70	36%	*KRAS* mutation not associated with radiation response	No association with OS
Demes et al. [294]	Pre-op CRT with 5FU	25	36%	*KRAS* mutation not associated with response	Not evaluated
Duldulao et al. [295]	Pre-op CRT with 5-FU	148	41%	*KRAS* mutated tumours less likely to have pCR (p=0.06). No pCR in patients with codon 13 mutation.	Not evaluated
Zauber et al.[296]	Pre-op CRT with 5-FU	33	34%	No association with TRG	Not evaluated
Sun et al.[300]	Pre-op CRT with Capecitabine and Cetuximab	63	31.2%	*KRAS* wild type associated with tumour downstaging (P=0.020)	Not evaluated
Garcia-Aguilar et al.[240]	Pre-op CRT with 5FU+/- Oxaliplatin	132	43%	*KRAS* mutation associated with non-pCR (p=0.012)	Not evaluated
Grimminger et al. [297]	Pre-op CRT with 5FU or Cape/Cetuximab +/- Oxaliplatin	130	42%	*KRAS* mutation associated with non pCR (p=0.037)	Not evaluated
Erben et al.[298]	Pre-op CRT with Cape/Irinotecan and Cetuximab	57	31.6	No association between *KRAS* mutation or loss of *PTEN* and response	Not evaluated
Kim et al.[209]	Pre-op CRT with Cape/Irinotecan and Cetuximab	40	13.2%	No association between *KRAS* mutation status and pCR	Not evaluated
Bengala et al.[299]	Pre-op CRT with 5FU	146	20.5%	No association between *KRAS* mutation status and pCR	No association with DFS or OS

b)PIK3CA and PTEN

There are a number of other molecular markers of interest, specifically *PIK3CA* and *PTEN*, which could give insight into the activation status of the PI3K signalling pathway but they have been less studied than *KRAS*. *PIK3CA* (phosphatidylinositol-3,4-bisphosphonate3-kinase, catalytic subunit alpha) encodes for the catalytic p110-alpha subunit of PI3K-alpha[302]. Mutations in the *PIK3CA* gene are reported to occur in up to 15% colorectal tumours[303], although one study in rectal tumours showed a prevalence of 7.9%[304] and a statistically significant association between *PIK3CA* mutation and the risk of local recurrence in non-irradiated patients. Subsequent to this it has been demonstrated in the context of samples from a prospective clinical trial, that the benefit of SCRT in reducing the risk of local recurrence in carriers of the mutation was three times greater than in those tumours lacking the mutation (although this was not statistically significant) [305]. A separate study has shown no association between *PIK3CA* mutation and response to RT but the proportion of patients with a mutation was small (4%)[306]. Two studies have suggested that loss of *PTEN* is not predictive of clinical outcome after neoadjuvant chemo radiotherapy[209, 298]. Further prospective data in larger numbers of patients is required to evaluate whether either of these markers may be valuable in clinical practice to predict response to RT or targeted agents, either separately or in combination.

c)Phospho-Akt and Phospho-PRAS 40

In terms of identifying tumours which may benefit from the Akt inhibitor nelfinavir, the detection of phosphorylated proteins in the PI3-kinase pathway e.g. phospho-Akt and phospho-PRAS40 may be more rational than individual molecular markers of the common EGFR-RAS-PI3K signalling pathways; they may also be more valuable as dynamic biomarkers, to assess the effect of Akt inhibition on the target in tissue.

Akt, the downstream effector of PI3K, has three isoforms, Akt-1, Akt-2 and Akt-3, of which AKt-1 is most important in oncogenic signalling[307]. Both total Akt and phosphorylation of Akt-1 at its

Ser473 residue can be detected immunohistochemically in cells in vitro and in human tissue using commercially available antibodies. Previous research has demonstrated specific expression of phospho-Akt (Ser473) in colonic tumours but absent expression in normal mucosa[308]. In a single study of 99 colonic tumours, it has been demonstrated that 63% of tumours had moderate/strong Akt expression, 30% weak expression and 7% were negative[309]. Phospho-Akt immunohistochemical expression has been evaluated in a range of tumour types but has been found to have variable prognostic value. In colorectal cancers, the majority of studies have suggested phopsho-Akt expression is not prognostic, [310-313] although the largest study, in tissue from 717 colorectal tumours, suggested phospho-Akt expression was associated with early tumours and a good prognosis[314].

Using a validated method, it has been demonstrated in the peripheral leucocytes of patients with HIV receiving nelfinavir at standard doses that phospho-Akt(Ser473) immunohistochemical expression is reliably inhibited, suggesting that it may have value as a dynamic biomarker of therapeutic Akt inhibition[315]. There is limited evidence that phospho-Akt expression in human tissue can predict response to radiation. A study of 38 patients in head and neck cancer showed an association between phospho-Akt expression and risk of local recurrence after RT, as well as an association between phospho-Akt expression and radio-resistance in cells in culture (antibody from New England Biolabs) [224]. Only two clinical studies have evaluated phospho-Akt expression in rectal cancer as a predictor of response to RT. The first demonstrated a statistically significant association between high phospho-Akt expression and response (Cell Signalling, Clone 736E11)[293], but a second study showed no statistically significant association between phospho-Akt expression and response to RT (Cell Signalling antibody used- clone not stipulated)[316].

A possible explanation for the contrasting findings of the two studies is the variation in immunohistochemical technique and tissue preparation and retrieval of antigens, which may

affect tumour antigenicity. There are multiple sources of commercially available anti-Akt antibodies. A comparison of 4 commercially available phospho-Akt (Ser473) antibodies (Cell signalling D9E, 736E11 and 587F11 and DAKO 14-5) for immunohistochemical analysis in cancer cell lines with a PIK3CA mutation, treated with a PIK3 inhibitor demonstrated that only immunohistochemistry assays using the D9E clone and 14-5 clone appeared to have sufficient sensitivity for dynamic monitoring. The 587F11 clone had lower sensitivity and therefore may have resulted in under-reporting of phospho-Akt expression in previous studies, whilst the 736E11 antibody demonstrated poor reduction in staining after PI3K-inhibition, due to cross-reactivity or non-specific staining[317]. Phospho-epitopes are also potentially unstable in tissue[318] and it is recommended that samples should be immediately fixed in 10% neutral buffered formalin[307]. A limitation of most published studies is that they do not describe the tissue preservation methods used; many specimens were analysed retrospectively and with respect to resected rectal tumours, it may take longer than the duration of stability of the phospho-epitope to fix tissue at the centre of the specimen. Further evaluation is required to evaluate the reproducibility of phospho-Akt staining and consider the feasibility of evaluating phospho-Akt as a predictive biomarker in rectal tumour biopsies.

PRAS 40 (Proline Rich Akt Substrate of 40KDa) is a downstream substrate of Akt1 and its activated form, phospho-PRAS40, regulates mTOR. In a bioinformatics pathway profiling analysis of phosphoproteins, designed to identify target biomarkers for predicting response to inhibitors of the PI3K pathway, Anderson et al[319] demonstrated that phospho-PRAS40 is highly regulated by PI3K inhibition and highlighted it as a potential candidate for biomarker development. Subsequent to this, a custom antibody directed against phospho-PRAS^{Thr246} was developed and evaluated in a panel of 96 lung and 67 breast cancer cell lines by reverse-phase protein array analyses. A strong correlation was observed between phospho-Akt(Ser473) and phospho-PRAS^{Thr246} for both cell lines. A potential advantage of using phospho-PRAS40 over phospho-Akt as a biomarker for PI3-K/Akt inhibition is that the stability of the phospho-PRAS40 was

demonstrated to be superior to phospho-Akt, being stable for an hour versus less than thirty minutes in non-fixed tissue; additionally phospho-PRAS40 immunohistochemistry demonstrated a robust signal[319]. A number of studies have shown that $PRAS^{Thr246}$ phosphorylation could predict hyper activation of the PI3K-Akt signalling pathways and sensitivity to its inhibitors in pre-clinical studies[320], [321, 322]. The proof of principle of using phospho-PRAS40 immunohistochemistry as a dynamic biomarker of Akt inhibition has also been demonstrated in human tumour xenografts and patients treated with an Akt inhibitor in an early phase clinical trial, where Akt inhibition resulted in significant downregulation of phospho-PRAS40 expression, in association with tumour growth delay[323]. To our knowledge, there are no published data relating to phospho-PRAS40 immunohistochemical expression in colorectal cancers nor regarding its role in predicting clinical response to radiotherapy.

In this thesis, phospho-Akt and Phospho-PRAS40 immunohistochemical expression are evaluated in pre-treatment and post-treatment rectal biopsies in patients receiving radiation and concurrent nelfinavir, to explore changes in expression and to further evaluate the feasibility of using these as biomarkers of response in this setting.

1C Perfusion CT in Rectal Cancer

C1 Principles of Perfusion CT

Perfusion CT (pCT) is an imaging modality which is based on the measurement of tumour enhancement and CT number on scan sequences acquired before, during and after the administration of intravenous contrast agents in order to plot time attenuation curves. From the latter a variety of semi-quantitative measures can be assessed and quantitative microcirculatory parameters relating to perfusion and permeability can be derived using pharmacokinetic modelling.

Figure 7 Time attenuation curves. The Y axis represents CT number (HU) and the X axis represents time (seconds) over which the scanning sequence occurs after injection of contrast starting at time 0s. The upper curve represents change in attenuation in an arterial region of interest over time, whilst the lower curve represents changes in attenuation in a tissue region of interest. The two curves are deconvoluted to produce an impulse residue function, R(t)

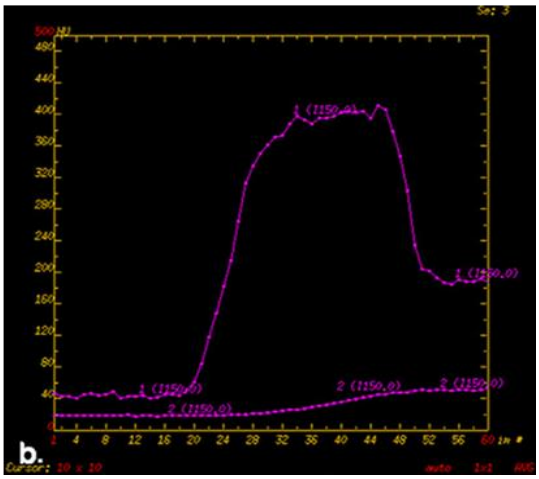

Perfusion CT in its earliest form was first devised by Leon Axel, in 1979[324]; the method he developed involved a rapid sequence of dynamic CT images after the injection of a bolus of contrast material to estimate cerebral tissue perfusion. One of the fundamental factors underlying pCT analysis is that attenuation (or CT number) is linearly proportional to iodinated contrast concentration. Baseline images are subtracted from the dynamic contrast enhanced sequence to provide accurate enhancement values. Time-attenuation curves from tumours are determined by contrast material in both intravascular and extravascular compartments. Immediately after administration, the contrast material remains largely in the intravascular space. This phase is termed the first pass and evaluation of contrast enhancement during this time will define perfusion i.e. blood flow per unit volume or mass of tissue (BF) and blood volume, the fraction of tissue that is blood (BV). Mean Transit Time (MTT) is the mean time taken for intravenous contrast to traverse the capillary network, the unit of which is seconds. It has been demonstrated that MTT is inversely proportional to perfusion pressure[325].

According to the central volume theory: BF = BV/ MTT

Delayed imaging is used to assess the extravascular phase which defines permeability since tumour blood vessels are abnormally “leaky” to circulating molecules including contrast material.

Permeability Surface area product (PS) is the product of the permeability and total surface area of the capillary endothelial network[326]. It reflects the leakage rate of the microvasculature.

The shape and nature of the arterial time attenuation curve can be summarised in terms of a few descriptive terms[327]. However these measures are influenced by the concentration of arterial contrast over time, which itself is related to patient physiology e.g. cardiac output.

Table 10 Summary of semi-quantitative terms used to describe the arterial time attenuation curve

Baseline interval	The time taken for the contrast to reach the region of interest, which may include an inbuilt delay from start of scanning to start of bolus contrast.
Time to peak attenuation (TTP)	The time interval when contrast attenuation rapidly increases due to arrival of the contrast bolus in the region of interest
Peak enhancement (PE)	The maximum attenuation value in the region of interest minus the baseline attenuation value.
Width	The width of the curve is usually evaluated at half the maximum enhancement value and reflects the speed of contrast uptake and disappearance from the region of interest.

C2 Models of pCT analysis

A number of different models for perfusion CT analysis have been proposed. In this research, the deconvolution method of analysis is used for pCT analysis and described in further detail below.

Table 11 Summary of models used for perfusion CT analysis and number of compartments assumed in the model

Model	**Compartments**
Deconvolution	Dual
Maximum Slope Method	Single
Patlak Analysis	Dual
Distributed Model (Johnson Wilson)	Dual

i)Deconvolution analysis

When contrast is injected via a peripheral vein, the arterial contrast concentration over time ($C_a(t)$) and the amount of contrast that remains in the tissue (tissue residual function, Q(*t*) can be measured on dynamic CT imaging as a change in CT number (see figure 7).It has been shown that:

$Q(t)=CBF(C_a(t) \otimes R(t))$

Where $\otimes$ is the convolution operator and R(t) is the impulse residue function[328], and CBF is Cerebral Blood Flow, worked out by deconvolution.

MTT is derived from the area over height formula initially put forward by Axel et al.[329]:

MTT= area underneath R(t) /height of R(t) plateau

CBV (Cerebral Blood Volume) in a capillary network is derived from the ratio of areas:

CBV=area underneath Q(t)/area underneath $C_a(t)$[324]

This latter equation only applies when there is no recirculation of contrast, which applies in the cerebrum when the blood brain barrier is intact but not in other tissues, where the capillaries are permeable. Following injection of contrast agent in such tissues there is an exchange of contrast molecules between the intravascular and extravascular space. Additional methods are required to correct for the effect of recirculation, which involve calculation of the extraction fraction of the contrast agent diffusing from the extravascular space to the intravascular space[330, 331]. Deconvolution of the arterial time attenuation curve and tissue time attenuation curve is sensitive to the effects of noise and in regions of low blood flow and blood volume, it may not be possible to determine perfusion parameters[331]. The deconvolution model for estimation of tumour blood flow has been validated in a rabbit cerebrum model using radioactive microspheres, where it was demonstrated that there was a significant linear correlation between

pCT and microsphere-derived BF values and that regional perfusion could be depicted using perfusion parameter maps[331, 332]. It has also been validated in patients with Xenon CT; correlation between BF derived from pCT and Xenon-CT was good but slightly inferior to that demonstrated in an animal model[333]. It has also been demonstrated that there is good correlation between BF measurements using pCT and those from $H_2(15)O$-PET, if vascular pixels are eliminated[334].

C3 Methods of Analysis

Commercially available software is now available to process perfusion CT data according to one or more of the models. The advent of multi-detector CT and helical scanning has enabled perfusion CT to be readily performed in clinical settings, with only fairly minor adaptations to standard CT scanning protocols. The anatomical coverage of pCT in the cranial-caudal axis has been limited until very recently, since CT data needed to be acquired without table movement; single row detectors are able to cover 5-10 mm, 2-32 row detectors are able to cover a maximum of 20 mm and 64 row detectors are able to cover 40 mm. Therefore the level to be covered is usually decided on a scout study.

Analysis of perfusion CT data using commercially available software involves selecting an appropriate protocol, windowing the CT data to focus on the tissue density of interest then defining an arterial region of interest (to derive an arterial time attenuation curve) and tumour region of interest to derive a tumour attenuation time curve. The software then usually automatically computes parameter values for the defined region of interest using one or more kinetic models. Functional perfusion parameter maps are also generated, in which a parameter value is assigned to each voxel in the dynamic CT data and represented by a colour scale (or gray scale) representing a range of parameter values of interest, which can be adjusted.

C4 Reproducibility

It has been suggested that pCT parameter measurements in rectal cancer are sufficiently robust to permit its use as a tool to monitor response to anti-cancer therapy. Goh et al described a number of intrinsic and extrinsic factors which may influence the reproducibility of pCT measurements[335]. Intrinsic factors include day to day changes in physiology, intra-tumoural regional heterogeneity and those factors specific to the technique. Extrinsic factors include differences in measurement due to different observers or scan acquisition protocols. There are data to suggest that intra-observer variation in colorectal tumour perfusion parameter estimation is lower than inter-observer variation but the limits of agreement can be wide and may be significant when using pCT for response assessment[336]. Goh et al have demonstrated that perfusion measurements from rectal tumours are less variable than those from skeletal muscle and on repeat pCT scans 48 hours apart that the within subject coefficient of variation for tumour mean BF, BV , MTT and PS are 23%, 14%, 35% and 17%, respectively. This means that when evaluating response to treatment in a group of patients, mean changes in parameter values below these levels could be due to measurement variation rather than treatment effect. In a series of colorectal tumours, Goh et al demonstrated that increasing the tumour coverage of colorectal tumours (from a single 0.5 cm slice to 4 x 0.5 cm slices) did not improve the reproducibility of measurement and have thus advocated pCT analysis of rectal cancers on a single central slice[337]. Conflicting results have been demonstrated elsewhere; improving pCT coverage (from 10 mm to 40 mm in the z axis) in a series of lung cancer improved the reproducibility of pCT measurement[338] and particularly high levels of reproducibility have been demonstrated when the whole tumour was covered[339].

C5 Technical Factors influencing pCT Analysis

There is published research evaluating the technical factors which influence pCT parameter values in rectal cancer, principally using commonly available commercial software packages. There are

multiple variables which can influence pCT parameters including acquisition time of pCT[340], the temporal interval between dynamic CT sequences (intervals >3 s potentially resulting in overestimates in BF and underestimates of MTT) [341], commercial software upgrades and the commercial software package used[342].

A number of factors relating to the post-processing of pCT data can contribute to the variability of the perfusion parameters and corresponding parametric colour maps derived .The definition of a region of interest is a potential source of inter-observer and intra-observer variability; Goh et al. demonstrated that there was poor inter- and intra-observer agreement in pCT parameters when standard circular tumour regions of interest (ROIs) (40 and 120 mm^2 respectively) were used to evaluate perfusion in rectal cancer. BF, BV and PS values were significantly higher when tumours ROIs were placed at the tumour edge than the tumour centre[343]. Improved reliability of parameter estimation was demonstrated when the tumour ROI was defined according to the outline of the rectal tumour.

Selection of the post-contrast enhancement image is a source of inter-operator variability using commercial software and can contribute significantly to variability in perfusion parameter values and the appearance of perfusion parameter maps, whereas selection of the pre-enhancement image is more reproducible[344].

Intra-sequence tumour motion is a technical challenge for pCT analysis, which has been studied very little in the context of rectal cancer. Since the assumption underlying pCT analysis is that it measures changes in enhancement in a defined tumour ROI in relation to an arterial ROI, it is important that the position of the ROIs is relatively stable throughout the temporal dynamic sequence. One study of pCT in 43 colorectal tumours demonstrated that in only 39% of all pCT studies was data capture accurate and free of motion artefact[345]; the authors performed manual correction of the tumour ROI position and used customised in-house software to extrapolate accurate data for the remaining patients, since few commercially available software

packages have a motion correction function. Of note, the majority of the tumours in this study were colonic rather than rectal and therefore more subject to respiratory and peristaltic motion; 80% of the rectal tumour studies were sufficiently free of motion for valid evaluation. Strategies which have been utilised to limit the impact of tumour motion include use of an anti-spasmodic, buscopan, and delineation of the tumour ROI such that it is within the confines of the tumour throughout the dynamic sequence.

In view of the multiple potential variables in pCT analysis and acquisition, consensus guidelines for the technique have been developed by a panel of experts[346] but have not been uniformly adopted.

C6 Perfusion CT in response assessment to radiotherapy in rectal cancer

A number of studies have evaluated changes in tumour perfusion parameters in rectal cancer in relation to pelvic radiotherapy (or chemo-radiotherapy) (see table 12). Three of these studies employed concomitant chemotherapy with a long course of radiotherapy [347-349]; only one studied the effects of radiation alone, without the confounding effect of chemotherapy[350].

The general aim of these studies was to evaluate the effect of treatment on tumour perfusion and in 3 of the 4 studies, to evaluate whether perfusion parameters might predict response to treatment. In the 3 studies which were performed in patients receiving a long-course of chemo-radiotherapy, significant reductions in mean BF were demonstrated between perfusion CT studies at baseline and 1-2 weeks after therapy, associated with significant decreases in PS and increases in MTT (where these parameters were studied). These findings have been interpreted as demonstrating that chemo-radiotherapy results in a reduction in angiogenesis and vascular shunting. However, conflicting results were presented regarding the ability of the baseline pCT parameters to predict response to CRT, with 2 studies suggesting that a high BF predicts a good

response to chemo-radiotherapy (CRT) [347, 351] and one suggesting that a low BF predicts a good response to CRT[349].

Table 12 Overview of Studies evaluating changes in pCT parameters during/after radiotherapy in rectal cancer

Study	Patient number	Modality	Treatment	Timing of scans	Baseline value	Method	Coverage and slice thickness	Change between baseline and post-treatment value
Bellomi et al 2007[347]	25	pCT	Pre-op long course chemo-RT (Capecitabine)	Before chemoRT (1-11 days) and within 1 week after therapy(n=19)	High BF, BV →response	GE Perfusion 3.0 software	2cm coverage 1 cm slice thickness	BF, BV↓ (p=0.002) PS↓ (p=0.009)
Sahani et al 2005[351]	15	pCT	Pre-op long-course chemo-RT (5-FU)	Before chemo-RT and within 1-2 weeks after therapy	High BF, low MTT →response	GE Perfusion 2.0 software	2cm coverage 0.5cm slice thickness	BF↓MTT↑ (p<0.05)
Curvo-Semedo et al 2012[349]	20	pCT	Long course chemo-RT (Capecitabine or tegafur-uracil)	Before chemo-RT and within 2 weeks of surgery	Low BF, high MTT →response	GE Perfusion 3.0 software	4cm coverage 0.5cm slice thickness	BF, BV ↓ (p=0.003) PS ↓ (p=0.008) MTT↑(p=0.006)
Janssen et al 2010[350]	23	pCT	Short course radiotherapy	Before and on the day of the last fraction of RT	Not evaluated	In-house software Matlab	2.88cm coverage 0.24cm slice thickness	Median K^{trans}↑ (p<0.001) Shift to higher k^{trans} values from lower k^{trans} values on voxel analysis

There are a number of possible explanations for the lack of consensus, the first being that each study used a different definition of 'response' and 'non-response', being defined in the former two studies on the basis of pathological tumour +/- nodal down-staging in comparison to pre-treatment ultrasound and/or MRI staging[347, 351] and based on Dworak pathological TRG in the third study (where TRG 0-2= non-response and TRG 3-4=response) [349]. The criticism of the former two methods is that imaging can under or over stage the T and N stage, so response assessment by this method may not be accurate; although potentially more objective than the

other methods, TRG assessment can be subject to inter-observer variability (as previously discussed) and in the study by Curvedo-Semedo, the assessment appears to have been performed by a single pathologist. A further explanation relates to the differing methods used for pCT acquisition and analysis. There were differences in the temporal duration of scanning, volume of contrast, CT tube voltage, range of the studies and CT slice thickness. A specific criticism of the studies is that a limited volume of the tumour was evaluated (2 cm in the z axis for 2 studies and 4 cm for the other) but their methods did not indicate that any attempts were made to scan the same region of the tumour when evaluating changes in parameter values; a mean of parameter values from the different slices was used to generate an overall parameter value for each tumour.

The study by Janssen et al is the only one to have evaluated the effect of RT alone on tumour perfusion in rectal cancer using pCT; it studied the effect of SCRT at an earlier time-point (last day of RT) [350]. In distinction from the other studies, it used a pCT acquisition protocol on a PET-scanner, allowing PET-pCT fusion and defined a tumour ROI according to segmentation of high PET SUV values[350], which is a novel method. This study applied a pharmacokinetic model which is more typically used in Dce-MRI analysis (and will be discussed in the next section) using in-house software and demonstrated significant increases in tumour perfusion (median K^{trans}) using pCT after 4 fractions of hypo-fractionated therapy.

C7 Perfusion CT in response assessment to systemic therapy in colorectal Cancer

Although pCT has been used in phase 1 trials to evaluate the vascular effect of anti-angiogenic drugs in a range of tumour types (as a pharmaco-dynamic marker) only one published study has previously utilised pCT to measure the effect of a systemic agent on vascular flow prior to pelvic chemo-radiotherapy for primary rectal cancer[111]. One other study [352] has used pCT to evaluate the acute vascular effects of a novel drug in primary colorectal cancer, although in this

study only 3 of 6 evaluable had pelvic disease, which was progressive or recurrent in all and systemic therapy was not being given as a prelude to or concurrent with radiotherapy.

Table 13 Overview of Studies evaluating changes in pCT parameters during systemic therapy in primary colorectal cancer

Study	Patient number	Treatment	Timing of scans	Method	Coverage and slice thickness	Change between baseline and post-treatment value
Falk et al.[352]	6	BW12C	Pre and post infusion BW12C	Maximum Slope	1 cm coverage 1 cm slice thickness	30% decrease BF (ns)
Willet et al.[111]	6	Neoadjuvant bevacizumab prior to chemo-RT	Before and 12 days after bevacizumab	GE Perfusion 3.0	2 cm coverage 0.5 cm slice thickness	40-44% decrease BF ($p<0.05$) 16-39% decrease BV ($p<0.05$)

Willet et al [111] demonstrated statistically significant reductions in blood flow and blood volume after a single treatment with bevacizumab in 5 primary rectal cancers, which was associated with reductions in tumour interstitial pressure and micro vessel density (on sequential tumour biopsy). A criticism of this study is that the authors provide limited details of the methodology used for pCT analysis and specifically no mention is made of any efforts to evaluate the same region of the tumour on each of the sequential pCT scans, which is also an issue in a number of the studies having used pCT to evaluate the effects of chemo-radiation [347, 349, 351]. Nor is the magnitude of change in perfusion parameters considered in the context of the reproducibility of the test (i.e. accounting for measurement error and normal variation in perfusion).

C8 Uncertainties regarding Perfusion CT for response assessment in rectal cancer

A number of technical factors have been demonstrated to influence the values derived from perfusion parameter estimation and in this thesis it is argued that an understanding of the technical factors which influence pCT parameter measurement is critical when using pCT as a tool for evaluating response to anti-cancer therapy and that sources of potential measurement

variation should be minimised and described. From the literature, it is unclear whether evaluating mean perfusion parameter values on a limited number of CT slices (in 2-D) is the optimum method for evaluating response to anti-cancer therapy in rectal cancer. In this thesis, intra-tumoural variation in perfusion parameters in rectal cancer is evaluated and methods of pCT analysis which account for such variation are developed.

1D Dynamic Contrast enhanced MRI in Rectal Cancer

D1 Principles of Dynamic contrast-enhanced MRI

Similar to pCT, Dce-MRI is based on differences in contrast kinetics between tumour and normal tissue but there are some important differences. Dce-MRI is based on the evaluation of changes in MRI signal in tissues over time after the injection of intravenous gadolinium contrast. Since gadolinium is a low molecular weight agent, its molecules are freely diffusible between the intravascular and extra-vascular extracellular space but they are unable to penetrate the intracellular compartment; dynamic MRI imaging of a volume of tissue allows evaluation of changes in the distribution of contrast over time. Dce-MRI is typically performed using gradient echo T1 MRI sequences, which requires the acquisition and analysis of baseline T1 values in the tissue of interest (T_{10}) since, unlike on pCT, there is a non-linear association between contrast concentration and signal enhancement. T_{10} can be estimated by using different flip angles. On T1 weighted sequences, contrast results in signal enhancement but a shortening of the T1 relaxation time (R_1), according to the formula:

$$R_1 = 1/T_1 = 1/T_{1,0} + r_1 C_T = R_{1,0} + C_T$$

where $T_{1,0}$ and $R_{1,0}$ are the relaxation time and relaxation rate of the tissue in the absence of contrast agent respectively , C_T is the mean tissue contrast agent concentration and r_1 is the relaxivity constant[353].

Changes in signal enhancement over time are typically evaluated over a period of time in excess of 5 minutes but at a lower temporal resolution than pCT. Since the technique does not involve ionising radiation, it is possible to image larger volumes of tissue than pCT, although a balance needs to be struck between temporal resolution, spatial resolution and volume of study. Qualitative description of time-signal intensity curves may have some value in distinguishing between benign and malignant lesions and three shapes have been defined: Type I-continuously rising, Type II- plateauing and Type III- delayed washout. In breast cancer, it has been demonstrated that a type III curve is a predictive indicator of malignancy[354]. As for pCT, the shape of the curve can be analysed semi-quantitatively by a number of descriptors: time to enhancement, maximum enhancement, initial slope of enhancement, enhancement ratio and area under the curve[355]. However, these parameters can be influenced by sequence interval, time of bolus contrast administration and do not have a direct relationship with the underlying tissue physiology. These semi-quantitative measures are not considered sufficiently robust for use in clinical trials[356].

D2 Pharmacokinetic models for analysis

Dce-MRI data can be quantitatively analysed by pharmacokinetic modelling. Modified versions of Toft's two compartmental model[357], which has its roots in Kety's dynamic model, are most commonly used. In this model K^{rans} describes the rate at which contrast passes between the intra-vascular and extravascular compartments, K_{ep} describes the rate at which contrast is extracted from the extra-vascular extracellular space to the plasma and V_e ,the volume of the extravascular extracellular space (see figure 8); V^p is the plasma volume.

Figure 8 Illustration of Toft's two compartmental model and related pharmacokinetic parameters.

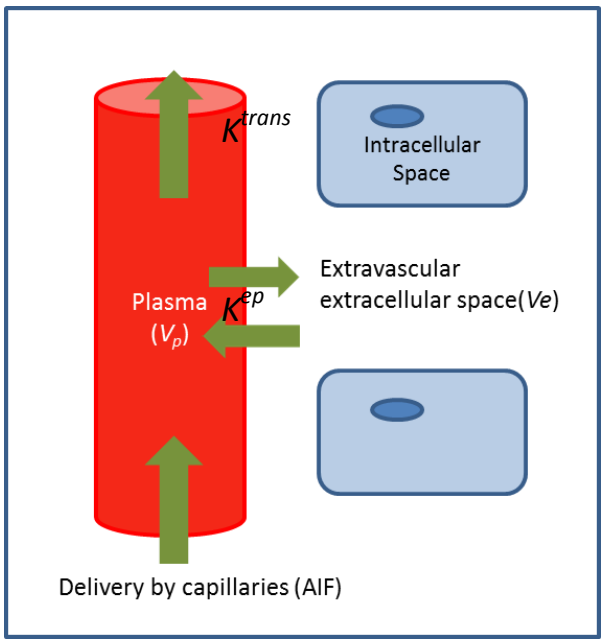

K^{rans} is dependent upon both blood flow and permeability. In situations where permeability is high compared to flow, as in many tumours, blood flow will determine the distribution of contrast and K^{trans} approximates to tissue perfusion per unit volume of tissue. In situations where diffusion of contrast into the interstitium is limited by permeability e.g. in fibrotic lesions or late after radiotherapy, K^{trans} approximates to the permeability surface area product[358]. The model is fitted to the signal time-intensity curves on a voxel by voxel basis. The derived contrast agent concentration is a convolution between the AIF and the tissue response, according to the formula:

$$Ct(t) = K^{trans} e^{-Kept} * Cp(t)$$

Where Ct(t)= the observed contrast agent concentration in tissue

Cp(t)= the arterial input function (AIF)

* = the convolution operator

K^{trans} can be used to derive other pharmacokinetic parameters according to the following equation:

$$K^{trans} = K_{ep} V_e$$

D3 Methods of analysis and Technical Factors influencing Dce-MRI analysis

A range of methods are available for Dce-MRI analysis. Although there are commercially available software packages for analysis, these are not widely available and many studies have used non-proprietary software; no standardised method has been adopted, which makes comparison between different centres difficult. Recently, guidance has been developed by a panel of UK based experts[359] and the Qualitative Imaging Biomarkers Alliance (http://www.rsna.org/QIBA_.aspx), in an attempt to standardise methods for reporting Dce-MRI in clinical trials.

Compared to pCT, Dce-MRI analysis is more complex and several steps are required in processing of data. Dce-MRI analysis usually involves delineation of a volume of interest, with pharmacokinetic parameter values being modelled for each voxel within that volume; typically mean or median parameter values of all of the voxels for which it is possible to fit a model to are used to summarise the data for a defined volume of interest. Other methods which have been shown to be of value in addition to summary statistics are the proportion of non-enhancing voxels[360] or histograms of the distribution of pharmacokinetic parameter values within the volume of interest[361-364], which are able to provide a measure of tumour heterogeneity. Specific technical factors which can influence the results of analysis are presence of intra-sequence motion and method of deriving an arterial input function[365], although studies utilising Dce-MRI in rectal cancer have seldom described how these issues have been managed in processing of the data.

D4 Reproducibility

The within-patient coefficient of variation for K^{trans} measurement using Dce-MRI is reported to be in the order of 20%[366] and thus changes in this parameter exceeding 40% to be clinically significant i.e. representative of a true change rather than measurement error. One published

study has specifically evaluated the reproducibility of K^{trans} measurements in pelvic tumours, which included colorectal cancers[367]. This demonstrated that the size of change in Dce-MRI parameters needed for significance in a group of 16 tumours was -14 to +16% for K^{trans}, 15 % for K_{ep} and 6% for V_e, whilst the magnitude of change required for significance in a single tumour would be -45 to +83% for K^{trans}, 60% for K_{ep} and 24% for V_e respectively[367].

D5 Response assessment to radiotherapy in rectal cancer

A number of studies have evaluated changes in tumour Dce-MRI parameters in rectal cancer in relation to pelvic radiotherapy or chemo-radiotherapy (see table 14). As with the studies using pCT, the aim was either to evaluate the effect of treatment on perfusion parameters or to explore the potential of perfusion parameters to predict response to treatment. Although the methodology and timing of scans used differ between the studies, those studies which evaluated changes in perfusion during chemo-RT suggested increases in perfusion in the first two weeks of treatment [368, 369] and those which evaluated changes in perfusion some weeks after chemo-RT showed significant decreases in perfusion parameters including K^{trans}[369-371].

Those studies which have explored the predictive value of post-treatment changes on Dce-MRI to predict response have in general found greater reductions in K^{trans} in responding tumours than non-responding tumours, although the definitions of response have varied between the studies [369, 371, 372, 376, 378].

Table 14 Summary of studies utilising Dce-MRI to evaluate changes in perfusion during pelvic chemo-radiotherapy for rectal cancer. Abbreviations: *Used a high molecular weight blood pool contrast agent; MPI= mean perfusion index; *KPS* =endothelial transfer coefficient; K_{21}=exchange rate constant

Study	Patient number	Timing of scans	Association between baseline value and response	Association between post-treatment value and response	Change between baseline and post treatment value
George et al 2001[372]	16	10-12 weeks after chemo and 3-6 weeks after chemo-RT	High K^{trans} associated with response		Significant decrease in K^{trans} in responders (at end of chemo-RT)
De Vries et al 2000[368]	11	Before Chemo-RT then weekly during therapy	High MPI associated with N downstaging		Significant increase in MPI in the 1st and 2nd weeks of chemo-RT
De Vries et al 2003[373]	34	Before Chemo-RT	Low MPI associated with response		
Lim et al 2011[83, 369]	39	Before chemo-RT End of week 2 Before surgery	High K^{trans} associated with response	Mean K^{trans} not associated with response	Significant increase in K^{trans} at end of week 2, decrease K^{trans} in post-therapy, mean decrease K^{trans} down staged group after therapy
De Lussanet et al 2005[374]	17	After long course CRT Before SCRT Before Surgery		K*PS* 77% lower in the group treated with RT vs no RT	
Oberholzer et al, 2013[370]	95	Baseline and after CRT	High 75th percentile *K21* associated with response		Significant reduction in median *K21* and 75th percentile *K21*
Kim et al. 2014[375]	50	Baseline and after CRT			Significant decrease in mean K^{trans} in group with T downstaging and in mean K^{trans} in those with pCR and non-pCR
Intven et al 2014[376]	51	1-2 weeks before CRT and 2 weeks before surgery	Median K^{trans} significantly higher in group with TRG 1 or 2 vs TRG 3-5	Median K^{trans} significantly higher in group with pCR vs non pCR and TRG 1 or 2 vs TRG 3-5	Relative change in mean K^{trans} significantly greater in patients with pCR or TRG 1-2 compared to non-pCR or TRG 3-5 respectively
De Vries et al 2014[377]	83	Baseline (before CRT)	MPI significantly higher in those with ypT0-2 than ypT3 tumours		
Martens et al 2014*[378]	30	Baseline After CRT	Late slope significantly different in those with TRG 1-2 vs TRG 3-5	No significant difference in AUC 60, AUC90, AUC120, between TRG 1-2 vs TRG 3-5	Percentage change in parameters higher for responders (TRG 1-2) than non-responders (TRG 3-5) but not statistically significant

Regarding the ability of baseline Dce-MRI parameters to predict response, initial studies were conflicting, with 2 studies suggesting that high pre-treatment tumour perfusion values (as defined by K^{trans} or MPI) were associated with response to treatment[372, 379] and a third suggesting an association between a low MPI and response[380]. Subsequent studies have added to the body of evidence suggesting that tumours with higher perfusion values are more likely to respond to chemo-radiation[370, 377]. However, since different studies have evaluated various parameters, it is not possible to derive a consensus regarding the thresholds of Dce-MRI parameter values which are likely to predict response to treatment and none of the findings from these Dce-MRI studies have been independently validated as yet.

D6 Response assessment to systemic treatments in colorectal cancer

Dce-MRI has been widely used in early phase studies in a range of tumour types, particularly metastatic tumours, to investigate the vascular effects of novel drugs, such as anti-angiogenics, with or without chemotherapy[381-385]. In general, studies have demonstrated that Dce-MRI is valuable in supporting the proposed mechanism of action for such drugs and in some studies, a relationship has been demonstrated between the dose of drugs given and change in Dce-MRI parameters, such that it also has a potential role in defining the biologically optimal dose for later phase studies[125, 358]. Dce-MRI parameters have also been shown to correlate with the clinical course in a number of studies[358]. Only one published study has utilised Dce-MRI to evaluate changes in tumour perfusion as a consequence of neoadjuvant systemic therapy in primary rectal cancer. In a prospective study of patients with rectal cancer, Dce-MRI was performed to evaluate whether it could predict pCR to pre-operative chemotherapy with FOLFOX and bevacizumab and thus have the potential to determine which patients can be spared pre-operative radiation. The results of this study are summarised in table 15. To our knowledge, Dce-MRI has not previously

been used to evaluate the vascular effects of a novel drug which may improve the efficacy of radiotherapy in rectal cancer.

Table 15 Overview of studies evaluating changes in DCE-MRI parameters during systemic therapy in primary colorectal cancer

Study	Patient number	Treatment	Timing of scans	Association between baseline value and response	Association between post-treatment value and response	Change between baseline and post-treatment value
Gollub et al 2012[386]	24	FOLFOX and bevacizumab (4 cycles) then 2 cycles FOLFOX	Baseline and within 3 weeks of completing therapy (range 0-29 days)	K^{trans}, V_e, K_{ep} not significantly associated with response	Low K^{trans} significantly associated with response	Trend to greater reduction in K^{trans} being associated with response

D7 Comparison of DCE-MRI and pCT

The main advantages of Dce-MRI over pCT are that it does not involve ionising radiation, has a better signal to noise ratio, and better spatial resolution, whilst the main advantages of pCT are that the technology is more accessible and the analysis is less complex. However, only one study has directly compared pCT with Dce-MRI in rectal cancer[387]. In a prospective study of 19 patients with locally advanced rectal cancer, pCT and Dce-MRI were performed before neo-adjuvant treatment and pharmacokinetic parameters were derived for the tumour in each. Tumour K^{trans} values between modalities correlated significantly for the voxel by voxel derived median, 80% quantile and averaged uptake but no significant correlations were found for V_e and V_p between pCT and Dce-MRI. These findings suggest that pCT may be reasonably used as an alternative to Dce-MRI for the evaluation of K^{trans} as a pharmacokinetic endpoint of tumour perfusion. However, correlation between the two modalities does not imply that the two modalities are interchangeable. A study in cervical cancer involving dual modality perfusion imaging with Dce-MRI and pCT performed a voxel-wise comparison of pharmacokinetic

parameters; although statistically significant correlations between the two modalities were demonstrated for all parameters, the parameter estimates were significantly different[388]. There is no current consensus regarding whether pCT or Dce-MRI represents the optimal test for the evaluation of changes in tumour perfusion in response to radiotherapy +/- vascular modifying drugs, particularly since no published studies have evaluated the use of both pCT and Dce-MRI at multiple time-points. Since there are no published studies comparing tumour K^{trans} values derived by pharmacokinetic modelling of Dce-MRI data with blood Flow or permeability surface area product in rectal cancer, it is not known whether the two modalities provide equivalent or complementary information in the response assessment of anti-cancer therapy.

In this project, the feasibility of performing dual modality perfusion imaging with Dce-MRI as well as pCT at multiple time points in patients with rectal cancer to evaluate the anti-vascular effects of the novel drug, nelfinavir, before and concurrent with radiotherapy was evaluated. It was assessed whether the evaluation of changes in tumour perfusion using Dce-MRI provides comparable information to the evaluation of changes in tumour perfusion using pCT.

1E Perfusion Imaging of Colorectal Liver Metastases.

E1 Perfusion imaging in response assessment to chemotherapy

Perfusion CT and Dce-MRI have both been used in the research setting to evaluate colorectal liver metastases, specifically to assess changes in tumour perfusion and explore whether parameters describing tumour perfusion may be able to predict response to treatment ahead of standard diagnostic imaging using RECIST criteria. There is a body of published data from studies utilising Dce-MRI to assess the effect of anti-angiogenic drugs in early phase clinical trials [384, 389-391].

Table 16 Studies evaluating Dce-MRI or pCT parameters in context of chemotherapy in colorectal liver metastases.

Study	Patient number	Modality	Treatment (number of patients)	Timing of scans	Association between baseline value and response	Association between post-treatment value and response	Association between change between baseline and post treatment values and response
Kim et al 2012[392]	17	pCT	XELOX(9) FOLFOX(6) FOLFIRI(2)	Baseline(0-6 days before chemo) Before cycle 2 chemotherapy(0-8 days, mean 2.1 days)			Reduction in BF and flow extraction product higher in responders vs non-responders
Anzidei et al 2011[393]	18	pCT	Chemotherapy and anti-angiogenic treatment for 6 months	Before chemotherapy 6 months after chemotherapy		Capillary permeability higher in responders than non-responders ; no difference in BF, BV	
Pauls et al 2009[394]	6	pCT	5FU+ FA(4) irinotecan +5FU(2)	Before chemotherapy and 3 monthly	Correlation between peripheral contrast enhancement and CEA	Correlation between peripheral contrast enhancement and CEA	
De Bruyne et al 2012[395]	19	Dce-MRI	FOLFOX/FOLFIRI 5 cycles and bevacizumab 4 cycles	Before chemotherapy After cycle 1 and after completion of chemotherapy; 4 days before surgery			Area Under the Curve (AUC) and initial AUC decreased after cycle 1 and again post-therapy. No significant change in mean k^{trans}
O'Connor et al 2011[396]	10	Dce-MRI	FOLFOX and bevacizumab 5 cycles	2 scans pre-therapy	86% variance in post-tumour shrinkage explained by median V_e tumour enhancing fraction		
Hirashima et al, 2012[397]	58	Dce-MRI	FOLFIRI and bevacizumab	Before chemotherapy Day 7 after first chemotherapy 8 weekly		Decrease in K^{trans} and K^{ep} after 7 days correlated with response	Reduction in mean K^{trans} and mean V_e 7 days after chemo
Vriens et al 2010[398]	23	Dce-MRI	irinotecan(7) capecitabine(5) CAPIRI(5) CAPOX(3) FOLFOX(3) 5FU/FA(1)	Before chemotherapy After 3 cycles chemotherapy			Significant increase in mean K^{trans} observed
Van Laarhoven et al 2007[399]	37	Dce-MRI	5FU/LV D1-5(27) capecitabine(5) CAPIRI(3) FOLFOX(2)	Before chemotherapy After 1, 2 or 3 cycles	K^{trans}, K^{ep} not correlated with response		No significant change mean K^{trans}, K^{ep}, V^e overall

Although decreases in K^{trans} on Dce-MRI have been demonstrated after 2 cycles of chemotherapy in breast cancer [364, 400], studies in other tumour types, including colorectal cancer, have not

replicated these findings. Overall, few studies have evaluated the perfusion of colorectal liver metastases in patients receiving standard cytotoxic chemotherapy, using either pCT or Dce-MRI (see table 17)[392-395, 397-399, 401]. A limitation of a number of these studies is that they involved the administration of anti-angiogenic drugs as well as chemotherapy; therefore it is not possible to separate the effect of chemotherapy from the effect of the anti-angiogenic drugs. Of the studies that involved systemic chemotherapy alone, only one study evaluated changes in tumour perfusion parameters in colorectal liver metastases during treatment using pCT[392] with two studies using Dce-MRI for this purpose[398, 399]. From these data, it is not possible to draw any definitive conclusions about the effects of cytotoxic chemotherapy on the perfusion of colorectal liver metastases, principally because each of these studies included patients receiving one of at least three different chemotherapy regimens but additionally because scans were performed at different time points across the studies. Of the Dce-MRI studies, both of which included scans at baseline and after 3 cycles of chemotherapy, results were conflicting with one demonstrating statistically significant increases in tumour K^{trans}[398] and the second demonstrating no statistically significant change in K^{trans} or any other parameter[399].

The study which used pCT to evaluate tumour perfusion parameters in patients receiving one of three standard first-line chemotherapy schedules for colorectal liver metastases demonstrated no statistically significant difference in perfusion parameters at baseline between responders and non-responders (based on RECIST criteria, however it did show that reduction rate in mean blood flow and flow extraction product after 1 cycle of chemotherapy was significantly greater for patients in the responder group (28.3% and 18.7%) compared to the non-responder group (5.2% and -13.0%)[p=0.036 and p=0.027 respectively] [392]. A limitation of this study was that it did not report the magnitude of change in perfusion parameters in individual patients or of the whole group of patients and did not consider the changes observed in the context of reproducibility statistics or technical factors which might influence the validity of the data. No published study to date has evaluated changes in perfusion parameters during first line chemotherapy at different

time points, where all patients receive the same regime. It is therefore uncertain what the effect of chemotherapy is on the perfusion of colorectal liver metastases or how this varies as a function of the type and number of cycles of chemotherapy being given. The effect of chemotherapy on the tumour perfusion in colorectal liver metastases is highly relevant to the timing of the delivery of SIRT, since significant changes in tumour vascularity as a result of chemotherapy might be expected to impact on the distribution of SIR-spheres and potentially the effectiveness of treatment. In this thesis, we evaluate the feasibility of evaluating changes in tumour perfusion in colorectal liver metastases at multiple time-points during oxaliplatin and modified de Gramont chemotherapy and test the hypothesis that multiple cycles of chemotherapy can result in changes in tumour perfusion which are unfavourable for subsequent SIRT.

E2 Perfusion imaging to guide delivery and response assessment for SIRT

Irrespective of the impact of chemotherapy on tumour perfusion, the vascularity of colorectal liver metastases at the time of SIRT might be expected to have a bearing on the distribution of Yttrium-90 microspheres and outcome of SIRT because it is an arterially directed treatment, which is dependent on the preferential deposition of microspheres in the abnormal tumour microvasculature and is itself influenced by blood flow dynamics[402]. Sato et al[403] retrospectively evaluated whether the vascularity of liver metastases (hypo- or hyper-vascularity), as defined on triple phase CT or hepatic angiography, was predictive of survival after SIRT (see table 17) but no association using either modality was demonstrated. Criticisms of this study are that it included patients with multiple tumour types (including colorectal cancer), used survival as an endpoint (which may have been influenced by other confounding factors such as the presence of extra-hepatic metastases) and there was substantial discordance between the definitions of a hypo-vascular or hyper-vascular metastasis between the two imaging modalities.

Table 17 Studies evaluating tumour vascularity in patients receiving SIRT

Study	Sample size	Imaging modality	Study design	Timing of scans	Outcome	Association between baseline value and outcome
Sato[403]	138	Triple phase CT and hepatic angiography	Retrospective	Pre-treatment	Median survival 1 and 2 year survival	No association between hypo/hypervascularity defined by either modality and outcome
Dhabuwala [404]	58	^{99}TC-MAA (SPECT)	Retrospective	2 hours before SIRT	Serial CEA and CT response	No association between MAA uptake and response
Dancey[405]	20	^{99}TC-MAA (SPECT)	Prospective	Pre-treatment	CT response Duration of response Time to progression Survival	^{99}TC-MAA tumour to liver uptake ratio significantly associated with survival
Morsbach [406]	38	pCT	Prospective	Mean of 20 days before SIRT	1 year survival RECIST response (mean 114 days after SIRT)	Arterial perfusion (AP) predicts RECIST response and 1 year survival
Morsbach [407]	40	Arterial and portal phase CT pCT ^{99}TC-MAA (SPECT)	Prospective	Mean of 20 days before SIRT	1 year survival RECIST response (4 months after SIRT)	Significantly higher AP and arterial enhancement in responders than non-responders; no significant difference in portal enhancement or TC-MAA uptake ratio and response. Higher AP associated with 1 year survival

As part of standard preparation for SIRT, patients undergo a preliminary arteriogram of the liver to determine vascular anatomy of the liver and to perform a Techneitium-99 macro-aggregated albumin (^{99}Tc-MAA) nuclear scan. The arteriogram provides a road map of the arterial supply of the liver in order to plan delivery of the SIR-Spheres. The primary purpose of the ^{99}Tc-MAA scan is to exclude the presence of a significant arteriovenous lung shunt. The distribution of ^{99}Tc-MAA using single photon emission CT (SPECT) has been used as a surrogate for the distribution of Yttrium-90 microspheres and investigated as a predictor of radiological and CEA response to SIRT. One study in colorectal liver metastases failed to demonstrate a predictive association between

^{99}Tc-MAA tumour uptake [404], whereas a different study in patients with hepatocellular carcinoma did show an association between higher tumour to liver uptake ratio of ^{99}Tc-MAA and improved survival[405]. It has been argued that there are flaws in using ^{99}Tc-MAA as a surrogate for the distribution of Yttrium-90 microspheres, since there are differences in flow dynamics between the two, for example resulting from different particle size and viscosity of the suspension, as well as different injection techniques[124].

Expert opinion has recommended that imaging modalities which are sensitive to tumour vascularity and perfusion, particularly perfusion CT, warrant further evaluation and development as potential biomarkers of response to SIRT in the context of clinical trials[124].Two specific areas for research have already been highlighted: the first, whether perfusion imaging might be able to help select which patients will benefit most from SIRT and the second, whether changes in tumour perfusion parameters on imaging might provide an early surrogate of subsequent response at later time-points e.g. CT response at 6-9 months or time to progression in the liver (both of which could allow modification of patient management)[124]. To date, only two studies have published data relating to pCT as a potential biomarker in patients treated with SIRT (see table 17)[406, 407].The first study of 38 patients with chemotherapy-refractory hepatic metastases evaluated the ability of pCT to predict morphologic response and survival after SIRT[406]. The second study in 40 patients, compared the ability of pCT and ^{99}Tc-MAA Uptake scans to predict these outcomes after SIRT[407]. Both studies demonstrated that a high pre-treatment arterial perfusion evaluated using a pre-SIRT pCT predicted RECIST response on CT and 1 year survival. However, limitations of the studies are that only half of the patients had metastatic colorectal cancer (tumour type potentially being related to vascularity), the remainder comprised other tumour types. Their findings have not been validated independently in a larger series. Patients did not receive concomitant radiosensitising chemotherapy.

These studies did not evaluate the effect of chemotherapy or SIRT on pCT parameters. Since it is ideal for a surrogate biomarker of response to be linked to the mechanism of treatment effect, it is desirable to improve understanding about the effect of SIRT on tumour perfusion parameters, through performing sequential pCT scans, although the optimum time-points after SIRT need to be determined. It has been hypothesised that the primary mode of action of SIRT is tumour irradiation rather than significant embolism[124]. Although there are some limited data from retrospective histopathological analysis of resected liver metastases to support this hypothesis[408], currently there are no published data from perfusion imaging to inform the debate. In this thesis, we evaluate the feasibility of evaluating changes in tumour perfusion in patients with colorectal liver metastases after SIRT and test the hypothesis that SIRT results in changes in tumour perfusion which are consistent with the effects of radiation, using pCT.

E3 Perfusion CT Liver

There are some important differences (as well as similarities) between pCT in the liver and pCT in the rectum, which need to be considered when evaluating tumour perfusion of colorectal liver metastases in patients receiving chemotherapy +/- SIRT.

i) Models for pCT analysis

Although the models for pCT analysis utilised in rectal cancer described in section 1C are applicable to pCT in the liver, their adaptation is required in the liver to account for the dual arterial supply, from the hepatic artery and hepatic portal vein. Analysis involves definition of additional regions of interest to generate supplementary tissue time attenuation curves, dependent on the model being used e.g. a portal venous ROI for deconvolution methods and a splenic ROI, liver ROI and portal venous ROI for the maximum slope and (dual-input) compartmental models. In the maximum slope method, liver enhancement is resolved into arterial and venous components by assuming that the start of splenic enhancement signifies the commencement of portal venous perfusion; arterial perfusion (AP) and portal perfusion

parameters are then calculated by dividing the maximum slopes of the arterial and perfusion time attenuation curves by the peak aortic enhancement[409].

Blomley proposed an adaptation of this method for deriving hepatic portal perfusion, which has been widely adopted[410]. A hepatic perfusion index (HPI) can be derived by dividing the arterial perfusion by the sum of the arterial and portal perfusion values. In dual compartmental modelling, the equations used in modelling of the perfusion data are modified to account for differences in contrast agent concentrations in the liver, hepatic artery, portal vein as well as the time delay in beginning of enhancement between the aorta or portal vein and liver[411]; this allows fitting of the data to estimate the hepatic arterial perfusion and portal venous perfusion, as well as the mean transit time of the contrast through the liver; HPI is calculated as for the maximum slope method. Deconvolution analysis can also be adapted to use a dual vascular input e.g. using a specific 'liver protocol' in commercially available software, which requires definition of a portal venous ROI as well as arterial ROI. Such algorithms allow derivation of a value for the hepatic arterial fraction (HAF), i.e. the proportion of the total liver blood flow which is derived from the hepatic artery. It has been shown that use of dual vascular inputs in deconvolution analysis of liver pCT results in significantly different absolute parameter values compared to single vascular input analysis and improved reproducibility[412]. Although by definition, the HAF should be equivalent to the HPI derived from the other models, it has been shown that hepatic perfusion measurements using the three methods are not interchangeable, although significant moderate correlations were observed. It has also been highlighted that the maximum slope method is more likely to be influenced by extra-hepatic systemic factors e.g. cardiac status and administration of contrast than the other two models, although there is no consensus as to the best model for clinical use [411].In this project, pCT liver scans are evaluated using dual vascular inputs and a deconvolution method of analysis, where technically possible.

ii)Technical Factors influencing liver pCT analysis

Table 18 Summary of methods to select and define a tumour ROI in liver pCT analysis

Study	Coverage in z axis	Selection of lesion	Boundaries/Size of ROI
Kim et al[392]	17.8 cm (entire liver)	Largest liver metastasis	Freehand delineation, covering as much of the tumour as possible, including the inner necrotic portion
Pauls et al[394]	2 cm (4 slices)	Not specified	Intensity of rim enhancement in the area of maximum enhancement (size not specified)
Yang et al[413]	Not specified (4 slices)	Largest Lesion	Not specified
Meijerink[414]	Entire liver	Not specified	ROI in hypo-dense lesion as defined on portal phase image and separate ROI in 1cm hypo-dense lesion
Veit Heibach[415]	4cm (8 slices)	Largest lesion on integrated FDG PET	Freehand delineation around border or lesion on each slice
Ippolito[416]	2.4cm (8 slices)	Not specified	Circular ROI within confines of apparent tumour on perfusion parameter map
Sahani[417]	2 cm (4 slices)	Scanned at level of largest tumour diameter	All tumours delineated as separate ROIs (mean parameters derived) on each slice
Ng[418]	2 cm (4 slices)	Not specified	Not specified
Miles[419]	Not specified	Largest metastasis	ROI over lesion as seen on unenhanced CT and separate ROI over lesion with additional 1cm rim
Reiner[420]	14.8 cm (Majority of liver)	Not specified	ROI within liver lesion, defined with reference to Tc^{99}-SPECT

As for pCT of rectal tumours, there are a number of technical factors which can potentially influence the perfusion values obtained from pCT analysis of liver metastases and there is no consensus regarding the optimum methodology for analysis. Common to most methods for post-processing of the pCT data, an arterial region of interest is defined in the aorta, some studies specifying placement of this at the level of the coeliac axis[411] or hepatic hilum[392] but many studies not specifying location[394, 413, 415-418, 420, 421]. A variety of different methods for defining a liver tumour ROI have been employed but to date no research has specifically addressed which of these methods is optimal.

Intra-sequence motion is a more significant issue for perfusion CT of the liver than perfusion CT of the rectum, because the liver is in close proximity to the diaphragm, which moves with each respiration. A number of perfusion CT liver protocols have utilised motion correction techniques[392, 418, 420], although these are not integral to all commercially available pCT analysis software. Ng et el. compared the impact of three different motion correction techniques on pCT analysis and demonstrated that the absolute values and reproducibility of perfusion parameters are markedly influenced by motion[418].The best reproducibility was obtained with a rigid registration method (deconvolution analysis), in which the within patient coefficient of variation for BF, BV, MTT and PS were 11.2%, 14.4%, 5.5% and 12.1% respectively[418].The authors concluded that motion correction techniques are required for analysis of delayed phase data and derivation of PS, which extend beyond a single breath hold. A separate study has suggested that semi-automated registration techniques are superior to manual alignment techniques for liver pCT analysis but that non-rigid registration was superior to rigid registration[422]. The presence of inter-sequence motion has the potential to influence tumour ROI definition, since the shape and size of the ROI will depend on the sequence used to define the tumour in the presence of motion; the impact of motion and motion correction on inter-observer variation in perfusion parameter estimation has not previously been explored.

In this thesis, the evaluation of changes in tumour perfusion of colorectal liver metastases after chemotherapy +/- SIRT are considered in the context of the technical limitations of the techniques used for pCT analysis. It is argued that previously published methods for evaluating changes in the perfusion of colorectal liver metastases using pCT in response to systemic therapy are not yet optimal and require further development.

2 Methods

In this section the materials and methods used to address the research hypotheses are described. In the first part of this chapter, the design and treatment schedule of a clinical trial designed to evaluate toxicity from the combination of nelfinavir and hypo fractionated radiotherapy and to assess changes in tumour perfusion during therapy in patients with rectal cancer is outlined. The specific acquisition protocols and methods of analysis for the imaging tests incorporated into the study (pCT and Dce-MRI) to assess changes in tumour perfusion are described. The acquisition of tissue from the patients is described along with the methods for evaluating tumour cell density in rectal tumour biopsies before and after nelfinavir and radiotherapy as a potential biomarker for assessing radio-sensitisation. The techniques used to evaluate immunohistochemical expression of tissue markers of hypoxia, vascularity and activation of the RAS-PI3K-Akt signalling pathway are reported. In the second part of this chapter, the design of a study to evaluate sequential changes in the tumour perfusion of colorectal liver metastases during oxaliplatin and 5-FU chemotherapy using pCT is described and the methods developed to assess the technical challenges of using pCT to evaluate the perfusion of colorectal liver metastases in patients receiving radioembolisation with Yttrium-90 SIR-spheres are outlined.

2A Materials

A1 Nelfinavir for clinical trial

Nelfinavir (VIRACEPT®) was sourced and funded locally from hospital own stock. It was stored and temperature monitored in line with Good Clinical Practice (GCP) and standard policy at the site.

A2 General laboratory supplies

10% neutral buffered formalin (Sigma-Aldrich, Gillingham, UK)

Aquamountant

Reagents for the Leica Bond-Max autostainer were obtained from Leica Biosystems (Newcastle Upon Tyne, UK):

- Dewax Solution
- Alcohol
- Wash Solution
- Buffer Solution
- Antibody diluent
- Peroxidase block
- Post primary antibody
- Polymer
- Deionised water
- Mixed Diaminobenzidine Tetrahydrochloride Refine
- Haematoxylin

A3 Antibodies

Primary antibodies directed against vascular markers (CD31, CD105) and hypoxia markers (CAIX, HIF 1 alpha) and proteins involved in Akt-signalling (Phospho-Akt, Phospho-PRAS-40) were acquired as summarised in Table 19.

Table 19 Primary antibodies used for tissue immunohistochemistry

Antigen detected	Antibody Clone	Species	Source
CD31	JC70	Mouse monoclonal	DAKO (Glostrup,Denmark)
Phospho-Akt	D9E	Rabbit monoclonal	Cell Signalling Technologies (Danvers, Massachusetts)
Phospho-PRAS40	C77D7	Rabbit monoclonal	Cell Signalling Technologies (Danvers, Massachusetts)
PRAS-40	D23C7	Rabbit monoclonal	Cell Signalling Technologies (Danvers, Massachusetts)
CD105	4G11	Mouse monoclonal	Novocastra Laboratories (Newcastle Upon Tyne, United Kingdom)
HIF-1 alpha	54	Mouse monoclonal	BD Biosciences (San Jose, CA)
CAIX	M75	Mouse monoclonal	Gift from Professor Adrian Harris, University of Oxford

A rabbit anti-mouse antibody purchased as part of the kit for the Leica Bond Max autostainer, Leica Biosystems (Newcastle Upon Tyne, UK) was used as a secondary antibody for immunohistochemistry.

2B Clinical assessment of nelfinavir and hypo-fractionated radiotherapy for rectal cancer

B1 Study Population

Patients with a diagnosis of metastatic rectal adenocarcinoma were recruited to a study designed to evaluate the safety and activity of nelfinavir and pelvic radiotherapy at the Churchill Hospital in Oxford. I contributed to the trial design, obtained regulatory approvals and led patient recruitment to this trial under the supervision of the 'chief investigator' (CI), Ricky Sharma and the 'trial management group' (TMG). Ethical approval for this research study was granted by Oxford Research Ethics Committee A.

In order to be eligible for study participation, patients were required to have a histologically proven adenocarcinoma of the rectum (≤ 15cm from the anal verge) with radiological evidence of metastatic disease and to require a short course of pelvic radiotherapy either to palliate local

tumour symptoms or to downstage the primary tumour with a view to delayed surgical resection (> 8 weeks after radiotherapy). Patients were also required to have an ECOG[423] performance status of 0-2 and satisfactory liver function, renal function and full blood count.

Potentially suitable patients were identified at Colorectal Multi-Disciplinary Team meetings and were subsequently seen in the Oncology Outpatient Department to discuss the clinical trial. Suitable patients were invited to participate in the study and were provided with verbal and written information about the study. Patients who were interested in study participation attended a screening visit, which constituted the following:

- History and physical examination, including height, weight, vital observations and ECOG Performance Status
- Assessment of active symtoms
- Review of current medications
- Informed consent for trial participation
- Screening blood tests, including Full Blood Count, Serum Renal and Liver Biochemistry, Tumour Markers
- Blood for research assays

B2. Study Treatment Schedule and Planning

Patients were scheduled to undergo a series of assessments as summarised in the study schedule of events.

Table 20 Schedule of Events

	Pre-treatment [6]	Daily from Day -7 to Day 7 [4]	Day -1	Daily from Day 1 to Day 7 on days of RT [5]	On last day of RT (Day 7)	7 days after RT[11] (Day 14 +/- 1 day)	8 weeks from last fraction of RT (+/- 2 weeks)	4 weekly from last day of RT for 5 months (+/-2 weeks)
EVENTS CONSISTENT WITH STANDARD NHS THERAPY								
History and physical exam	X				X			X
Histology [15]	X							
Diagnostic MRI scan pelvis [8,9]	X						X	
Diagnostic CT scan thorax, abdomen, pelvis	X						X	
Treatment planning CT scan (for SCRT)	X							
Radiotherapy treatment [5,7]				X				
FBC + differentials [1]	X				X			X
Serum chemistries [2]	X				X			X
Pregnancy test Applicable to adults of child bearing age	X							
Serum tumour markers [3]	X							X
EVENTS SPECIFIC TO CLINICAL TRIAL:								
Complete informed consent A	X							
Diagnostic scans: perfusion CT and DCE-MRI pelvis [10]	X		X		X			
Blood for research assays[13]	X		X		X			
Nelfinavir dosing[4]		X						
Tumour biopsies						X		
Optional Tumour biopsies (complete Consent Form B) [12]	X							
CTCAE v 4.0	X		X		X	X		X

[1] FBC: Haemoglobin, leukocytes, platelets, differential blood count

[2] Clinical chemistry: electrolytes, calcium, creatinine, bilirubin, alkaline phosphatase, magnesium, ALT, albumin, glucose (non-fasting), Urea

[3] CEA, CA125 and CA19.9 (only repeated if initial sample at pre-treatment was elevated above normal range)

[4] Applicable to first 16 patients in clinical trial and then only patients randomised to active treatment arm: Nelfinavir 1250 mg bd each day (7 days per week) from day -7 (Wednesday) to last day of RT (Tuesday)

[5] 5 Gy delivered daily from first (Day 1) to last day (Day 7), excluding weekends, of radiotherapy (total dose prescribed to ICRU reference point = 25 Gy)

[6] Within 4 weeks of commencement of dosing with Nelfinavir

[7] Any oncological intervention, including standard systemic chemotherapy, was permitted ≥14 days from the last fraction of radiotherapy.

[8] RECIST measurements of primary tumour required on pre-treatment and post-treatment MRI scans mrTRG required on post-treatment MRI scans.

[9] Imaging reviewed at Multi-Disciplinary Team Meeting with surgical representation.

[10] Perfusion CT and DCE-MRI scans according to standard protocols: If tolerated, both modalities performed. If patients were unable to tolerate both scans, only perfusion CT was performed.

[12] See section 7.3 Optional biopsy performed only in patients who offered informed consent on Consent Form B.

[13] See section 7.3 Assay 1 was completed at pre-treatment time point only, whereas assay 2 was done pre-treatment, day -1 and last day of radiotherapy.

[14] Visit done at 6 months post last fraction of radiotherapy or at any time for those patients that withdraw from the study.

[15] Needed to be performed within 6 months of study entry.

Patients were administered 14 days in total of the study drug, oral nelfinavir 1250 mg bd, with 7 days of nelfinavir being given prior to the commencement of radiotherapy and 7 days of nelfinavir being administered during radiotherapy (see figure 9). The radiotherapy schedule consisted of 25 Gy in 5# of 5 Gy per # over 7 days (commencing on a Wednesday and the final fraction on a Tuesday, with no radiotherapy on Saturday or Sunday). Patients were permitted to commence systemic chemotherapy a minimum of 14 days after completion of radiotherapy.

Figure 9 Treatment schedule for the administration of nelfinavir and radiotherapy.* Starting on a Wednesday and continuing for 5 weekdays.

Day number	**-7**	**-6**	**-5**	**-4**	**-3**	**-2**	**-1**	**1**	**2**	**3**	**4**	**5**	**6**	**7**
Nelfinavir 1250mg bd for 14 days														
Radiotherapy*														

For radiotherapy planning, patients were immobilised and simulated on a flat-top CT couch in a supine or prone position. Patients were advised to drink fluids prior to simulation in order to have a comfortably full bladder during the CT planning scan and intravenous contrast was administered unless contra-indicated. An anal marker was placed at the anal verge. A planning CT scan was performed with 2.5 mm slice thickness to cover the L3 space to at least 4 cm below the anal marker.

Tumour volumes were delineated on planning CT images using ECLIPSE planning software according to a standardised radiotherapy planning protocol, based on the ARISTOTLE Trial Group contouring guidance, using modest size fields. Radiotherapy was planned using 3-D conformal radiotherapy techniques, involving the use of 3-7 beams to meet the planning criteria. Dose volume histograms were calculated for the planning target volume (PTV) and organs at risk (OARs) and two clinicians, a planner and a physicist reviewed and approved the plan prior to

delivery. The aim was to encompass the PTV within the 95% iso-dose, with dose constraints set such that at least 95% of the PTV was required to receive 99% of the dose. Other dose constraints are detailed in Table 21 and were documented on a radiotherapy plan assessment form for each patient. The radiotherapy plan and plan assessment form were reviewed and approved by an independent clinician on the 'Radiotherapy Quality Assurance Team' prior to delivery of the treatment.

25 Gy in 5 # of 5 Gy per # was prescribed to the ICRU reference point, with all fields being treated daily. Verification imaging to localize the treatment volume was required prior to every fraction. The technique of verification imaging was in accordance with local policy and consisted of a minimum of one pair of orthogonal verification images to confirm the position of the iso-centre, either kV or MV imaging. Repositioning was recommended for all target offsets greater than 3 mm from the planned position.

Table 21 Dose constraints used for radiotherapy planning approval and quality assurance

Dose volume constraints region of interest/organ at risk	Dose constraint
PTV	$V_{95\%} > 99.0\%$
DMAX	< 107% (to a volume of approximately 2 cm as per ICRU guidelines)
Femoral head [left]	V_{20} Gy < 40%
Femoral head [right]	V_{20} Gy < 40%
Small intestine	Document volume (cc) receiving 103%, 105% and 107% of dose
Bladder	Document volume (cc) receiving 105% and 107% of dose

B3 Assessment of Toxicity

Treatment toxicity was evaluated according to Common Toxicity Criteria for Adverse Events (CTCAE) Version 4.0 at intervals according to a pre-defined schedule as follows:

- Day -1 (seventh day of nelfinavir administration, the day before commencement of radiotherapy)
- Day 7 (the last day of radiotherapy)

- Day 14 (7 days after completion of radiotherapy)
- Every 4 weeks (+/- 1 week) for 6 months after the last dose of radiotherapy

Blood sampling for full blood count, urea & electrolytes, liver function tests and random glucose was perfomed at the following timepoints:

- Day -1
- Day 7
- Every 4 weeks (+/- 1 week) for 6 months after the last dose of radiotherapy

An adverse event was defined as “any untoward medical occurrence in a patient or clinical investigation subject administered a pharmaceutical product and which does not necessarily have a causal relationship with this treatment.” For each adverse event the CTCAE Grade was documented and an assessment was made regarding the likely causality: disease-related, nelfinavir- related, radiotherapy-related or study-related (with reference to known side effects of pelvic radiotherapy and nelfinavir, as detailed in the Investigator Brochure and Summary of Product Characteristics (SmPc) for nelfinavir according to the following score system:

1. Definitely related
2. Probably related
3. Possibly related
4. Probably unrelated
5. Definitely unrelated

Abnormal laboratory findings detected during the study or which were present at baseline and significantly worsened during the study (unless related to the disease and consistent with the patients’s condition) were recorded as adverse events if considered to be clinically significant.

Clinical data was collated by Oxford Clinical Trials Office (OCTO), whose trial statisticians contributed to the production of the end of study report.

B4 Radiological Response Assessment

All patients were required to have a diagnostic pelvic MRI scan at baseline (≤28 days before commencing nelfinavir) and a further diagnostic pelvic MRI scan 8 weeks following completion of radiotherapy. Revised RECIST guidelines (version 1.1) were used in the assessment of disease response of the primary tumour or radiological N1-2 disease on MRI scans at baseline and at 8 weeks post-SCRT[119] and RECIST measurements were reported by a radiologist.

The TNM status and status of the Circumferential Resection Margin (CRM), whether involved, threatened or clear was evaluated on the baseline and follow-up MRI scan as described in the MERCURY trial[424].

Tumour response to treatment was also evaluated by radiological assessment of the Tumour Regression Grade on MRI scan 8 weeks post-radiotherapy (mrTRG) using the scoring system developed by Patel et al.[123], as described in Chapter 1A. As described by Patel et al. [123] patients with a mrTRG score of 1-3 on their 8 week MRI scan were classified as having a 'good mrTRG score' and patients with a mrTRG score of 4 or 5 were classified as having a 'poor mrTRG score'.

TNM stage, CRM status and mrTRG score on pelvic MRI scans were reported by two independent consultant radiologists at the Churchill Hospital. In cases of discrepancy the review of a third expert radiologist, was sought and the final classification was decided by the consensus of two of the radiologists or the judgment of the third expert radiologist, in the few circumstances where there was a difference between the assessment of all 3 radiologists.

2C General Methods for Imaging Rectal Cancer

C1 Perfusion CT Rectum

In order to explore changes in tumour perfusion parameters occurring as a result of nelfinavir on its own and nelfinavir concurrent with radiotherapy, perfusion CT(pCT)scans of the rectum were incorporated into the schedule at three time-points. Patients were scheduled to have a pCT scan at baseline (i.e. before the commencement of nelfinavir), a second pCT scan the day before commencement of radiotherapy (i.e. the 7th day of nelfinavir) and a third pCT scan at the end of radiotherapy (where possible on the last day of radiotherapy before the final fraction).

Patients were asked to fast for 2 hours prior to the pCT, except to drink a litre of water before the scan. The pCT scan was performed on a 64-row detector GE Medical LightSpeed VCT scanner. Initially, a CT study of the abdomen and pelvis was acquired without contrast in order to localise the CT spatial co-ordinates of the primary tumour. The location of the tumour was identified, and the spatial CT co-ordinates for the dynamic study specified with the aim of centering the dynamic scan over the bulkiest part of the tumour if it exceeded 4 cm in cranio-caudal dimension. Dynamic images of the pelvis were acquired starting 10 s after commencement of intravenous contrast using 60-100 ml of an iodine based contrast agent (Omnipaque 300) injected at a rate of 5 ml/sec using a pump injector (Medrad) via a 20 Guage cannula. Eight contiguous sections, each collimated at 5 mm (providing a z axis coverage of 4 cm) were acquired at 1 s intervals for 45 s by using a cine-mode acquisition (120 kv, 60 mA, 1 s rotation speed, 36 cm field of view and 512 x 512 mm matrix, 17 mSV effective dose).

Images were transferred to a GE Advantage Windows Workstation (Version 4.2, GE Healthcare Technologies). Viewing and analysis was performed using the Body Protocol of GE Perfusion 3.0 software (GE Health care Technologies) which is based on a deconvolution method. A processing threshold of -45 to 120 Hounsfield Units (HU) was used to view the images in order to optimise

soft tissue visualisation. In order to minimise partial volume averaging (through arterial ROI definition in a small artery), to promote acceptable signal to noise ratio (small arterial ROI) and for consistency, the arterial ROI was manually defined by a 12mm² circle annually in the centre of the right iliac artery in our analysis of pCT data. Cine images were reviewed to check that the ROI did not encompass intra-arterial calcification or become displaced outside the arterial wall due to motion. The software was used to automatically derive an arterial enhancement curve and to define the pre-enhancement image. The end of the first pass or post-enhancement image was manually selected by reviewing the arterial enhancement curve and identifying the lowest point after the peak[425].

Parameter maps were produced for Blood Flow (BF), Blood Volume (BV) and Mean Transit Time (MTT), with each pixel representing a parameter value. Parameter values for the tumour were calculated by defining a tumour ROI. A tumour region of interest was defined freehand by tracing a mouse around the perceived margins of the tumour in each of 8 CT slices in the z axis. The tumour ROI was drawn on the CT image defined by the end of the first pass for consistency and since tumour contrast enhancement was usually greatest at the end of the arterial enhancement phase. The entire temporal sequence of images were reviewed for each slice, in order to check for intra-sequence motion, to exclude in bowel gas from the tumour ROI and try to keep the ROI within the margins of the tumour on all slices where possible. Tumour ROIs were independently annotated by a radiologist according to this method and inter-observer variation in perfusion parameters between two observers was analysed using a weighted kappa score using the software package SPSS version 21.0

Figure 10 Steps involved in pCT analysis of primary rectal tumours using GE software

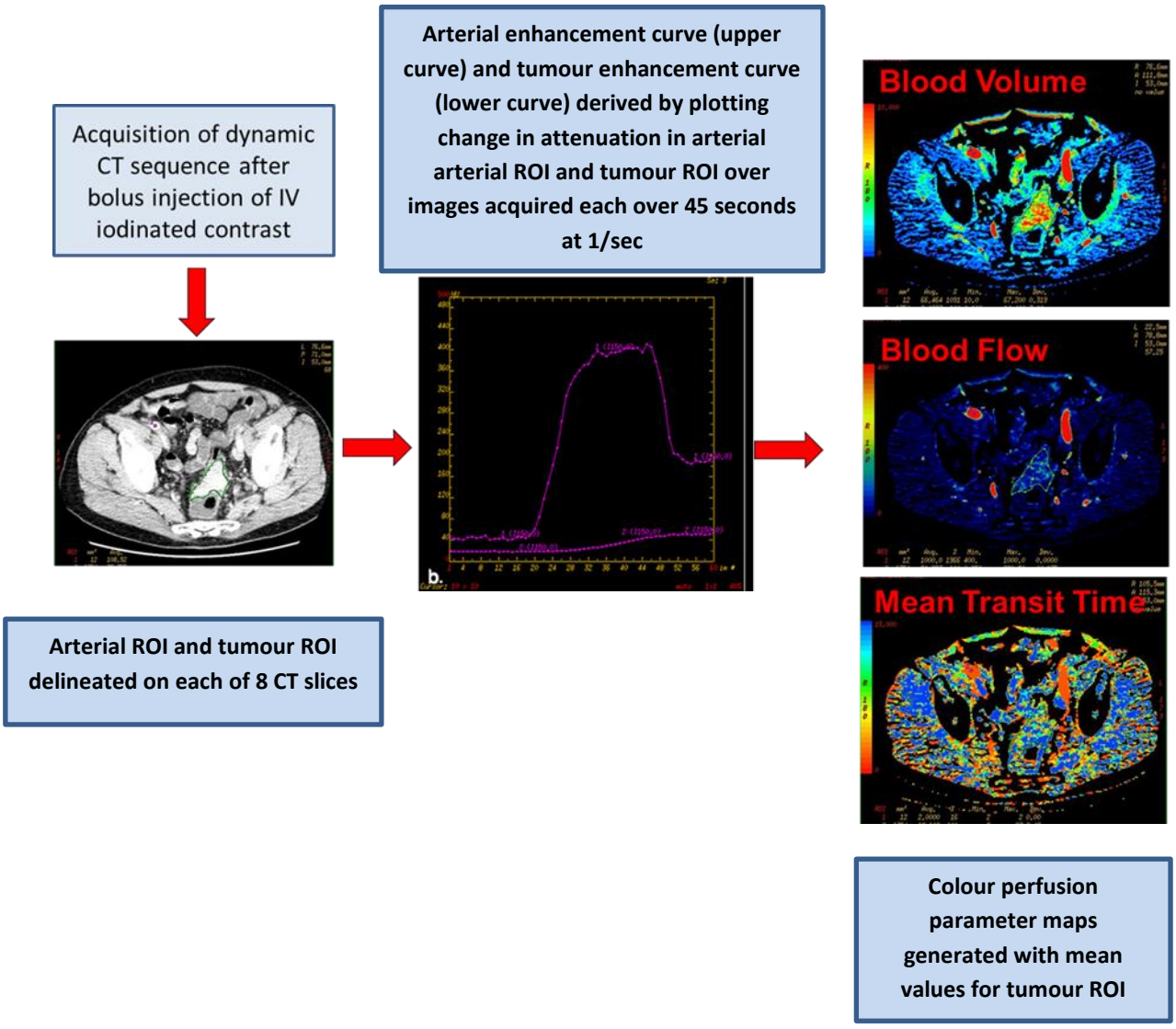

The mean parameter values and their standard deviations for the tumour ROI in each CT slice were manually entered into an excel spreadsheet for each scan and each patient for further analysis. The arterial input function curves were extracted from the software by viewing the mean enhancement value(HU) for the arterial ROI in each image in the temporal sequence and manually entering it into an excel spreadsheet before plotting the data in graphical format.

In order to compare parameter maps from sequential scans in the same patient, screensave shots of the colour parameter maps and CT images for each slice were saved and imported to Image J (a JAVA based software).

In order to perform advanced image analysis, the parameter maps first had to be converted to grayscale images, saved as screensave DICOM images using the GE Perfusion 3.0 software and subsequently saved to an external storage device. CT images for each of the 8 z axis slices were also saved and extracted in this format. In collaboration with a data programmer Jun Li, a customised program was developed using Matlab (Mathworks 2012b) for further analysis of these images. This program was designed to allow freehand definition of a tumour ROI on a CT slice, extraction of the ROI as a binary mask and application of the mask co-ordinates to DICOM images of the grayscale parameter maps at the same location. The number of divisions in the gray levels (1 to 255) of each of the pixels in the ROI was read from the DICOM file of the grayscale parameter map and a mean gray level value for the ROI derived. The mean gray level for the ROI was converted to the mean parameter values by the program by adjusting the scale of the different gray levels according to the scale of the parameter maps (0- 400 for BF, 0-10 for BV and 0-15 for MTT). A function was derived to plot a histogram of the parameter values within a ROI for each CT slice (2D analysis) and to subsequently combine the data from the ROI in each of 8 CT slice in the z axis to produce a histogram of parameter values within the defined tumour volume (3-D analysis). This function was also used to derive statistics for the 3-D tumour ROI (mean, minimum, maximum, standard deviation and descriptors for the shape of the histogram, namely skewness and kurtosis).

Statistical analysis was performed using SPSS 21.0. The normality of the distribution of parameter values in the population studied was evaluated using the Shapiro-Wilk test. Paired parametric data was analysed using the Wilcoxon Signed Rank test and paired parametric data was analysed using the paired *t* test for significant differences between sequential scans.

C2 Dce-MRI Rectum

In order to explore changes in tumour perfusion parameters occurring as a result of nelfinavir on its own and nelfinavir concurrent with radiotherapy Dce-MRI scans of the rectum were incorporated into the study schedule. Patients were scheduled to have a Dce-MRI scan at baseline (i.e. before the commencement of nelfinavir), a second Dce-MRI scan the day before commencement of radiotherapy (i.e. the 7th day of nelfinavir) and a third Dce- MRI scan at the end of radiotherapy (where possible on the last day of radiotherapy before the final fraction).

MRI images were acquired on a 3 Tesla GE Medical System. T2 weighted images of the pelvis were performed followed by T1 mapping sequences. The dynamic sequences were performed using the LAVA Protocol which is based on a spoiled gradient echo sequence. Images with dimensions of 512 x 512 mm x 52 mm were acquired every 9.5 s for 5 minutes after the administration of intravenous ProHance (Gadoteriol contrast) using a pump injector. The in-plane resolution of the images was 0.7813 x 0.7813 mm and the slice thickness was 2 mm. Flip-angle images were not interpretable and a uniform T10 map of 1 was assumed in the subsequent analysis.

Scans were analysed by Dr Monica Enescu in the Department of Biomedical Engineering, University of Oxford. The first processing step involved manual selection of a volume of interest (VOI) measuring 120 x 120mm encompassing the mesorectum (see figure 11). In the temporal dimension, frames 4-17 were selected for analysis as they contained the uptake curve and part of the plateau phase of the signal enhancement. Pharmacokinetic modelling was used to derive pharmacokinetic parameters reflecting the underlying tissue physiology, namely K^{trans}, K_{ep} and V_e. This involved two steps. The first step consisted of estimation of the contrast agent concentration from the MRI signal enhancement time curve in each voxel within the selected VOI. A non-linear

relationship was assumed between the MRI Signal concentration, *S*, and the contrast agent concentration, *C(t):*

$$S(t) = S0\ \frac{(1 - e^{-TR/T10} - r1C(t)TR)\sin\theta}{1 - e^{-TR/T10 - r1C(t)TR}\cos\theta}$$

Where S0 = pre-enhancement (baseline) signal

TR=repetition time

r1 = the tissue relaxivity constant

θ = the flip angle

T10 = the unenhanced relaxation time of the tissue (typically calculated from variable flip-angle sequences using the DESPOT protocol)

Once the contrast agent contrast agent concentration had been derived for each voxel, the modified Tofts pharmacokinetic model was fitted to each of them to calculate pharmacokinetic parameters, according to the principles described in Chapter 1D. A population derived AIF was used for Dce MRI analysis namely, the Orton bi-exponential model [426].

A novel framework was used for motion correction using deformable image registration and simultaneous pharmacokinetic parameter estimation[427]. Intra-sequence tumour motion on the dynamic T1 scans was evaluated for each scan before and after application of the motion correction algorithm, using a 4D image viewer incorporated into the Image Registration Toolkit (IRTK), used under license from Ixico Ltd. Pharmacokinetic parameters were derived for each voxel in the mesorectal VOI for each scan and represented pictorially as perfusion parameter maps.

Figure 11 Steps involved in DCE-MRI analysis

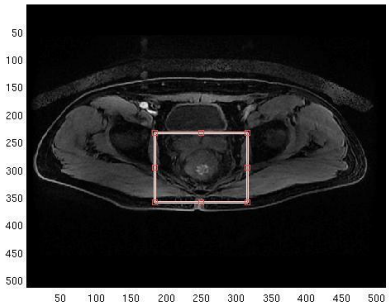

Manual selection of 12x12cm VOI centred on mesorectum on T1 images

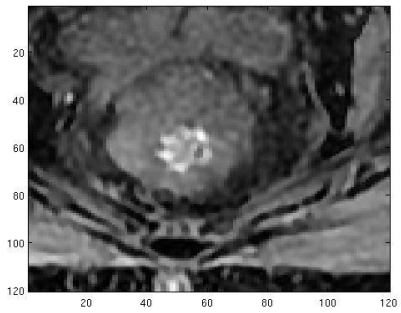

Algorithm for simultaneous motion correction/pharmacokinetic modelling applied to volume of interest on dynamic T1 images.

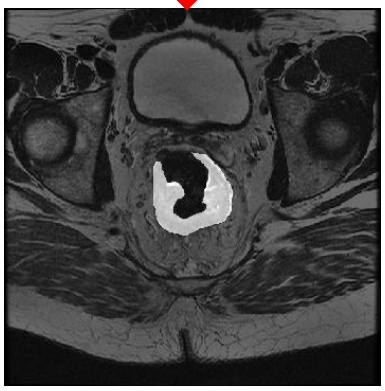

Delineation of tumour VOI on T2W MRI and creation of a mask

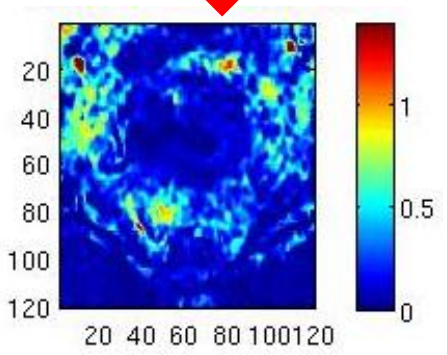

Pharmacokinetic parameters Derived for VOI (*Ktrans, Kep, Ve*)

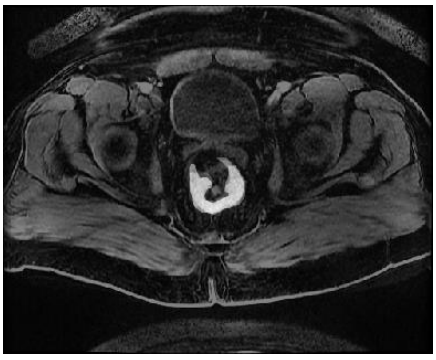

Superimposition of mask on co-registered T1W DCE-MRI sequence

In order to derive perfusion parameters within the tumour VOI, the rectal tumour was outlined on T2 weighted MRI images by a radiologist using OsiriX, an image processing software for DICOM

images. This is in line with draft guidance, published since the conception of this research, which recommends that quantitative parameters (e.g. K^{trans}) for a tumour are derived from Dce-MRI scans by segmentation of the tumour tissues using either correlative images from the same scanning episode (e.g. T2W MRI) or summation images from the dynamic T1W images[428].The co-ordinates of the delineations were saved and exported as XML files. The delineations were imported into the IRTK and co-registered with the T2W MRI scans, where they were viewed as masks. The accuracy of co-registration of the masks with the tumour was assessed by manual checking of tumour coverage by the masks on the T2W scans. T2 images were co-registered with the first volume of the corresponding T1 Dce-MRI sequences in two steps, the first involving rigid registration with normalised mutual information (NMI) as a similarity metric using Insight Toolkit Software (ITK) and the second step involving refinement using a multi-modal neighbourhood-based similarity metric (MIND). The accuracy of the automated registrations was manually checked and adjusted where sub-optimal using the transformation function in the IRTK. The T2 masks were than mapped to the co-registered T1 Dce-MRI dynamic images and the position of the masks in relation to the tumour on the T1 scans were manually checked. The co-ordinates of the T1 maps were superimposed on the corresponding perfusion parameter maps for the mesorectal VOI for each scan and used to derive the mean K^{trans}, mean K^{ep} and mean V^{e} (with associated standard deviations) of the voxel values within the delineated tumour VOI.

For qualitative analysis of the Dce-MRI scans, modifications were made to the program designed to perform the pharmacokinetic analysis, such that it was possible to select the entire pelvis as the VOI rather than a 120 x 120 mm VOI. This allowed comparison between scans at comparable anatomical levels.

2D General Methods for Tissue Biomarkers in Rectal Cancer

Tissue samples were collected, processed and stored according to the schedule defined in the study protocol.

Table 22 Summary of arrangements for collection, storage and processing of tissue samples acquired in the study schedule.

	ASSAY 1	**ASSAY 2**	**ASSAY 3 (7 days post-radiotherapy)**	**ASSAY 4 (voluntary biopsy pre-treatment)**
Purpose of Assay	Genotype analysis	Phospho-Akt expression	Fixation/storage of biopsy tissue	Fixation/storage of biopsy tissue
Assay	To be determined by ongoing preclinical research	Western blot	To be determined by ongoing preclinical research	To be determined by ongoing preclinical research
Type of sample	Whole blood	PBMC	Biopsy tissue	Biopsy tissue
Vials Used	7.5 ml EDTA	10 ml EDTA	Standard	Standard
Total volume per visit	15 ml	20 ml	Standard biopsy	Standard biopsy
Total volume per patient	15 ml	60 ml	Seven biopsies obtained at proctoscopy (note that one biopsy is from non-malignant mucosa)	Seven biopsies obtained at proctoscopy(note that one biopsy is from non-malignant mucosa)
Time points	Pre-treatment only	Pre-treatment, day -1, last day of radiotherapy	Pre-treatment and 7 days post-RT	Pre-treatment
Clinical Handling /Storage/ Transport	To Sample handling/ GCLP lab at room temperature for immediate freezing as whole blood.	On ice to Sample handling/GCLP lab for immediate PBMC isolation, following isolation freeze PBMCs or platelets immediately	Five biopsies formalin fixed using standard procedures, one biopsy snap frozen in liquid nitrogen and one biopsy stored in RNA-later	Five biopsies formalin fixed using standard procedures, one biopsies snap frozen in liquid nitrogen and one biopsy stored in RNA-later
Storage Conditions	-70^{o}C Freezer	– 70^{o}C Freezer	Liquid nitrogen for biopsies, vials of cultured cells stored in – 70^{0}C Freezer	Liquid nitrogen for biopsies, vials of cultured cells stored in – 70^{0}C Freezer

D1 Tumour Cell Density Analysis

Patients in the study were asked to provide consent to post-treatment research biopsies of the primary rectal tumour, which was undertaken 7 days (+/- 1 day) after completion of pelvic radiotherapy, with the primary intention of evaluating Tumour Cell Density in the primary tumour at this time point. In addition, patients were asked for consent for an optional pre-treatment research biopsy; for patients agreeing to this optional biopsy, it was performed between the time-point at which the patient gave consent to participate in the study and the commencement of nelfinavir. A sample handling manual was written detailing the processes required for correct acquisition, processing and storage of tissue samples to ensure standardisation and quality control. Patients underwent biopsies in the Endoscopy Suite at Oxford University Hospitals. Biopsies were taken under visual guidance using flexible sigmoidoscopy tools, with the aim of taking biopsies of 5 mm in diameter from the luminal surface of the tumour/rectal mucosa. Six tumour biopsies were taken from the rectal tumour at each procedure, 4 of which were immediately placed in 10% neutral buffered formalin in a single sample pot and left for 6 to 24h for fixation prior to briefly washing the specimens in distilled water, placing in 70% ethanol. Transfer to cassettes for paraffin embedding was carried out by OCHRe (Oxford Centre for Histopathology Research). From the tumour blocks, 3 levels of the tissue were taken for slides (at 5 micro-meter intervals according to local practice). Additionally, paraffin- embedded tissue from the patients' diagnostic biopsies were retrieved and processed for slides. Slides were stained with haematoxylin and eosin. The slides were then reviewed initially by a consultant pathologist to confirm the presence of adenocarcinoma cells.

Subsequently, the haematoxylin and eosin stained slides were digitally scanned using an automated scanning system (Aperio XT, Aperio Technologies, Vista CA) at 200x magnification. The entire region of the tumour on slides at each of the time points was manually annotated by a Colorectal Pathologist using Image Scope software (version 10, Aperio Technologies), which was

used to superimpose a systematic random sample of 300 points using virtual graticule software (RandomSpot , University of Leeds, Leeds), as illustrated in figure 12.

Figure 12 Diagramatic representation of steps involved in Tumour Cell Density analysis of rectal tumour biopsies

Haematoxylin & eosin stained biopsy scanned at 200x magnification using Aperio Digital scanner

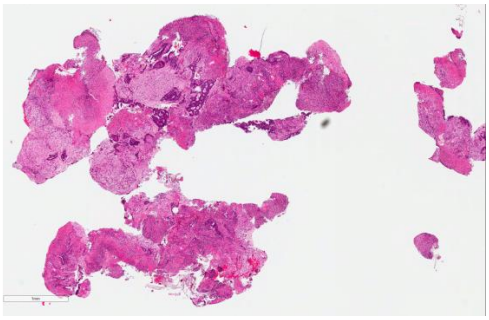

Entire biopsy manually annotated and grid with 300 random points superimposed

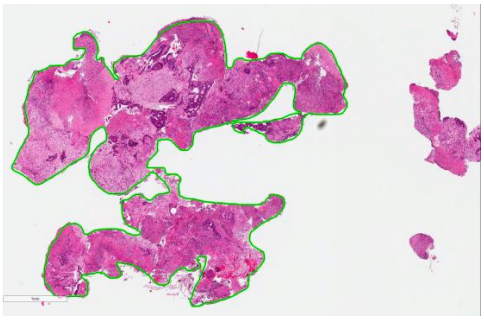

Each point manually scored according to whether it falls on tumour, stroma, mucin, muscle, vessel, lumen, necrosis or inflammation

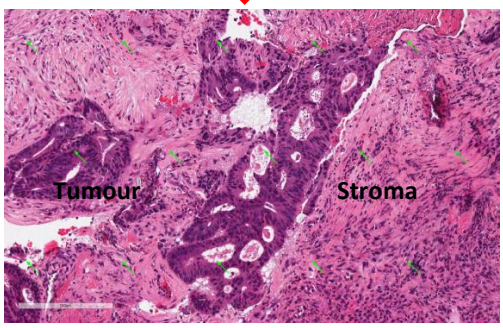

The pathologist then manually scored each point according to whether it fell on one of the following 8 categories:

1.Tumour

2. Stroma

3.Blood Vessel

4.Necrosis

5.Inflammation

6.Lumen

7.Mucin

8.Muscle.

Tumour Cell Density was calculated as the percentage of points falling on tumour out of all of the informative points and calculated for each pre-treatment and post-treatment biopsy. For statistical analysis, the median TCD (and interquartile range) was derived for the evaluable pre-treatment (diagnostic biopsies) and post-treatment biopsies. Subsequently the percentage change in TCD between the pre-treatment and post-treatment biopsies was calculated for each individual patient. These results were compared with TCD results from paired pre-treatment biopsies and post-treatment resection tumour specimens in an historical series of patients[255] with rectal cancer treated at St James Hospital, Leeds with either surgery alone (no pre-operative radiotherapy) or hypo fractionated radiotherapy 25 Gy in 5# over 7 days (surgery in a median of 7 days [28]).The paired *t* test was used for comparison of TCD in pre-treatment and post-treatment samples. TCD in trial samples were compared with historical controls using the Mann-Whitney U test for independent non-parametric data. The paired *t* test was used to evaluate the statistical significance of differences in percentage change in TCD for individual patients between those with a good versus a poor mrTRG on the post-treatment MRI scan. Statistical analyses were performed in EXCEL and SPSS version 21.

D2 *KRAS* mutational analysis

Diagnostic pre-treatment biopsies were evaluated for common mutations in the *KRAS* gene by Molecular Pathology services at the referring hospital.

D3 Hypoxia, Vascular and Proliferative Markers

Immunohistochemistry was carried out using the Leica Bond-Max automated immunostainer (Leica Microsystems, Wetzlar, Germany) using a two-step method and the materials described in section 2A on 5 µM sections cut from paraffin-embedded tissue biopsies using the antibodies summarized in table 19.

i) CAIX

Tissue sections were stained using Protocol F on the autostainer. Tissue sections were heated and dewaxed to retrieve antigen, washed in epitope retrieval solution then incubated with peroxidase for 5 minutes to block endogenous peroxidase. The specificity of staining was optimized in control tissue by evaluating staining with different combinations of antigen retrieval times (10 minutes or 20 minutes), buffer pH (6.0 or 9.0) and dilution (1: 500, 1:1000, and 1:1500). Tissue sections were incubated with the primary antibody for 15 minutes followed by the secondary antibody for 8 minutes. Sections were washed with the manufacturer's washer buffer (diluted 1:10). Sections were incubated with the manufacturer's polymer for 8 minutes, incubated with DAB for 10 minutes and counterstained with hematoxylin for 5 minutes. Slides were washed in distilled water and mounted with a coverslip using Aquamountant. Renal cell carcinoma tissue sections were used as a positive control and also as a negative control with omission of the primary antibody (incubation with antibody diluent only). Stained slides were examined under a light microscope. Two independent assessors evaluated slides for intensity of membrane staining, scoring them as weak (1) or strong (2) and percentage of cells staining (%). These two scores were multiplied to derive a composite score (0-200) [266]. Samples were also classified as positive or negatively staining for CAIX, with negative samples being defined as those containing less than

10% positively staining cells. In cases of disagreement, the assessors examined the slide together and reached a consensus.

ii) HIF- 1 alpha

Immunohistochemical expression of the hypoxia marker HIF 1-alpha was evaluated in tissue biopsies on the Leica Bond-Max automated immunostainer using a primary antibody at a dilution of 1:400. Tissue sections were stained using a previously optimized protocol. Tissue sections were baked to retrieve antigen, dewaxed, washed in epitope retrieval solution with a pH of 9.0 (ER2) for 40minutes then incubated with peroxidase for 5 minutes to block endogenous peroxidase. Tissue sections were then incubated with the primary antibody for 60 minutes and with secondary antibody for 8minutes. Sections were washed with the manufacturer's washer buffer (diluted 1:10). Sections were incubated with the manufacturer's polymer for 8 minutes, incubated with DAB for 10 minutes and counterstained with haematoxylin for 5 minutes. Positively staining pancreatic tissue sections were used as positive controls and as negative controls (with omission of the primary antibody) [281, 285] Stained slides were mounted with a coverslip using Aquamountant and evaluated under a light microscope. Two independent assessors evaluated slides for intensity of nuclear staining, scoring them as weak (1) or strong (2) and the percentage of cells staining (%). Although several methods of scoring HIF 1 alpha expression have previously been reported [281, 285, 429], for ease of direct comparison with CAIX expression, the frequency of staining was not categorized and the composite score (0-200) was similarly derived by multiplying the intensity score by the percentage of cells staining. Samples were classified as positively or negative staining using the method described for CAIX expression.

iii) CD31, CD105 and Micro vessel Density Analysis

CD105 was carried out using the Leica Bond-Max automated immunostainer according to manufacturer's instructions. Tissue sections were stained using Protocol J60 on the autostainer. Tissue sections were baked to retrieve antigen, dewaxed, washed in epitope retrieval solution

then incubated with peroxidase for 5 minutes to block endogenous peroxidase. The specificity of staining was optimized in control tissue by evaluating staining with different combinations of antigen retrieval times (20 minutes or 40 minutes), buffer pH (6.0 or 9.0) and dilution (1: 50, 1:100, 1:150). Tissue sections were incubated with the primary antibody for 60 minutes followed by the secondary antibody for 8 minutes. Sections were washed with the manufacturer's washer buffer (diluted 1:10). Sections were incubated with the manufacturer's polymer for 8 minutes, incubated with a red chromagen for 10 minutes and counterstained with haematoxylin for 5 minutes. Slides were washed in distilled water and mounted with a coverslip using Aquamountant. Full face rectal tumour sections incubated with the antibody were used as a positive control and rectal tumour without the antibody was used as a negative control.

Immunohistochemical expression of the pan-endothelial marker CD31 was performed using a previously optimized protocol at a dilution of 1:2000, according to the general methods used for CD105 employing heat antigen retrieval, incubating with an epitope retrieval solution with pH 9.0 for 20 minutes and DAB as a chromagen. Slides were washed and mounted as described previously. Full face rectal tumour sections known to stain positively for CD31 were used as control tissue (with the antibody as a positive control and without the antibody as a negative control).

Micro vessel density (MVD) was evaluated in the CD31 and CD105 stained tissue sections using the Chalkley counting method [261]. Stained tissue sections were evaluated under a double-headed light microscope at 100 x magnification by two assessors and 3 micro vessel hotspots identified in each biopsy by consensus agreement. A Chalkley graticule was employed over each hot-spot and orientated so that the maximum number of points were on, or within stained vessels at 250 x magnification. Two assessors then independently counted the number of points falling on staining vessels. In this analysis, stained vessels with a clearly defined lumen or well

defined linear shape were counted as vessels but single endothelial cells or vessel lumens were not counted as vessels [430, 431]. A mean count was derived from the 3 hotspots of greatest micro vessel density for each tumour. The mean of the two assessors' scores was used to derive the final micro vessel count.

D4 Phospho-Akt and Phospho-PRAS40

To facilitate optimization of immunohistochemical staining for the phospho-Akt and phospho-PRAS 40 antibodies for immunohistochemical staining, colorectal cancer cell lines with known constitutive activation of the PIK3CA gene (RKO and HCT116) which, from first principles would be expected to express the activated/phosphorylated from of Akt and PRAS 40 were cultured and cell lysates were prepared for analysis of phospho-Akt and phospho-PRAS 40 expression using Western blotting by Dr Rebecca Carter. Western Blotting confirmed the presence of a band at 60kDa, the expected molecular weight for phospho-Akt and the presence of a band at 40 kDa for phospho-PRAS40.

On this basis, RKO and HCT cell pellets were prepared for imunohistochemical examination and optimization of phospho-Akt and phospho-PRAS prior to staining of study biopsies and these positively staining cells were used as controls. Cell pellets were paraffin embedded by Ms Leticia Campo and tissue sections cut and mounted on glass slides by Dr Thomas Macgregor. Immunohistochemical expression of the phospho-Akt and phospho-PRAS40 proteins was performed using the general methods previously described using Protocol F on the autostainer. Tissue sections were heated to retrieve antigen, dewaxed, washed in epitope retrieval solution then incubated with peroxidase for 5 minutes. The specificity of staining was optimized in cell pellets by evaluating staining with different combinations of antigen retrieval times (10 minutes or 20 minutes), buffer pH(6.0 or 9.0) and dilutions (1: 50, 1:100, 1:200 for phospho-Akt and 1:200, 1:400, 1:800 for phospho-PRAS40). Tissue sections were incubated with the primary antibody for 15 minutes followed by the secondary antibody for 8 minutes. Sections were washed with the

manufacturer's washer buffer (diluted 1:10). Sections were incubated with the manufacturer's polymer for 8 minutes, incubated with DAB for 10 minutes and counterstained with haematoxylin for 5 minutes. Slides were washed in distilled water and mounted with a coverslip using Aquamountant. Staining was repeated on 3 separate occasions under the same conditions to ensure consistency of staining across runs.

2E General methods for Imaging of liver metastases

E1 Study Population

Patients with a diagnosis of unresectable liver-only or liver-dominant colorectal liver metastases having already consented to participate in the Phase 3 randomised controlled trial, FOXFIRE, were recruited to an imaging sub-study designed to evaluate the feasibility of measuring changes in the perfusion of colorectal liver metastases using pCT liver scans occurring in response to therapy. This study was designed, regulatory approvals obtained and patient recruitment led by myself under the supervision of the CI, Ricky Sharma and the TMG. Specific inclusion criteria for recruitment to the perfusion CT sub-study were as follows:

- Patients having consented to participate in the FOXFIRE clinical trial but not yet started chemotherapy treatment in the trial.
- Serum creatinine and calculated glomerular filtration rate $\leq$ upper limit of normal (ULN) in blood tests performed up to 29 days before entry into the FOXFIRE clinical trial.
- Liver metastasis 1.0-4.0 cm in cranio-caudal diameter on imaging performed up to 29 days before entry into the FOXFIRE clinical trial.

Exclusion criteria were defined as follows:

- True allergy to intravenous iodinated CT contrast
- Active medical or psychological illness that would render the patient unsuitable for the additional imaging proposed in this pilot study, at the discretion of the investigator

E2 Study Schedule

All patients in the FOXFIRE trial and imaging sub-study were scheduled to receive 12 cycles (6months) of oxaliplatin and modified de Gramont chemotherapy, each cycle being scheduled 2 weeks apart, with a standard contrast-enhanced CT after 3 months of therapy to assess radiological response according to RECIST criteria Version 1.0. Selective Internal radiotherapy was scheduled on Day 3 of the 2nd or 3rd cycle of chemotherapy where possible.

Figure 13 Schedule for perfusion CT liver scans and therapy in Arm A and Arm B of the FOXFIRE imaging sub-study

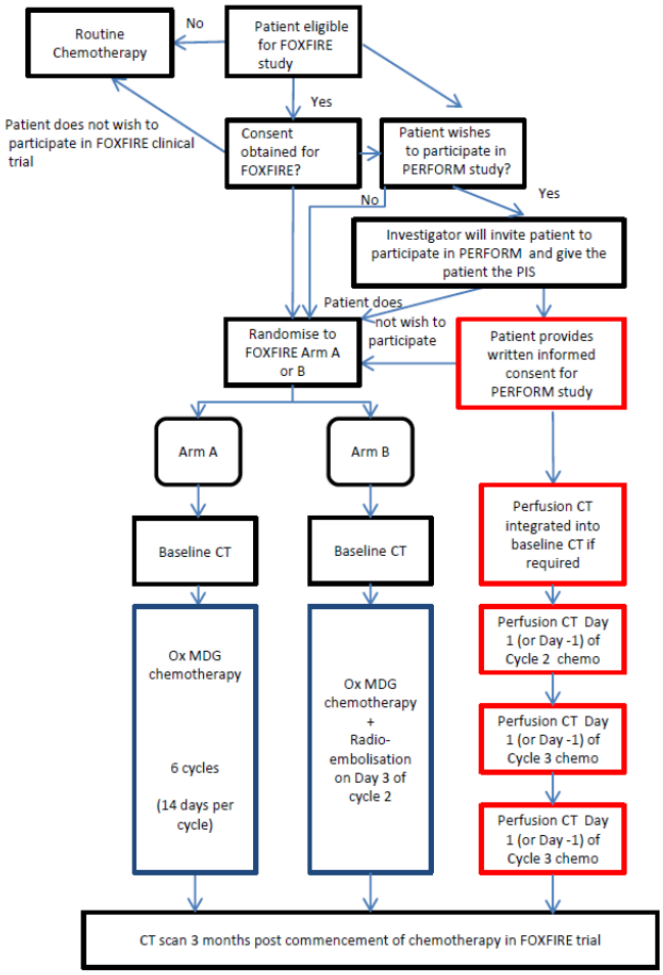

Abbreviations
OxMDG = Oxaliplatin and Modified de Gramont chemotherapy
PIS = Participant Information Sheet

E3 Perfusion CT Liver

Perfusion CT scans were scheduled at 4 time points: baseline (pre-treatment), Day 1 Cycle 2 chemotherapy, Day 1 Cycle 3 chemotherapy and Day 1 Cycle 5 chemotherapy (in all cases prior to the administration of chemotherapy the same day).

Patients were asked to fast for 2 h prior to the pCT, except to drink a litre of water before the scan. The pCT scan was performed on a 64-row detector GE Medical Light-Speed VCT scanner. Initially, a CT study of the abdomen was acquired without contrast in order to localise the CT spatial co-ordinates of a liver metastasis suitable for perfusion imaging. A metastasis suitable for perfusion imaging was identified by the supervising clinician, who specified the spatial CT co-ordinates for the dynamic study, with the aim of centering the dynamic scan over the metastasis, if possible, to cover the entire metastasis. An abdominal compression band was applied to the patient's abdomen to help minimise motion due to breathing. Patients were asked to hold their breath for 45 s or where this was not possible, to take shallow breaths as required. Dynamic images of the liver were acquired starting 10 s after commencement of intravenous contrast using 60-100ml of an iodine based contrast agent (Omnipaque 300) injected at a rate of 5 ml/s using a pump injector (Medrad) via a 20 Guage cannula. Eight contiguous sections, each collimated at 5 mm (providing a z axis coverage of 4 cm) were acquired at 1 s intervals for 45 s by using a cine-mode acquisition (120 kv, 60 mA, 1 second rotation speed, 36 cm field of view and 512 x 512 mm matrix, 20 mSV effective dose).

Images were transferred to a GE Advantage Windows Workstation (Version 4.2, GE Healthcare Technologies). Viewing and analysis was performed using the "Liver Protocol" of GE Perfusion 3.0 software (GE Health care Technologies) which is based on dual vessel input function, except for scans in which the portal vein was not included (the "Body Protocol" which uses a single arterial input was employed for these scans). A processing threshold of -45 to 120 Hounsfield Units (HU)

was used to view the images in order to optimise soft tissue visualisation. An arterial input was manually defined in a single slice freehand to place a circular region of interest (ROI) measuring 12-15mm² in the centre of the aorta at the level of the coeliac axis. Cine images were reviewed to check that the ROI did not encompass intra-arterial calcification or become displaced outside the arterial wall due to motion. The software was used to automatically derive an arterial enhancement curve and to define the pre-enhancement image (arrival time of contrast). The end of the first pass or post-enhancement image was manually selected by reviewing the arterial enhancement curve and identifying the lowest point after the peak of arterial contrast enhancement[425].

A second circular ROI measuring 12-15mm² was defined in the portal vein (where present) to derive a portal venous input (see figure 14). Cine images were reviewed to check whether the ROI became displaced outside the portal vein due to motion. Scans which did not cover the portal vein or where there was significant motion affecting the portal venous input were analysed according to the Body Protocol, which depends on a single arterial input to derive perfusion parameters. Parameter maps were produced for Blood Flow (BF), Blood Volume (BV) and Mean Transit Time (MTT) and Hepatic Arterial Fraction (HAF), with each pixel representing a parameter value. Parameter values for the tumour were calculated by defining a tumour ROI. A tumour region of interest was defined freehand by drawing around the perceived margins of the selected metastasis in each of 8 CT slices in the z axis. The tumour ROI was drawn on the CT image defined by the end of the first pass for consistency and since tumour contrast enhancement was usually greatest at the end of the arterial enhancement phase. The entire temporal sequence of images were reviewed for each slice, in order to evaluate intra-sequence motion and try to keep the ROI within the margins of the tumour on all slices where possible. The tumour ROIs were independently delineated by a radiologist according to the same method.

Figure 14 Delineation of regions of interest in the aorta, the portal vein and liver metastasis to derive arterial enhancement, portal venous enhancement and tumour enhancement curve and to generate BF, BV, MTT and HAF parameter maps

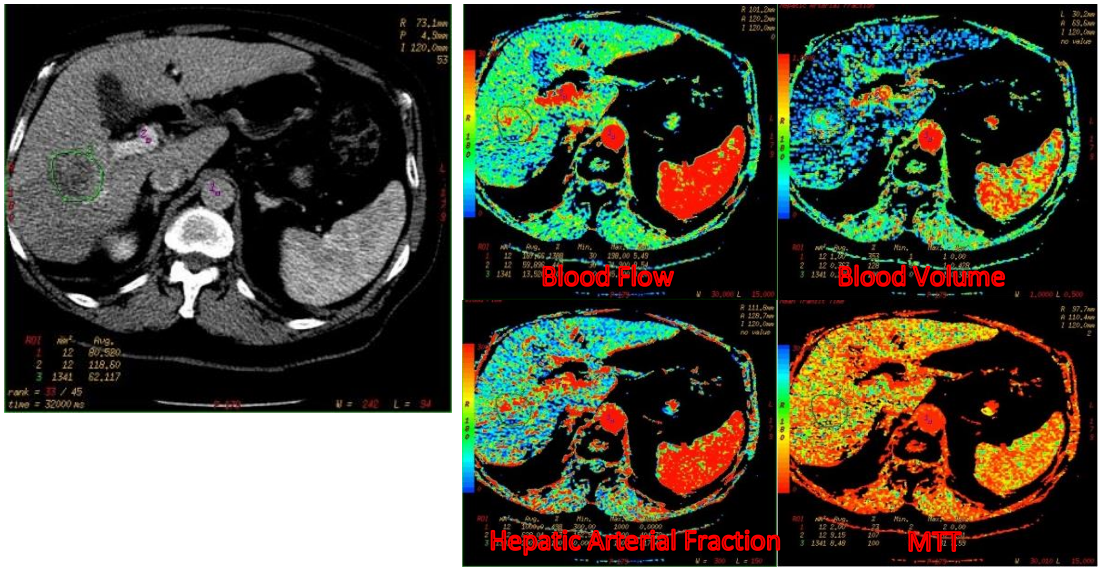

The mean parameter values for each tumour ROI in each CT slice were manually entered into an excel spreadsheet for each scan and each patient for further analysis. The arterial input function curves and portal venous input curves were extracted from the software by viewing the mean enhancement value(HU) for the arterial and portal vein ROI in each image in the temporal sequence and manually entering it into an excel spreadsheet before plotting the data in graphical format. In order to compare parameter maps from sequential scans in the same patient, screen save shots of the colour parameter maps and CT images for each slice were saved and imported to Image J (JAVA based software).

Intra-sequence motion was evaluated scan and scored for each pCT scan. As it was not possible to correct for motion using GE software, the DICOM data for each pCT was exported electronically and motion-corrected using a 2-step method, developed and applied by Dr Amalia Cifor. The first step involved rigid registration of image sequences from different time-points and corrected for motion in the z axis (cranio-caudal) using a technique called 'local phase', which is independent of

the phase of contrast enhancement and emphasised structures. The second step involved a non-linear registration based on both similarity of local phase and image intensity (dependent on contrast enhancement) to produce a reformatted volume. Motion corrected scans were re-imported for repeat analysis using GE perfusion software.

In order to perform advanced image analysis, the parameter maps first had to be converted to grayscale images, saved as screen save DICOM images using the GE Perfusion 3.0 software and subsequently saved to an external storage device. CT images for each of the 8 z axis slices were also saved and extracted in this format. The Matlab program previously referred to was customised for further analysis of these images. In addition to the functions already described, this program was developed to allow freehand delineation of each metastasis on a grayscale parameter map and propagation of a concentric outline within or outside the initial delineation and segmentation of the ring structure (of selected width or drawn freehand) and associated mean parameter values between the two outlines.

Figure 15 Illustration of segmentation of a metastasis (1), propagation and extraction of rim 0.5cm outside metastasis (2), rim 0.5cm inside outline of metastasis (3) and corresponding core (3) on perfusion CT image

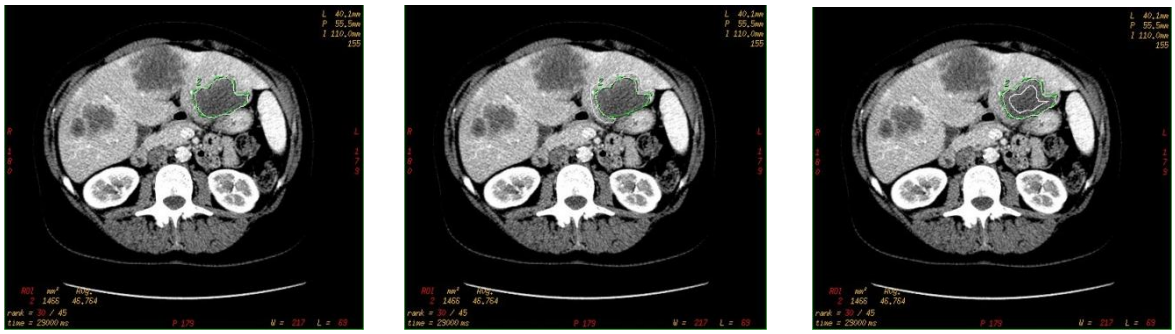

(1) **(2)** **(3)**

For each scan selected, the single metastasis selected and outlined for perfusion CT analysis using the GE software was delineated in Matlab, using the ROI contours saved in the GE software to ensure consistency of delineation. The whole metastasis, a rim 0.5cm around the outline of the

whole metastasis and core/rim 0.5cm inside the whole metastasis were separately segmented and the co-ordinates of the segmentations applied to the corresponding grayscale perfusion parameter maps for BF, BV, MTT and HAF to extract mean perfusion parameters for the whole metastasis, the outer rim, the inner rim and core on each CT slice in which the metastasis was present. The weighted mean BF, BV, MTT and HAF of the segmented volume of the metastasis across all 8 CT slices (3D) were derived as for rectal pCT scans. Mean values and standard deviations were entered into an EXCEL spreadsheet for further analysis.

3 Results

3A Assessment of Toxicity and Activity of Nelfinavir and Hypo-fractionated Radiotherapy

In this chapter, the hypothesis that the combination of nelfinavir and hypo-fractionated pelvic radiotherapy is tolerated with acceptable toxicity in humans with rectal cancer is tested. The effectiveness of treatment with nelfinavir and concurrent hypo-fractionated pelvic radiotherapy (followed by systemic chemotherapy after a minimum of 14 days where indicated) for patients with T3/4 N0-2 M1 rectal cancers using conventional tools of response assessment (namely pelvic MRI) is evaluated. The feasibility of using quantitative TCD measurement in post-treatment rectal tumour biopsies as an early pathological biomarker to evaluate the efficacy of pelvic radiotherapy in combination with a novel radio-sensitizer, such as nelfinavir, is assessed. Since the premise on which nelfinavir is being investigated as a clinical radio-sensitizer is the pre-clinical finding that nelfinavir can improve tumour vascularity and reduce tumour hypoxia in tumours with activation of the RAS-PI3K-Akt pathway, immunohistochemical tissue markers of hypoxia (CAIX and HIF 1-α), vascularity (CD31 and CD105a MVD) and activation status of the Akt pathway are evaluated in rectal tumour biopsies before and after treatment and association with treatment response is explored. Specifically phospho-Akt expression using immunohistochemistry is evaluated and compared with expression of the downstream effector protein, phospho-PRAS40.

A1 Patient recruitment and Baseline Characteristics

Ten patients with metastatic rectal cancer were recruited to a clinical study designed to assess the tolerability of nelfinavir 1250 mg bd for 7 days before and 7 days concurrent with 25 Gy in 5# radiotherapy to the pelvis (followed by systemic chemotherapy where appropriate). Table 23 summarises the patient characteristics at study entry. The main rationale for delivering a short course of pelvic radiotherapy in all 10 cases was to palliate local tumour symptoms, although for

2 of the 10 patients (with liver-only metastases), an additional aim was to downstage the primary tumour with a view to considering delayed resection of the primary and metastatic disease.

Table 23 Summary of baseline characteristics of patients recruited to the study

Characteristic	No of patients (N=10)	(%)
Age (years)		
Median	65	
Range	45-81	
Gender		
Male	5	50
Female	5	50
ECOG Performance status		
0	4	40
1	6	60
Sub-site of tumour in rectum		
Low	7	70
Mid	2	20
Upper	1	10
MRI defined T stage		
T3	4	40
T4	6	60
MRI defined N stage		
N0	2	20
N1	3	30
N2	5	50
Extramural vascular invasión (EMVI)		
Yes	5	50
No	5	50
Circumferential Resection Margin Status (MRI)		
Involved/threatened	8	80
Clear	2	20
Sites of metastatic disease (CT)		
Liver	8	80
Distant lymph nodes	5	50
Lung	6	60
Other	1	10

Abbreviations: MRI magnetic resonance imaging; CT computed tomography

A2 Toxicity of Nelfinavir and Hypo-fractionated Radiotherapy

It was hypothesised that the rates of toxicity associated with nelfinavir and concurrent SCRT to the pelvis would not significantly exceed the historical rates of toxicity associated with SCRT alone. Defining historical rates of toxicity due to SCRT in rectal cancer for comparison is somewhat challenging since this schedule has most commonly been used in patients proceeding to immediate surgery rather than proceeding to delayed surgery or as palliative treatment. Only one prospective clinical trial [432]and retrospective studies have reported rates of toxicity due to SCRT and delayed surgery[33, 34].

When comparing rates of acute toxicity due to radiation and nelfinavir in this study with rates of acute toxicity due to SCRT and delayed surgery alone in historical series, for a fair comparison it was considered necessary to limit the toxicities used for the analysis to Grade 3 or 4 non-laboratory toxicities thought to be causally linked to radiation or nelfinavir (but not chemotherapy) within 3 months of study treatment. From the viewpoint of what would be a clinically acceptable level of acute toxicity for the combination of nelfinavir and short-course radiation, Phase I radiotherapy dose escalation studies (with or without radiosensitising drugs) typically define the acceptable dose for a regime(MTD) as the cohort in which <1/3 patients have dose limiting toxicity (defined as Grade 3/4 toxicity)[433]. Using this principle, it was pre-specified that less than one third of patients receiving nelfinavir and radiotherapy should have dose-limiting toxicity (necessitating interruption or early cessation of either nelfinavir or radiotherapy) to demonstrate acceptable tolerability of the regime.

Table 24 summarises compliance with the treatment schedule. Six of the 10 patients received all of the nelfinavir and the radiotherapy as per-protocol, without missing any doses. One patient (ST1003) missed one dose of nelfinavir and another (ST1008) missed their last two doses of nelfinavir (for reasons other than toxicity). Two patients (20%) stopped taking nelfinavir early

because of toxicity; patient ST1001 stopped a day early because of the development of a rash and patient ST1010 stopped 10 days early due to vomiting. All patients completed radiotherapy per-protocol.

Table 24 Summary of patient compliance with nelfinavir and radiotherapy treatment schedules

Patient number	Doses of Nelfinavir delivered	Reason stopped Nelfinavir	Reason for missed doses	Dose of radiotherapy received
1	25	Toxicity	Drug skin reaction.	25 Gy in 5#
2	28	End of treatment	-	25 Gy in 5#
3	27	End of treatment	One dose missed – reason unknown.	25 Gy in 5#
4	28	End of treatment	-	25 Gy in 5#
5	28	End of treatment	-	25 Gy in 5#
6	28	End of treatment	-	25 Gy in 5#
7	28	End of treatment	-	25 Gy in 5#
8	26	End of treatment	Drowsy following small seizure (known Epilepsy)	25 Gy in 5#
9	28	End of treatment	-	25 Gy in 5#
10	8	Toxicity	Patient stopped study drug due to vomiting.	25 Gy in 5#

Table 25 summarises toxicities occurring within 6 months of nelfinavir and SCRT. Gastro-intestinal toxicities were the most common type of toxicity, in particular diarrhoea and nausea/vomiting, which are both documented side effects of pelvic radiotherapy and nelfinavir individually. Fatigue and urinary symptoms were common, which are also anticipated side effects from pelvic radiotherapy.

Table 25 Summary of acute non-haematological toxicities within 6 months of nelfinavir

Toxicity	Grade 0-2	Grade 3	Grade 4
Nausea/vomiting	13	1	-
Diarrhoea	13	2	-
Proctitis	3	--	-
Tenesmus	1	-	-
Urinary symptoms	6	-	-
Rash	5	1	-
Fatigue	9	-	-
Anorexia	2	-	-
Fever	2	-	-
Pain	5	1	-
Peripheral neuropathy	3	-	-
Labyrinthitis	1	-	-
Dizziness	1	-	-
Trismus	1	-	
Insomnia	1	-	-
Bleeding/bruising	2	-	-

There were no Grade 4 toxicities within 6 months of therapy. Five patients had Grade 3 non-haematological toxicities (summarised in table 26) 28 days of nelfinavir and SCRT. Patient ST1001 developed a widespread maculopapular rash on the last day of nelfinavir and radiotherapy, which was typical of a drug reaction and thought to be related to nelfinavir, as the patient had not commenced any other new medication. The nelfinavir was stopped and the patient given a course of oral steroids and antihistamines; the rash resolved fully on this treatment. Patient ST1003 was admitted to hospital with Grade 3 diarrhoea (>10 stools a day) 23 days after completion of radiotherapy and nelfinavir, 7 days after commencement of oxaliplatin and 5FU chemotherapy. The patient was not dehydrated; loperamide was administered, the diarrhoea

settled and the patient was discharged after 2 days. This patient had diarrhoea at baseline (up to 4 stools a day) related to his rectal tumour; the episode of Grade 3 diarrhoea (representing a Grade 2 increase) was considered to be related to chemotherapy and possibly related to radiotherapy but unrelated to nelfinavir. The same patient had a further episode of Grade 3 diarrhoea 6 weeks after completion of nelfinavir and radiation, which was again thought to be related to chemotherapy but possibly related to radiotherapy. This was also managed with loperamide. Patient ST1005 developed Grade 3 diarrhoea 4 days after completion of nelfinavir and radiotherapy; the patient was not dehydrated, loperamide was administered and the diarrhoea improved to ≤ Grade 2 within a day. The diarrhoea was considered to be causally related to radiotherapy and nelfinavir rather than the tumour. Three days after completion of nelfinavir and radiotherapy, Patient 9 developed Grade 3 perianal pain due to haemorrhoids. This required treatment with oral analgesia, topical ointment containing local anaesthetic and steroids as well as nursing support. Symptoms persisted for 3 months in total. This toxicity was felt to be causally related to the radiotherapy component of the treatment. Patient 10 was admitted to hospital with grade 3 vomiting and associated dehydration 3 days after commencing nelfinavir; although the patient had Grade 1 nausea and vomiting prior to commencement of nelfinavir, it was initially thought that the nelfinavir may be causally related and this treatment was discontinued. The patient was treated with intravenous fluids and anti-emetics and the vomiting improved but did not resolve prior to, during or after the pelvic radiotherapy. This patient had extensive liver metastases and it was considered likely that the nausea and vomiting were due to partial gastric outlet obstruction from hepatomegaly.

Table 26 Summary of Grade ≥ 3 non-haematological toxicities within 28 days of therapy, with details of causality and onset in relation to study treatment

Patient number	Event	CTCAE grade	CTCAE grade at baseline (if any)	Increase in CTCAE grade from baseline	Nelfinavir causality	Disease causality	RT causality	Time after last RT
1	Skin Reaction	3	-	+3	Probably related	Probably not related	Definitely not related	Last day of RT
3	Diarrhoea	3	1	+2	Probably not related	Possibly related	Possibly related	Within 28 days
5	Diarrhoea	3	-	+3	Probably related	Probably not related	Probably related	Within 28 days
9	Peri-anal Pain	3	-	+3	Probably not related	Probably not related	Probably related	Within 28 days
10	Vomiting	3			Possibly related	Probably related	Definitely not related	Started whilst taking NFV

Tables 27 a, b and c summarise laboratory abnormalities occurring within 28 days of nelfinavir and radiotherapy.

Table 27 Summary of Laboratory abnormalities within 28 days after completing nelfinavir and radiotherapy

(a) Frequency of abnormal blood results on baseline blood tests with CTCAE grade

Blood test	Grade 1	Grade 2	Grade 3	Total
Haemoglobin	1	0	0	**1**
Neutrophils	1	0	0	**1**
Lymphocytes – Lymphopenia (low)	1	0	0	**1**
Sodium – Hyponatremia (low)	1	0	0	**1**
Potassium – Hyperkalaemia (high)	1	0	0	**1**
AST	1	0	0	**1**
ALT	1	0	0	**1**
Alk-Phos	2	1	0	**3**
Fasting glucose	1	0	0	**1**
Albumin	0	0	0	**0**
Magnesium	0	0	0	**0**

(b) Frequency of abnormal blood results on day 7 nelfinavir with CTCAE grade

Blood test	Grade 1	Grade 2	Grade 3	Total
Haemoglobin	2	0	0	**2**
Neutrophils	1	0	0	**1**
Lymphocytes – Lymphopenia (low)	1	3	2	**6**
Sodium – Hyponatremia (low)	1	0	1	**2**
Potassium – Hyperkalaemia (high)	2	0	0	**2**
AST	2	0	0	**2**
ALT	2	1	0	**3**
Alk-Phos	2	1	0	**3**
Fasting glucose	2	1	0	**3**
Albumin	0	0	0	**0**
Magnesium	1	0	0	**1**

(c) Frequency of abnormal blood results 28 days after end of radiotherapy and nelfinavir

Blood test	Grade 1	Grade 2	Grade 3	Total
Haemoglobin	3	0	0	**3**
White blood cells	2	0	0	**2**
Neutrophils	1	0	0	**1**
Lymphocytes – Lymphopenia (low)	4	1	1	**6**
Platelets	1	0	0	**1**
Sodium – Hyponatremia (low)	0	0	1	**1**
Potassium – Hyperkalaemia (high)	1	0	0	**1**
AST	2	0	0	**2**
ALT	1	0	0	**1**
Alk-Phos	1	1	0	**2**
Fasting glucose	0	0	0	**0**
Albumin	0	1	0	**1**
Magnesium	0	0	0	**0**

Lymphopenia was the most commonly occurring laboratory abnormality, with 2 patients (2 and 3) developing Grade 3 lymphopenia. Patient 2 had Grade 1 lymphopenia at baseline and developed grade 3 lymphopenia 2 months after completion of nelfinavir and radiotherapy, whilst receiving chemotherapy. Patient 3 developed Grade 3 lymphopenia on the last day of nelfinavir and radiotherapy; this persisted on a blood test one month following completion of therapy. In both cases, the lymphopenia developed in the context of a normal total white cell count and the patients had no evidence of active infection. These abnormalities were considered to be possibly related to nelfinavir and/or radiotherapy. No other Grade 3 or 4 haematological toxicities were

observed within 3 months of nelfinavir. Two patients developed Grade 3 hyponatremia (patients 1 and 7) within 3 months of nelfinavir and radiotherapy. Patient 1 developed Grade 3 hyponatremia 5 weeks after completion of nelfinavir; patient 7 had Grade 1 hyponatremia at baseline and developed Grade 3 hyponatremia on the last day of radiotherapy. In neither case was the laboratory abnormality associated with clinical symptomatology; the findings were considered to be probably unrelated to nelfinavir. A number of Grade 1 or 2 abnormalities in liver function tests were observed within 3 months of therapy but since 8 of the patients had liver metastases these were considered likely to be disease related; of note, there were no Grade 3 hepatotoxicities. Since a known long term consequence of nelfinavir is the development of Diabetes Mellitus, fasting glucose was checked during nelfinavir treatment and at follow-up. One patient (patient 1, who was known to have Diabetes Mellitus) had elevated blood glucose at baseline. Three patients had Grade 1 or 2 hyperglycaemia after 7 days of nelfinavir but blood glucose was normal on subsequent testing, 28 days after completion of therapy.

A3 Clinical response assessment

Nine of 10 patients successfully completed a MRI scan of the pelvis 8 weeks after completion of nelfinavir and radiotherapy to assess radiological response of the primary tumour. Patient 10 deteriorated due to progressive liver metastases and died 5 weeks after completion of therapy. Since patients were permitted to commence systemic chemotherapy for metastatic disease ≥ 14 days after completing nelfinavir and radiotherapy, details of chemotherapy received between the end of protocol therapy and the MRI scan at 8 weeks are summarised in table 28. Inter-observer agreement between two independent radiologists, who scored tumour regression grade on MRI scan (mrTRG) after radiotherapy according to a 5 point scoring system, was substantial/good, with a weighted kappa score of 0.79. In cases of disagreement, a consensus score was derived by seeking review by a third expert radiologist (scores are summarised in table 29). Five of 9 evaluable patients had a good mrTRG score.

Table 28 Number of Cycles of Chemotherapy between end of study therapy and MRI scan

Patient number	Type of Chemotherapy	Number of Cycles	Frequency
1	oxaliplatin/modified de Gramont	3	2 weekly
2	oxaliplatin/modified de Gramont	3	2 weekly
3	oxaliplatin/modified de Gramont	3	2 weekly
4	capecitabine/oxaliplatin	2	3 weekly
5	capecitabine/oxaliplatin	1	3 weekly
6	capecitabine/oxaliplatin	1	3 weekly
7	oxaliplatin/modified De Gramont	2	2 weekly
8	oxaliplatin/modified De Gramont	2	2 weekly
9	-	0	-
10	-	0	-

Table 29 Independent mrTRG scores and classification (good/poor) on MRI scans 8 weeks after completion of nelfinavir and radiation by 3 independent radiologists for individual patients

Patient number	Radiologist 1 mrTRG score	Radiologist 2 mrTRG score	Radiologist 3 mrTRG score	Consensus mrTRG score	Consensus mrTRG class
1	2	3	3	3	good
2	5	5		5	poor
3	1	1		1	good
4	3	4	4	4	poor
5	1	1		1	good
6	4	4		4	poor
7	4	4		4	poor
8	1	2	2	2	good
9	2	2		2	good
10*	-	-	-	-	-

***Patient 10 died prior to 8 week MRI scan so mrTRG not assessed**

Agreement	Expected agreement	Weighted Kappa	Std. Error	Z	Prob>Z
91.67%	60.19%	0.7907	0.2341	3.38	0.0004

A baseline tumour T stage of ≥T3c on MRI scan has been associated with a greater likelihood of poor mrTRG score on MRI scan after radiotherapy[123]. In some studies *KRAS* mutations have been associated with poor response to radiotherapy in rectal tumours[292, 295]. Systemic chemotherapy may result in significant tumour regression of advanced rectal cancers[39]. Therefore, the pattern of association with each of these features and response to nelfinavir and radiotherapy (mrTRG) in the study patients was explored (see table 30). Three out of 4 patients

with baseline ≤T3b tumours had a good mrTRG score as opposed to 2 of 5 evaluable patients with T4 tumours. The mean number of cycles of chemotherapy delivered before the 8 week MRI scan was 1.8 for patients with a good mrTRG score (range 0 – 3) and 2 for patients with a poor mrTRG score (range 1-3). Seven out of 10 tumours (70%) had a *KRAS* mutation; 2 of 5 evaluable patients with a *KRAS* mutation had a good mrTRG response, whilst 2 of 3 patients with wild type *KRAS* had a good response. In summary, there was no consistent pattern of association between either baseline T stage of the rectal tumour, *KRAS* mutational status nor number of chemotherapy cycles administered with mrTRG score 8 weeks after radiotherapy.

Table 30 Baseline tumour stage on pelvic MRI, *KRAS* mutational status of the primary tumour and details of chemotherapy administered for individual patients in relation to mrTRG score on MRI pelvis 8 weeks after study therapy

Patient number	**Baseline MRI stage**	***KRAS* mutation status**	**No. cycles of chemotherapy between end of study therapy and MRI**	**mrTRG class**
1	T3b N2	Wild-type	3 x Ox/MDG	good
2	T4 N2	Mutant (G12Val)	3 x Ox/MDG	poor
3	T3a N2	Wild-type	3 x Ox/MDG	good
4	T3b N2	Mutant (G12Asp)	2 x CAPOX	poor
5	T3a N2	Mutant (G12Serc)	1 x CAPOX	good
6	T4 N2	Mutant (G12Val)	1 x CAPOX	poor
7	T4 N2	Wild-type	2 x Ox/MDG	poor
8	T4 N2	Mutant (G12Val)	2 x Ox/MDG	good
9	T4 N1	Mutant (G12C)	-	good
10	T4 N2	Mutant (G13Asp)	-	-

A4 Tumour Cell Density Analysis

TCD was evaluable in all of the pre-treatment rectal biopsy specimens and in 9 out of 10 post-radiotherapy biopsy specimens. One of the post-treatment biopsies contained adenoma cells but no malignant tumour cells, which is likely to have been the result of a sampling error (as the cancer arose within an adenoma); this sample wasn't included in subsequent analyses. TCD decreased between the pre-treatment and post-treatment rectal biopsies for all but one individual (see figure 16) with a median percentage reduction in TCD (normalised to pre-treatment TCD) of 60% (n=9). The median TCD decreased from 24.3% (IQR= 13.4-44.5%) at baseline to 9.2% (IQR=3.4-16.3%) after radiotherapy and nelfinavir (*P*=0.01; Wilcoxon signed-rank test).

Figure 16 Tumour Cell Density in rectal tumour biopsies for individual patients before treatment and 7 days after completion of nelfinavir and radiotherapy

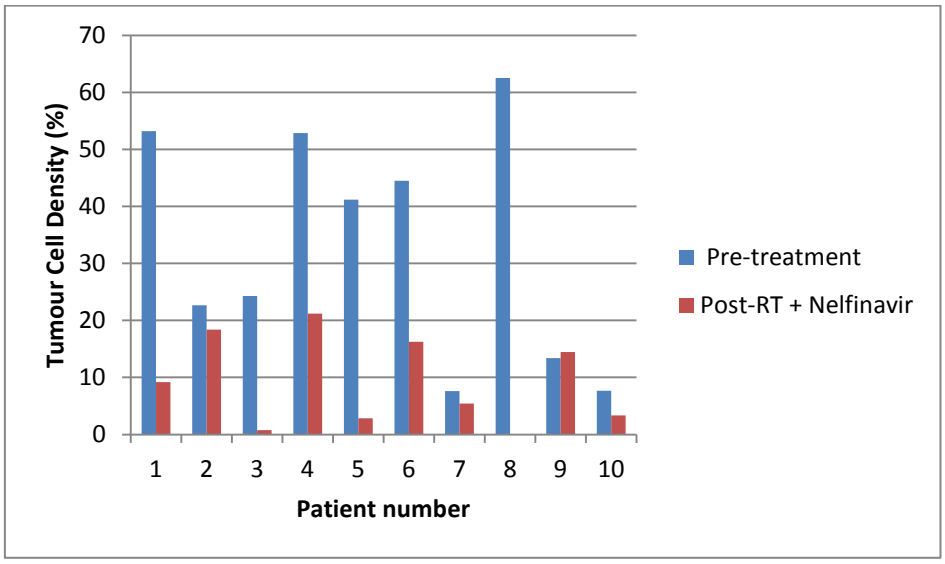

Since the technique for quantitative TCD scores not only tumour cells but other stromal components including necrosis and radiotherapy can result in tumour necrosis, the percentage of points scored as falling on areas of necrosis out of all the informative points was evaluated on pre-treatment and post-treatment rectal tumour biopsies for individual patients (see figure 17). Necrosis was present in 7 out of 10 pre-treatment biopsies and 5 out of 9 evaluable post-

treatment biopsies. There was >10% necrosis in the pre-treatment biopsies for patient 7 and 10 and in the post-treatment biopsies for patient 3 and 10; this was associated with a low TCD (<10%) in all cases.

Figure 17 Percentage necrosis in rectal tumour biopsies for individual patients before and 7 days after completion of nelfinavir and radiotherapy

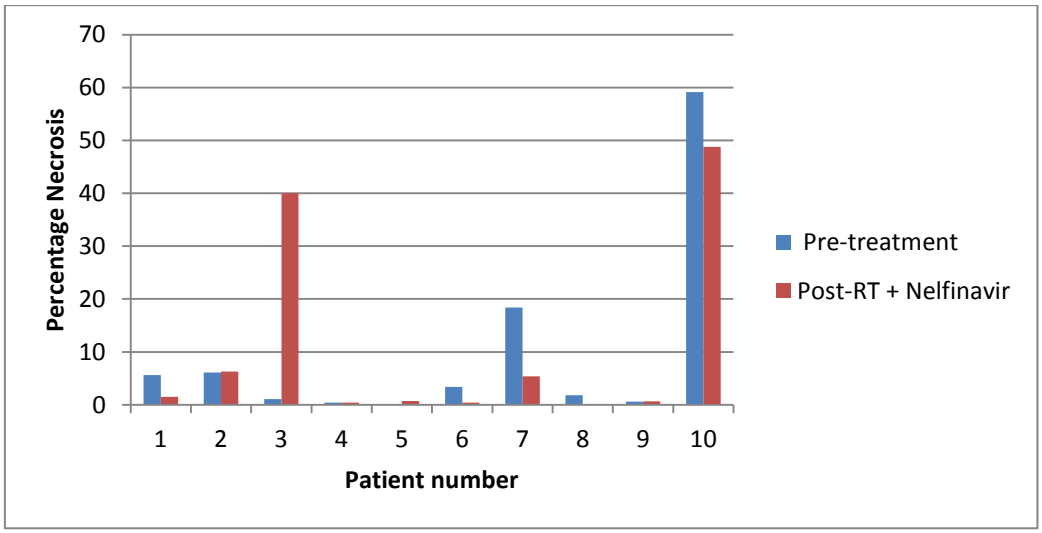

In order to evaluate the treatment effect of nelfinavir added to hypo-fractionated pelvic radiotherapy in patients with rectal cancer on tumour cell kill, TCD measurements before and the treatment combination in study patients were compared with TCD measurements in historical controls (19 rectal cancer patients treated in Leeds) who received 25Gy in 5 fractions of radiotherapy to the pelvis followed by surgery, typically within 7 days after the end of radiotherapy. The effect of radiotherapy alone on TCD was evaluated by comparison of this latter historical group of patients with another series of 22 historical controls (also treated in Leeds) who received no pre-operative radiotherapy prior to resection of their rectal tumours. TCD was evaluated in 31 pre-treatment biopsies and all post-treatment resection specimens. This comparison is represented graphically in figure 18.

Although it is not known which is the optimum method for TCD analysis ("greatest TCD", "luminal TCD" or "whole tumour TCD"), it would be expected that luminal TCD measurements would be most comparable with TCD measured in biopsies taken from the luminal surface of the tumour.

Evaluation of paired TCD measurements from historical controls who received no SCRT suggests that biopsies may underestimate luminal TCD measurements, whilst they overestimate whole tumour TCD measurements. Therefore, in this analysis, both the "whole tumour" TCD measurements and the "luminal TCD" measurements are presented for the historical controls.

Figure 18 Box and whisker plots illustrating median TCD (central line) with interquartile range (upper and lower boundaries of box) and range (upper and lower extent of whiskers) for rectal tumour biopsies in the SONATINA study before and after treatment with nelfinavir and RT, in comparison to two separate series of historical controls from Leeds (having received 25Gy in 5#) or no radiotherapy prior to surgical resection of the tumours. Spots indicate outliers. Post-treatment TCD in resection specimens for historical controls is shown for two methods of TCD analysis (based on analysis of whole tumour versus the luminal surface of the tumour).

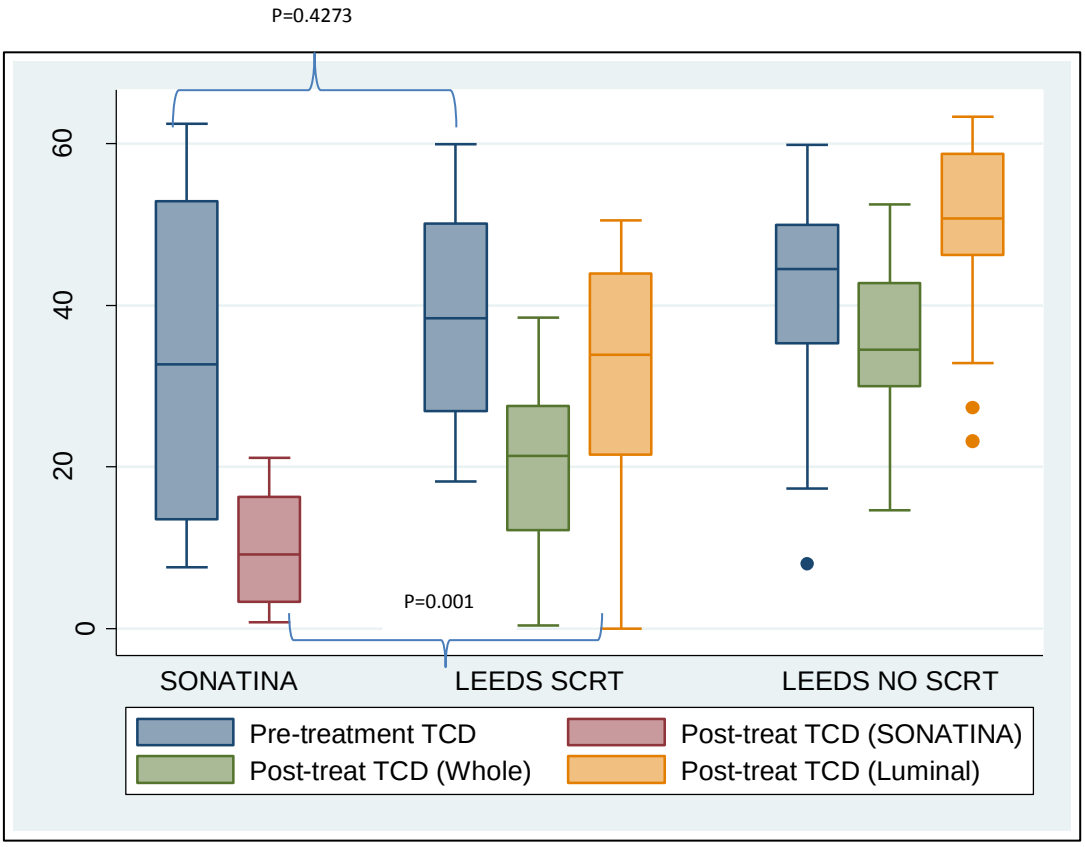

Hypo-fractionated radiotherapy alone had a significant effect on post-treatment TCD. The median TCD in pre-treatment biopsies from historic controls who received SCRT before surgery and historic controls who did not receive any radiotherapy prior to surgery were not statistically different (p=0.43, Mann-Whitney U test). Post-treatment TCD was significantly lower in the

patients who received SCRT than for the patients who did not receive SCRT (median 21.35 (range 0.35-38.46) versus 34.5(14.62-52.49) for 'whole' TCD analysis and median 33.9 (range 0-50.51) versus 50.78(23.18-63.37) for 'luminal' TCD analysis). Both the post-treatment 'whole' median TCD and the post-treatment 'luminal' median TCD were statistically different for these two groups at the 5% significance level (p=0.0002 and p=0.0001 respectively).

The median TCD in pre-treatment biopsies from historic controls who received SCRT before surgery and study patients who received nelfinavir and SCRT were not statistically different (p=0.45, Mann-Whitney U test). However, the median post-treatment TCD for the patients receiving SCRT and nelfinavir was significantly lower at 9.19 (range 0.77-21.18), compared to 21.35 (0.35-38.46) for the historical controls receiving SCRT patients post-treatment based on 'whole' TCD analysis and 33.9 (0-50.51) based on 'luminal' TCD analysis. The post-treatment median 'whole' TCD in tumours treated with radiotherapy and nelfinavir was statistically different from historical tumours treated with radiotherapy alone, at the 5% level (p=0.0113). The post-treatment median 'luminal' TCD was also statistically different between these two groups (p=0.0023). This suggests that the addition of nelfinavir to hypo-fractionated radiotherapy results in additional tumour cell kill compared to radiotherapy alone.

Tumour Cell Density (TCD) has not previously been evaluated as a surrogate for clinical response nor as a measure of tumour cell kill at an early time point in response to radiotherapy. An association between changes in TCD and radiological response using mrTRG assessment (on MRI scan at 8 weeks post-SCRT) was investigated (see table 31) by splitting the patients into two equally sized groups based on their TCD values; the median percentage decrease in TCD from pre to post-treatment was used as a cut off (i.e. 60%). In this preliminary analysis based on a small number of patients, the proportion of tumours demonstrating a good mrTRG score was not statistically different between the two groups of tumours- those with as ≥ 60% decrease in TCD

and those with a < 60% decrease in TCD between pre-treatment and post-treatment biopsies (p = 0.486, Fisher's exact test).

Table 31 Two by two table demonstrating association between percentage reduction in TCD (< median or ≥ median) and tumour response on MRI scan (mrTRG) 8 weeks after completion of study therapy

		Percentage decrease in TCD from pre to post treatment		
		<60% TCD decrease	≥60% TCD decrease	Total
mrTRG overall score	Good	1	3	**4**
	Poor	3	1	**4**
	Total	**4**	**4**	**8***

*Only 8 patients as patient ST1008 was non-evaluable for post-treatment TCD, and patient ST1010 died before the mrTRG assessment at 8 weeks post SCRT

A5 Hypoxia and Vascular Markers

Since hypoxia is associated with radiation resistance and nelfinavir has been demonstrated in pre-clinical studies to improve tumour radio sensitivity by a mechanism involving improvement in tumour perfusion and a reduction in hypoxia[229], MVD (using CD31 and CD105a) and immunohistochemical markers of hypoxia (CAIX and HIF- 1α) were evaluated in rectal tumour biopsies before and after treatment with nelfinavir and hypo-fractionated pelvic radiotherapy. Figure 19 illustrates micro vessel staining of tumour biopsies with the endothelial markers CD31 and CD105a. There was less non-specific staining using CD105a in comparison to CD31 and inter-observer agreement for MVD scores was greater for CD105a than CD31 (see table 10). MVD scores were lower using CD105a than CD31 both on pre-treatment and post-treatment biopsies, which can be explained by the greater specificity of CD105a for vessels. There was a statistically significant increase in mean MVD assessed using CD105a between pre-treatment and post-treatment biopsies but no significant difference in mean MVD score using CD31 (see table 33).

Figure 19 Panel shows positive micro vessel staining of rectal biopsy tissue with (a) CD105a and (b) CD31 (shown at x 20 magnification)

(a) **(b)**

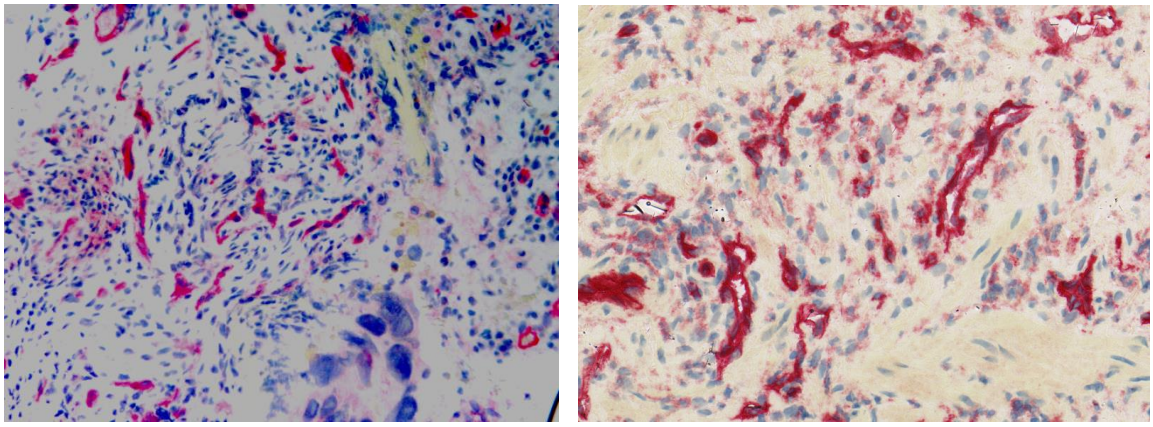

Table 32 Inter-observer agreement for Microvessel density analysis using weighted kappa score

MVD analysis	Agreement	Kappa	P-value
CD105	93.39%	0.7440	<0.00001
CD31	90.30%	0.5600	<0.00001

Table 33 Microvessel density before and after nelfinavir and radiotherapy using CD105 and CD31 immunohistochemistry (scores represent mean of two observers' scores)

	Mean MVD Pre-treatment (SD)	Mean MVD Post-treatment (SD)	Mean difference (95% CI)	Paired *t* test
CD105 MVD	4.28 (0.67)	5.35 (1.67)	1.07(0.13 to 2.12)	P=0.046
CD31 MVD	6.11 (0.83)	5.98 (1.85)	-0.13(-1.73 to 1.47)	P=0.857

Immunohistochemical staining of biopsies and control tissue for CAIX and HIF1-1α is illustrated in Figures 20 and 21. Three tumours demonstrated positive CAIX expression before treatment, in comparison to 4 tumours post-treatment; 4 demonstrated positive expression of HIF-1 α before treatment, in comparison to 6 post-treatment (see table 34). There was no statistically significant

difference in the median composite score for CAIX or HIF-1α between pre-treatment and post-treatment rectal biopsies (see table 35).

Figure 20. Illustration of (a) positive membrane staining with CAIX antibody in positive control (renal cell carcinoma) (b) absent membrane staining in negative control (renal cell carcinoma without CAIX antibody (c) example of weak positive CAIX expression (d) strong positive expression and (e) absent (negative) expression of CAIX on immunohistochemical staining of pre-treatment rectal tumour biopsies (all shown at x20 magnification)

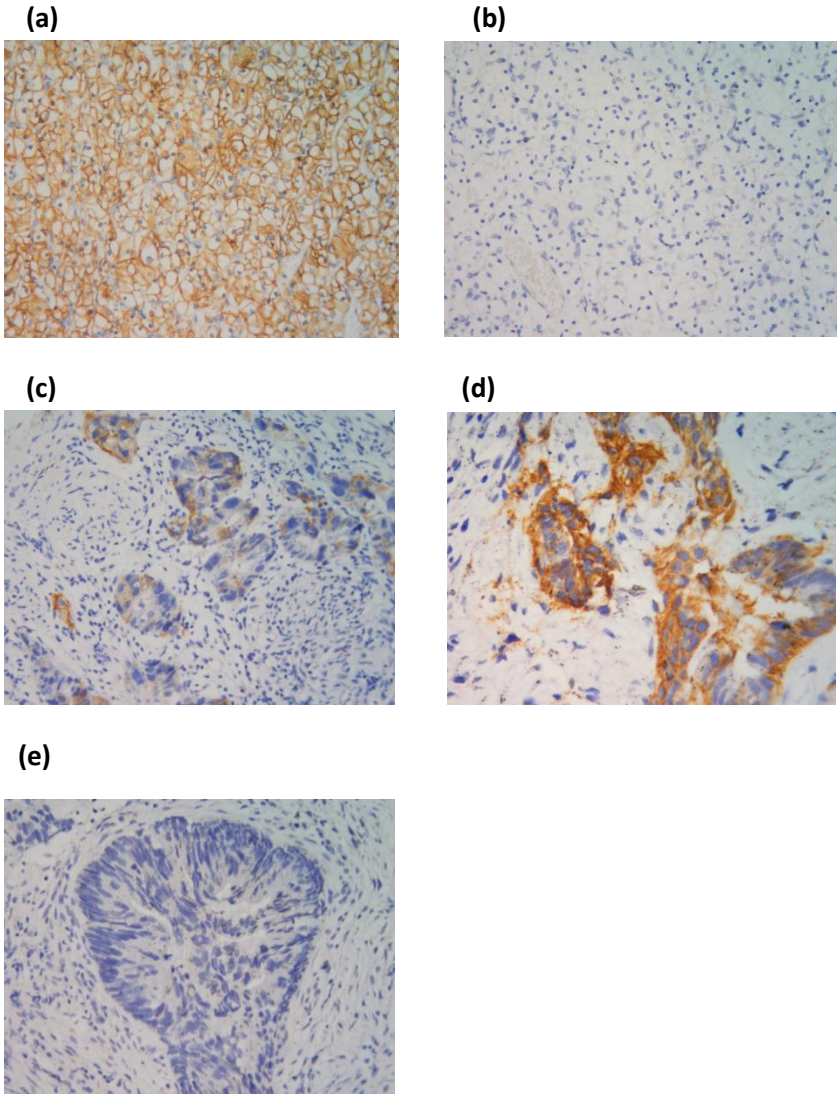

Figure 21 Illustration of (a) positive nuclear staining with HIF-1 α antibody in positive control (pancreatic adenocarcinoma) (b) absent nuclear staining in negative control (pancreatic adenocarcinoma without antibody) (c) example of strong positive nuclear staining in pre-treatment(20577) rectal tumour biopsy (d) example of moderate positive nuclear staining in rectal tumour biopsy (2290) (e) example of absent nuclear staining in rectal tumour biopsy (all shown at x20 magnification).

(a)

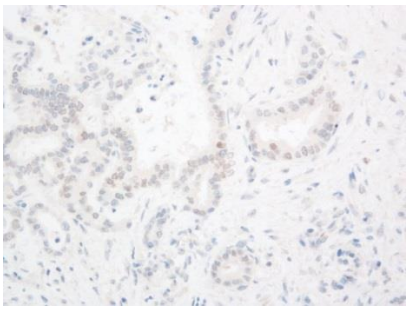

(b)

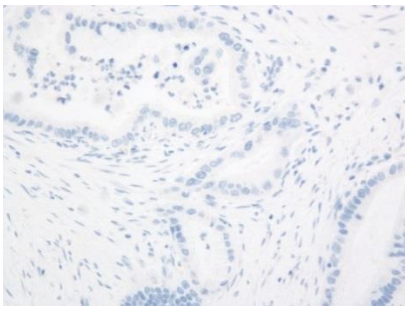

(c)

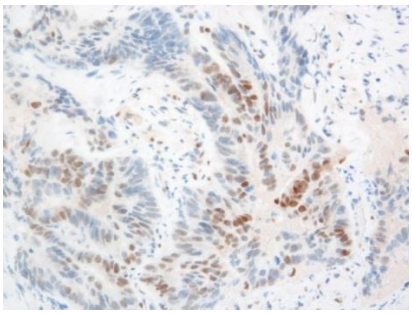

(d)

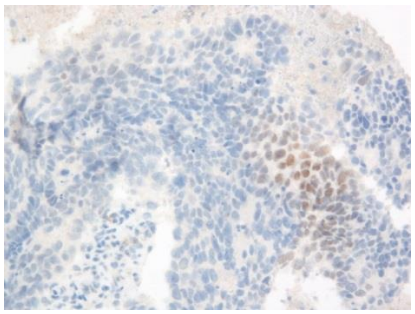

(e)

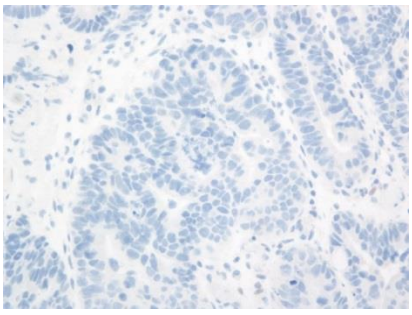

Table 34 Composite immunohistochemical scores for CAIX and HIF-1αexpression in pre-treatment and post-treatment biopsies for individual patients (shaded cells indicate positive expression of hypoxia markers)

Patient number	CAIX (pre-treatment)	HIF1 -α (pre-treatment)	CAIX (post-treatment)	HIF 1-α (post-treatment)
1	0	0	60	0
2	0	0	0	10
3	0	60	80	120
4	140	No tumour	5	0
5	0	30	0	5
6	0	0	<1	30
7	120	0	80	0
8	No tumour	0	No-tumour	No tumour
9	140	20	140	30
10	0	20	0	10

Table 35 Hypoxia marker expression before and after nelfinavir and radiotherapy using CAIX and HIF-1 alpha immunohistochemistry.

	Median Composite Score Pre-treatment (IQR)	Median Composite Score Post-treatment (IQR)	Wilcoxon Rank Sum test
CAIX	44.44 (0-120)	45.63 (0-80)	P=1.0
HIF-1 alpha	10 (0-20)	10 (0-30)	P=0.233

A6 Markers associated with activation of the RAS-PI3K-Akt signalling pathway

Colorectal cancer cell lines known to have PI3-Kinase mutations (and therefore presumed to express the phosphorylated form of Akt) were selected to evaluate relative expression of Phospho-Akt and Phospho-PRAS40 antibodies (in relation to total Akt and PRAS40) by Western blotting.

Figure 22 Western Blot of phospho-Akt, total Akt, phospho-PRAS40, total PRAS40 and alphatubulin protein expression in human colon cancer cell lines RKO, DLD1 and HCT116

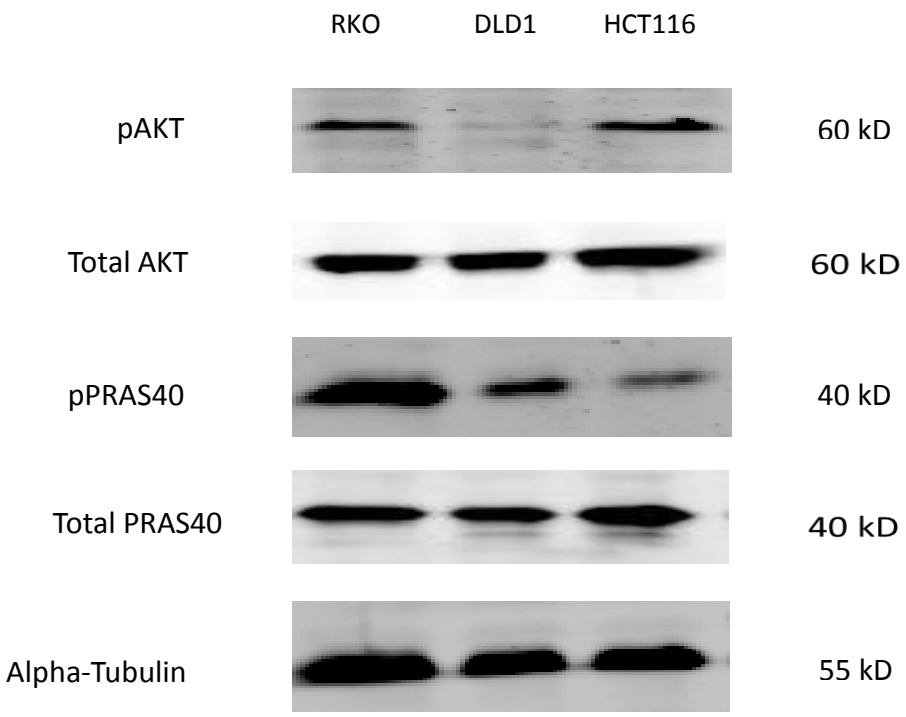

RKO and HCT116 cancer cell lines both demonstrated positive phospho-Akt and phospho-PRAS40 protein expression. These cell lines were therefore selected to produce cell pellets for optimising immunohistochemistry with phospho-Akt and Phospho-PRAS40 antibodies using an automated staining protocol. The reproducibility of staining using the optimised protocol was confirmed by antibody staining of cell pellets on three separate runs. Pre-treatment and post-treatment tumour biopsies were stained for phospho-Akt and phospho-PRAS40 using cell pellets incubated with antibody as a positive control and cell pellets without antibody as a negative control. Figure 23 illustrates the immunohistochemical staining of the cell pellets with phospho-Akt and phospho-PRAS40 antibodies in HCT 116 cell pellets, which were used as control tissue.

Figure 23. Illustration of (a) positive cytoplasmic staining with phospho-Akt antibody in positive control (HCT116 cell pellets) in optimised conditions (b) absent cytoplasmic staining in negative control (HCT116 cell pellets without phospho-Akt antibody at optimised conditions) (c) positive cytoplasmic staining with phospho-PRAS40 in HCT116 cell pellets (d) absent cytoplasmic staining in negative control (HCT116 cell pellets without phospho-PRAS40 at optimised conditions).

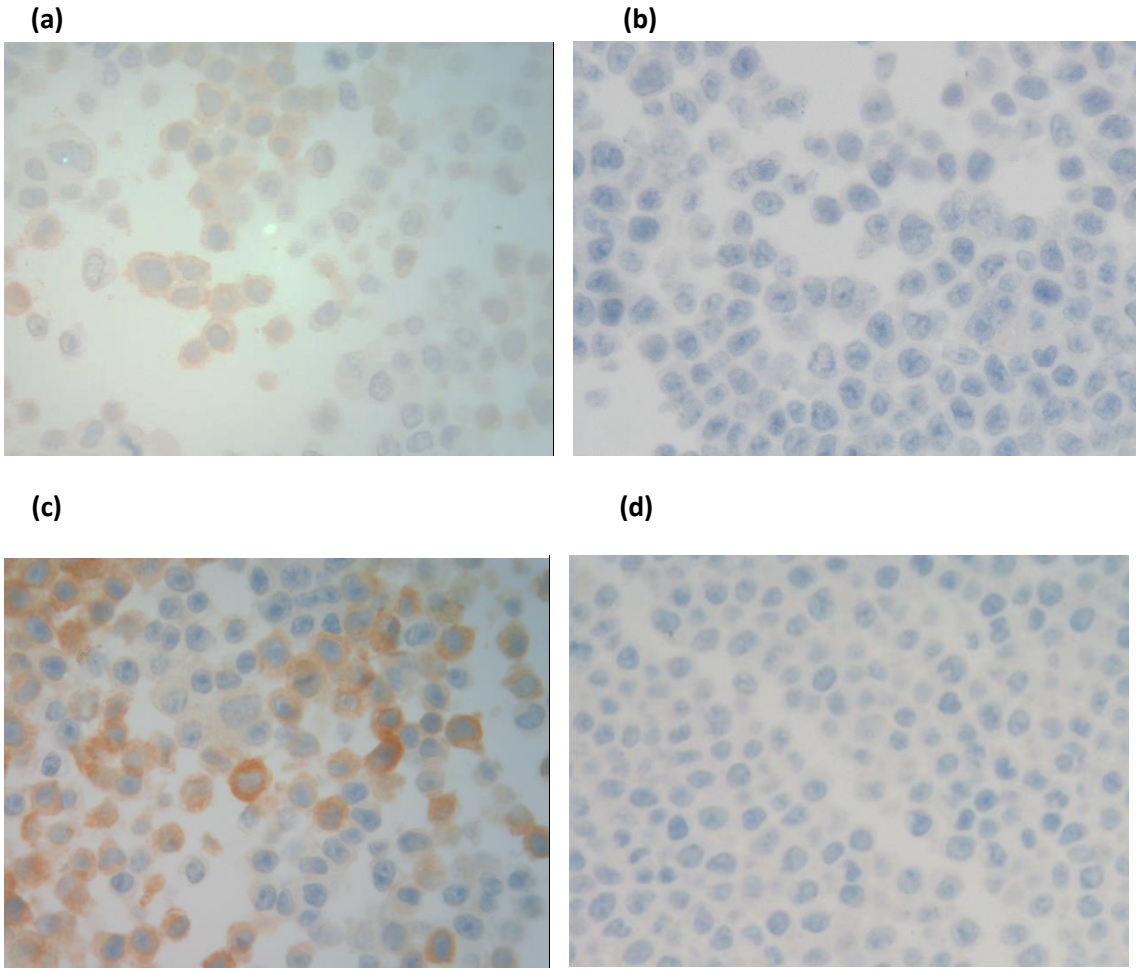

Figures 24 and 25 illustrate representative staining of individual tumour samples with phospho-Akt and phospho-PRAS40 respectively. Only one pre-treatment tumour sample (patient 9) demonstrated positive phospho-Akt expression compared to 3 post-treatment tumour samples, whereas 3 pre-treatment tumour samples and 2 post-treatment samples demonstrated positive expression of phospho-PRAS40 (see table 36). Overall, there was no significant difference in the median composite score for phospho-Akt or phospho-PRAS40 between pre-treatment and post-treatment samples (table 37). No obvious pattern of association between phospho-Akt, phospho-

PRAS40, CAIX or HIF1-α expression on pre-treatment or post-treatment biopsies and tumour response to treatment on MRI (mrTRG) was observable (see table 38).

Figure 24 Illustration of immunohistochemical staining of rectal biopsies(pre-treatment and post-nelfinavir/ radiation therapy) with phospho-Akt antibody for individual patients.

Patient 1 (Pre-treatment)

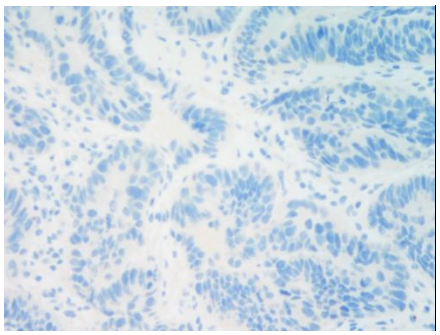

Patient 1 (Post-treatment)

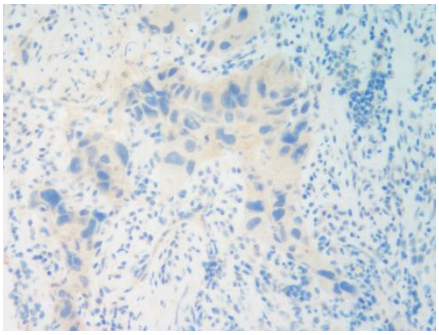

Patient 2 (Pre-treatment)

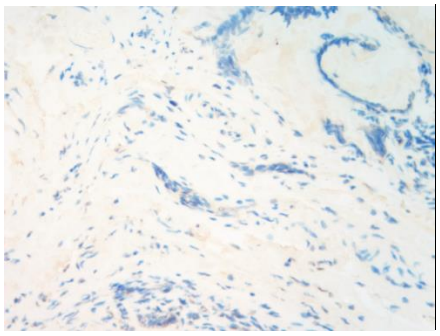

Patient 2 (Post-treatment)

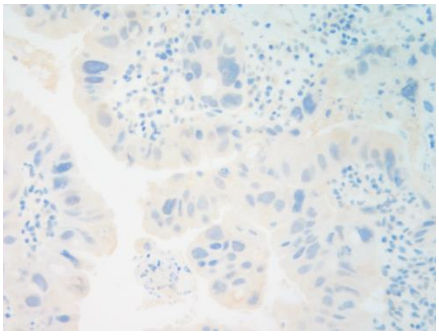

Patient 3 (Pre-treatment)

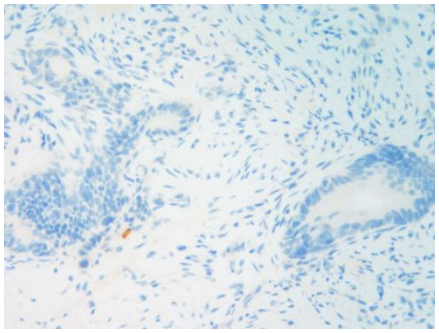

Patient 3 (Post-treatment)

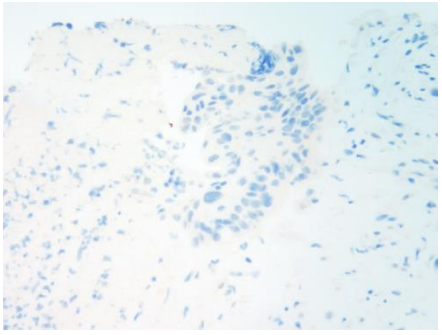

Patient 4 (Pre-treatment)

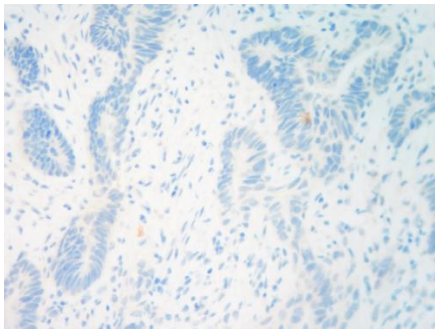

Patient 4 (Post-treatment)

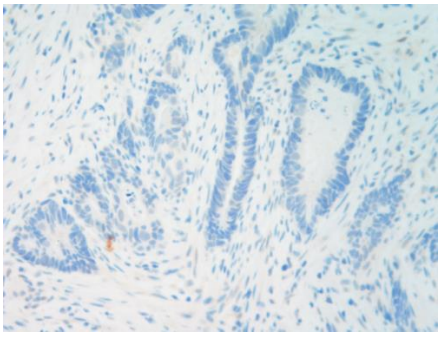

Patient 5 (Pre-treatment)

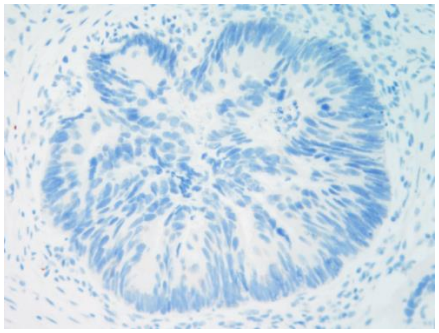

Patient 5 (Post-treatment)

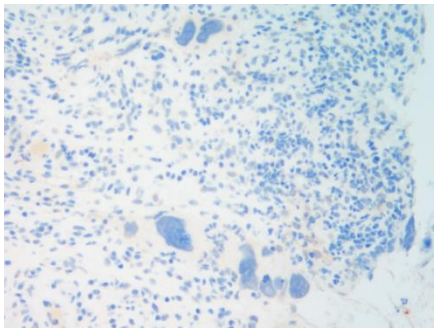

Patient 6 (Pre-treatment)

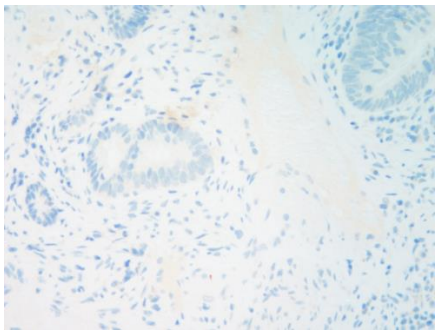

Patient 6 (Post-treatment)

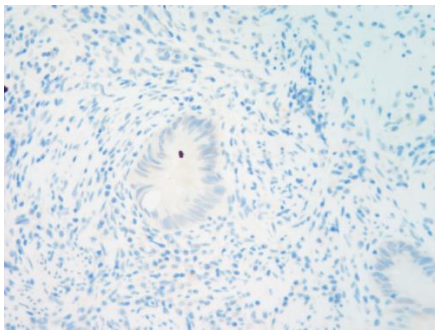

Patient 7 (Pre-treatment)

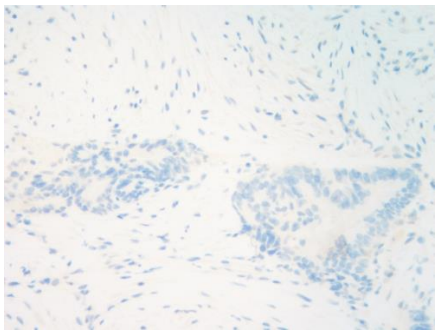

Patient 7 (Post-treatment)

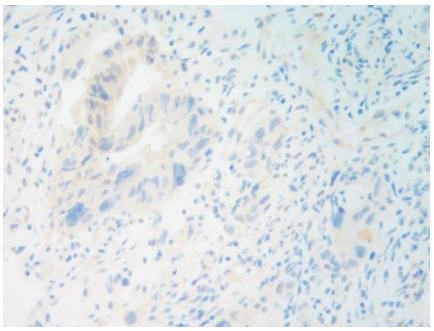

Patient 8 (Pre-treatment) **Patient 8 (Post-treatment –no tumour)**

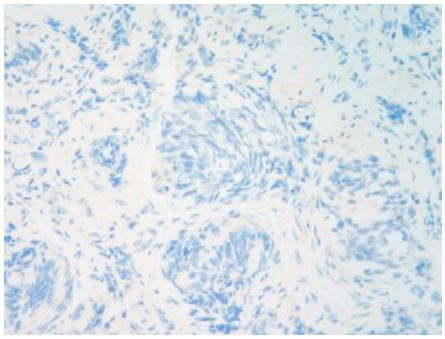

Patient 9 (Pre-treatment) **Patient 9 (Post-treatment)**

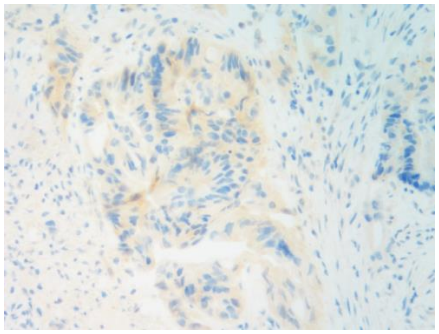

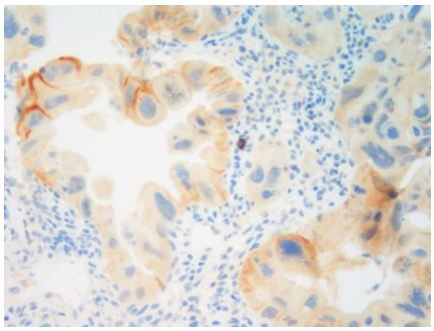

Patient 10 (Pre-treatment) **Patient 10 (Post-treatment)**

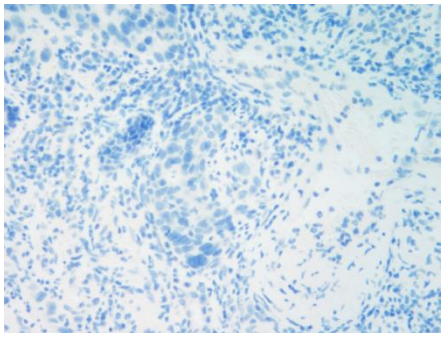

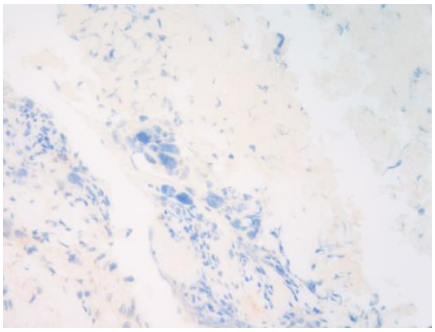

Figure 25 Illustration of immunohistochemical staining of rectal biopsies pre-treatment and post-treatment (with nelfinavir and radiotherapy) with phospho-PRAS40 antibody for individual patients.

Patient 1 (Pre-treatment) **Patient 1 (Pre-treatment)**

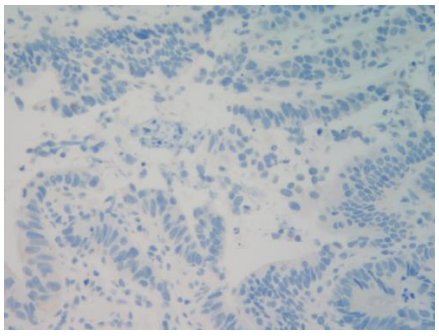

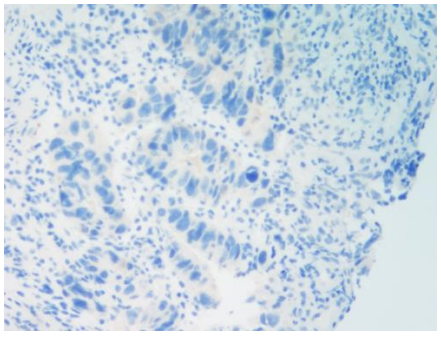

Patient 2 (Pre-treatment)

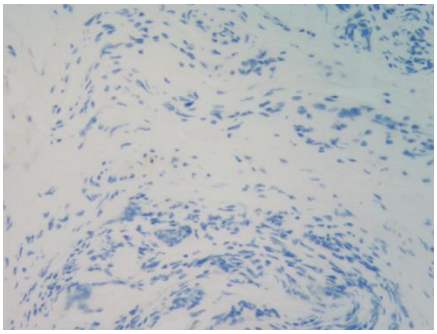

Patient 2 (Pre-treatment)

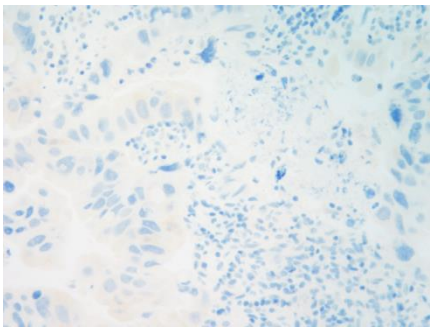

Patient 3 (Pre-treatment)

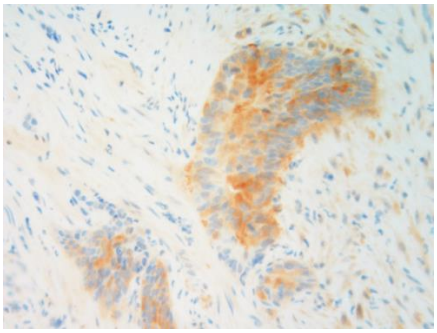

Patient 3 (Post-treatment)

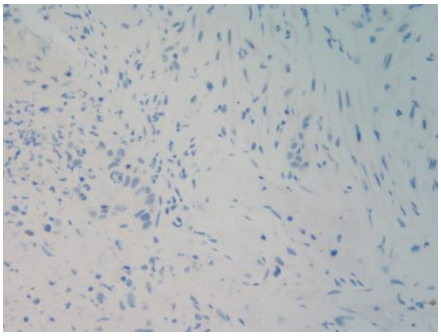

Patient 4 (Pre-treatment)

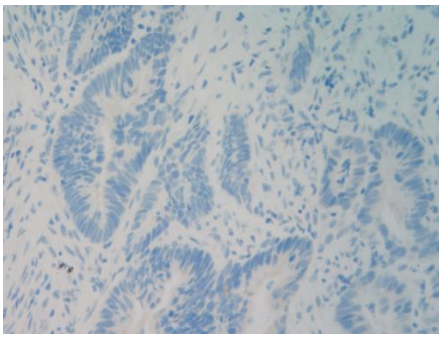

Patient 4 (Post-treatment)

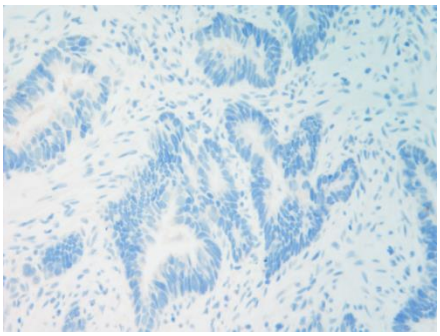

Patient 5 (Pre-treatment)

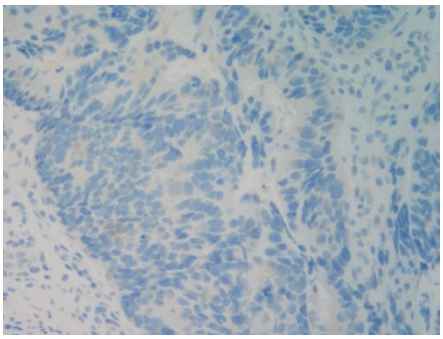

Patient 5 (Post-treatment)

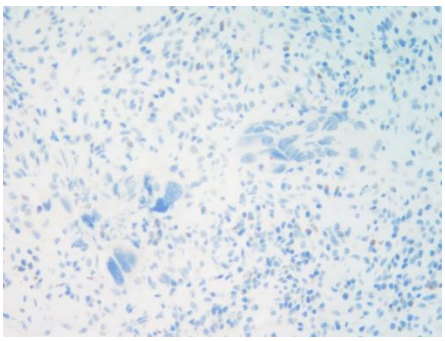

Patient 6 (Pre-treatment)

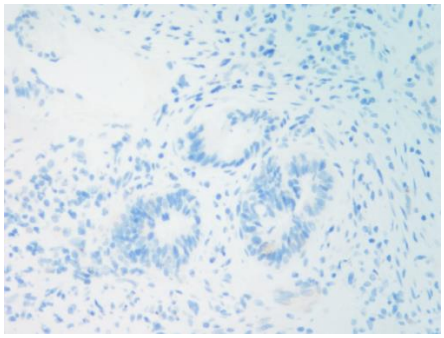

Patient 6 (Post-treatment)

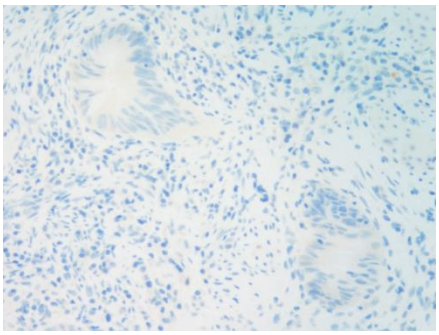

Patient 7 (Pre-treatment)

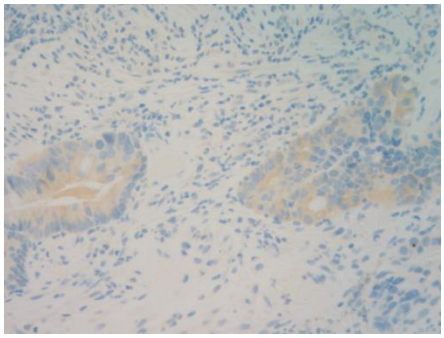

Patient 7 (Post-treatment)

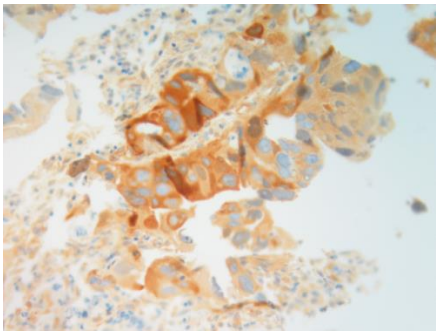

Patient 8 (Pre-treatment)

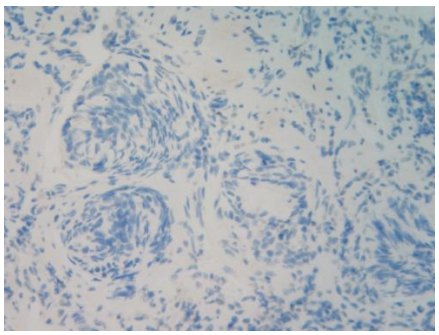

Patient 8 (post-treatment)- no tumour

Patient 9 (Pre-treatment)

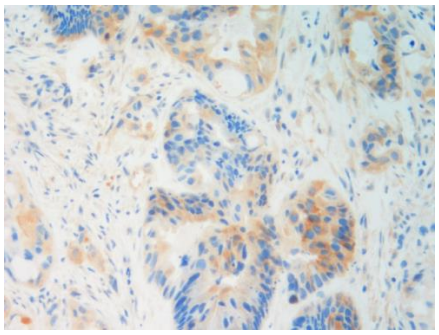

Patient 9 (Post-treatment)

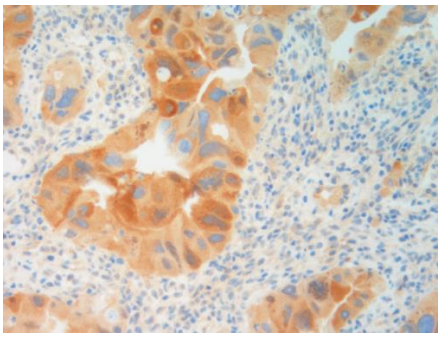

Patient 10 (Pre-treatment) **Patient 10 (Post-treatment)**

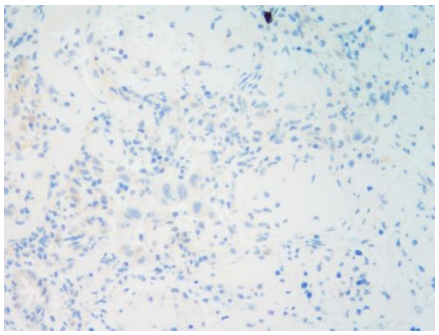

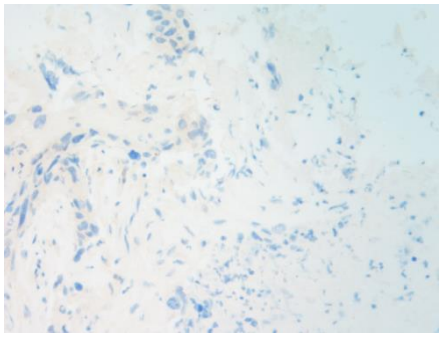

Table 36 Composite immunohistochemical scores for Phospho-Akt and Phospho-PRAS40 antibody staining in rectal tumour biopsies before and after nelfinavir therapy for individual patients (shaded cells indicate positive expression).

Patient number	Phospho-Akt (pre-treatment)	Phospho-PRAS40 (pre-treatment)	Phospho-Akt (post-treatment)	Phospho-PRAS40 (post-treatment)
1	0	0	0	0
2	0	0	50	0
3	0	80	0	0
4	0	0	5	0
5	0	0	0	0
6	0	0	0	0
7	0	10	10	100
8	No tumour	No tumour	No tumour	No tumour
9	90	80	180	180
10	0	0	0	0

Table 37 Phospho-Akt and Phospho-PRAS40 immunohistochemical expression in rectal tumour biopsies before and after nelfinavir and radiotherapy.

	Median Composite Score Pre-treatment (IQR)	Median Composite Score Post-treatment (IQR)	Wilcoxon Rank Sum test
Phospho-Akt	0 (0;0)	0 (0-10)	P=0.068
Phospho-PRAS40	0 (0-10)	0 (0;0)	P=0.285

Table 38 Summary of hypoxia marker and phospho-Akt/ phospho-PRAS40 immunohistochemical expression on pre-treatment and post-treatment biopsies in relation to radiological response on MRI 8 weeks post nelfinavir and radiotherapy.

Patient no.	CAIX (pre-RT)	HIF1 -α (pre-RT)	CAIX (post-RT)	HIF 1-α (post-RT)	Phospho-Akt (pre-RT)	Phospho-PRAS40 (pre-RT)	Phospho-Akt (post-RT)	Phospho-PRAS40 (post-RT)	mrTRG class
1	-ve	-ve	+ve	-ve	-ve	-ve	-ve	-ve	good
2	-ve	-ve	-ve	+ve	-ve	-ve	+ve	-ve	poor
3	-ve	-ve	+ve	+ve	-ve	+ve	-ve	-ve	good
4	+ve	No tumour	-ve	-ve	-ve	-ve	+ve	-ve	poor
5	-ve	+ve	-ve	-ve	-ve	-ve	-ve	-ve	good
6	-ve	-ve	-ve	+ve	-ve	-ve	-ve	-ve	poor
7	+ve	-ve	+ve	-ve	-ve	+ve	+ve	+ve	poor
8	No tumour	-ve	No-tumour	No tumour	No tumour	No tumour	No tumour	No tumour	good
9	+ve	+ve	+ve	+ve	+ve	+ve	+ve	+ve	good
10	-ve	+ve	-ve	+ve	-ve	-ve	-ve	-ve	Not assessed

A7 Summary

In summary, in a clinical trial of 10 patients with T3/4 N0-2 M1 rectal cancer, it has been demonstrated that the combination of nelfinavir and hypo-fractionated pelvic radiotherapy resulted in dose limiting toxicity (necessitating interruption of therapy) in 2 patients. Five patients developed Grade 3 non-laboratory toxicities within 28 days of therapy, of which 3 were probably/possibly causally related to nelfinavir. Additionally 2 patients developed Grade 3 lymphopenia (thought to be causally related to nelfinavir) and 2 patients developed Grade 3

hyponatremia (not thought to be causally related). Gastrointestinal toxicities were the most common type of toxicity from the treatment combination. The rate of good tumour response (mrTRG score 1-3) 8 weeks after treatment with nelfinavir and concurrent hypo fractionated pelvic radiotherapy was 5/9, including patients who started systemic chemotherapy between the end of RT and the MRI scan.

The feasibility of evaluating quantitative TCD in rectal tumour biopsies after radiotherapy has been demonstrated and significant reductions in TCD were observed after nelfinavir and radiotherapy. Comparison of TCD in tumours treated with nelfinavir and hypo-fractionated radiotherapy and historical controls treated with radiotherapy alone indicated a significantly lower TCD after but not before treatment with nelfinavir; this suggests not only that nelfinavir results in additional tumour cell kill but that it is feasible to use TCD as an early endpoint to evaluate the efficacy of radiosensitising drugs. Evidence of tumour hypoxia using CAIX and HIF-1α immunohistochemistry on pre-treatment biopsies was demonstrable in a small proportion of tumours but no significant change in hypoxia marker immunohistochemistry scores was observed on biopsies taken after treatment with nelfinavir and radiotherapy. Immunohistochemical staining using the phospho-PRAS40 antibody was optimised for use in colorectal tissue. Only 10% of tumours demonstrated positive expression of phospho-Akt and 30% positive expression of phospho-PRAS40 expression on pre-treatment biopsies, despite 70% of patients having a *KRAS* mutation. No pattern of association between phospho-Akt, phospho-PRAS40, CAIX or HIF1-α expression in tumour biopsies and radiological response to treatment (mrTRG) was observed.

3B Perfusion Imaging of Rectal Cancer using pCT

B1 pCT Imaging of Rectal Cancer

In this section, the pCT scans acquired and analysed as part of the study protocol are described. The impact of technical factors on pCT analysis in the acquired scans is investigated, notably

differences in bowel and bladder filling between sequential scans. Variability in the tumour perfusion parameters being evaluated between different CT slices within the same scan is evaluated. Methods for analysing tumour perfusion parameters on multiple slices of the tumour CT volume to compare comparable tumour volumes on sequential scans are presented, and compared to methods of analysis advocated in the literature based on analysis of a single CT slice. The results of quantitative and qualitative evaluation of pCT scans during nelfinavir and radiotherapy are presented to test the hypothesis that nelfinavir improves blood flow to human rectal tumours.

B2 Scans performed and evaluated

All 10 patients in the rectal study successfully completed pCT scans of the rectum at three time points. Table 39 summarises the timing of the scans in relation to commencement of nelfinavir and completion of radiotherapy, specifically detailing the number of days between the baseline study and start of treatment, number of days between start of nelfinavir and second scan and number of days between final fraction of radiotherapy and third scan.

Figure 26 Perfusion CT Scans acquired and evaluated

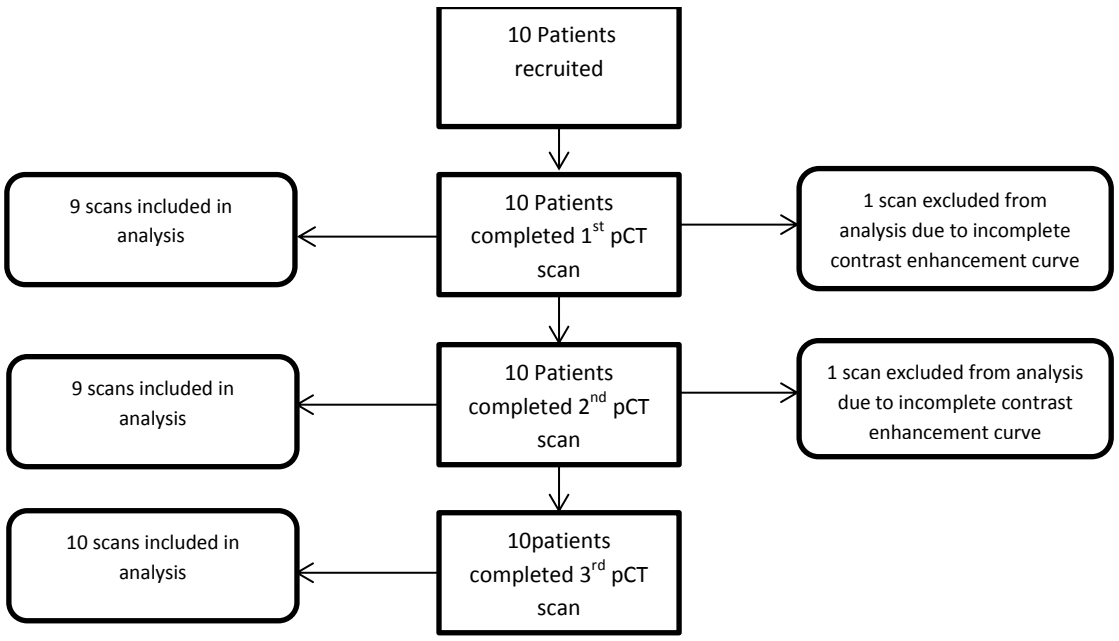

Table 39 Timing of pCT scans. Protocol specified that baseline scan should be performed ≤28 days before start of nelfinavir, scan 2 should be performed on day 7 after commencement of nelfinavir and scan 3 should be performed on final day of nelfinavir and RT.

Patient number	Number of days between scan 1 and start of nelfinavir	Number of days between commencement of nelfinavir and scan 2	Numbers of days between last fraction of radiotherapy and scan 3
ST1001	7	6	0
ST1002	7	7	2*
ST1003	8	6	1*
ST1004	1	7	0
ST1005	5	5*	1*
ST1006	1	6	0
ST1007	14	6	0
ST1008	1	6	0
ST1009	1	6	0
ST1010	1	6	0

***Deviation from trial protocol**

B3 Technical factors influencing perfusion parameter analysis

Intra-sequence motion has been highlighted as a potential technical challenge when evaluating colorectal tumours with pCT[345], since excessive tumour motion, particularly due to respiration, can result in tumour displacement out of the scanning field along the pCT time sequence, resulting in inaccurate data capture. However significant intra-sequence motion was not a major limitation in our analysis of rectal tumours using sequential pCT scans. Rectal tumour was identifiable throughout the dynamic sequences on all pCT scans for all patients and peristalsis rather than respiration was identifiable as the most common type of motion affecting the shape and position of the tumour. As no standardised tools are currently in clinical use for evaluating the degree of intra-sequence tumour motion on pCT, the degree to which the tumours were affected by intra-sequence motion was semi-quantitatively assessed. Using a scale from 1 to 4, which has previously been employed by researchers in one study of Dce-MRI of the liver [396], we categorised the severity of motion for each pCT rectum scan (see table 41) was categorised according to the magnitude of tumour displacement or motion during the pCT time sequence from its original position at the start of the sequence.

Table 40 Qualitative assessment of rectal tumour motion on pCT scans at each time point for individual patients. The degree of motion affecting the tumour on dynamic pCT images was categorised according to the following scale: Score 0= No motion, Score 1= Slight Motion, Score 2= Moderate motion, Score 3=Significant Motion, Score 4= Severe Motion

	Scan1 Motion Score	Scan 2 Motion Score	Scan 3 Motion Score
ST1001	2	2	2
ST1002	1	1	1
ST1003	3	2	2
ST1004	0	1	2
ST1005	2	2	2
ST1006	2	1	2
ST1007	1	1	1
ST1008	1	2	3
ST1009	1	1	1
ST1010	0	0	1

Significant motion was evident in only two scans, in both cases being due to peristaltic motion affecting the intra-luminal shape of the tumour and the amount of intra-luminal air. The majority of tumours were positioned in the lower rectum, with no evident association between the severity of motion and tumour site. No pCT scan was excluded from analysis on account of motion, as out of plane movement within the pCT image sequence did not occur, presumably due to the relative fixation of these locally advanced rectal tumours. No pCT scans were excluded from analysis due to intra-sequence motion as changes in shape of the tumour and amount of intra-luminal gas was allowed for by defining a tumour ROI based on review of the cine loop of the entire dynamic sequence, specifically to avoid inclusion of intra-luminal gas and extension of the tumour ROI outside the tumour, in accordance with published guidelines[425].

An additional technical issue that may potentially influence the accuracy of measuring changes in tumour perfusion on sequential pCT scans are differences in rectal and bladder filling between sequential scans, which to date has been given cursory mention in the published literature[350, 434]. It has been observed in studies of image guided radiotherapy for rectal cancer that changes in rectal and bladder filling can affect rectal and mesorectal tumour shape and position, with

changes in rectal filling contributing most to those changes, and shape changes being greater in the upper rectum than the lower rectum[435]. One team of researchers attempted to control rectal distension by administering laxatives and an enema the day before the pCT and giving a water enema immediately prior to the pCT scan[347]. We evaluated whether there were differences in bladder filling on sequential pCT scans by identifying pCT slices at comparable anatomical levels on successive scans for individual patients and calculating the volume of the bladder on those slices.

Figure 27 Comparison of bowel and bladder filling between sequential scans. The upper panel (a) illustrates an example of differences in rectal filling/distension between sequential scans for patient ST1003. The lower panel illustrates differences in bladder filling (b) between sequential pCT scans for patient ST1004

Scan 1 **Scan 2** **Scan 3**

(a)

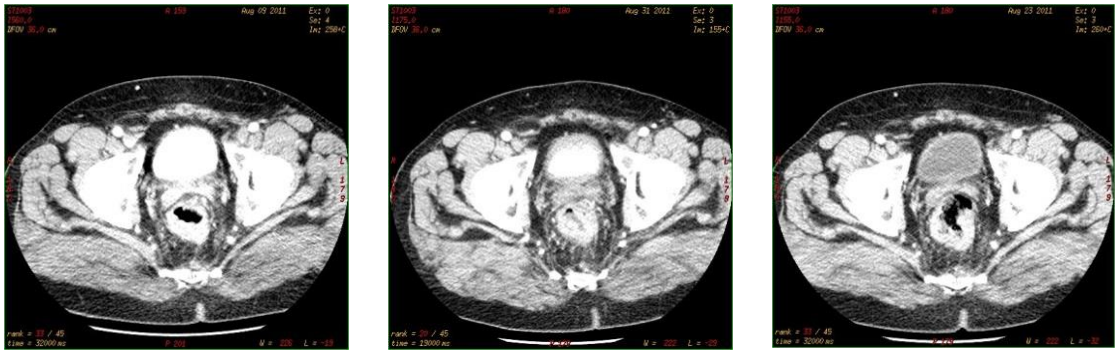

(b)

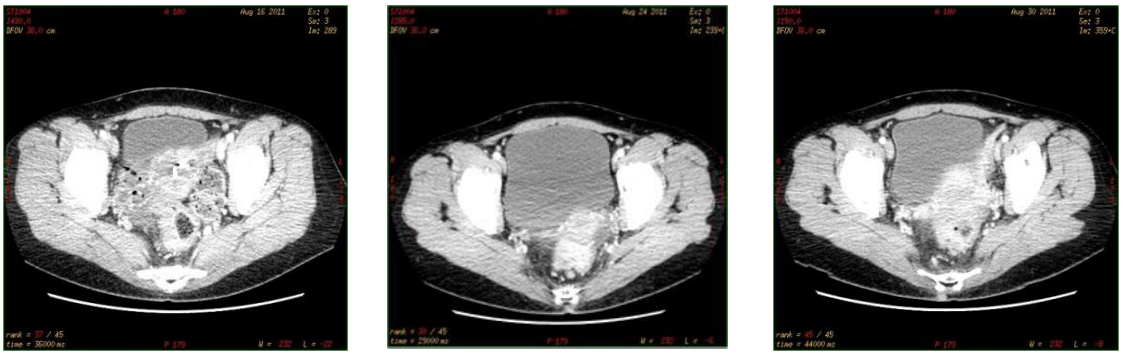

Table 41 summarises the results of this analysis and demonstrates that there was variability in bladder filling between sequential scans for all of the patients, excluding ST1008, where bladder

was below the level of the pCT, between at least two of the time points. Changes in the position of the tumour on successive scans could influence the evaluation of changes in tumour perfusion if there is significant variation in tumour perfusion at different levels of the tumour in the cranio-caudal axis perfusion, particularly if the perfusion parameters are derived from a single slice.

Table 41 Volume of bladder on pCT slices at comparable anatomical levels on successive pCT scans

Patient	Bladder Volume (cm^3)			Number of pCT slices overlapping on sequential scans on which bladder present
	Scan 1	Scan 2	Scan3	
ST1001	7.76	29.6	30.64	1
ST1002	106.97	70.54	61.2	7
ST1003	50.64	48.28	38.36	6
ST1004	90.4	210.43	45.74	2
ST1005	53.47	96.15	51.47	6
ST1006	135.86	105.77	53.14	5
ST1007	17.9	18.86	58.91	1
ST1008	0	0	0	8
ST1009	47.15	57.74	70.51	7
ST1010	359.66	453.73	391.89	8

B4 Development of methods for perfusion CT analysis

Initial analysis of tumour perfusion parameters on the baseline pCT scan was performed on a single CT slice (the slice with greatest tumour bulk) according to the method advocated by Goh et al. [337, 343] and inter-observer variability was evaluated between two observers (see figure 28 and table 42).

Figure 28 Bland Altman plots and scatter plots demonstrating inter-observer variability in BF, BV and MTT measurements for a single slice on the baseline pCT scans

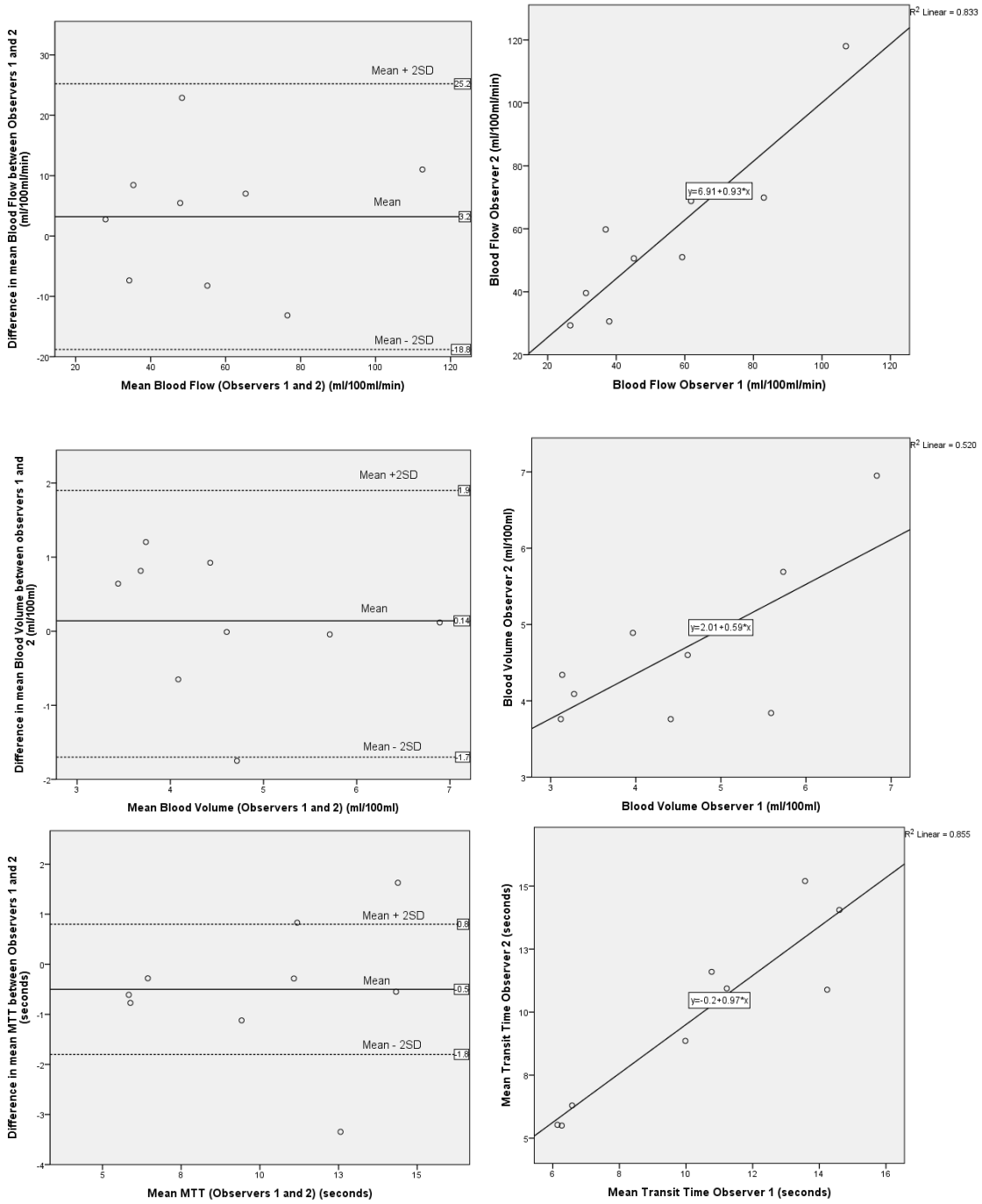

Table 42 Table summarising inter-observer variation in perfusion parameters based on delineation of a tumour ROI on a single pCT slice

Perfusion parameter	Mean difference between Observers 1 and 2	Bland Altman 95% limits of agreement	Intra-class correlation coefficient (ICC)	95% Confidence Interval for ICC
Blood Flow (ml/100ml/min)	3.20	-18.77 to 25.18	0.95	0.80-0.99
Blood Volume (ml/100ml)	0.66	-1.66 to 1.93	0.83	0.24-0.96
Mean Transit Time (Seconds)	0.31	-1.83 to 0.83	0.96	0.82-0.99

Figure 29 Scatter plots illustrating variation in mean BF, BV and MTT derived for the tumour ROI between different pCT slices for each patient on the baseline pCT scan

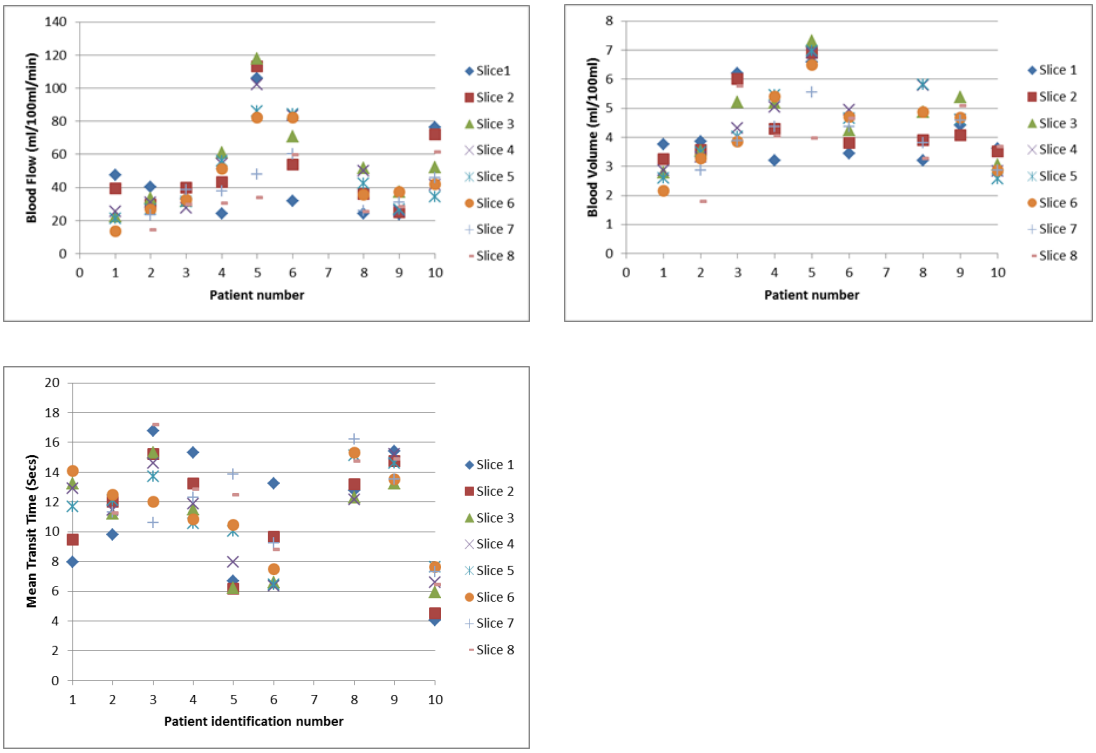

It was postulated that there would be significant variation in perfusion parameters derived within the tumour ROI at different levels in the tumour, corresponding to consecutive pCT slices in the z axis, based on the pathological observations that tumours typically have disordered

vasculature [436] with heterogeneity in the distribution of blood vessels[91]. Inter-slice variation in all perfusion parameters was observed for all baseline scans (see figure 29), with the highest coefficient of variation being demonstrated for mean BF followed by MTT then BV (table 43).

Table 43 Summary of variation in mean BF(a), BV(b) and MTT(c) for the tumour ROI between 8 pCT slices for each patient on the baseline pCT scan.

(a)

Patient identification number	Mean Blood Flow (ml/100ml/min)	Standard Deviation of Mean Blood Flow (ml/100ml/min)	Coefficient of Variation (%)
ST1001	28.33	12.70	44.83
ST1002	28.23	7.59	26.89
ST1003	33.11	4.21	12.70
ST1004	44.80	13.14	29.34
ST1005	86.23	30.68	35.58
ST1006	65.79	18.26	27.76
ST1007	Not evaluable	Not evaluable	Not evaluable
ST1008	36.47	10.90	29.88
ST1009	29.43	5.33	18.12
ST1010	53.22	15.30	28.75

(b)

Patient identification number	Mean Blood Volume (ml/100ml)	Standard Deviation of Mean Blood Volume (ml/100ml)	Coefficient of Variation (%)
ST1001	2.90	0.55	18.89
ST1002	3.21	0.64	19.79
ST1003	4.91	1.00	20.38
ST1004	4.62	0.78	16.92
ST1005	6.34	1.09	17.19
ST1006	4.35	0.51	11.65
ST1007	Not evaluable	Not evaluable	Not evaluable
ST1008	4.43	1.04	23.55
ST1009	4.68	0.40	8.46
ST1010	3.12	0.42	13.51

(c)

Patient identification number	Mean Mean Transit Time (Seconds)	Standard Deviation of Mean Transit Time (Seconds)	Coefficient of Variation (%)
ST1001	11.57	2.39	20.68
ST1002	11.45	0.81	7.10
ST1003	14.43	2.25	15.59
ST1004	12.31	1.54	12.48
ST1005	9.24	2.94	31.79
ST1006	8.47	2.33	27.47
ST1007	Not evaluable	Not evaluable	Not evaluable
ST1008	13.97	1.55	11.11
ST1009	14.39	0.84	5.86
ST1010	6.27	1.37	21.79

Although, Goh et al. demonstrated that multi-slice pCT parameter estimation does not improve the reproducibility of the test for colorectal tumours compared to single-slice pCT parameter estimation[337], since intra-tumour vascularity and perfusion is heterogeneous, a single slice may misrepresent the perfusion characteristics of the tumour and unless the same region of the tumour in the z axis is evaluated on sequential scans, changes in perfusion parameters may reflect regional variation in perfusion rather than change due to tumour progression or treatment response. Goh et al.[337] discussed the possibility that the lack of significant difference between reproducibility of pCT measurement between analysis of a single slice with 5 mm z axis coverage of tumour and 4 slice analysis with 20 mm coverage might be due to the difficulty in ensuring that the same level of the tumour was assessed on all 4 slices, as the repeat scan may have imaged a slightly different level of the tumour.

Figure 30 Alignment of pCT slices from sequential pCT scans for a single patient according to pelvic anatomical landmarks

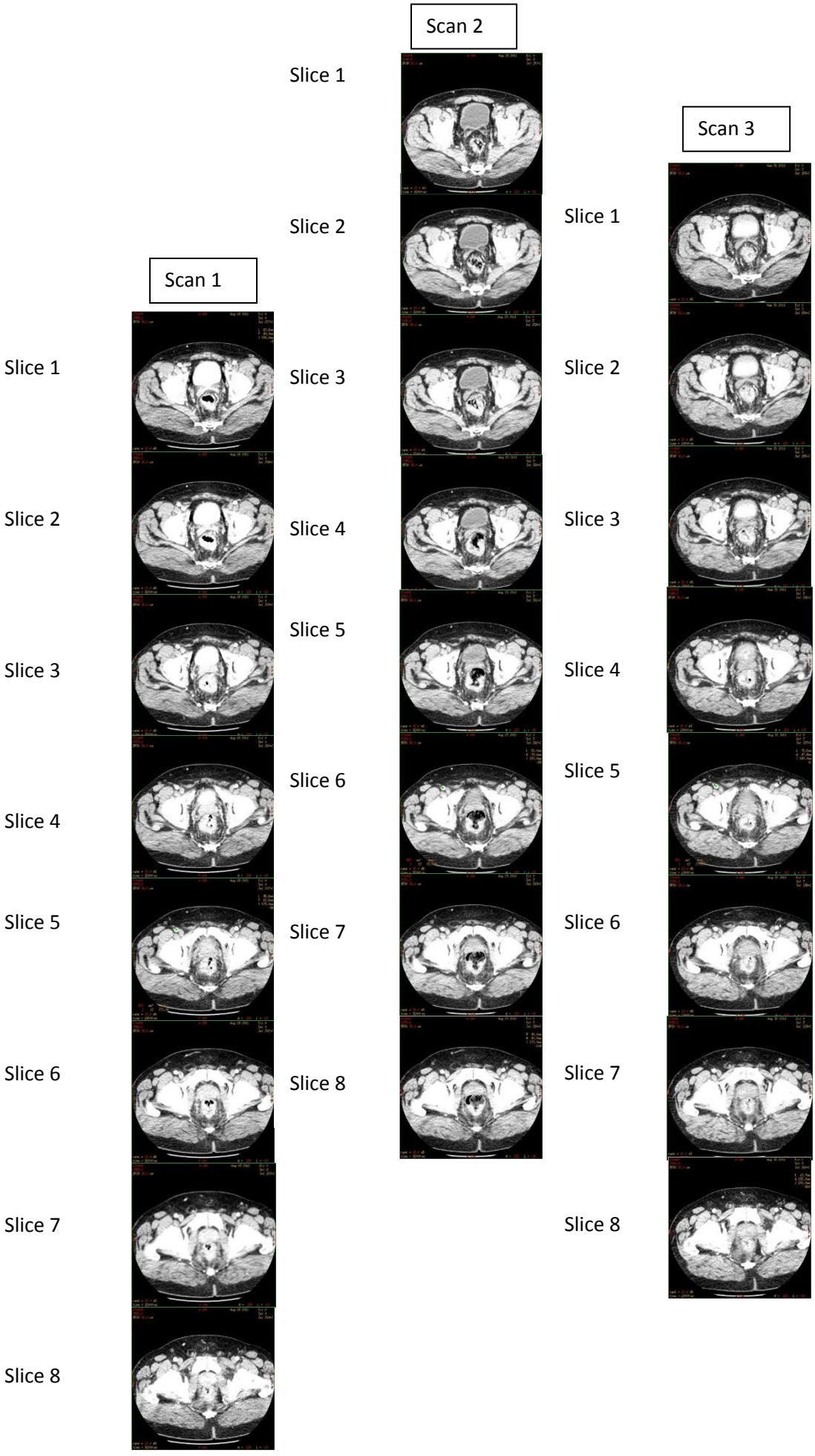

As the pCT coverage was limited to 4 cm in our study and most tumours exceeded this distance, we evaluated whether the same portion of the tumour was successfully imaged on sequential pCT scans for each patient by aligning sequential pCT scans according to bony pelvic landmarks using Image J (see figure 30). We observed that the anatomical overlap of sequential pCT scans in the z axis ranged from 1.5 cm to 4 cm between scans 1 and 2 (median 3.5cm),3cm to 4cm (median 3.5cm) 0.5 cm to 4 cm (median 2.75 cm) between scans 1, 2 and 3 (see table 44).

Table 44 Comparison of anatomical overlap between sequential pCT Scans for individual patients

Patient identification number	Number of overlapping pCT slices between scans 1 and 2 (Z axis coverage)	Number of overlapping pCT slices between scans 2 and 3 (Z axis coverage)	Number of overlapping pCT slices between all 3 scans (Z axis coverage)
ST1001	3(1.5cm)	6(3cm)	1(0.5cm)
ST1002	8(4cm)	7(3.5cm)	7(3.5cm)
ST1003	6(3cm)	7(3.5cm)	6(3cm)
ST1004	2(1cm)	8(4cm)	2(1cm)
ST1005	8(4cm)	6(3cm)	4(2cm)
ST1006	5(2.5cm)	7(3.5cm)	5(2.5cm)
ST1007	6(3cm)	6(3cm)	4(2cm)
ST1008	8(4cm)	8(4cm)	8(4cm)
ST1009	8(4cm)	8(4cm)	7(3.5cm)
ST1010	8(4cm)	8(4cm)	8(4cm)

Based on our findings of significant inter-slice variation in tumour perfusion and the observation that the anatomical level of the tumour imaged was not always consistent between successive scans, the method subsequently used for analysis of changes in tumour perfusion on sequential scans involved calculation of tumour perfusion parameters for each of 8 pCT slices in the z axis for

each tumour and derivation of a weighted mean value for the perfusion parameters (based on the relative area of the ROI on each slice) from all of the anatomically comparable slices between successive pCT scans.

It was hypothesised that this method of analysis would reduce inter-observer variation in perfusion parameters derived, by virtue of having removed the influence of slice selection and averaging differences in tumour area delineated on different slices over the scanned tumour volume. This hypothesis was tested by 2 observers repeating analysis of the baseline pCT scans using the method based on derivation of a weighted mean for the tumour volume (see figure 31 and table 45). Analysis revealed that the mean difference in BF and BV between 2 observers and the Bland Altman limits of agreement were less using analysis of a weighted mean of multiple pCT slices than for analysis using a single pCT slice (although little different for MTT); the intra-class correlation coefficient between 2 observers for BF, BV and MTT were also higher using the former method.

Table 45 Table summarising inter-observer variation in perfusion parameters based on delineation of a tumour ROI on multiple slices and derivation of a weighted mean

Perfusion parameter	**Mean difference between Observers 1 and 2**	**Bland Altman 95% limits of agreement**	**Intra-class correlation coefficient (ICC)**	**95% Confidence Interval for ICC**
Blood Flow (ml/100ml/min)	1.34	-4.67 to 7.35	0.995	0.979-0.999
Blood Volume (ml/100ml)	0.11	-0.87 to 0.64	0.972	0.877-0.994
Mean Transit Time (Seconds)	-0.56	-2.1 to 1.05	0.98	0.911-0.995

Figure 31 Bland Altman plots and scatter plots demonstrating inter-observer variability in BF, BV and MTT measurements derived from multiple slices using a weighted mean on the baseline pCT scans

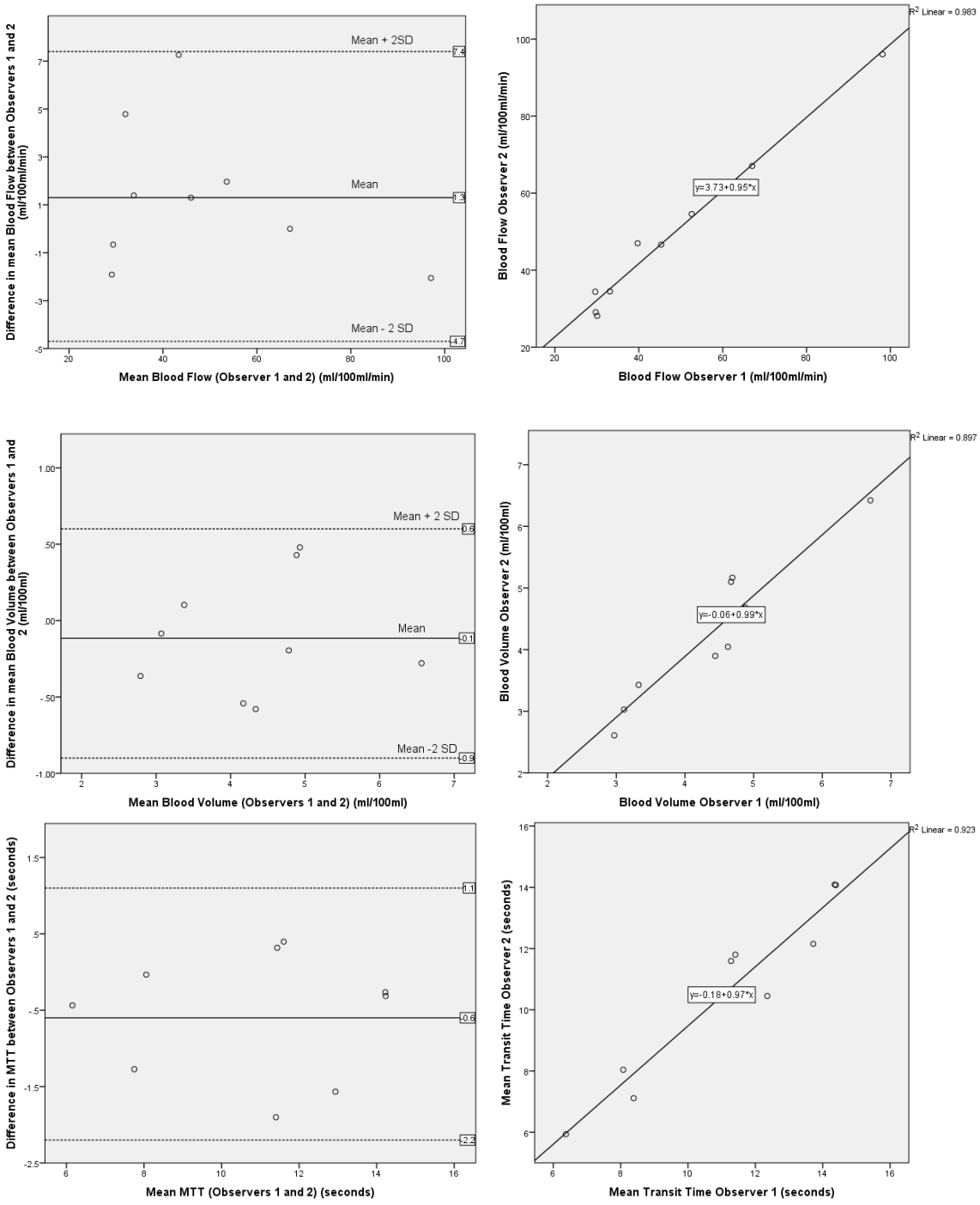

It was evaluated whether the derivation of perfusion parameters for the tumour volume using a weighted mean of values acquired using GE software for each pCT slice (2-D analysis) was equivalent to direct derivation of the mean by averaging all of the voxels within the tumour ROI

(3-D analysis). A statistically significant positive correlation was demonstrated between the mean perfusion parameters derived for the tumour using 3-D and 2-D analysis in Matlab (see figure 32 and table 46).

Figure 32 Scatter plots demonstrating correlation between mean perfusion parameters and the standard deviation of perfusion parameters derived by 2-D analysis (weighted mean of 8 slices) versus 3-D Analysis (mean of volume) using Matlab.

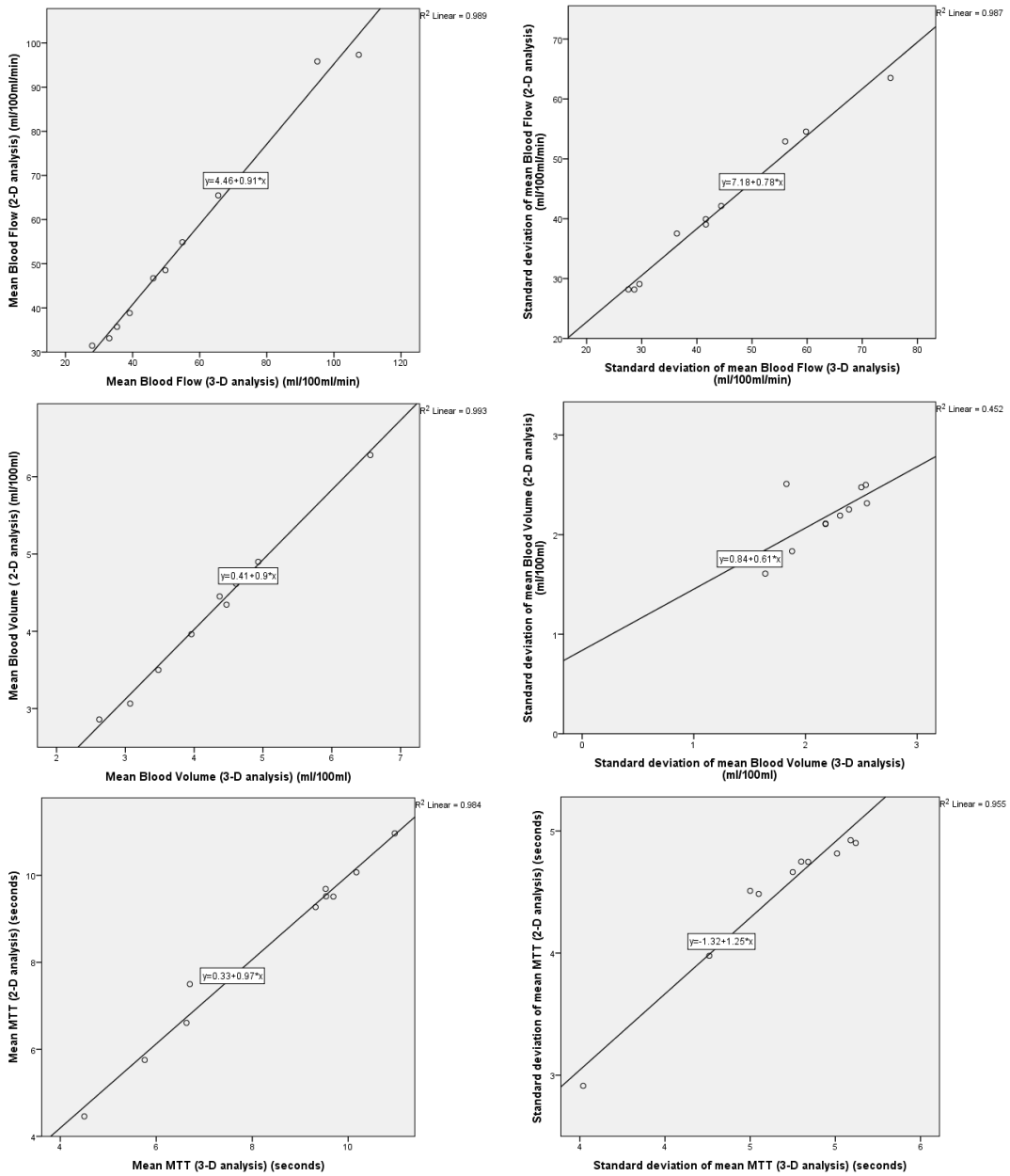

Table 46 Table summarising Pearson's correlation coefficient and statistical significance for perfusion parameters derived using 2-D and 3-D analysis in Matlab

Parameter	Pearson's correlation coefficient (R)	R^2	Statistical significance (2-sided)
Mean Blood Flow	0.995	0.989	P=0.000
Standard Deviation of Mean Blood Flow	0.993	0.987	P=0.000
Mean Blood Volume	0.996	0.993	P=0.000
Standard Deviation of Mean blood Volume	0.672	0.452	P=0.033
Mean Mean Transit Time	0.992	0.984	P=0.000
Standard Deviation of Mean Mean Transit Time	0.977	0.955	P=0.000

In order to validate the Matlab program for pCT analysis, the mean perfusion parameters and their associated standard deviation derived by 2D analysis of all 8 pCT slices using Matlab were compared with the mean perfusion parameters (and their associated standard deviation) derived from 2D analysis of all 8 pCT slices using GE software for the baseline scans of all 10 patients. Positive correlation was demonstrated between perfusion parameters derived by the 2 methods (as illustrated in the scatterplots in figure 33). This correlation was statistically significant (table 47).Positive correlation was strongest for mean BF, being weaker for mean BV and mean MTT. However, there were statistically significant differences between the mean values derived using Matlab and GE software (table 48). In view of these findings, 2D analysis of perfusion parameters for the tumour volume, based on multiple slices as comparable anatomical levels using GE software, was used for the final analysis of changes in tumour perfusion between sequential scans.

Figure 33 Scatter plots demonstrating degree of correlation between BF, BV and MTT derived using GE Software and Matlab Program

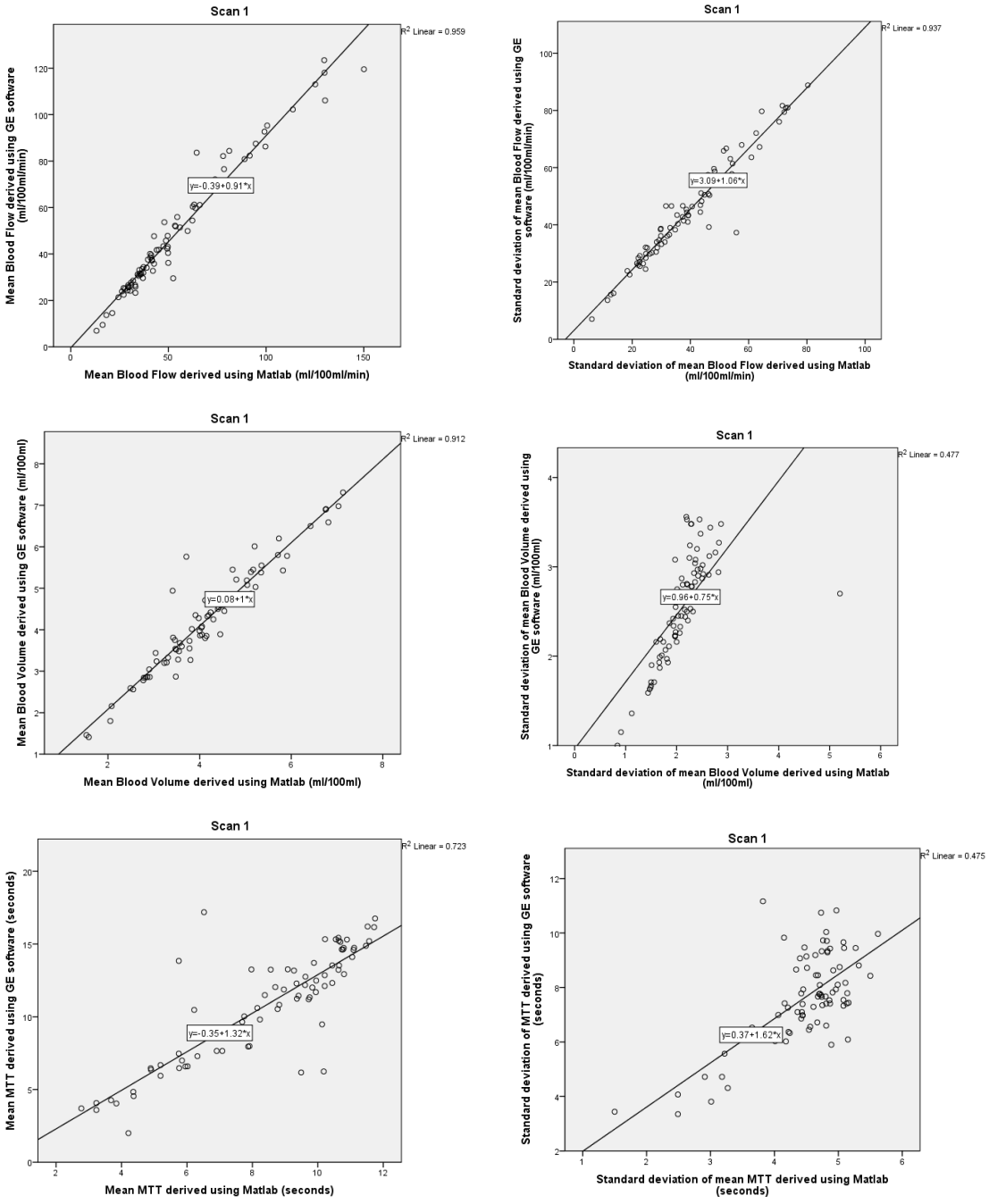

Table 47 Table summarising Pearson's correlation coefficient and statistical significance between parameters derived using GE software and Matlab

Parameter for comparison between analysis using GE software and Matlab	Pearson's correlation coefficient (R)	R^2	Statistical Significance (2-sided)
Mean Blood Flow (ml/100ml/min)	0.979	0.959	P=0.000
Standard Deviation of Mean Blood Flow (ml/100ml/min)	0.968	0.937	P=0.000
Mean Blood Volume (ml/100ml)	0.955	0.912	P=0.000
Standard Deviation of Mean Blood Volume (ml/100ml/min)	0.691	0.477	P=0.000
Mean Mean Transit Time (Seconds)	0.85	0.723	P=0.000
Standard Deviation of Mean Mean Transit Time (Seconds)	0.689	0.475	P=0.000

Table 48 Table comparing mean perfusion parameter values and their associated standard deviations derived using GE Software and Matlab

Parameter	Median difference between values derived using GE software and Matlab	Statistical significance (2-sided) Wilcoxon Signed Rank test
Mean Blood Flow (ml/100ml/min)	6.91	P=0.000
Standard Deviation of Mean Blood Flow (ml/100ml/min)	10.61	P=0.000
Mean Blood Volume (ml/100ml)	0.18	P=0.036
Standard Deviation of Mean Blood Volume (ml/100ml)	-2.79	P=0.000
Mean Mean Transit Time (Seconds)	-0.63	P=0.000
Standard Deviation of Mean Mean Transit Time (Seconds)	-0.3	P=0.000

B5 Quantitative and qualitative evaluation of changes in tumour perfusion parameters during nelfinavir and radiotherapy

In order to test the hypothesis that nelfinavir improves tumour perfusion in patients with rectal cancer, we evaluated quantitative and qualitative changes in tumour perfusion on pCT scans performed before nelfinavir, after 7 days of nelfinavir and after 14 days of nelfinavir. No consistent pattern of percentage change in any perfusion parameter was observed between the pre-treatment pCT (scan 1) and the pCT on the 7th day of nelfinavir (scan 2) as illustrated in figure 34 and on statistical analysis of the evaluable scans, overall no statistically significant changes in tumour perfusion parameters were demonstrated (table 49).

Figure 34 Bar chart demonstrating percentage change in tumour parameters between baseline pCT scan and second pCT scan (on 7th day of nelfinavir administration)

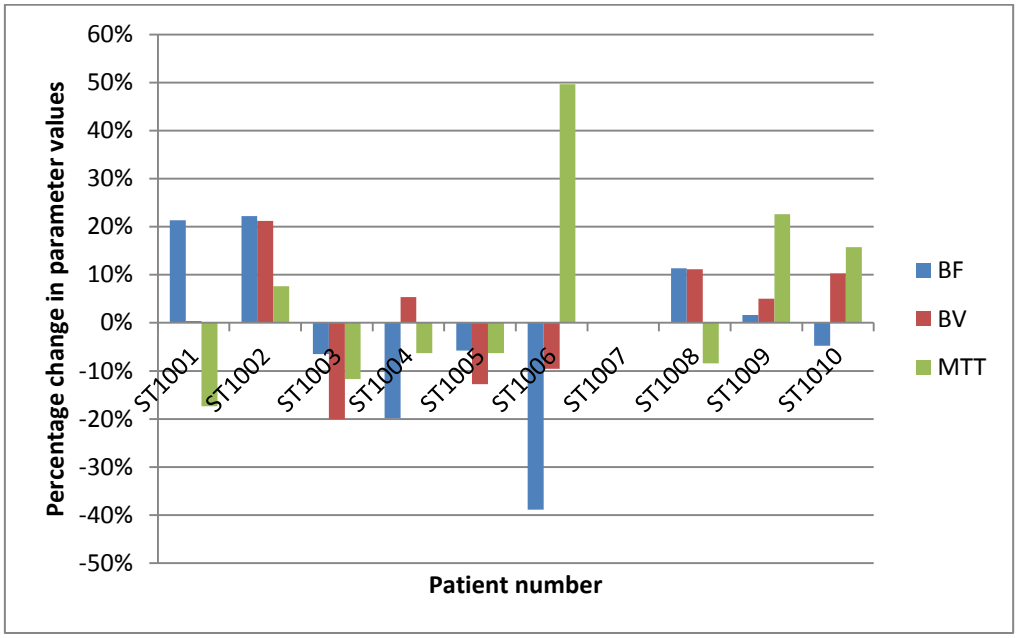

Table 49 Summary of percentage change and median absolute differences in parameter values between scans 1 and 2.

Perfusion Parameter	Mean percentage change in mean parameter values (difference in mean absolute values)
BF	- 0.02% (-0.12/100ml/min) P=0.566[1]
BV	+0.51% (+6.17ml/100ml) P=0.24[2]
MTT	+3.55% (+0.13secs) P=0.876[2]

1.Wilcoxon Signed Rank test 2. Paired *t* test

However, between the pCT on the 7th day of nelfinavir (scan 2) and the scan at the end of radiotherapy (scan 3) an increase in BF in association with a decrease in MTT was observed in 8 of 9 evaluable patients (see figure 35). Overall, a statistically significant difference in mean BF and mean MTT between scan 2 and 3 was demonstrated which amounted to a 40% mean increase in BF and 24% reduction in MTT, indicating improved tumour perfusion (table 50).

Figure 35 Bar chart demonstrating percentage change in pCT parameters between second scan (on seventh day of nelfinavir administration) and third scan (on last day of nelfinavir and radiotherapy)

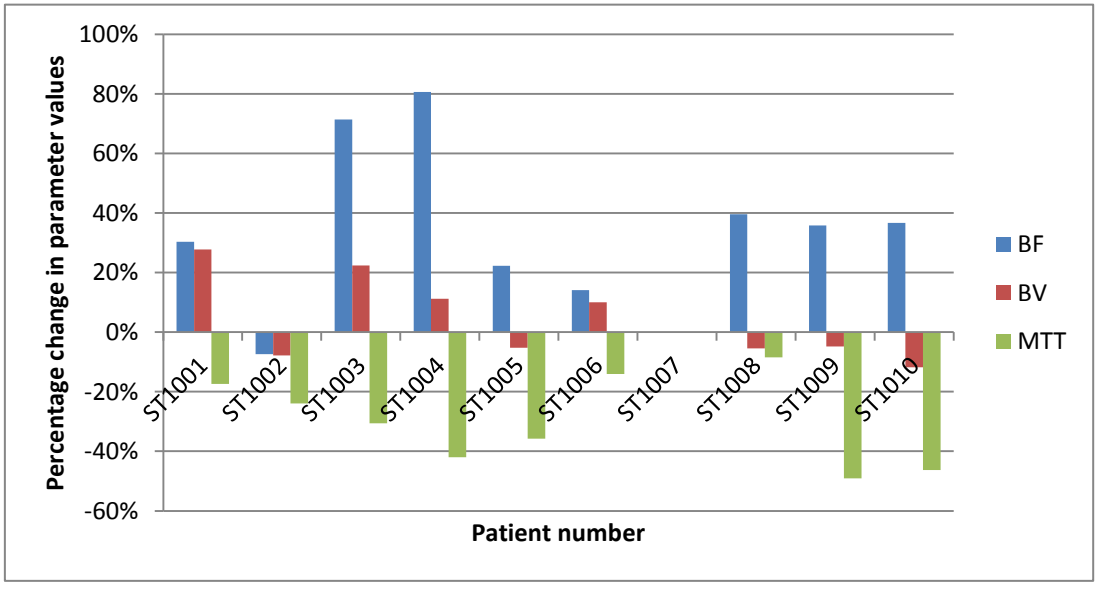

Table 50 Summary of percentage change and mean absolute differences in parameter values between scans 2 and 3

Perfusion Parameter	Mean percentage change in mean parameter values (difference in mean absolute values)
BF	+40% (15 ml/100ml/min) **P=0.001**
BV	+6% (0.25 ml/100ml) P=0.199
MTT	-28% (-3secs) **P=0.007**

Paired *t* test

A limitation of the quantitative evaluation of mean perfusion parameters is that it averages perfusion parameters across the voxels in the region of interest and does not represent the heterogeneity of perfusion parameters within tumours. Therefore, a visual analysis of the spatial pattern of tumour perfusion parameters was performed by review of perfusion parameter maps from each of the scans. On qualitative analysis of perfusion parameter maps from the baseline scans it was observed that a number of the rectal tumour regions of interest appeared to have higher BF, higher BV and lower MTT than adjacent normal rectal mucosa (see figure 36). The greatest degree of contrast between tumour and normal rectum was observed on BV parameter maps, in which BV was greater in the tumour ROI than the normal rectal mucosa for all 7 evaluable patients. BF was visibly higher and MTT lower in the tumour ROI than the normal rectum for 5 evaluable patients. Intra-tumour heterogeneity in all perfusion parameters was observed and was a feature which distinguished the tumours from surrounding tissue on BV and BF maps but not for MTT maps where there was considerable heterogeneity of MTT values within normal tissues (see figure 36).

Figure 36 Example of pCT colour perfusion parameter maps for patient ST1008 demonstrating higher BF and BV in tumour (outline in purple) in comparison to normal rectal mucosa

Blood Flow **Blood Volume** **Mean Transit Time**

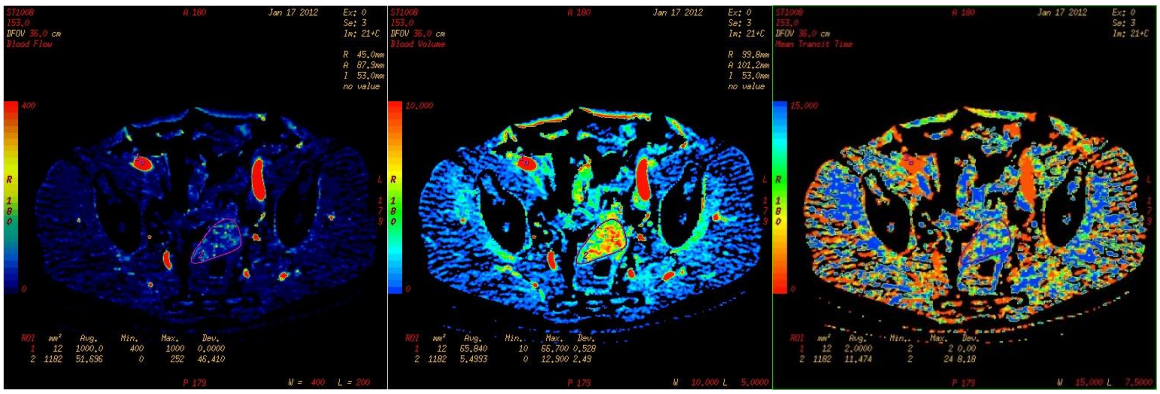

On review of delineated tumour ROIs at comparable anatomical levels on perfusion parameter maps from successive scans for each patient, changes in tumour perfusion were visually appreciable. For example, figure 37 illustrates a reduction in the proportion of yellow/red voxels in the tumour ROI corresponding to tumour regions with high BF values between scans 1 and 2 for patient ST1006.

Figure 37 Blood Flow parameter maps from Scans 1 and 2 for patient ST1006 illustrating an apparent reduction in Blood Flow after 7 days of nelfinavir

Scan 1 **Scan 2**

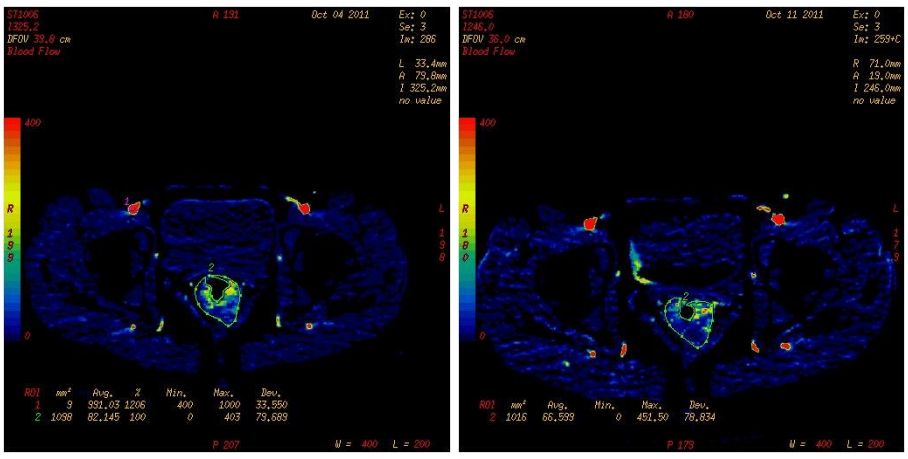

After 7 days of nelfinavir (between scans 1 and 2) there were appreciable increases in the proportion of tumour with high BF values for patients ST1001 and ST1002. After a further 7 days

of nelfinavir and concomitant radiotherapy there were appreciable increases in tumour BF in 6 of 7 evaluable patients (all but ST1002) and reductions in MTT were apparent for all evaluable patients, an example of which is illustrated in figure 38, consistent with the quantitative changes observed in mean perfusion parameters.

Figure 38 Perfusion parameter maps for patient ST1005 illustrating an apparent increase in Blood Flow and reduction in MTT between Scans 2 and 3

Scan 2 **Scan 3**

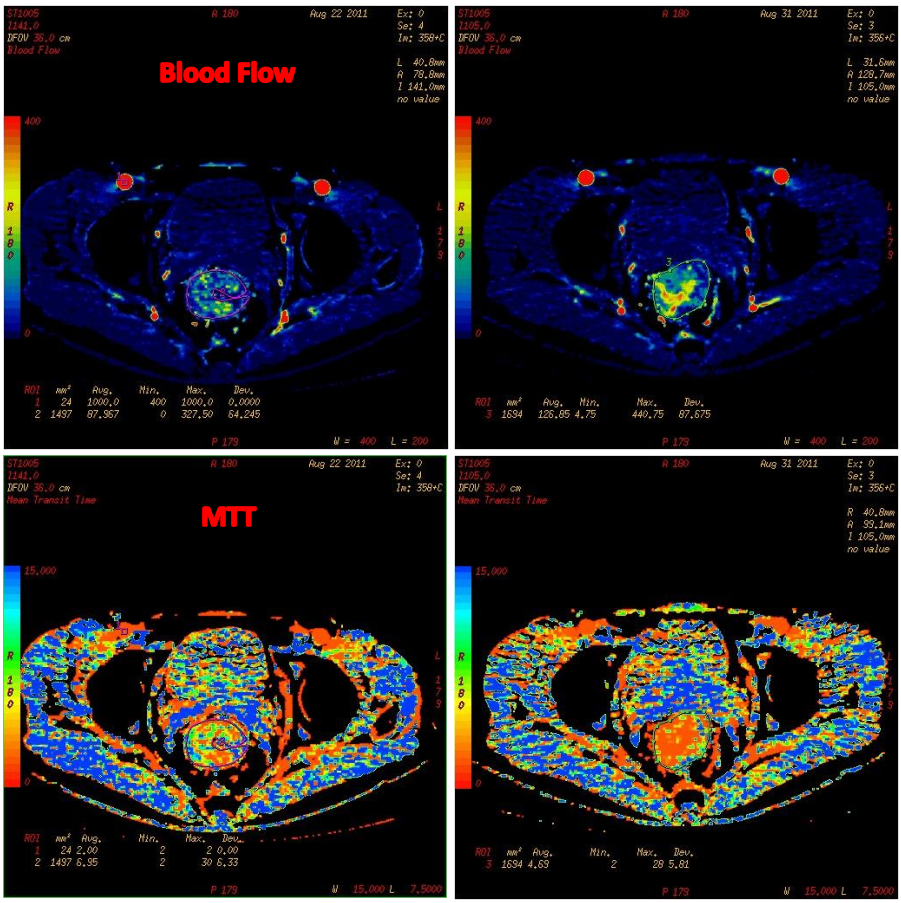

The pCT scan in patient 10 demonstrated high perfusion parameter values in a malignant right inguinal node as well as in the primary tumour (see figure 39). Although this patient discontinued nelfinavir after 3 days of treatment due to toxicity, appreciable visual and quantitative changes in tumour perfusion were observed in the primary tumour between the second and third scans but not between the first and second scan, suggesting that the significant changes between the second and third scans were caused by radiation plus nelfinavir. No significant changes in

perfusion were observed in the metastatic lymph node for this patient (which was outside the radiation field), adding further support to the interpretation of perfusion changes being due to radiotherapy, rather than the effect of nelfinavir alone.

Figure 39 Perfusion CT parameter maps for patient ST1010 from scans 2 and 3, demonstrating appreciable increase in perfusion within the irradiated primary tumour and no appreciable change in the right inguinal lymph node

Scan 2 **Scan 3**

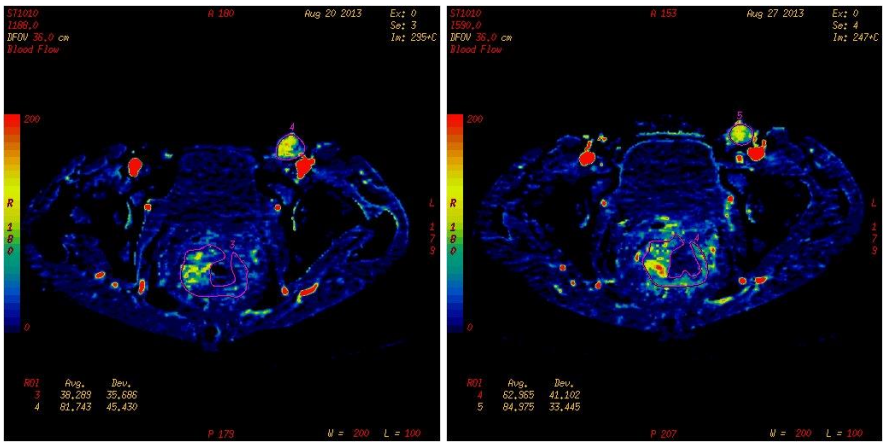

A semi-quantitative method for evaluating perfusion in a region of interest, which has potential to take account of heterogeneity, is histogram analysis of the relative frequency of voxels with perfusion parameter values within the range of values represented in the perfusion parameter map. To date, no published studies have evaluated tumour BF, BV and MTT heterogeneity in colorectal cancers using pCT, which is likely to be due to the limitation of commercially available software which has no functional capability to produce histograms of perfusion parameter values (i.e. BF, BV, MTT) within a ROI[425].

Using a customised computer program, developed in Matlab by Dr Jun Li, histograms were derived from grayscale perfusion parameter maps for each tumour volume. Distinctive histogram distributions were demonstrated for each of the perfusion parameters consistently across individual tumours. BF histograms for the tumour ROI were positively skewed, with the majority of voxels tending towards lower BF values. In general BV histograms were normally distributed

and MTT histograms had a bimodal distribution (see figure 40). This finding suggests that mean perfusion parameter values for the tumour ROI may not be the best measure for evaluation of changes in perfusion.

Figure 40 Representative histograms of BF, BV and MTT for tumour volume of interest .

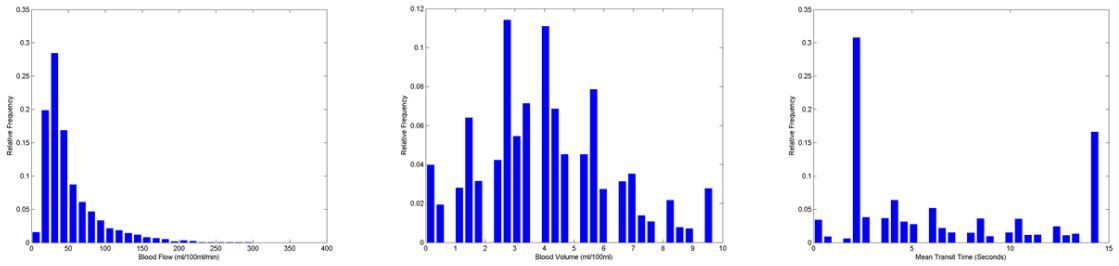

It was hypothesised that, although no changes in mean perfusion parameters were observed on pCT after 7 days of nelfinavir, nelfinavir could result in a change in the distribution of parameter values on histogram analysis of the tumour ROIs. Qualitative analysis of perfusion parameter value histograms derived for the tumour volume at comparable anatomical levels on pCT scans at the first and second time points demonstrated a rightward shift (reduced positive skew) in the BF distribution for 1 patient (ST1001) and leftward shift (increased positive skew) for one patient but the other histogram distributions were otherwise consistent between the first and second scans for individual patients (see figure 41 for example and Appendix 1 for data from all patients).

Figure 41 Histograms of BF, BV and MTT for tumour volume at comparable anatomical levels on scan 1 (pre-treatment) and Scan 2 (after 7 days of nelfinavir) for patient ST1008

Pre-Nelfinavir **After 7 days Nelfinavir**

Blood Flow

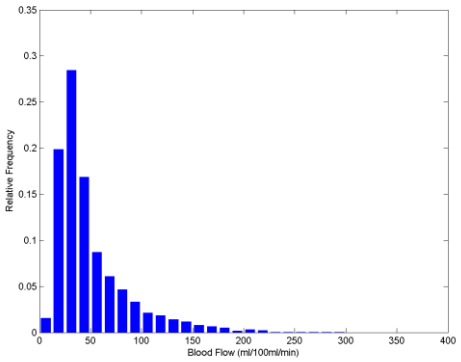

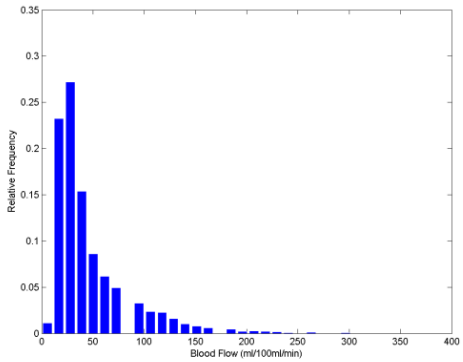

Blood Volume

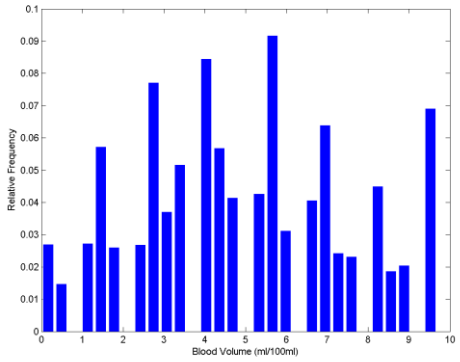

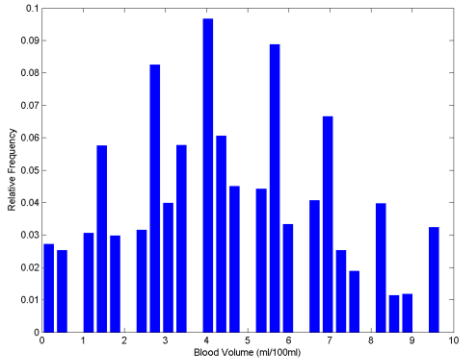

Mean Transit Time

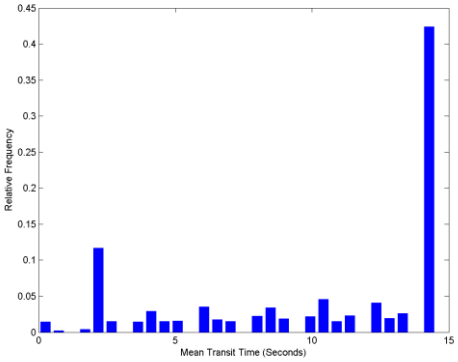

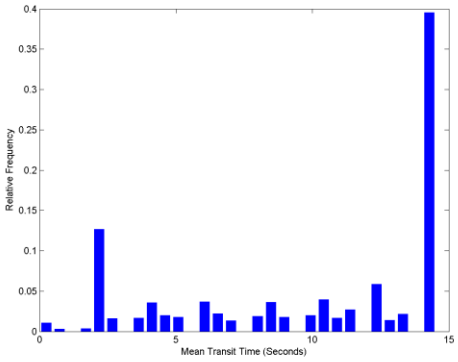

However, between the second and third scans, there was a rightward shift in the BF distribution for all but 1 patient (ST1002) representing a reduction of the proportion of tumour voxels with

low BF values and an increase in the proportion of tumour voxels with higher BF values (example illustrated in figure 42).

Figure 42 Blood Flow histograms for tumour VOI on scan 2 (after 7 days of nelfinavir) and scan 3 (after 14 days of nelfinavir and radiotherapy) for patient ST1005, demonstrating rightwards shift in relative frequency distribution of BF values

Scan 2 **Scan 3**

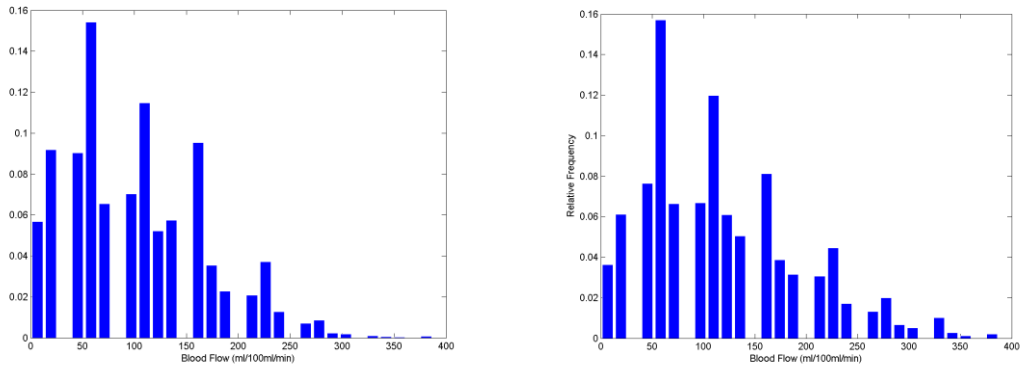

On analysis of BV histograms at the same time points, there appeared to be a flattening of the distribution curve (or "peakiness") for certain patients and an increase in the proportion of voxels with BV values >9 ml/100 ml for 6 of 10 patients (see figure 43), although visual interpretation was challenging due to steps in the curves. On analysis of MTT histograms, there was a reduction in the second peak at high MTT values for all evaluable patients, which was accompanied by an increase in the first peak at low perfusion values for 6 patients (ST1003, ST1004, ST1005, and ST1008, ST1009 and ST1010). An example of this is illustrated in figure 44.

Figure 43 Blood Volume histograms on scan 2 (after 7 days of nelfinavir) and scan 3 (after 14 days of nelfinavir and radiotherapy) for patient ST1003, demonstrating a flattening of the distribution and increase in the proportion of voxels with high BV (>9ml/100ml)

Scan 2 **Scan 3**

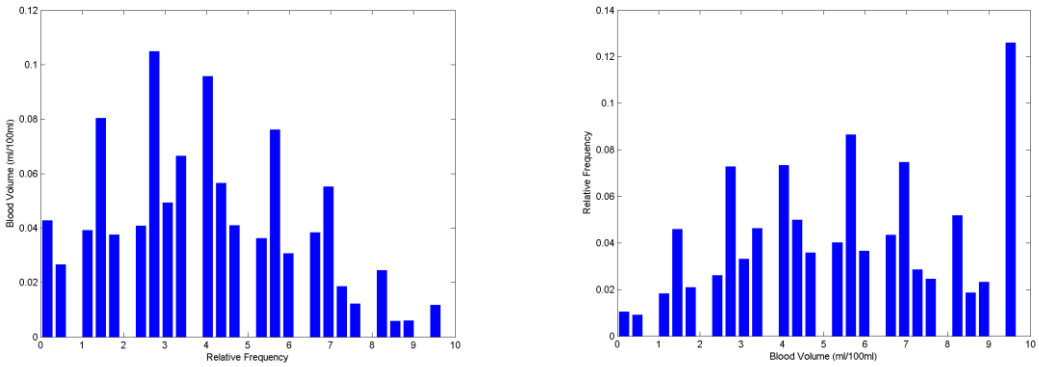

Figure 44 Mean Transit Time histograms on scan 2 (after 7 days of nelfinavir) and scan 3 (after 14 days of nelfinavir and radiotherapy) for patient ST1003, demonstrating a reduction in the first peak in the distribution and increase in the second peak.

Scan 2 **Scan 3**

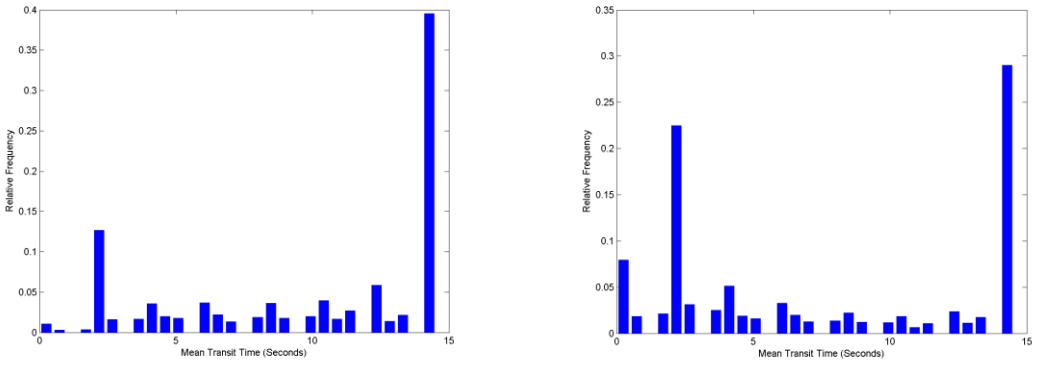

On the basis of this qualitative analysis we evaluated whether there was a statistical change in histogram distributions for perfusion parameters on successive scans in terms of “skewness” and “kurtosis”. Skewness is a measure of the asymmetry of data around the sample mean (Mathworks R2013b documentation), with normally distributed data having a skewness of 0. Histograms with a longer tail to the right of the mean have positive skewness and those with a longer tail to the left of the mean have a negative skewness. Kurtosis is a measure of how outlier

prone a distribution is (Mathworks R2013b documentation), with a normal distribution having a kurtosis of 3, distributions which are more outlier prone having a kurtosis of greater than 3, and distributions which are less outlier prone having a kurtosis of less than 3. On analysis of histograms derived from the baseline pCT scan and subsequent pCT scan after 7 days of nelfinavir (scans 1 and 2), there was no statistically significant difference in the mean skewness nor mean kurtosis of BF, BV and MTT histograms of the tumour volumes (see table 51 and 52).

Table 51 Table summarising changes in mean skewness between the tumour volume at comparable anatomical levels between scans 1 and 2

Parameter	**Mean (Range) on Scan 1**	**Mean (Range)on Scan 2**	**Mean Difference between Scan 1 and 2**	**95% CI of the Difference**		**Significance (2 tailed) Paired t test**
				Lower	Upper	
Blood Flow (ml/100ml /min)	2.44 (1.18-3.89)	2.25 (1.23-2.75)	-0.2	-0.32	0.71	P=0.409
Blood Volume (ml/100ml)	1.09 (0.44-2.52)	0.95 (0.59-1.76)	0.14	-0.32	0.61	P=0.495
Mean Transit Time (Secs)	4.11 (2.67-4.93)	4.11 (3.14-4.88)	0.00	-0.43	0.43	P=0.995

Table 52 Table summarising changes in mean kurtosis between the tumour volume at comparable anatomical levels between scans 1 and 2

Parameter	**Mean (Range) on Scan 1**	**Mean (Range)on Scan 2**	**Mean Difference between Scan 1 and 2**	**95% CI of the Difference**		**Significance (2 tailed) Paired t test**
				Lower	Upper	
Blood Flow (ml/100ml /min)	8.81 (3.42-18.36)	7.24 (3.57- 9.33)	1.57	-1.52	4.66	0.276
Blood Volume (ml/100ml)	4.10 (2.33-10.7)	3.41 (2.66-5.59)	0.7	-1.30	2.69	0.445
Mean Transit Time (Secs)	20.17 (10.01-26.22)	20.04 (12.02 - 25.7)	0.13	-3.13	3.39	0.931

On analysis of histograms derived from pCT scans after 7 days of nelfinavir and at the end of 14 days of nelfinavir and concomitant pelvic radiotherapy (scans 2 and 3) there was no statistically significant change in the mean skewness nor mean kurtosis of BF, BV and MTT histograms of tumour volumes (see tables 53 and 54). However, there was a trend towards reduction in mean positive skewness of the BF histograms and a trend towards reduction in mean positive skewness of the MTT histograms after radiotherapy and nelfinavir.

Table 53 Table summarising changes in mean skewness of histograms for the tumour volume at comparable anatomical levels between scans 2 and 3

Parameter	**Mean (Range) on Scan 2**	**Mean (Range)on Scan 3**	**Mean Difference between Scan 2 and 3**	**95% CI of the Difference**		**Significance (2 tailed) Paired t test**
				Lower	Upper	
Blood Flow (ml/100ml /min)	2.14 (1.13-2.97)	1.80 (0.64-2.55)	0.34	-0.03	0.71	P=0.064
Blood Volume (ml/100ml)	0.95 (0.59 - 1.76)	1.1 (0. 64-1.89)	-0.13	-0.53	0.24	P=0.400
Mean Transit Time (Secs)	4.19 (3.44-4.55)	3.48 (2.14-4.94)	0.84	-0.17	1.84	P=0.091

Table 54 Table summarising changes in mean kurtosis between the tumour volume at comparable anatomical levels between scans 2 and 3

Parameter	**Mean (Range) on Scan 2**	**Mean (Range)on Scan 3**	**Mean Difference between Scan 2 and 3**	**95% CI of the Difference**		**Significance (2 tailed) Paired t test**
				Lower	Upper	
Blood Flow (ml/100ml /min)	6.97 (3.11-11.5)	5.72 (1.86- 8.29)	1.41	-0.53	3.36	P=0.132
Blood Volume (ml/100ml)	3.41 (2.66-5.59)	3.92 (1.86-6.49)	-0.5	-1.76	0.76	P=0.384
Mean Transit Time (Secs)	19.19 (12.33-25.64)	15.03 (7.7-26.32)	2.6	-1.3	11.13	P=0.445

B6 Summary

In summary, it has been demonstrated that there can be considerable variability in mean pCT parameters between different pCT slices in the cranio-caudal axis. This suggests that derivation of pCT parameters from a single slice may be non-representative and be a source of measurement error when evaluating changes in perfusion on sequential pCT scans. Methods of pCT analysis have been developed which take into account tumour perfusion heterogeneity and permits evaluation of changes in pCT parameters in anatomically comparable regions of tumour on successive scans. Findings demonstrate that this method of analysis can reduce inter-observer variation in parameter estimation compared to single pCT slice analysis. No significant changes in rectal tumour pCT parameters were demonstrated after 7 days of nelfinavir before radiotherapy but statistically significant increases in tumour BF and decrease in MTT were demonstrated after 7 days of nelfinavir in combination with hypo-fractionated radiotherapy. Histogram analysis showed that following nelfinavir and radiation there is an increase in the proportion of voxels in the tumour VOIs with higher BV, higher BF and low MTT values, in association with a reduction in the proportion of voxels with lower BF and higher MTT values.

3D Perfusion Imaging of Rectal Cancer using Dce-MRI

In this section, results from the Dce-MRI scans acquired and analysed as part of the study protocol are described. The technical challenges that are encountered in derivation of pharmacokinetic parameters from the Dce-MRI scans are evaluated. The feasibility of performing dual modality perfusion imaging with Dce-MRI as well as pCT at multiple time points in patients with rectal cancer receiving drug therapy before and concurrent with radiotherapy is evaluated. The results of quantitative and qualitative analysis of MRI scans during nelfinavir and radiotherapy are presented to test the hypothesis that nelfinavir can improve perfusion to human rectal tumours. Specifically, it is postulated that nelfinavir might be expected to increase the pharmacokinetic parameter K^{trans} in human rectal cancers and this is analysed. It is assessed

whether the evaluation of changes in tumour perfusion using Dce-MRI provides comparable information to the evaluation of changes in tumour perfusion using pCT.

D1 Scans Performed and evaluated

Nine patients underwent Dce-MRI scanning at all 3 time points (see figure 45). Table 55 summarises the timing of the scans in relation to the commencement of nelfinavir and completion of radiotherapy. All baseline scans were performed within 14 days of commencing nelfinavir, in line with recommendations which suggest that baseline Dce-MRI studies should be within 14 days of treatment[428].

Figure 45 Dce-MRI Scans performed and evaluated

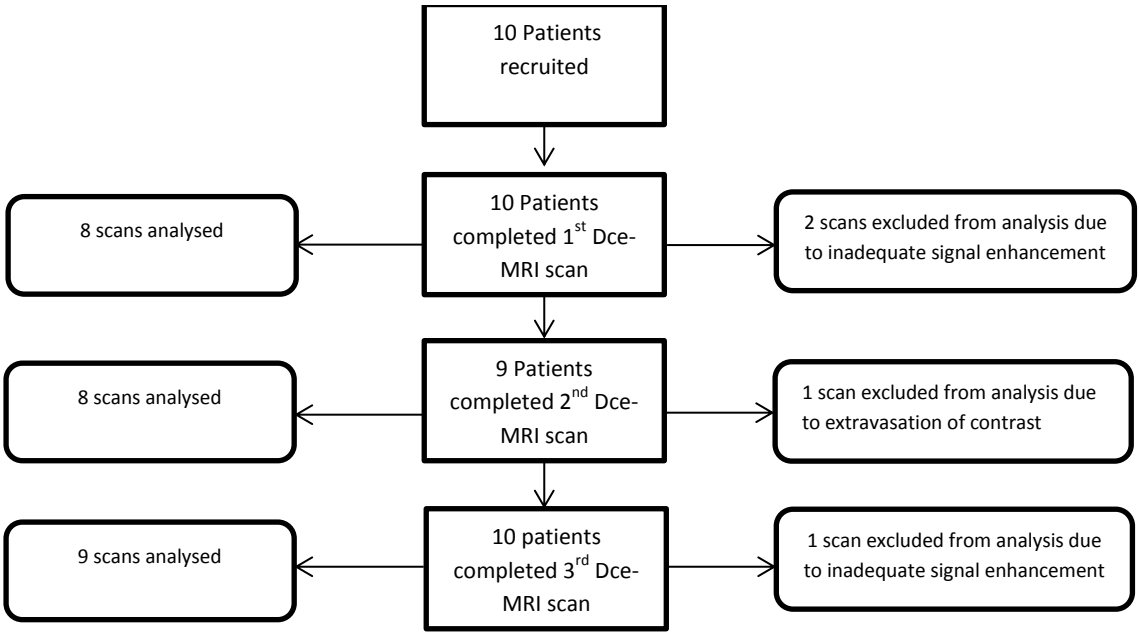

Table 55 Timing of Dce-MRI scans in relation to nelfinavir and radiotherapy

	Number of days between scan 1 and start of nelfinavir	Number of days between commencement of nelfinavir and scan 2	Numbers of days between last fraction of radiotherapy and scan 3
ST1001	**7**	**Not performed**	**0**
ST1002	**7**	**7**	**2***
ST1003	**8**	**6**	**1***
ST1004	**1**	**7**	**0**
ST1005	**5**	**5***	**1***
ST1006	**1**	**6**	**0**
ST1007	**14**	**6**	**0**
ST1008	**1**	**6**	**0**
ST1009	**1**	**6**	**0**
ST1010	**1**	**6**	**0**

***deviation from protocol**

One patient (patient 1) did not undergo the second Dce-MRI scan because of illness (vertigo). A further 4 scans were excluded from analysis because of: extravasation of gadolinium contrast (second scan for patient 5) and inadequate contrast enhancement (baseline scans for patient 1 and 6; third scan for patient 8). Seven patients (2, 3, 4, 7, 8, 9 and 10) successfully underwent dual modality perfusion imaging (Dce-MRI and perfusion CT) at all three time points and both types of scan were evaluable at all three time points for 5 patients.

D2 Technical factors influencing perfusion parameter analysis

Few published studies integrating Dce-MRI into the assessment of rectal cancer have documented the effects of intra-sequence tumour motion or use of motion correction strategies [437, 438]. However, recently drafted guidance on the use of Dce-MRI as an imaging biomarker (not limited to rectal cancer) recommends that Dce-MRI data affected by motion should be motion corrected before analysis or excluded from pharmacokinetic analysis[428]. Using a modified version of a semi-quantitative scoring system used in a previous study of Dce-MRI in colorectal liver metastases[439], the severity of intra-sequence rectal tumour motion on dynamic contrast-enhanced images was evaluated for each of the scans in this study. Although rectal tumours are

considered to be relatively fixed tumours, the presence of some degree of intra-sequence tumour motion was demonstrated for all uncorrected Dce-MRI scans in this study (see table 56).

Respiratory and peristaltic motions were both evident, with each type of motion predominating in some studies but contributing equally in others. Intra-sequence tumour motion was re-evaluated after motion correction using the deformable image registration algorithm using the same scoring system. Improvements in the severity of intra-sequence tumour motion were demonstrated for all studies, with 24 of 27 evaluable studies being given a motion severity score of 0 or 1 (no or slight motion) after motion correction. However, in three studies classified as exhibiting severe intra-sequence tumour motion, the uncorrected studies still displayed a moderate degree of tumour motion after motion correction. As none of the corrected studies were classed as demonstrating "significant" or "severe" intra-sequence tumour motion, all studies were included in subsequent analyses.

Table 56 Table of motion score for Dce-MRI score before and after motion correction (MC) for each patient on each scan. The degree of motion affecting the tumour on dynamic images was categorised according to the following scale: Score 0= No motion, Score 1= Slight motion, Score 2= Moderate motion, Score 3=Significant motion, Score 4= Severe motion

Patient number	Scan 1 Motion Score		Scan 2 Motion Score		Scan 3 Motion Score	
	Non MC	MC	Non MC	MC	Non MC	MC
1					3	1
2	1	0	1	0	1	0
3	2	0	2	0	2	0
4	3	1	3	1	3	1
5	1	0	1	0	1	0
6	2	0	2	0	2	0
7	1	0	1	0	1	0
8	4	2	4	2	4	2
9	2	1	2	1	2	1
10	2	0	2	0	2	0

A number of technical challenges were encountered in the process of co-registering dynamic T1W MRI scans with T2W MRI scans (acquired from the same scanning episode) in order to translate the co-ordinates of delineation "masks" from the T2W MRI images to the T1W images

and associated parameter maps, for extraction of mean quantitative parameters for the tumour VOI. Manual adjustments were required to produce a registration that was acceptable in 18 of 25 (72%) evaluable scans. Figure 46 illustrates an example of misaligned T1 and T2W MRI images of a rectal tumour before and after manual correction using Insight Toolkit Software. Figure 47 summarises the registration errors between T2W and T1W MRI scans in the x, y and z axes for individual scans; the mean (SD) transformation vectors to correct the misalignment of the T1 and T2W MRI scans were -9.13 mm (14.51), 0.5 mm (11.43) and 10.125 mm (25.89) respectively. Additionally, rotational adjustments were required for 6 scans (Patient 4- scans 1, 2 and 3; Patient 5 scan 1; Patient 6 scans 1 and 3). An issue which may have contributed to errors in registration in this study is the acquisition of T1W and T2W MRI images in different planes; guidelines now recommend that T1W and correlative imaging should be acquired in the same plane[428]. Further challenges were encountered when the transformations were applied to the tumour masks having been delineated on T2W MRI images but co-registered to the T1 images.

Figure 46 Illustration of co-registration of T1 and T2 MRI images for patient 4 (scan 1). Image (a) shows misalignment of T1 and T2W MRI scans using automated co-registration. Image (b) shows isoline contours of structures on T1W MRI superimposed on T2W MRI images before manual transformation of alignment and (c) shows the same co-registration after manual transformation.

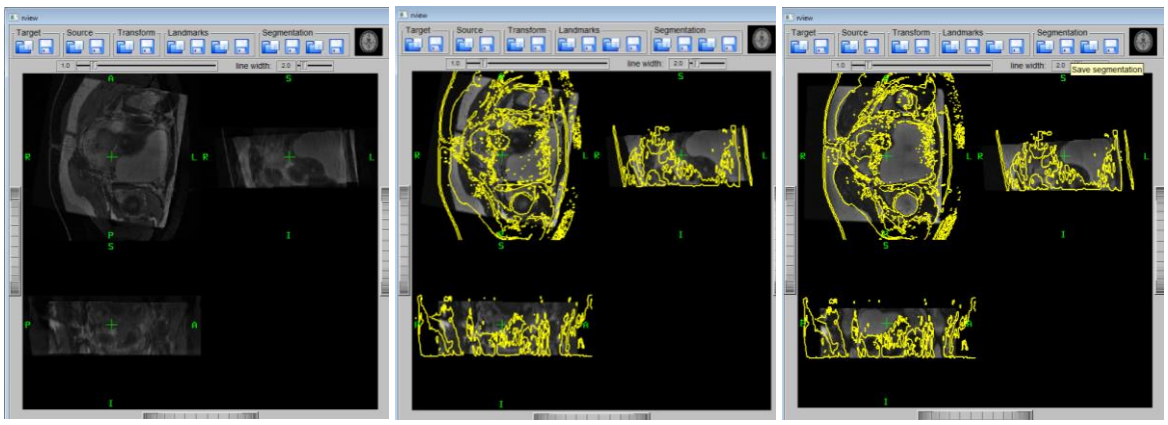

(a) **(b)** **(c)**

Figure 47 Summary of transformations of T1/T2 registrations. Y axis indicates manual adjustment of T2 images required in the X, Y and Z axes after automated co-registration to permit accurate registration with T1 images.

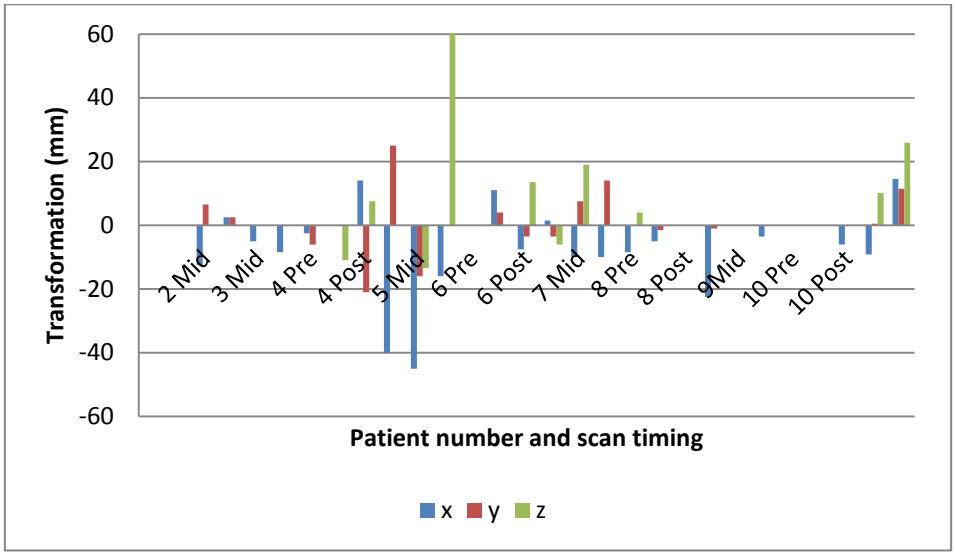

Figure 48 Illustration of (a)T2W MRI (b)T2WMRI with superimposed mask (c) T1WMRI and (d) T1W MRI with superimposed mask, illustrating some discordance between tumour on T1W MRI and mask for patient 4

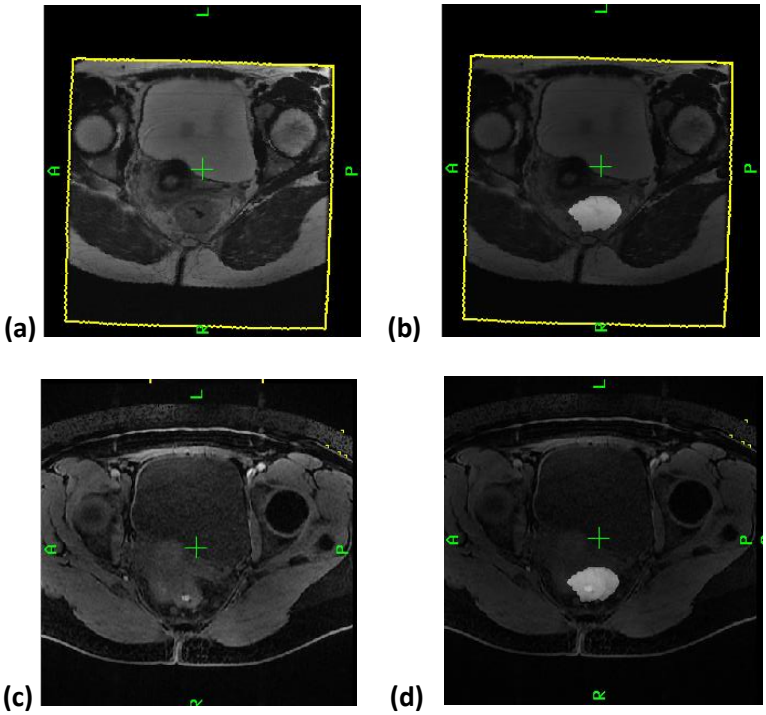

In a minority of cases, there was some visible discordance between the mask and apparent boundary of the tumour on T1W MRI images. The discordance appeared significant for patient 4

(illustrated in figure 48), in which the upper/mid rectal tumour appeared to have changed position between the T2 W MRI and T1W MRI images acquired during the same scanning episode (this interval is typically 45 minutes). For this patient, the tumour was re-delineated on the T1W images with reference to the T2W MRI images. Another issue specific to transposition of masks delineated on T2W images to T1W images in this study is that the resolution of the T1W MRI images was greater than that for the T2W MRI images (slice thickness 2 mm versus 3 mm), such that it was necessary to interpolate the tumour mask derived from T2W MRI analysis between slices. Setting different intensity thresholds for interpolating the masks resulted in slightly different tumour volumes. Although this step may be a source of systematic error when translating tumour ROIs delineated on the T2W MRI images to T1W MRI images, an interpolation threshold of 1 was consistently applied across all scans analysed to minimise inclusion of non-tumour regions when extracting perfusion parameters from the parameter maps.

An additional problem when delineating tumour ROIs on T2W MRI images to apply toT1W dynamic sequences is that it is challenging to reproducibly edit out luminal air, since the T2W image is static and the position and amount of luminal air can vary with peristaltic motion, as demonstrated on review of the T1W MRI images in this study. In practice, small volumes of intra-luminal air were not edited out on the T2W MRI and this resulted in variable amounts of air being covered by the tumour masks on successive T1W dynamic MRI sequences. As luminal air is non-enhancing, inclusion of these voxels in the derivation of the tumour VOI for extraction of mean perfusion parameters may have influenced the values derived. Delineation of the tumour ROIs on T2W MRI scans performed at the end of radiotherapy was more difficult than on the pre-radiotherapy scan due to the presence of radiotherapy related oedema, which blurred the boundaries of the tumour in some cases.

Finally, it is recommended that prior to pharmacokinetic parameter estimation from the dynamic T1 image, a native T1 map is generated of the pre-contrast T1 values for the imaged tissue

volume (T10 estimation)[356, 428], which is used when converting changes in signal intensity to gadolinium concentration, as the intrinsic relaxation rate of the tissue determines the signal produced after gadolinium contrast injection[440]. T1 mapping is typically derived from T1 images acquired immediately prior to the dynamic T1 sequence using variable flip angle sequences. After acquisition of the Dce-MRI scans in this study, it became apparent that the variable flip angle sequences acquired as part of the DESPOT sequence in our scanning protocol was sub-optimal for T1 mapping and therefore a uniform T10 value was assumed for the scanned volume. This issue may have affected the accuracy of the PK parameters derived from Dce-MRI analysis in this research, since it has been demonstrated that lack of flip angle correction for quantitative T1 determination results in underestimation of T1 values[441].

D3 Qualitative and Quantitative Evaluation of Changes in Tumour Perfusion during Nelfinavir and Radiation Therapy for Rectal Cancer

In order to further test the hypothesis that nelfinavir improves tumour perfusion in patients with rectal cancer, we evaluated qualitative and quantitative changes in tumour perfusion on Dce-MRI scans performed before nelfinavir, after 7 days of nelfinavir and after 14 days of nelfinavir. Since the pharmacokinetic parameter K^{trans} approximates to blood flow in tissues with high permeability (such as tumours), it was postulated that nelfinavir might be expected to result in increased tumour K^{trans}.

Table 57 Intra-patient and inter-patient variation in pharmacokinetic parameters

	Mean K^{trans}	Mean V_e	Mean K_{ep}
Mean intra-patient coefficient of variation on scans 1 to 3 (range)	0.18 (0.06-0.39)	0.08 (0- 0.16)	0.11 (0.03-0.26)
Inter-patient coefficient of variation			
Scan 1	0.33	0.09	0.25
Scan 2	0.39	0.12	0.29
Scan 3	0.42	0.18	0.24

In general, inter-patient variation in the mean pharmacokinetic parameters K^{trans}, V_e and K_{ep} for tumour volumes of interest was greater than the intra-patient variation for successive scans. Therefore, percentage change in the pharmacokinetic parameters for individuals was evaluated in addition to absolute changes between successive scans. In accordance with published recommendations, the mean, median and standard deviation of pixel values within the tumour VOI were calculated for the pharmacokinetic parameters[428] on successive scans(figure 49). The percentage change in median parameters is also represented graphically, as the median figures are the figures considered of most value[428].

Figure 49 Bar charts representing absolute values for (a)mean K^{trans}, (b)standard deviation of mean K^{trans} and (c)median K^{trans} within the tumour VOI on successive Dce-MRI scans

(a)

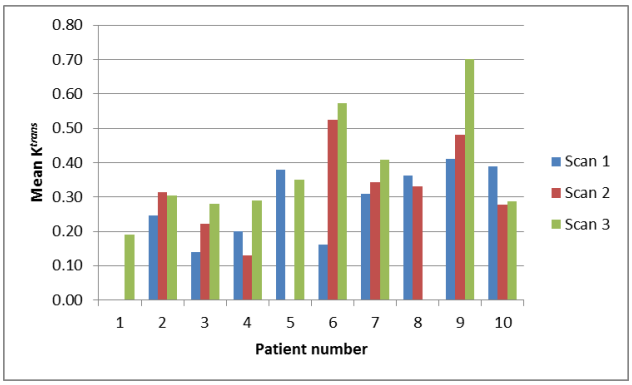

(b)

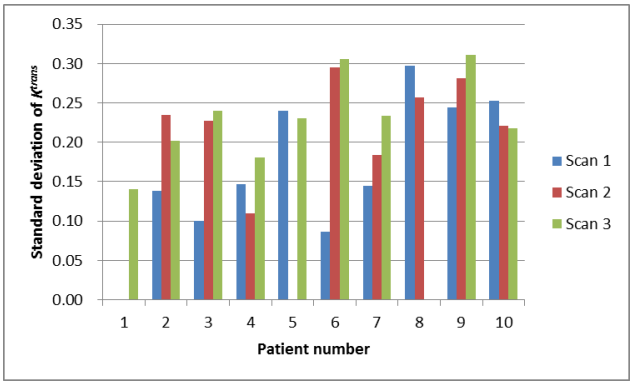

(c)

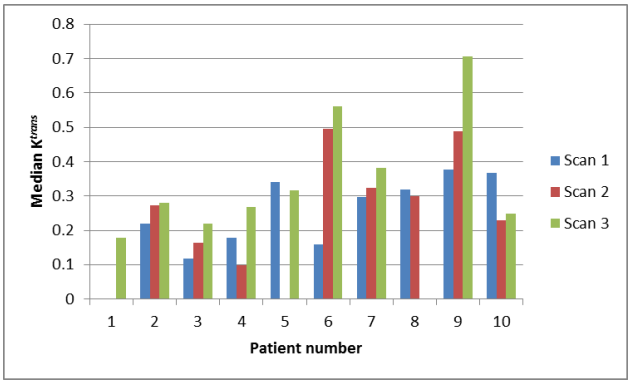

On analysis of the percentage change in median pharmacokinetic parameters between sequential scans for the 10 patients evaluated, no consistent pattern of change in percentage change of any of the parameters was observed between the pre-treatment Dce-MRI (scan 1) and the Dce-MRI on the 7th day of nelfinavir (scan 2) as illustrated in figure 50.

Figure 50 Percentage change in median pharmacokinetic parameters for tumour VOI after 7 days of nelfinavir

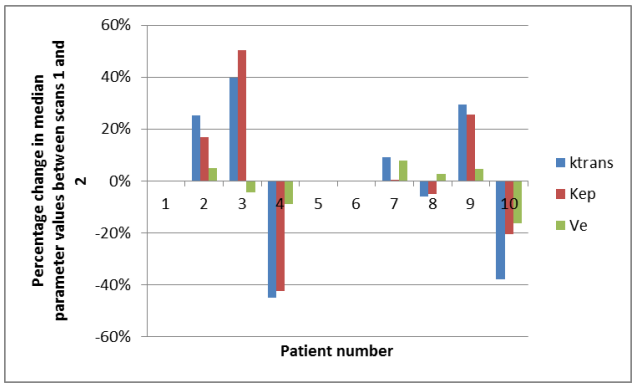

Figure 51 Percentage change in pharmacokinetic parameter values after a further 7 days of nelfinavir and pelvic radiotherapy (*magnitude of change extends beyond 100%)

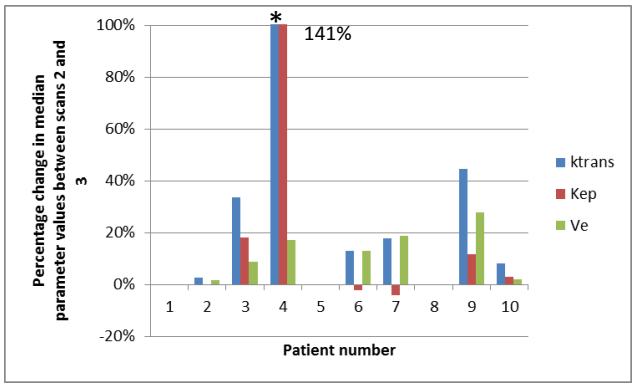

Between the Dce-MRI on the 7th day of nelfinavir (scan2) and the scan at the end of radiotherapy (scan 3) an increase in median K^{trans} in association with an increase in median V_e was observed in all 7 evaluable patients (see figure 51). Overall, a statistically significant difference in mean/median K^{trans} and mean/median V_e between scan 2 and 3 was demonstrated which amounted to a 42% mean increase in median K^{trans} and 13% increase in V_e(table 58).

Table 58 Summary of percentage change and mean absolute differences in parameter values between scans 1 and 2. Changes were non-significant statistically (paired t test).

Pharmacokinetic Parameter	Mean percentage change in mean parameter values (difference in absolute values)	Mean percentage change in median parameter values (difference in absolute values)
K^{trans}	+33% (0.05)	+29% (0.04)
K_{ep}	+19% (+0.06)	+22% (+0.07)
V_e	+14% (+0.01)	+2% (+0.007)

Table 59 Summary of percentage change and mean absolute difference in parameter values between scans 2 and 3

Pharmacokinetic Parameter	Mean percentage change in mean parameter values (difference in absolute mean values)	Mean percentage change in median parameter values (difference in absolute median values)
K^{trans}	+32% (+0.08) **P=0.04**	+42% (+0.08) **P=0.03**
K_{ep}	+15% (+0.06) P=0.14	+24% (+0.07) P=0.208
V_e	+14% (+0.07) **P=0.02**	+13% (+0.07) **P=0.018**

(Paired *t* test)

As for perfusion CT, a limitation of the quantitative evaluation of mean perfusion parameters using Dce-MRI is that perfusion parameters are averaged across the voxels in the region of interest and the heterogeneity of perfusion parameters within tumours is not represented. Therefore, a visual analysis of the spatial pattern of tumour perfusion parameters was performed by review of perfusion parameter maps from each of the scans. As tumour volume outlines were generated independently of the perfusion parameter maps, parameter maps were fused with T2W MRI scans (on which tumours were visualised and delineated) in order that the anatomical and functional information could be combined (see figure 52). On qualitative analysis of perfusion parameter maps from the baseline scans, it was observed that there was intra-tumoural heterogeneity in K^{trans}, K_{ep} and V_e; some tumours had predominantly low K^{trans} values overall (e.g. ST1002, ST1003) whilst others had relatively high K^{trans} values (e.g. ST1005, ST1008)in contrast to surrounding tissues.

Figure 52 Illustration of co-registration of *Ktrans* parameter map with T2W MRI scan for patient ST1008. This method was used to review the spatial pattern of pharmacokinetic parameters in relation to tumour localisation on T2W MRI scans.

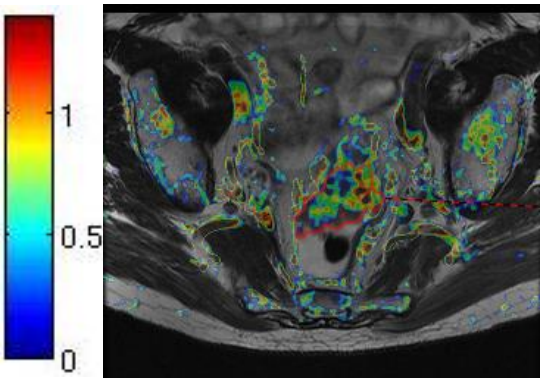

(tumour outlined on T2W MRI in red).

On review of delineated tumour VOIs on perfusion parameter maps at comparable anatomical levels from evaluable scans at the first two time points (i.e. after 7 days of nelfinavir), minor increases in K^{trans} were appreciable for patients ST1002 and ST1009, as was a minor decrease in K^{trans} for ST1008 and no appreciable change for the remaining patients. On review of perfusion parameter maps from the second and third time points (i.e. after a further 7 days of nelfinavir and 25Gy in 5# radiotherapy) in evaluable scans, appreciable increases in K^{trans} were observed within the tumour VOI and surrounding tissues for patient ST1003, ST1004, ST1006, ST1007 and ST1009.

Figure 53 K^{trans} parameter maps at comparable anatomical levels for patient ST1008 demonstrating no apparent change in K^{trans} within the tumour VOI between (a) baseline and (b)scan after 7 days of nelfinavir.

(a) **(b)**

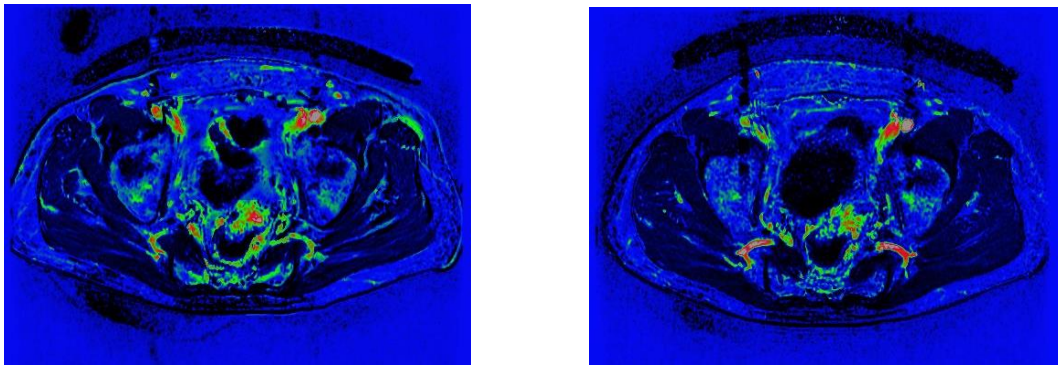

Figure 54 (a)K^{trans} and (b)V_e parameter maps for patient 9 demonstrating increase in K^{trans} within tumour VOI between scan after 7 days of nelfinavir and scan on last day of radiotherapy and nelfinavir for patient ST1009

(a) Scan 2 **Scan 3**

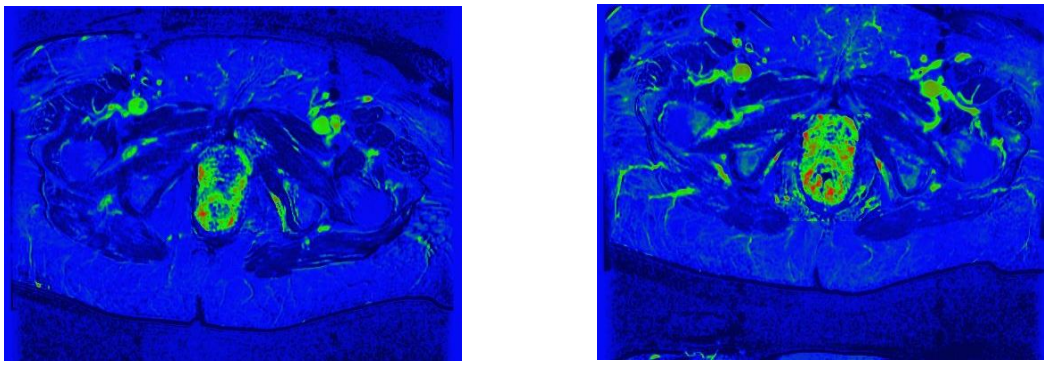

(b)

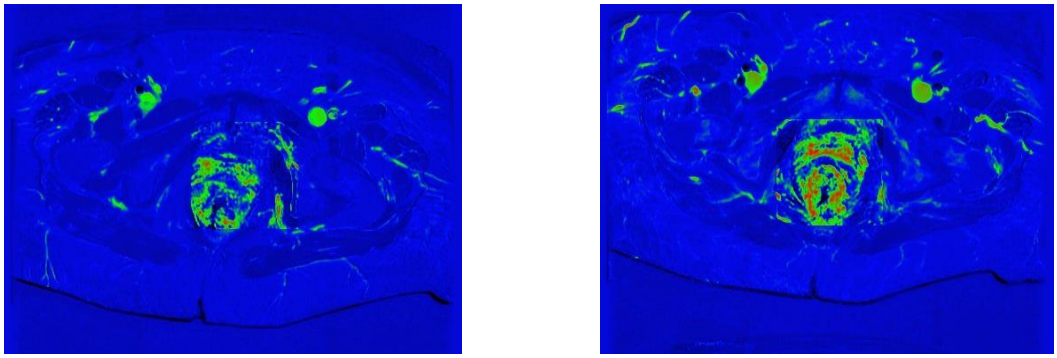

In contrast with the analysis of pCT scans using commercially available software, it was possible to derive histograms (representing the distribution of pharmacokinetic parameters within the tumour VOI) from Dce-MRI scans with relative ease. Consistent with previously published studies which have incorporated Dce-MRI histogram analysis[361, 364], it was demonstrated that histograms of K^{trans} values within the rectal tumour volume of interest on the baseline Dce-MRI scans were characteristically positively skewed (see figure 55 a for an example and Appendix 2 for all histograms).

Figure 55 Examples of histograms of pharmacokinetic parameters for tumour VOI on baseline study (a) K^{trans} (b) K_{ep} (c) V_e

(a) Patient 2 (positively skewed)

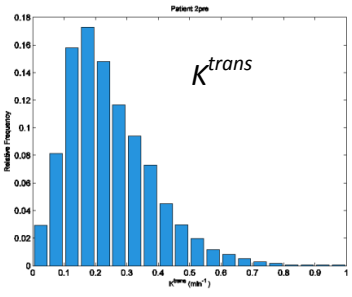

(b) Patient 2 (normally distributed) **Patient 7 (negatively skewed)** **Patient 9 (positively skewed)**

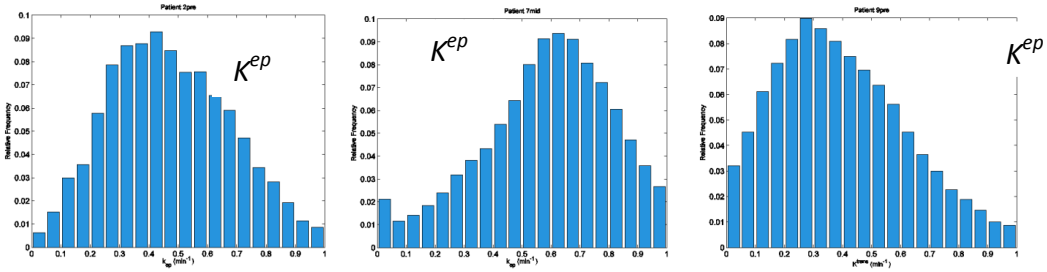

(c) Patient 2 (normally distributed)

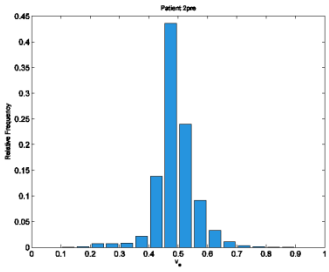

No consistent histogram shape was observed for K_{ep} values but histograms of V_e values within the tumour VOI were normally distributed (see figure 55 b and c). Evaluation of changes in the distribution of Dce-MRI parameter histograms have previously been demonstrated to provide supplementary benefit over and above summary statistics like the mean and median for response assessment for cancer therapies[361-364, 442]. Although no significant changes in average pharmacokinetic parameters were observed on Dce-MRI after 7 days of nelfinavir, it was postulated that nelfinavir may result in a change in the distribution of parameter values on

histogram analysis of the tumour VOIs, with the expectation that nelfinavir would result in a rightward shift in the distribution of K^{trans} histograms and a reduction in the proportion of voxels with lower K^{trans} values towards higher values.

Figure 56 Changes in K^{trans} histograms after 7 days of nelfinavir. K^{trans} Histograms at baseline and after 7 days of nelfinavir demonstrate (a) rightwards shift in distribution in patient 9 (b) leftwards shift in distribution for patient 10

(a) Baseline **After 7 days of nelfinavir**

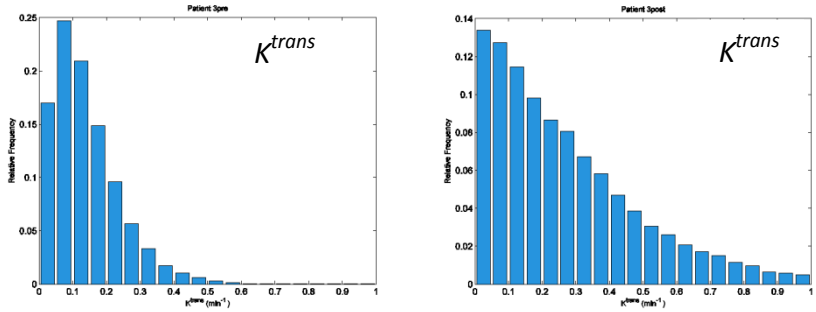

(b) Baseline **After 7 days of nelfinavir**

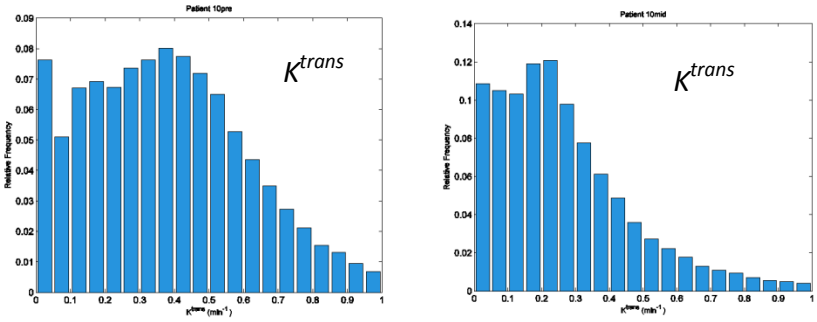

Qualitative analysis of pharmacokinetic parameter histograms derived for the tumour volume from Dce-MRI scans at the first and second time points demonstrated a rightward shift (reduced positive skew) in the K^{trans} distribution for four evaluable patients (ST1002, ST1003, ST1007, ST1009), leftward shift (increased positive skew) for two patients (ST1004, ST1010) [see figure 56] and no apparent change in the shape of the K^{trans} histogram for one patient (ST1008). Of note, a substantial proportion of the K^{trans} histograms showed a high proportion of voxels with very low K^{trans} values, which was frequently variable between sequential scans. This may be at least partly

explained by the inability to edit it out all of the intra-luminal air from the volume of interest in the dynamic MRI sequences, which would not be expected to enhance with contrast.

Between the second and third scans (after a further 7 days of nelfinavir and 25Gy in 5# radiotherapy), there was a rightward shift in the K^{trans} distribution for 4 evaluable patients (ST1004, ST1006, ST1007, ST1009) representing a reduction of the proportion of tumour voxels with low K^{trans} values and an increase in the proportion of tumour voxels with higher K^{trans} values (see figure 57), and no apparent change in the shape of the K^{trans} distribution for 2 patients (ST1002 and ST1010).

Figure 57 Change in K^{trans} histograms between scan after 7 days of nelfinavir and scan of last day of radiotherapy and nelfinavir. K^{trans} histograms for scans 2 and 3 demonstrate rightwards shift in K^{trans} distribution for (a) patient 6 and (b) no marked change for patient 2

(a)

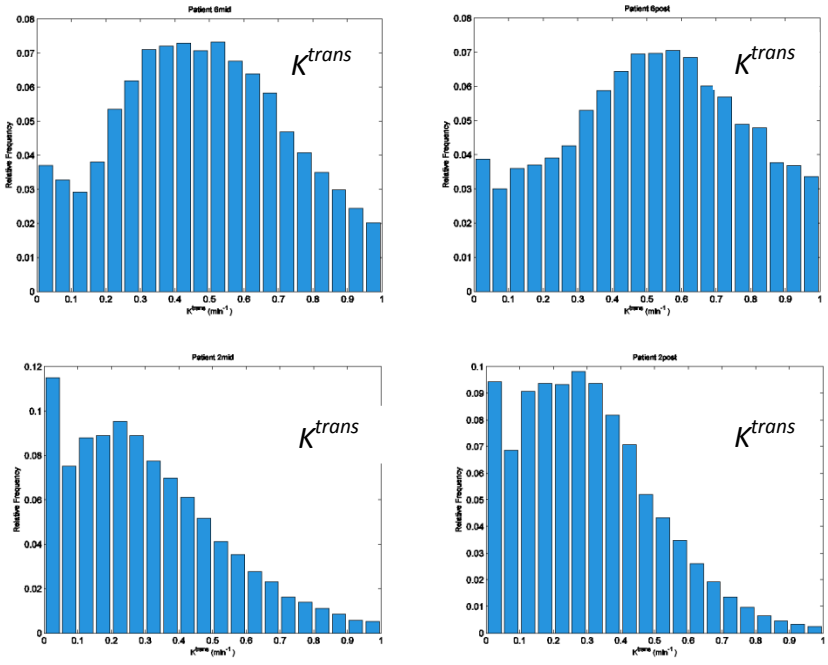

(b)

For one patient (ST1003), changes in the shape of the K^{trans} histogram were difficult to interpret, as there was a marked increase in the proportion of voxels with very low K^{trans} but otherwise little change in the distribution overall. For K_{ep}, no consistent patterns of change in the K^{trans} histograms were observed but the shape of the histograms were relatively consistent between scans 2 and 3

for the majority of patients (see Appendix 2). For V_e, a broadening of the histogram and a reduction in the height of the modal peak was observed for 3 patients between the first and second scans (ST1002, ST1003 and ST1006) and a narrowing of the curve associated with an increase in the height of the modal peak was observed for 2 patients (ST1008 and ST1010). Between the second and third scans, there was a rightwards shift in the shape of the V_e histograms (from a normal distribution to a negative skew) for 4 of 7 evaluable patients (ST1003, ST1006, ST1007 and ST1009). There was no change in the shape of the V_e histogram for 3 patients (ST1002, ST1004 and ST1010).

As for perfusion CT, on the basis of this qualitative analysis, an evaluation was carried out to see whether there was a statistical change in histogram distributions for Dce-MRI perfusion parameters on successive scans in terms of "skewness" and "kurtosis". On analysis of histograms derived from the baseline Dce-MRI scan and subsequent Dce-MRI scan after 7 days of nelfinavir (scans 1 and 2), there was no statistically significant difference in the mean skewness or mean kurtosis of K^{trans}, K_{ep} and V_e histograms of the tumour volumes (see table 60 and 61).

Table 60 Table summarising changes in skewness of histograms for Dce-MRI parameters on scans at baseline (scan 1) and after 7 days of nelfinavir (scan 2)

Parameter	Mean (Range) on Scan 1	Mean (Range) on Scan 2	Mean Difference between Scan 1 and 2	95% CI of the Difference		Significance (2 tailed) Paired *t* test
				Lower	Upper	
K^{trans}	1.01 (-0.4 -2.54)	1.20 (-0.39-3.12)	0.183	-0.77	1.13	P=0.654
K_{ep}	0.65 (-1.52 -3.48)	0.87 (-1.18 -3.86)	0.22	-1.33	1.78	P=0.737
V_e	1.97 (1.09-3.66)	1.76 (0.77-2.46)	-0.21	-1.09	0.67	P=0.581

Table 61 Table summarising changes in kurtosis of histograms for Dce-MRI parameters on scans at baseline (scan 1) and after 7 days of nelfinavir (scan 2)

Parameter	Mean (Range) on Scan 1	Mean (Range) on Scan 2	Mean Difference between Scan 1 and 2	95% CI of the Difference		Significance (2 tailed) Paired *t* test
				Lower	Upper	
K^{trans}	3.85 (1.56 – 10.78)	4.87 (1.61 – 13.03)	1.02	-2.97	5.00	P=0.555
K_{ep}	3.96 (1.54-15.64)	6.30 (1.67-17.10)	2.34	-3.51	8.19	P=0.365
V_e	6.65 (3.07 - 15.43)	5.40 (2.07 - 7.79)	-1.15	-5.49	3.20	P=0.543

On analysis of histograms derived from Dce-MRI scans after 7 days of nelfinavir and at the end of 14 days of nelfinavir and concomitant pelvic radiotherapy (scans 2 and 3) there was a statistically significant decrease in the mean skewness for K^{trans} and trend towards reduction in V_e but no statistically significant difference in skewness for K_{ep} (see table 62). There was a trend towards a reduction in mean positive kurtosis of the V_e histograms (see table 63) but no statistically significant change in the kurtosis of the Dce-MRI parameter histograms after radiotherapy and nelfinavir.

Table 62 Table summarising changes in skewness of histograms for Dce-MRI parameters on scans at baseline (scan 1) and after 7 days of nelfinavir (scan 2)

Parameter	Mean (Range) on Scan 2	Mean (Range) on Scan 3	Mean Difference between Scan 2 and 3	95% CI of the Difference		Significance (2 tailed) Paired *t* test
				Lower	Upper	
K^{trans}	0.92 (-0.39 – 3.12)	0.12 (-0.7 -0.98)	-0.80	-0.02	-1.58	**P=0.046**
K_{ep}	0.58 (-1.18-3.86)	-0.18 (-1.77 - 0.97)	-0.76	-2.66	1.14	P=0.367
V_e	1.64 (0.77 - 2.46)	1.08 (-0.2 -1.98)	-0.56	-1.12	0.01	P=0.053

Table 63 Table summarising changes in kurtosis of histograms for Dce-MRI parameters on scans after 7 days of nelfinavir (scan 2) and on last day of nelfinavir and radiotherapy (scan 3)

Parameter	Mean (Range) on Scan 2	Mean (Range) on Scan3	Mean Difference between Scan 2 and 3	95% CI of the Difference		Significance (2 tailed) Paired *t* test
				Lower	Upper	
K^{trans}	4.22 (1.61 - 13.03)	2.10 (1.34-3.71)	-2.13	-6.09	1.84	P=0.238
K_{ep}	5.02 (1.67-17.10)	2.96 (1.76-5.47)	-2.06	-3.5	8.19	P=0.365
V_e	4.85 (2.07-7.79)	3.49 (1.22-6.61)	-1.36	-2.98	0.25	P=0.084

D4 Comparison of Dce-MRI and pCT scans

In this study, both pCT and Dce-MRI scans were performed at multiple time points to evaluate the effect of a novel radio-sensitiser on tumour blood flow before and during radiotherapy. It is not known which of these modalities is optimal for evaluating the vascular effects of such drugs. Although K^{trans} is theoretically dependent on blood flow and permeability, and believed to approximate to blood flow in highly permeable tissues such as tumours, no previous studies in rectal cancer have evaluated the association between BF derived from pCT and K^{trans} derived from Dce-MRI. In this study the absolute mean BF values from pCT were plotted against mean K^{trans} values for the tumour from all evaluable scans (see figure 58) and there was no statistically significant positive correlation. However, there was weak statistically significant positive correlation between the percentage change in mean BF and mean K^{trans} on successive pCT and Dce-MRI scans respectively (see figure 59).

Figure 58 Scatter plot of absolute mean K^{trans} values on Dce-MRI against mean blood flow values on pCT (with line of best fit) and correlation statistics.

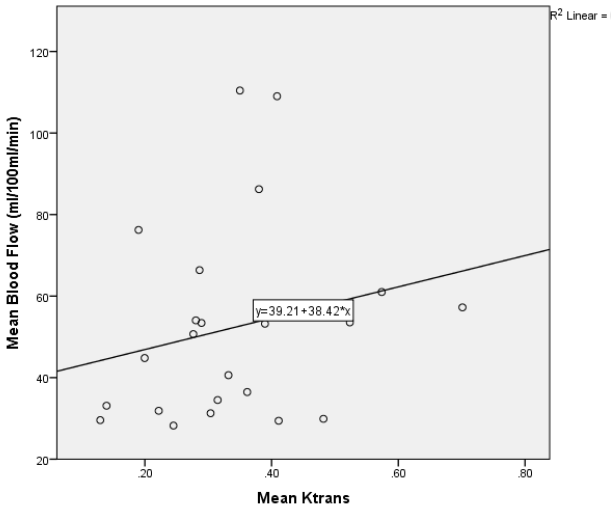

		Mean K^{trans}	Mean BF
Mean K^{trans}	Pearson Correlation	1	.220
	Sig. (2-tailed)		.313
	N	25	23
Mean BF	Pearson Correlation	.220	1
	Sig. (2-tailed)	.313	
	N	23	28

Figure 59 Scatter plot of percentage change in mean K^{trans} on Dce-MRI scans against percentage change in mean blood flow on pCT (with line of best fit) and correlation statistics, showing positive correlation between mean BF and mean K^{trans}.

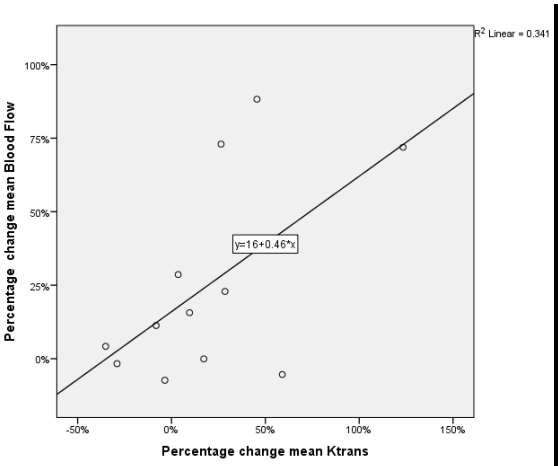

		% change mean K^{trans}	% change mean BF
% change mean K^{trans}	Pearson Correlation	1	.584*
	Sig. (2-tailed)		.046
	N	14	12
% change mean BF	Pearson Correlation	.584*	1
	Sig. (2-tailed)	.046	
	N	12	18

*Correlation is significant at the 0.05 level (2-tailed).

Blood Flow parameter maps from pCT and K^{trans} maps from Dce-MRI at a comparable anatomical level were compared qualitatively on contemporaneous scans for individual tumours (see figure 60). On visual assessment, similarities were observed in the spatial distribution of high BF and high K^{trans} regions of tumours, although the Dce-MRI K^{trans} maps were of higher resolution (and less noisy) in comparison to pCT BF maps. The mean Signal to Noise Ratio (SNR) for the tumour on parameter maps were 1.78 for BV, 1.51 for BF, 0.96 for MTT, 2.14 for K^{trans}, 2.38 for K_{ep} and 5.77 for V_e respectively, in support of the qualitative findings.

Figure 60 Comparison of pCT Blood Flow parameter maps (left-hand pictures) and Dce-MRI K^{trans} parameter maps (right-hand pictures) for ST1010 on evaluable baseline scans. Images show similar pattern of spatial distribution of high BF and K^{trans} values in tumour ROI (see arrow).

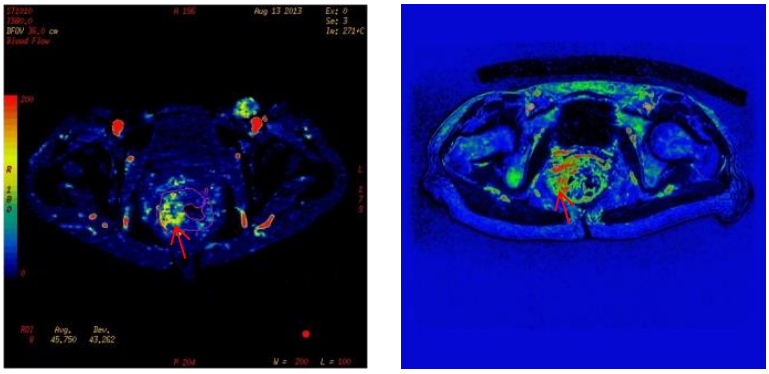

D5 Summary

In summary, it has been demonstrated that it is feasible to perform dual modality perfusion imaging using Dce-MRI and pCT at multiple time points to evaluate the microvascular effects of a novel radiosensitising drug given before and concurrent with radiotherapy. This chapter highlights the technical challenges associated with tumour ROI definition for perfusion parameter analysis, which have relevance for interpretation of qualitative and quantitative Dce-parameter value analysis. Although no consistent or statistically significant change in K^{trans} was demonstrated after 7 days of nelfinavir alone in evaluable patients, the data presented demonstrate a consistent increase in K^{trans} after 7 days of nelfinavir and concurrent hypo-fractionated radiotherapy which is

statistically significant overall. Although, these findings are consistent with those obtained using pCT analysis of changes in BF, there was no positive correlation between mean K^{trans} (from Dce-MRI) and BF from pCT but weak positive statistically significant correlation between the percentage change in each of these parameter values between sequential scans. Nevertheless, similarities were demonstrated in the spatial distribution of high BF and high K^{trans} regions of tumours.

3E Results for Imaging of Colorectal Liver Metastases

In this section, the pCT scans acquired and analysed as part of the study protocol are described. The feasibility of performing sequential pCT scans in patients with colorectal liver metastases receiving oxaliplatin and modified de Gramont chemotherapy, with and without the addition of SIRT using SIR-spheres, is evaluated. The impact of technical factors on pCT analysis in the acquired scans is investigated, including intra-sequence motion, and a motion correction strategy is evaluated. Variability in the tumour perfusion parameters being evaluated between different CT slices within the same scan is evaluated. Methods for analysing tumour perfusion parameters on multiple slices of the tumour CT volume to compare tumour volumes on sequential scans are presented, and compared to methods of analysis based on a single CT slice. The results of quantitative and qualitative evaluation of pCT scans during oxaliplatin and modified de Gramont chemotherapy are presented to test the hypothesis that multiple cycles of chemotherapy result in changes in perfusion which are unfavourable for subsequent SIRT. The results of quantitative and qualitative evaluation of pCT scans before and after SIRT with concurrent oxaliplatin and modified de Gramont chemotherapy are presented to test the hypothesis that SIRT of colorectal liver metastases results in acute increases in perfusion followed by subsequent decreases in perfusion, consistent with the effect of radiotherapy in rectal cancers.

E1 Scans performed and evaluated

Thirteen out of fourteen patients in the liver study successfully completed pCT scans of the liver at four time points.

Figure 61. Perfusion CT Scans acquired and evaluated

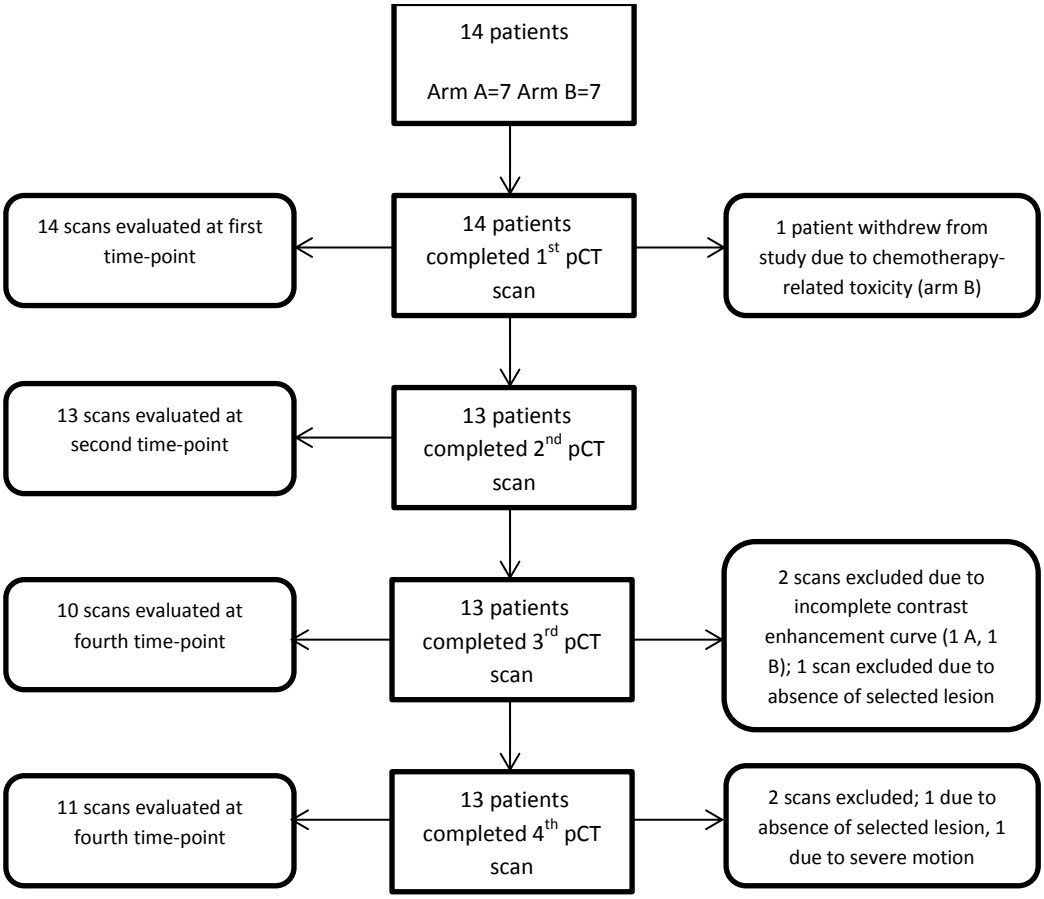

The first patient recruited to the study (P1048) withdrew after the first scan because the patient developed 5-FU-related coronary artery spasm, necessitating cessation of protocol chemotherapy. Within the trial, she received SIRT without concurrent chemotherapy. Table 64 summarises the timing of the scans in relation to systemic chemotherapy for patients in Arm A and Arm B; table 65 summarises the timing of scans in relation to SIRT, for patients in Arm B. The third scans for patients P1085 and P1170 were excluded from analysis due to the detection of an incomplete arterial enhancement time curve on post-processing of the perfusion CT data, leading to an inability to accurately select the post-enhancement image. Scan 3 for patient P1204 and

scan 4 for patient P1056 were excluded from further analysis because the selected metastasis was not present in the scanned volume. Scan 4 for patient P1099 was excluded from further analysis because of severe motion affecting the ability to derive a satisfactory portal venous input.

Table 64 Timing of pCT scans in relation to day 1 of each cycle of chemotherapy. The study protocol specified that scans should be performed at baseline (before cycle 1), day 1 cycle 2, day 1 cycle 3 and day 1 cycle 5 of chemotherapy respectively.

Patient number	Number of days between scan 1 and Day 1 cycle 1 of chemotherapy	Number of days between Day 1 cycle 2 of chemotherapy and scan 2	Numbers of days between Day 1 cycle 3 of chemotherapy and scan 3	Number of days between Day 1 cycle 5 of chemotherapy and scan 4
P1048	0	No scan	No scan	No scan
P1053	0	0	0	0
P1056	4	0	7	3
P1085	2	0	14	1
P1099	1	0	0	0
P1005	0	9	0	0
P1009	1	0	0	0
P1131	0	0	0	8
P1154	4	0	0	0
P1170	0	0	0	0
P1172	0	0	0	0
P1182	0	0	0	0
P1200	0	7	7	0
P1204	0	0	0	8

Table 65 Timing of pCT scans in relation to SIRT. Table indicates number of days between delivery of SIRT and scans 2, 3 and 4, which varies according to cycle number during which SIRT was delivered.

Patient number	Timing of SIRT in relation to chemotherapy	Timing of SIRT in relation to scan 2 (days)	Timing of Scan 3 in relation to SIRT (days)	Timing of Scan 4 in relation to SIRT (days)
P1048	**withdrew**	**-**	**-**	**-**
P1053	**Day 3 Cycle 3**	**16**	**-2**	**26**
P1085	**Day 4 Cycle 3**	**17**	**-3**	**39**
P1105	**Day 3 Cycle 2**	**2**	**12**	**40**
P1154	**Day 4 Cycle 2**	**3**	**10**	**39**
P1182	**Day 3 Cycle 2**	**2**	**12**	**39**
P1200	**Day 3 Cycle 2**	**2**	**12**	**47**

E2 Technical factors influencing perfusion parameter analysis

A liver metastasis suitable for perfusion analysis was present in 100% of scans performed. However, for two patients, the lesion selected on the baseline scan was absent in one of the subsequent scans, precluding evaluation of changes in perfusion in that metastasis at all time-points. One or more liver metastases were visible in at least 2 CT slices (i.e. over 1 cm) in 100% scans. The entire lesion was covered in the cranio-caudal axis by the perfusion CT scan in 12(23%) of the 53 scans.

Since the modelling of perfusion parameters using a liver–specific algorithm depends on definition of a dual vascular input, i.e. portal venous input, as well as arterial input, the visibility of the portal vein in each of the imaging studies was assessed. The portal vein was visible in 22 of the 29 (76%) perfusion CT scans performed in the first eight patients and subsequent to this, the scanning protocol was amended to select a liver metastasis for evaluation within the 4 cm block to be scanned which also incorporated the portal vein. In the subsequent 6 patients, the portal vein was visible in 23 of the 24 (96%) scans, making it feasible to study hepatic arterial fraction in this study. Scans in which the portal vein was not visible were analysed using the “Body” Protocol in GE Perfusion 3.0 software, which requires only a single arterial input but only permits derivation of BF, BV and MTT, not HAF. Since the “Body” and “Liver” protocols result in significantly different estimates of BF and BV[412] for evaluation of changes in perfusion parameters in these patients (P1056, P1085, P1170) the “Body” protocol was consistently used.

The portal venous enhancement curves for all patients were notably more erratic than the corresponding arterial enhancement curves, which is likely to be due to the greater mobility of this vessel and in some cases partial volume averaging. Placing a ROI in the portal vein that remained in the vessel throughout the study in the presence of intra-sequence motion was challenging (see figure 62); in scan 4 for patient P1099, the severity of motion was such that this

was not possible, resulting in a large dip in the shape of the portal venous curve, towards the end of the image sequence, at which point the curve should have plateaued.

Figure 62 Portal venous time-enhancement curves for patient P1099 on sequential pCT scans

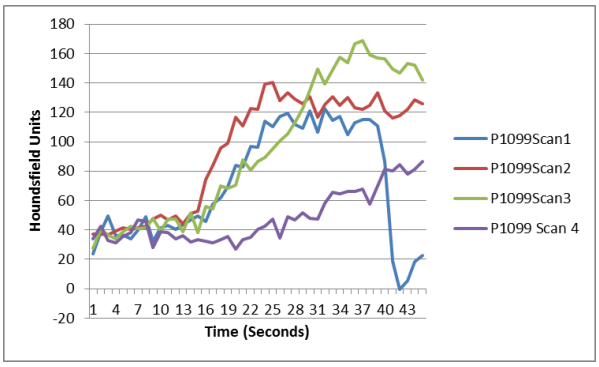

Intra-sequence motion has been mentioned as a potential technical challenge when evaluating liver tumours with pCT[409], although few studies involving perfusion imaging of the liver have sought to evaluate and report the extent of motion. Our acquisition protocol sought to limit motion using an abdominal compression device and breath-holding techniques; despite this, intra-sequence motion affected the majority of liver pCT scans to some degree. Respiratory motion was the most common type of motion (see Figure 63a for example), but there was evidence of gastric peristalsis in a minority of scans. Motion artefact affected only 5 out of 53 scans (see figure 63b for example).

Figure 63 Illustration of (a) paired images from same z axis co-ordinates acquired at different time-points during perfusion CT scan acquisition; displacement of the selected metastasis (highlighted by an arrow) out of plane is demonstrated (b)perfusion CT image affected by motion artefact

(a)

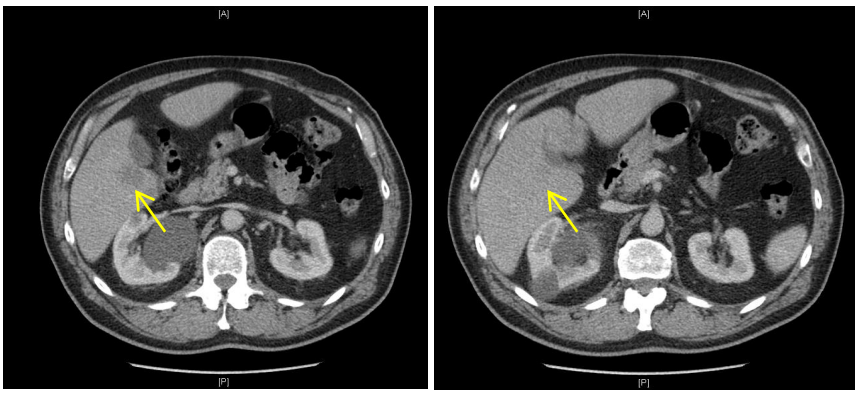

(b)

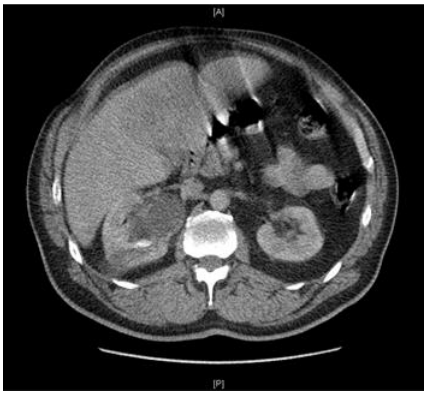

As for pCT scans of the rectum, using a scale from 1 to 4, which has previously been employed by researchers in one study of Dce-MRI of the liver[401], the severity of tumour motion for each pCT liver scan was categorised (see table 66) according to the magnitude of tumour displacement during the pCT time sequence from its position at baseline. The severity of intra-sequence tumour motion was re-evaluated on the same pCT scans after they had been "motion corrected" using a deformable image registration algorithm developed by our collaborators, in order to evaluate the effect of the motion correction algorithm on motion.

Table 66 Qualitative assessment of liver tumour motion on pCT scans at each time point for individual patients. The degree of motion affecting the tumour on dynamic pCT images was categorised according to the following scale: Score 0= No motion, Score 1= Slight motion, Score 2= Moderate motion, Score 3=Significant motion, Score 4= Severe motion scored by a single observer*Non-correctable **Not evaluated. MC= motion corrected by method described in Chapter 2E.

Patient number	Scan 1 Motion Score		Scan 2 Motion Score		Scan 3 Motion Score		Scan 4 Motion Score	
	Non MC	MC	Non MC	MC	Non MC	MC	Non MC	MC
P1048	3	2	No Scan	No Scan	No Scan	No Scan	No Scan	No Scan
P1053	1	0	1	0	1	1	1	0
P1056	3	2	3	2	3	1	3	2
P1085	2	0	2	1	3	1	3	1
P1099	3	4	2	*	3	*	3	*
P1105	1	1	1	1	1	**	1	1
P1109	2	1	2	1	2	1	3	1
P1131	1	1	1	1	1	1	1	**
P1154	2	1	2	2	3	3	3	4
P1170	1	1	2	1	2	1	1	0
P1172	**	**	**	**	**	**	**	**
P1182	1	1	3	3	2	1	4	4
P1200	4	**	2	2	2	3	2	**
P1204	2	1	1	0	1	0	3	1

Improvements in the severity of intra-sequence tumour motion, were demonstrated for a significant proportion of studies, with 23 of 44 evaluable studies being given a lower motion severity score after motion correction; however there was no change in the motion severity score in 13 scans, and the motion score increased in 3 scans. Scans for P1172 were excluded from this analysis, as the selected metastasis was difficult to visualise throughout the image sequence. It was not possible to apply the motion correction algorithm in a further 3 scans; in 2 cases this was due to the presence of coil artefacts. Even after motion correction, six studies still exhibited significant or severe motion. The application of the algorithm resulted in a decrease in the number of perfusion CT slices available for analysis in each scan, since data was lost in 2 slices on

average within the 4cm volume of interest, usually the most cranial and most caudal slices, depending on the severity of motion.

Figure 64 Illustration of a perfusion CT image affected by coil artefact; the red arrow highlights a metastasis affected by artefact and the yellow arrow highlights a metastasis unaffected by artefact and therefore more suitable for perfusion analysis

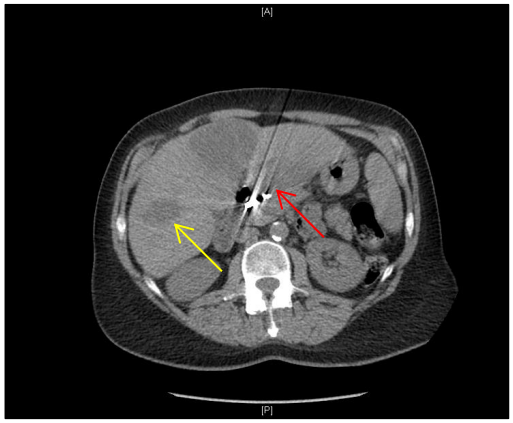

Coil artefacts were present in 12 of 25 pCT scans performed in patients from Arm B of the PERFORM trial (see figure 64 for example). As none of the patients in Arm A underwent coil embolization prior and SIRT, coil artefacts were not present in any of the 28 scans performed in this group. Of the 12 scans where coil artefacts were present, they occurred in the selected tumour region of interest for six of the scans, but not in every slice; after analysis of the first 4 patients recruited to Arm B, the protocol was modified to select a metastasis for analysis distant from the hepatic arterial system.

E3 Development of Methods for Analysis

Initial analysis of tumour perfusion parameters on the baseline pCT scan (non-motion corrected) was performed on a single CT slice (the central slice) according to the method advocated by Goh et al. for colorectal cancer [337, 343] and inter-observer variability was evaluated between two observers. The mean value for each perfusion parameter and the mean difference, standard deviation of the difference and 95% limits of agreement are summarised in Bland Altman plots, with corresponding scatter plots.

Figure 65 Bland Altman plots and scatter plots demonstrating inter-observer variability in BF, BV MTT, and HAF measurements for a single slice on the baseline pCT scans

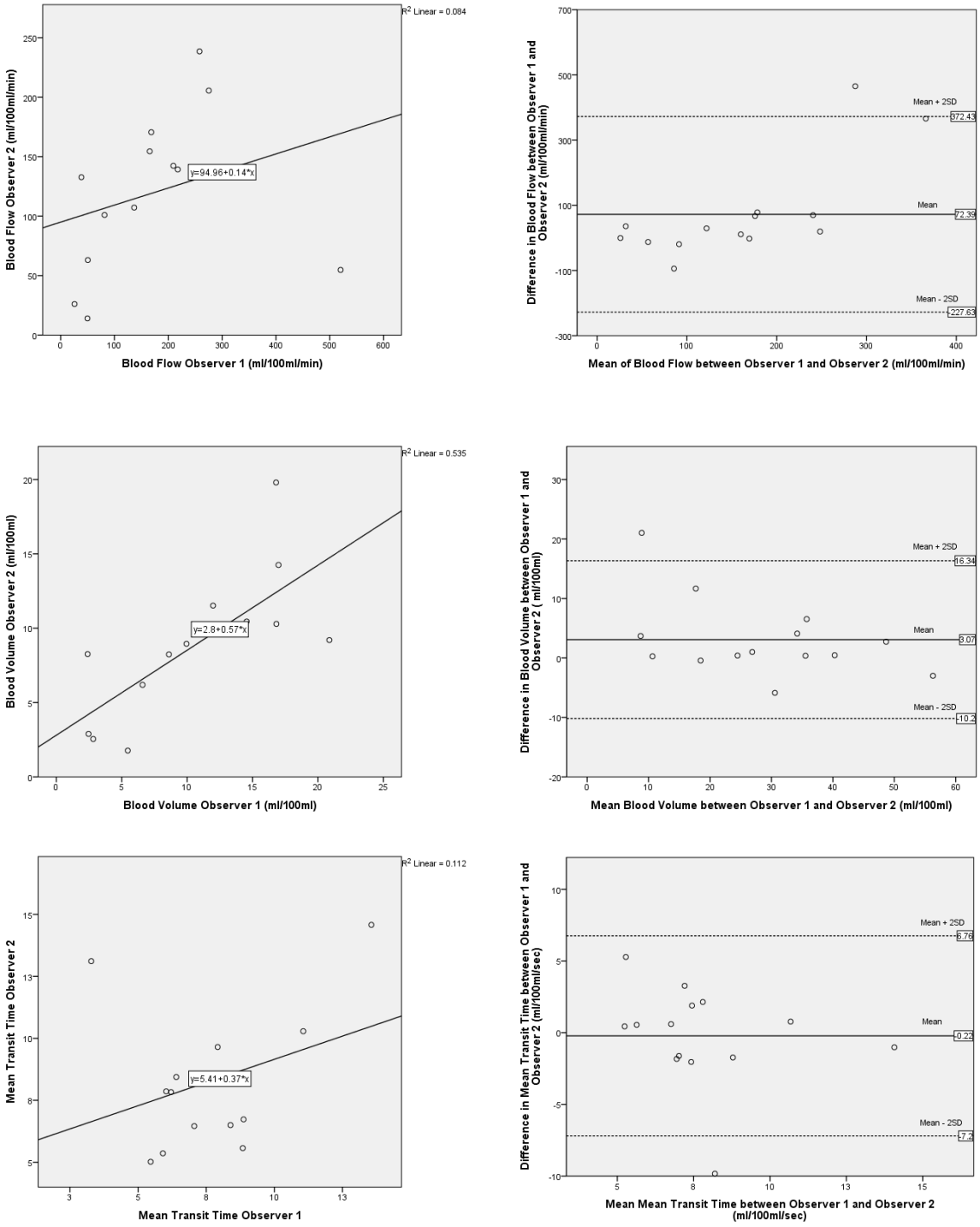

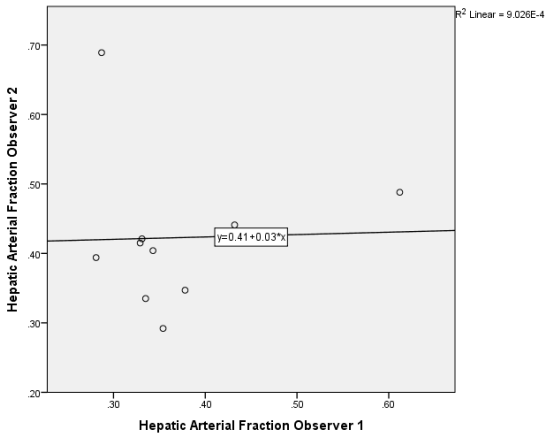

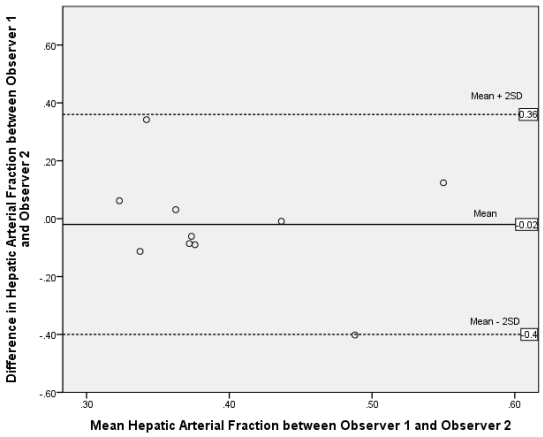

Table 67 Table summarising inter-observer variation in perfusion parameters based on delineation of a tumour ROI on a single pCT slice

Perfusion parameter	Mean difference between observers 1 and 2	Bland Altman 95% limits of agreement	Intra-class correlation coefficient (ICC)	95% Confidence Interval for ICC
Blood Flow (ml/100ml/min)	72.39	-16 to 160.77	0.88	0.67 to 0.96
Blood Volume (ml/100ml)	3.07	-0.76 to 6.90	0.68	-0.26 to 0.89
Mean Transit Time(Secs)	-0.22	-2.24 to 1.79	0.33	-0.24 to 0.74
Hepatic Arterial Fraction	-0.02	-0.16 to 0.12	0.03	-0.58 to 0.62

We postulated that there would be significant variation in perfusion parameters derived within the tumour ROI at different levels in the tumour, although potentially less so than for primary rectal tumours since liver metastases typically grow as spheres.

Figure 66 Scatter plots illustrating variation in mean BF, BV, MTT and HAF derived for the tumour ROI between different pCT slices for each patient on the baseline pCT

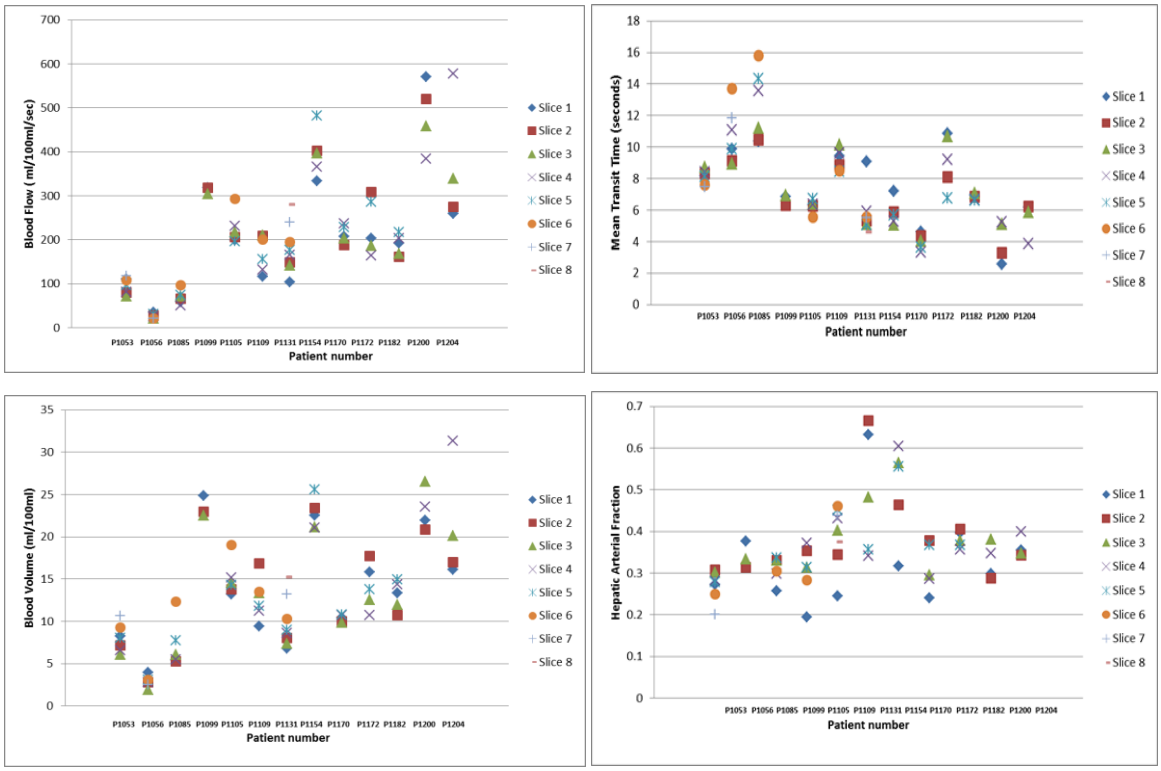

Inter-slice variation in all perfusion parameters was observed for the majority of baseline scans (see figure 66), with the highest coefficient of variation being demonstrated for mean BF followed by BV, MTT then HAF (table 68).

Table 68 Summary of variation in mean BF,BV, MTT and HAF for the tumour ROI between 8 pCT slices for each patient on the baseline pCT scan.

Patient identification number	Mean Blood Flow (ml/100ml/min)	Standard Deviation of Mean Blood Flow (ml/100ml/min)	Coefficient of Variation (%)
P1048	47.37	38.60	81.47
P1053	94.93	17.58	18.52
P1056	26.05	5.44	20.89
P1085	69.39	15.95	22.99
P1099	313.37	8.63	2.76
P1105	223.81	36.25	16.19
P1109	0.3917	41.86	24.56
P1131	166.95	43.24	25.9
P1154	396.15	55.45	14.00
P1170	212.66	20.20	9.56
P1172	229.43	63.47	27.67
P1182	188.35	23.35	12.4
P1200	483.47	80.25	16.60
P1204	362.86	147.51	40.66

Patient identification number	Mean Blood Volume (ml/100ml)	Standard Deviation of Mean Blood Volume (ml/100ml)	Coefficient of Variation (%)
P1048	2.51	1.42	56.73
P1053	8.0	1.54	19.86
P1056	2.87	0.64	22.29
P1085	7.05	2.74	38.95
P1099	23.45	1.26	5.36
P1105	15.00	2.08	13.85
P1109	12.70	2.52	19.83
P1131	9.03	2.15	23.79
P1154	22.74	1.89	8.29
P1170	10.36	0.41	4.01
P1172	14.11	2.74	19.43
P1182	13.06	1.73	13.23
P1200	23.22	2.47	10.62
P1204	21.14	7.02	33.22

Patient identification number	Mean Transit Time (seconds)	Standard Deviation of Mean Transit Time (seconds)	Coefficient of Variation (%)
P1048	8.44	3.58	42.45
P1053	8.12	0.43	5.35
P1056	10.63	1.70	15.95
P1085	12.63	2.26	17.93
P1099	6.69	0.35	5.26
P1105	6.26	0.39	6.15
P1109	9.16	0.67	7.33
P1131	5.94	1.42	23.86
P1154	5.81	0.84	14.39
P1170	3.99	0.52	12.98
P1172	9.12	1.74	19.06
P1182	6.82	0.19	2.77
P1200	4.05	1.33	32.95
P1204	5.54	1.12	20.16

Patient identification number	Hepatic Arterial Fraction	Standard Deviation of Hepatic Arterial Fraction	Coefficient of Variation (%)
P1048	0.59	0.11	18.85
P1053	0.27	0.04	13.4
P1099	0.34	0.03	9.32
P1105	0.31	0.03	9.74
P1109	0.31	0.06	20.52
P1131	0.40	0.08	19.48
P1154	0.50	0.15	30.42
P1170	0.50	0.12	22.99
P1172	0.31	0.06	18.48
P1182	0.38	0.02	5.35
P1200	0.33	0.04	13.34
P1204	0.36	0.03	7.28

Since intra-tumour vascularity and perfusion can be heterogeneous, a single slice may misrepresent the perfusion characteristics of the tumour and unless the same region of the tumour in the z axis is evaluated on sequential scans, changes in perfusion parameters may reflect regional variation in perfusion rather than change due to tumour progression or treatment response. Selecting the same slice of the tumour for analysis on serial pCT scans is challenging

since it is not always possible to image an entire metastasis within the 4 cm z axis coverage. The liver moves relative to other intra-abdominal structures, such that it is not possible to accurately align serial scans using anatomical landmarks and also metastases can change in size and shape over time. A further issue, specific to the perfusion analysis of liver metastases, as opposed to primary rectal tumours, relates to the delineation of the tumours; since liver tumours move more, the delineated tumour contour can vary depending on which position the tumour is in on the specific image selected for contouring and it is not always possible to edit the contour such that the metastasis is in its confines throughout the cine loop, without cropping the tumour rim, which often has high perfusion. This may be a source of inter-observer variation in contouring and perfusion parameter estimation. Based on our findings of significant inter-slice variation in tumour perfusion and the observation that the entire metastasis was not always fully imaged, the method subsequently selected for analysis of changes in tumour perfusion on sequential scans involved calculation of tumour perfusion parameters for each of the evaluable pCT slices in the z axis for each tumour and derivation of a weighted mean value for the perfusion parameters (based on the relative area of the ROI on each slice) from all of the evaluable slices between successive pCT scans. It was hypothesised that this method of analysis would reduce inter-observer variation in perfusion parameters derived, by virtue of having removed the influence of averaging differences in tumour area delineated on different slices over the scanned tumour volume. This hypothesis was tested by 2 observers repeating analysis of the baseline pCT scans using the method based on derivation of a weighted mean for the tumour volume (see figure 67).

Figure 67 Bland Altman plots and scatter plots demonstrating inter-observer variability in BF, BV, MTT and HAF measurements derived from multiple slices using a weighted mean on the baseline pCT scans

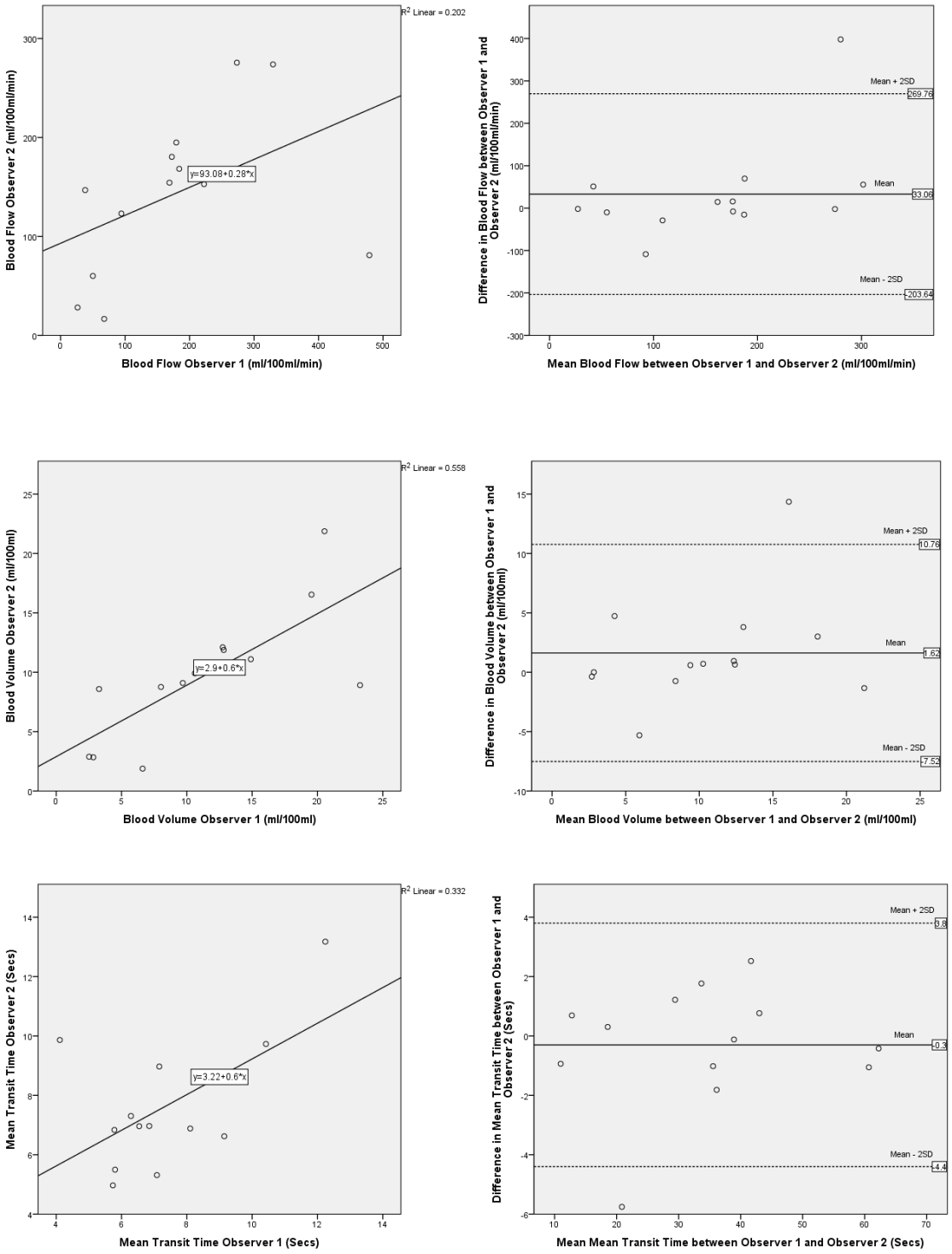

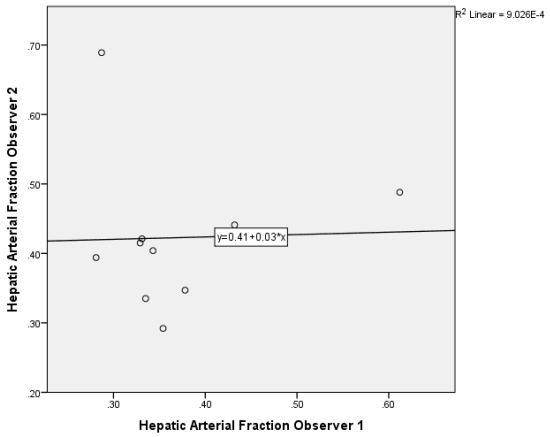

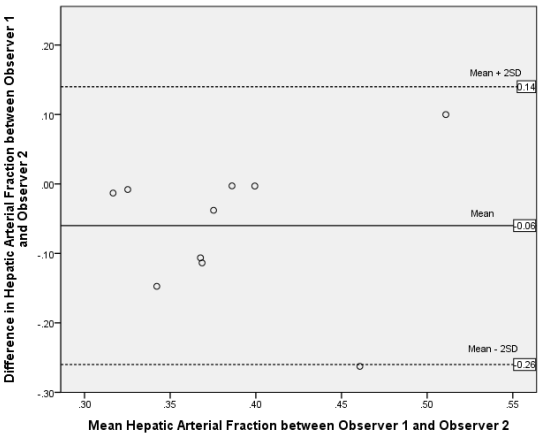

Analysis revealed that the mean difference in BF and BV between 2 observers and the Bland Altman limits of agreement were less using analysis of a weighted mean of multiple pCT slices (see table 69) than for analysis using a single pCT slice (although little different for MTT); the intra-class correlation coefficient between 2 observers for BF, BV and MTT were also higher using the former method.

Table 69 Table summarising inter-observer variation in perfusion parameters based on delineation of a tumour ROI on multiple slices and derivation of a weighted mean

Perfusion parameter	**Mean difference between Observers 1 and 2**	**Bland Altman 95% limits of agreement**	**Intra-class correlation coefficient (ICC)**	**95% Confidence Interval for ICC**
Blood Flow (ml/100ml/min)	33.06	-38.46 to 104.58	0.41	-0.16 to 0.77
Blood Volume (ml/100ml)	1.62	-1.14 to 4.38	0.73	0.32 to 0.91
Mean Transit Time (Seconds)	-0.30	-1.54 to 0.96	0.58	0.06 to 0.85
Hepatic Arterial Fraction	-0.06	-0.13 to 0.01	0.18	-0.48 to 0.70

We speculated that motion correction of perfusion CT images would reduce inter-observer variation in perfusion parameters, since it should improve consistency of tumour position throughout the perfusion time sequence and reduce variability in contour delineation. We tested this speculation by 2 observers repeating analysis of nine baseline pCT scans (before and after motion correction) using the method based on derivation of a weighted mean for the tumour volume (figure 68). Table 70 summarises the mean differences in perfusion parameters between the 2 observers on the 9 scans before and after motion correction, the intra-class correlation coefficient and the corresponding 95% confidence limits for intra-class correlation.

Table 70 Table summarising inter-observer variation in perfusion parameters based on delineation of a tumour ROI on multiple slices and derivation of a weighted mean without motion correction (Non-MC) and after motion correction (MC) for nine baseline scans

Perfusion parameter	**Mean difference between Observers 1 and 2**		**Bland Altman 95% limits of agreement**		**Intra-class correlation coefficient (ICC)**		**95% Confidence Interval for ICC**	
	Non-MC	**MC**	**Non-MC**	**MC**	**Non-MC**	**MC**	**Non-MC**	**MC**
Blood Flow (ml/100ml/min)	15.11	20.4	-11.91 to 42.12	-14 to 54.80	0.93	0.93	0.73 to 0.98	0.73 to 0.98
Blood Volume (ml/100ml)	1.29	0.92	-0.31 to 2.90	-0.95 to 2.80	0.94	0.93	0.76 to 0.99	0.73 to 0.98
Mean Transit Time (Seconds)	0.18	-0.19	-0.75 to 1.12	-0.76 to 0.37	0.86	0.93	0.51 to 0.97	0.70 to 0.98
Hepatic Arterial Fraction	-0.06	-0.01	-0.12 to 0.004	-0.12 to 0.09	-0.09	0.34	-0.75 to 0.66	-0.5 to 0.84

The analysis reveals that the mean difference in parameter estimation between the two observers was greater on the motion corrected scans compared to the non-motion corrected scans for BF and MTT, although lesser for BV and HAF (but with wider 95% confidence intervals).

The intra-class **c**orrelation for BF was comparable before and after motion correction, slightly lower on the motion corrected studies for Blood Volume but higher on the motion corrected studies for MTT and HAF. Therefore, in this limited analysis no evidence was found to suggest that motion correction reduces inter-observer variation in pCT parameters. It was evaluated whether motion correction resulted in significant differences to the parameter values estimated by a single observer; no statistically significant differences in any of the parameters were demonstrated, with a low coefficient of variation between the analyses (see table 71). In view of these findings, for the purpose of analysis of pCT data in this research, it was decided to analyse changes in perfusion parameters based on sequential non-motion corrected scans using the method based on deriving a weighted mean of multiple slices.

Figure 68 Bland Altman plots and scatter plots demonstrating inter-observer variability in BF, BV, MTT and HAF measurements derived from multiple slices using a weighted mean on the baseline pCT scans after motion correction

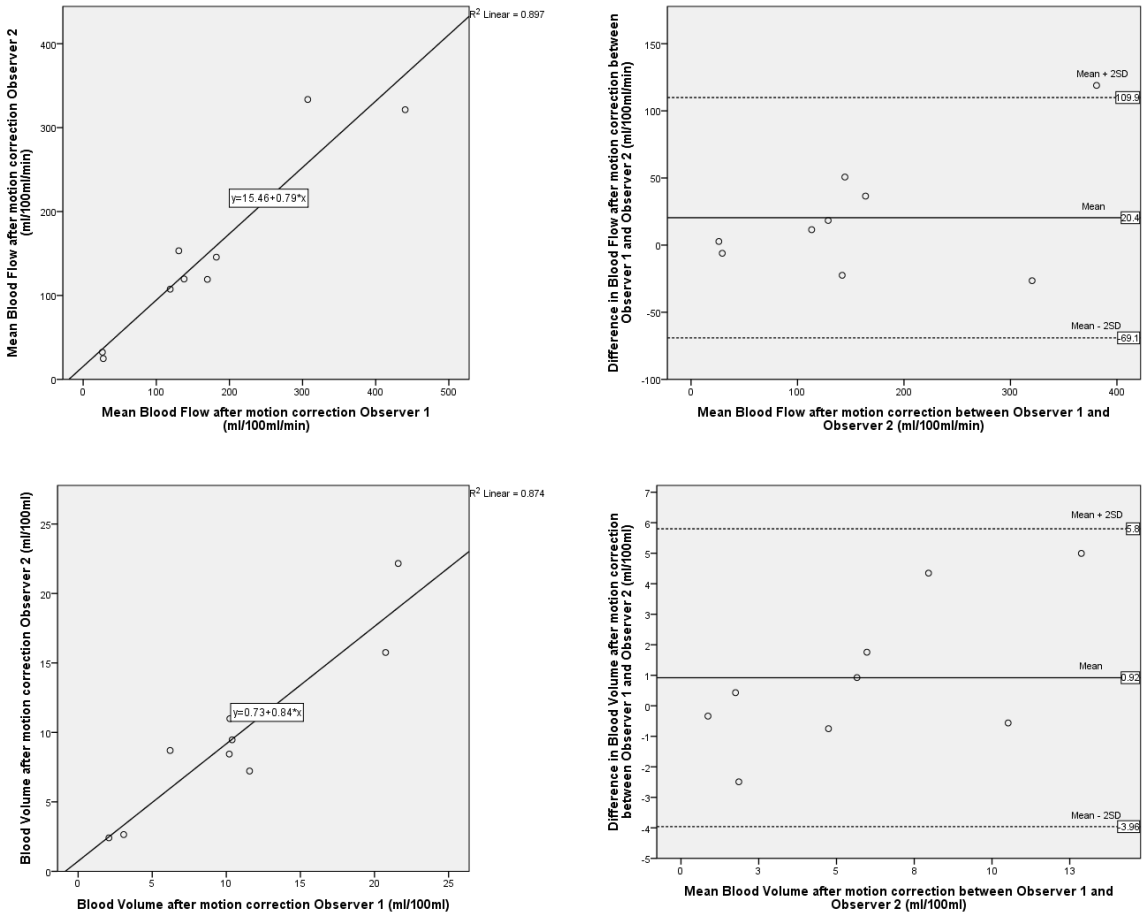

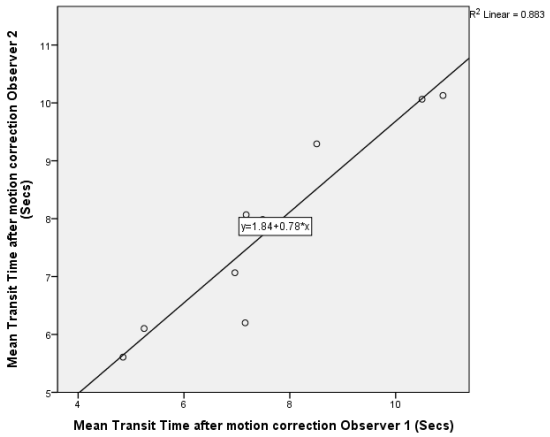

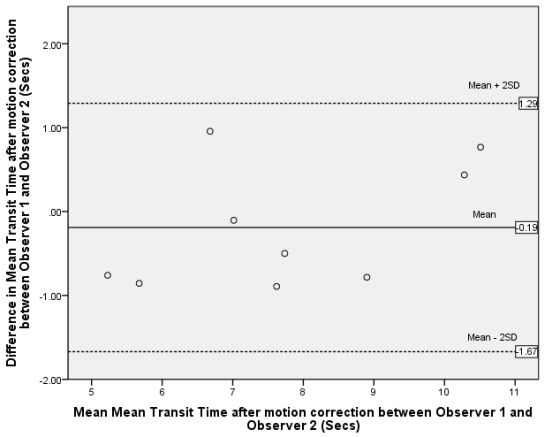

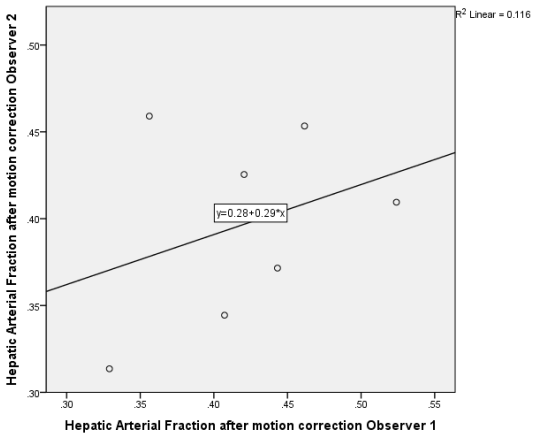

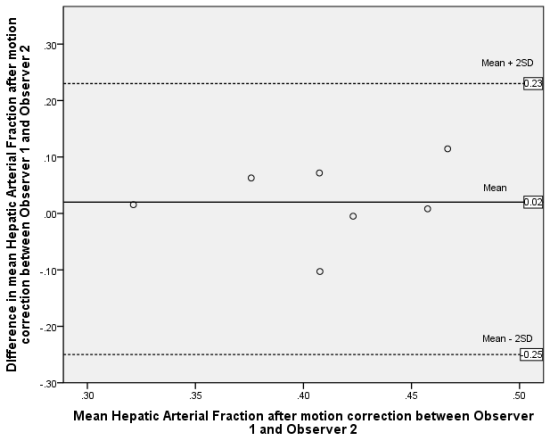

Table 71 Table summarising differences in perfusion parameters measured by a single observer before (non-MC) and after motion correction (MC) on the baseline pCT scan

Parameter	Mean difference between parameter on non-MC and MC scans	95% Confidence interval of the difference	Statistical significance (2-sided)	Coefficient of Variation (%) between 2 measurements
Blood Flow (ml/100ml/min)	13.74	-23.4 to 50.88	P=0.418	3.51
Blood Volume (ml/100ml)	1.50	-1.17 to 4.17	0.231	2.32
Mean Transit Time (Secs)	0.18	-0.86 to 1.27	0.702	7.5
Hepatic Arterial Fraction	-0.06	-0.16 to 0.41	0.201	1.83

E4 Quantitative and qualitative evaluation of perfusion parameters on baseline scans

The mean tumour BF on the baseline perfusion CT scans was 217.95 ml/100ml/min (+/-129.40) and the mean BV was 13.73 ml/100ml (+/-6.69).Qualitative analysis of the baseline perfusion parameter maps demonstrated appreciable differences in the appearance of metastases with high BF and high BV (hyper-vascular metastases) in comparison to those with low BV and low BF (hypo-vascular metastases).

Figure 69 Blood Flow and Blood Volume parameter maps illustrating (a) hypo-vascular metastases and (b) metastases with a hyper-vascular rim

(a)

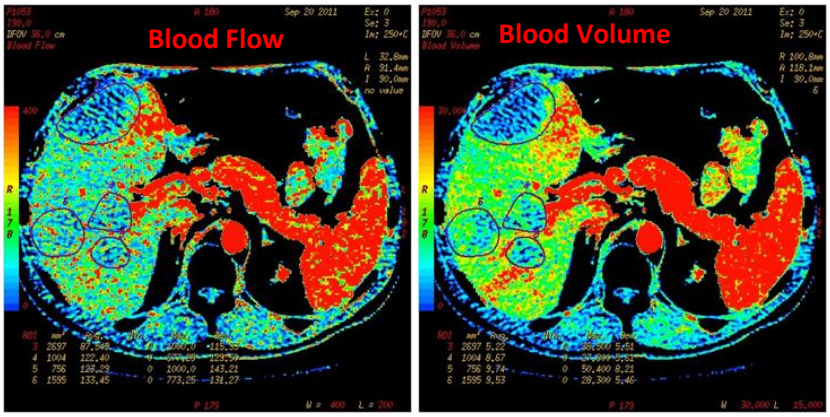

(b)

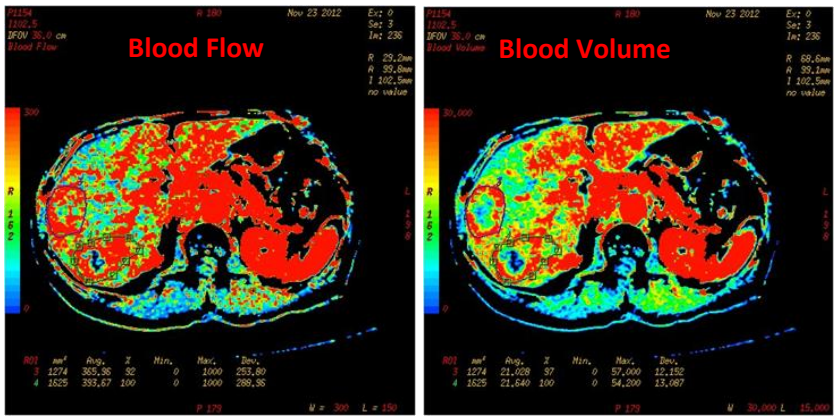

Spatial variation in blood flow and blood volume was demonstrable; eleven of the fourteen metastases demonstrated some rim enhancement on the baseline study. Hyper-vascular metastases characteristically had a thick rim of voxels with high BF and BV, with a less perfused core; even a number of the hypo-vascular metastases demonstrated high perfusion peripherally,

often appearing to be outside the edge of the tumour seen on CT images. HAF perfusion maps demonstrated an appreciably higher hepatic arterial fraction in metastases than the normal liver.

Figure 70 Hepatic Arterial Flow parameter map and corresponding contrast-enhanced CT for patient P1099 (tumour ROI outlined)

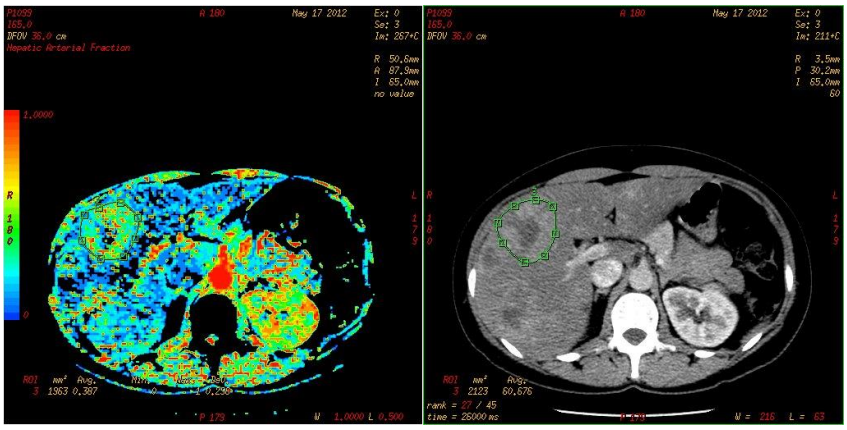

The variability of mean tumour perfusion parameters within different metastases within the same individual, where there was more than one evaluable metastasis within the cranio-caudal coverage of the pCT scan and between different patients was explored, as illustrated in figure 71. In general, there was greater variation in mean tumour perfusion parameters between the metastases of different patients than between different metastases within individual patients, although there was wide variation in mean pCT between metastases within a few patients e.g. P1204, which might be explained by the different z axis coverage of some of the metastases, which had not been specifically selected for the primary pCT analysis.

Figure 71 Scatter plots illustrating variation in (a) mean Blood Flow (b) mean Blood Volume (c) mean MTT and (d) mean HAF of different metastases within individual patients (points joined up) as well as variation between patients.

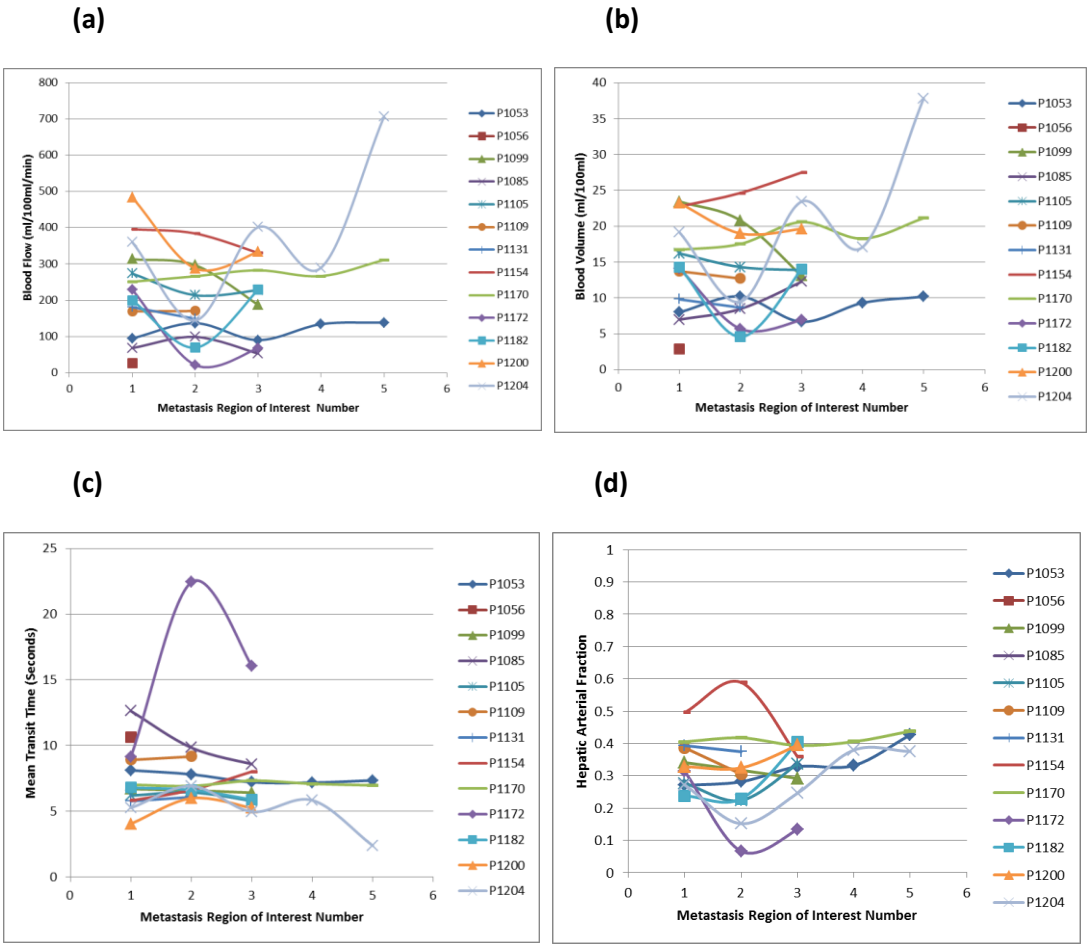

Using a customised Matlab program to quantify differences in mean perfusion parameters in the rim of tissue outside the liver as well as the rim inside the tumour and core), quantifiable differences in perfusion parameter values were demonstrated in different regions of interest (outer rim, inner rim and core) (see figure 72). For the studied patient, the 0.5 and 1 cm rims outside the tumour had the highest BF, BV and MTT; the core 1 cm inside the tumour contour had the lowest perfusion values. However, the HAF was lowest in the 0.5-1 cm region of interests outside the tumour with higher values in all regions of interest within the tumour (both inner rim and core, which were comparable).

Figure 72 Bar charts illustrating spatial variation in perfusion parameters in different regions of interest for selected liver metastasis in patient P1053 on baseline scan.

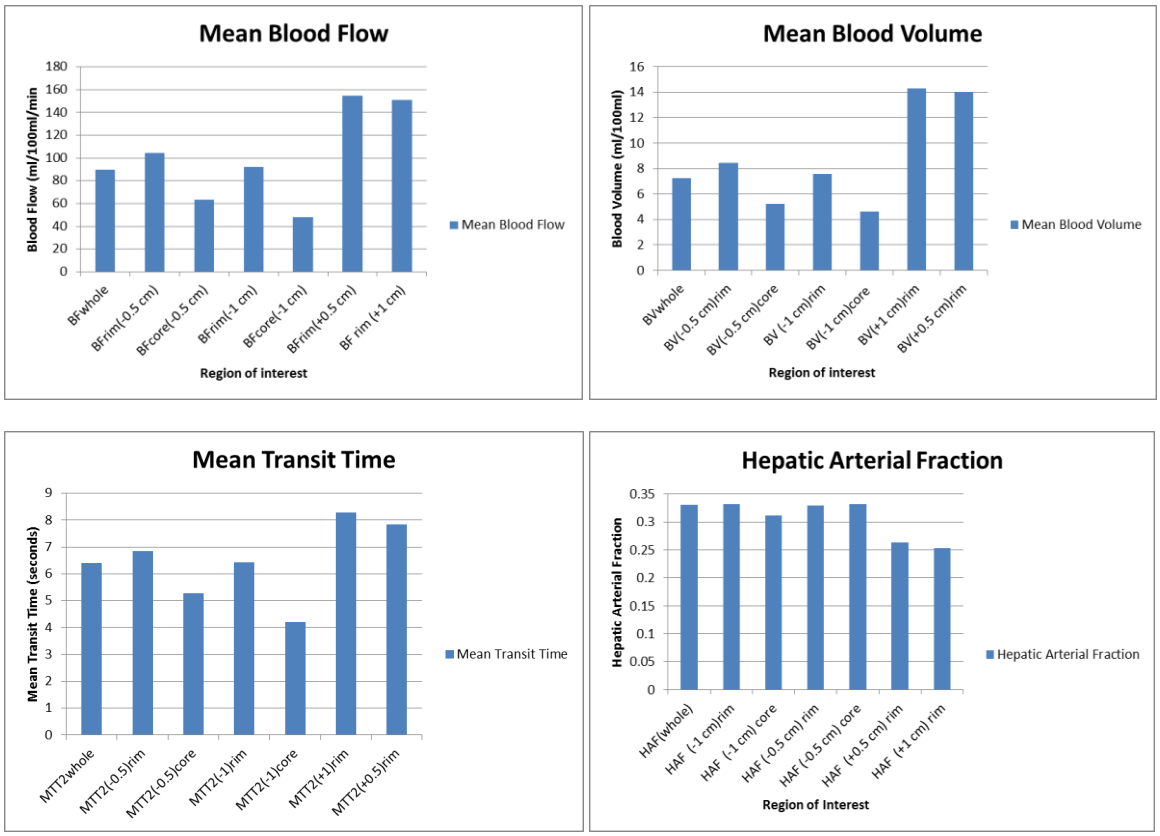

E5 Quantitative and qualitative evaluation of changes in tumour perfusion parameters during oxaliplatin and modified de Gramont chemotherapy

In order to test the hypothesis that oxaliplatin and modified de Gramont chemotherapy results in changes in the perfusion of colorectal liver metastases, which are unfavourable for subsequent radioembolisation with yttrium-90 SIR-spheres, we evaluated quantitative and qualitative changes in tumour perfusion between pCT scans performed: before chemotherapy, after 1 cycle of chemotherapy, after 2 cycles of chemotherapy and after 4 cycles of chemotherapy. We postulated that multiple cycles of chemotherapy would cause a decrease in BF, BV and HAF, which would potentially reduce the selective deposition of the SIR-spheres in the metastasis. On

analysis of the percentage change in perfusion parameters between sequential scans for the patients evaluated, no consistent pattern of change in percentage change of any of perfusion parameter was observed between the pre-treatment pCT (scan 1) and the pCT after 1 cycle of chemotherapy (scan 2), the pCT after 2 cycles of chemotherapy (scan 3) or the pCT scan after 4 cycles of chemotherapy (scan 4). However, mean BF decreased in 5/13 evaluable tumours after 1 cycle of chemotherapy, in 5/8 evaluable tumours after 2 cycles of chemotherapy and 4/5 patients after 4 cycles of chemotherapy. HAF decreased in 6/10 evaluable tumours after 1 cycle of chemotherapy, in 4/6 tumours after 2 cycles of chemotherapy and in all 5 evaluable tumours after 4 cycles of chemotherapy.

Figure 73 Percentage change in mean BF, BV and MTT between baseline scan and (a) scan 2, after 1 cycle of Chemotherapy (arms A and B), (b) scan 3, after 2 cycles of Chemotherapy (arm A and patients in Arm B not receiving SIRT until after Cycle 3), (c)scan 3, after 4 cycles of chemotherapy (arm A).

(a)

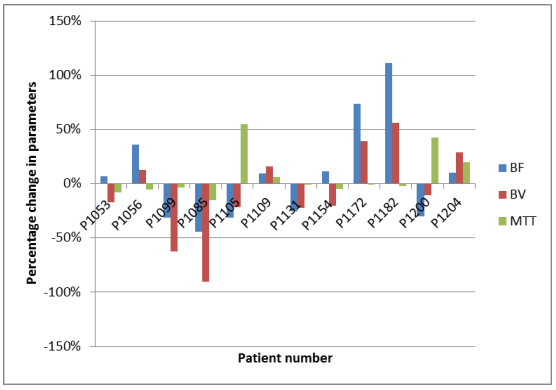

(b)

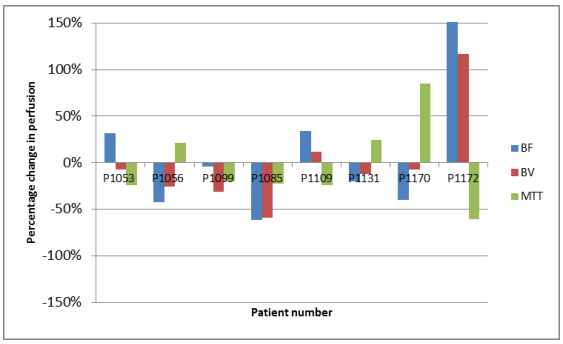

(c)

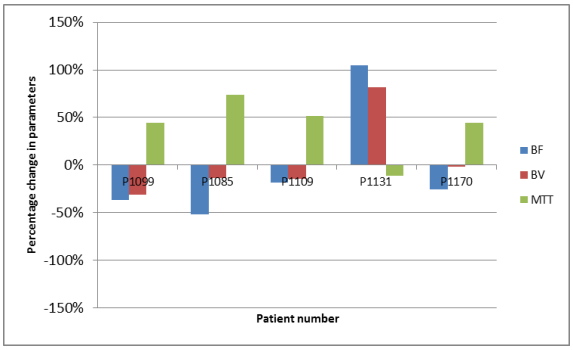

Figure 74 Percentage change in HAF after (a) 1 cycle of chemotherapy (Arms A and B), (b) 2 cycles of chemotherapy chemotherapy (Arm A and patients in Arm B receiving SIRT after cycle 3), (c) 4 cycles of chemotherapy

(a)

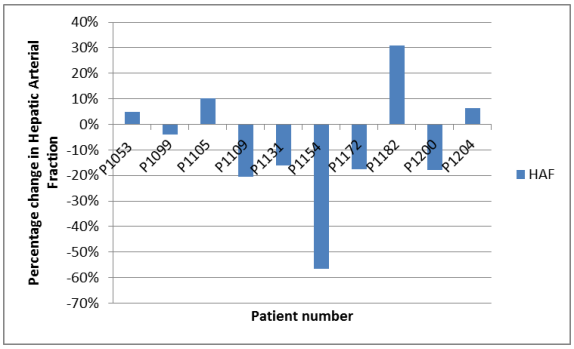

(b)

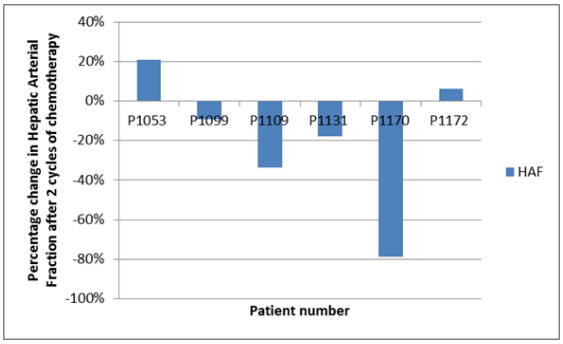

(c)

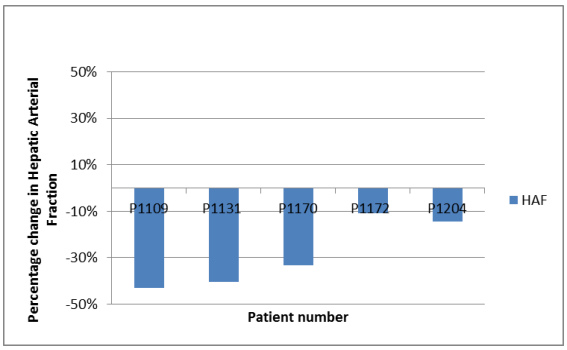

On statistical analysis of the evaluable scans, overall no statistically significant changes in tumour perfusion parameters were demonstrated after 1 cycle or 2 cycles of chemotherapy (table 72). However, a statistically significant difference in HAF was demonstrated between baseline and after 4 cycles of chemotherapy, which amounted to a 28.43% mean reduction in HAF from baseline; there was also an increase in mean MTT of 40.46%, which bordered on statistical significance, suggestive of reduced tumour perfusion.

Table 72 Summary of percentage change, mean absolute differences and 95% confidence intervals in parameter values between (a) baseline study and after 1 cycle of chemotherapy (between scans 1 and 2, Arms A and B) (b)2 cycles of chemotherapy (between scans 1 and 3, Arm A and patients in Arm B receiving SIRT with cycle 3) and (c) 4 cycles of chemotherapy (between scans 1 and 4, Arm A only); statistical significance assessed using paired *t* test.

(a)

Perfusion parameter	**Mean difference in parameter after 1 cycle of chemotherapy (n=13)**	**95 % confidence interval of the difference**	**Statistical significance Paired *t* test (2 – sided)**
Blood Flow (ml/100ml/min)	+11.57 (+10.92%)	- 41.99 to +65.14	P=0.646
Blood Volume (ml/100ml)	+1.24 (+11.92%)	-2.61 to +5.1	P=0.497
Mean Transit Time (seconds)	+0.17 (+3.79%)	-0.47 to +0.81	P=0.58
Hepatic Arterial Fraction	-0.03 (-13.84%)	-0.1 to +0.04	P=0.344

(b)

Perfusion parameter	Mean difference in parameter after 2 cycles of chemotherapy (n=6)	95 % confidence interval of the difference	Statistical significance Paired t test (2 – sided)
Blood Flow (ml/100ml/min)	-9.95 (-6.89%)	- 62.18 to + 42.28	P=0.645
Blood Volume (ml/100ml)	-1.48 (-11.99%)	-4.64 to + 1.68	P=0.282
Mean Transit Time (seconds)	+0.26 (+10.48%)	-2.20 to +2.72	P=0.798
Hepatic Arterial Fraction (n=5)	-0.12 (-23.73%)	-0.34 to + 0.10	P=0.213

(c)

Perfusion parameter	Mean difference in parameter after 4 cycles of chemotherapy (n=7)	95 % confidence interval of the difference	Statistical significance Paired t test (2 – sided)
Blood Flow (ml/100ml/min)	-20.27 (-5.59%)	- 159.9 to +119.36	P=0.708
Blood Volume (ml/100ml)	+0.23 (+ 4.11%)	-5.90 to +6.36	P=0.922
Mean Transit Time (seconds)	+2.39 (+ 40.46%)	-0.11 to + 4.89	P=0.057
Hepatic Arterial Fraction	-0.118 (-28.43%)	-0.202 to -0.033	P=0.018

On qualitative evaluation of perfusion parameter maps, changes in perfusion were appreciable for some patients, most commonly after 2 or 4 cycles of chemotherapy but not always appreciable after 1 cycle. For example, figure 75 illustrates a reduction in BF in the tumour rim after 2 cycles of chemotherapy, reductions in BV and MTT after 1 and 2 cycles of chemotherapy associated with a decrease in tumour size although no obvious change in the hepatic arterial fraction. A decrease in the size of the metastasis was observed in 6 of 7 patients after 4 cycles of chemotherapy (Arm A), although no consistent pattern of change in perfusion was observed. It

was evaluated whether there were differential changes in mean perfusion parameters within different regions of interest (rim versus core, as previously defined).

Figure 75 Perfusion parameter maps (Blood Flow, Blood Volume, MTT, HAF) for patient P1099 (Arm A) (a) at baseline (b) after 1 cycle of chemotherapy (c) after 2 cycles of chemotherapy illustrating changes in tumour ROI (outlined)

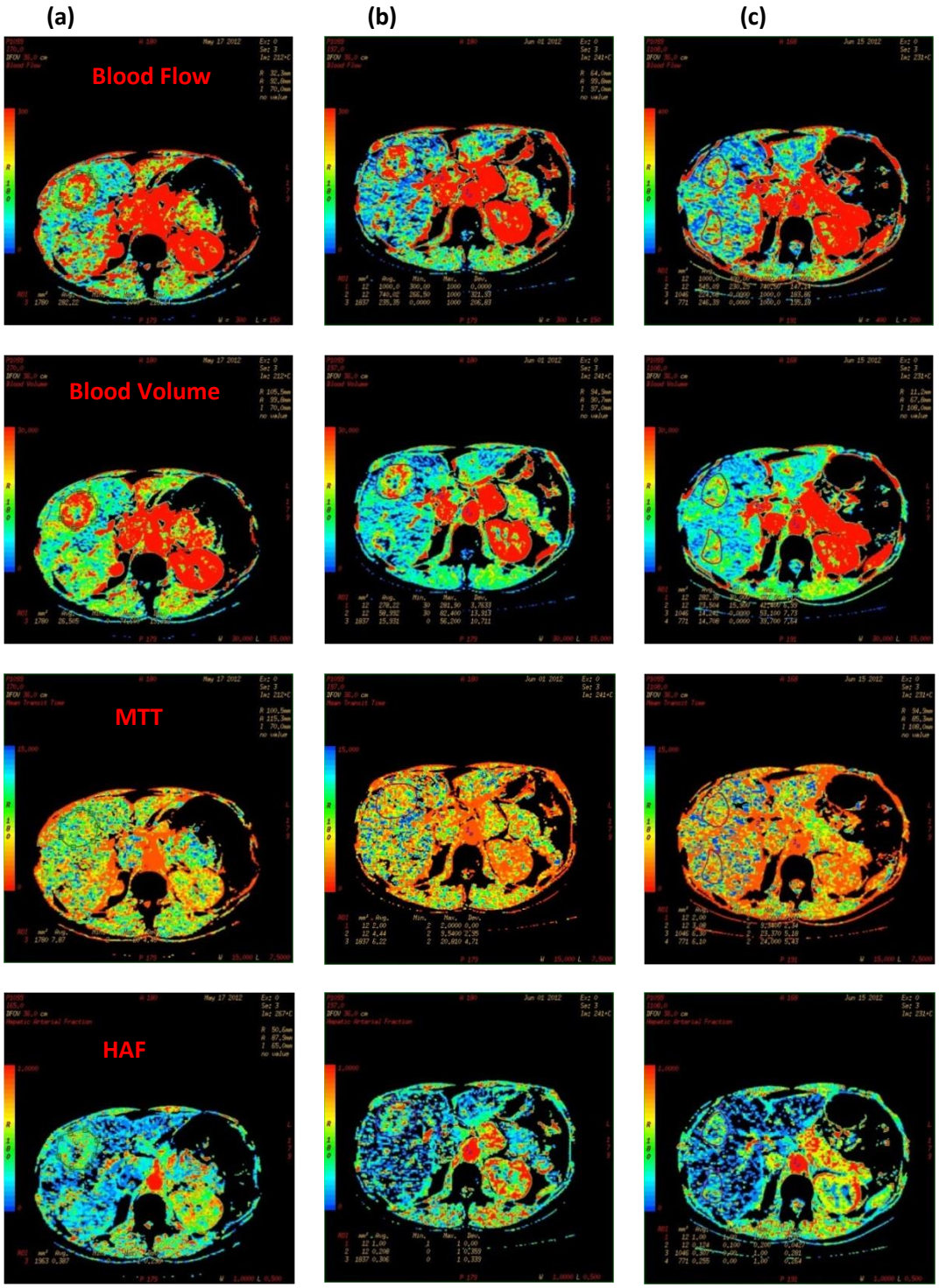

Figure 76 illustrates that after 1 cycle of chemotherapy, differences in the magnitude and sometimes direction of change in perfusion parameters were seen between the rim and the core of some metastases. This suggests that mean perfusion parameters for the whole tumour region of interest may not always reflect differential changes in perfusion within a metastasis. However, these data need to be interpreted with some caution, since this analysis was based on-motion corrected images and in some cases, mis-registration of CT-defined ROIs with perfusion maps was observed.

Figure 76 Change in mean BF after 1 cycle of chemotherapy according to ROI: a) whole metastasis b) 0.5cm rim inside metastasis c) corresponding core inside metastasis d)0.5cm rim outside metastasis

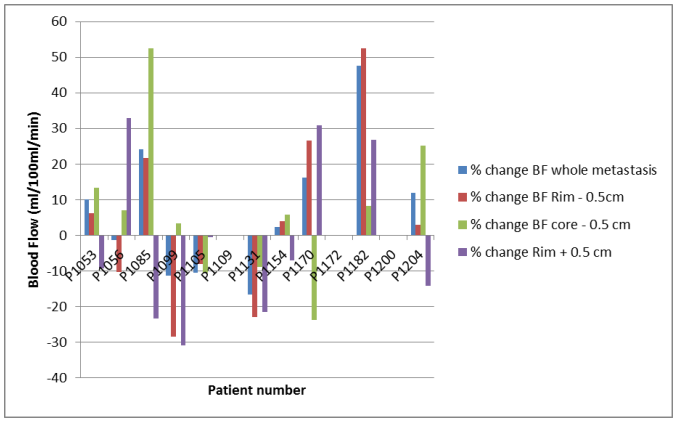

Differential changes in the histogram distributions of perfusion parameters within different tumour regions of interest after 1 cycle of chemotherapy were also evaluated. Figure 77 illustrates a reduction in the proportion of voxels with very high BF values in the whole tumour, the inner and outer rim after 1 cycle of chemotherapy for patient 1099, although no change in the proportion of voxels with high BF in the core. It also demonstrates an increase in the proportion of voxels with very low BF, for all regions of interest and a leftwards shift in the distribution of voxels from higher to lower values in the 0.5 cm rim outside and 0.5 cm rim inside the whole tumour outline. It was not possible to evaluate all parameters at all time-points using these methods due to the limits of time but the potential for these methods to detect changes in

perfusion where changes in mean perfusion parameter values may not be apparent has been demonstrated.

Figure 77 Histograms of BF for patient P1099 on baseline scan and scan after 1 cycle of chemotherapy in the following regions of interest: (a) whole metastasis (b) 0.5 cm rim outside tumour (c) 0.5 cm rim inside tumour (d) core of metastasis (0.5 cm from edge)

(a)

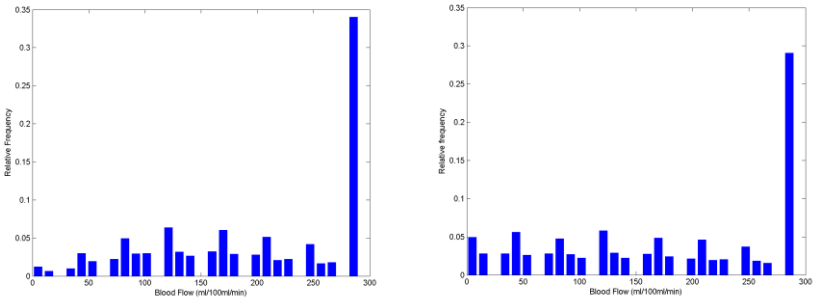

(b)

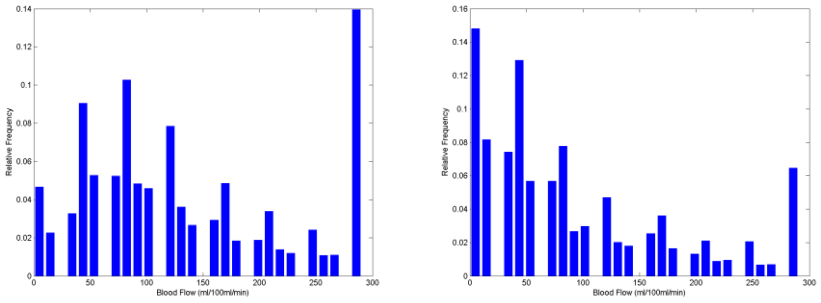

(c)

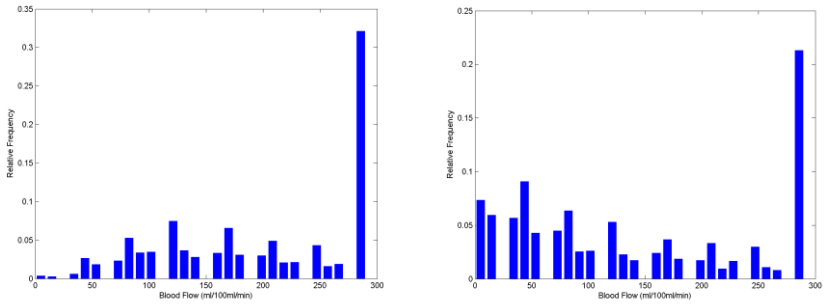

(d)

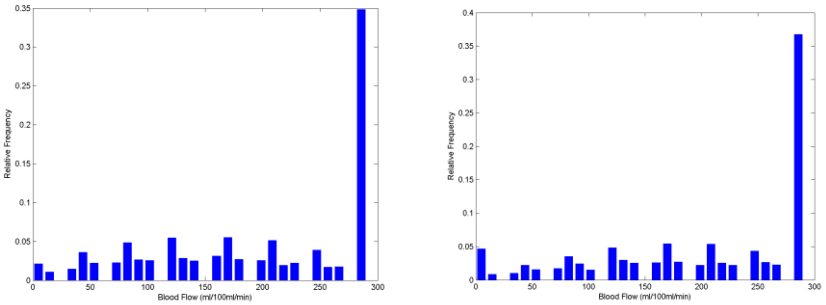

E6 Quantitative and qualitative evaluation of changes in tumour perfusion parameters after SIRT using yttrium-90 SIR-spheres and concurrent oxaliplatin and modified de Gramont chemotherapy

In order to test the hypothesis that SIRT using yttrium-90 SIR-spheres of colorectal liver metastases results in significant changes in perfusion consistent with the effects expected from radiotherapy, we evaluated quantitative and qualitative changes in tumour perfusion between pCT scans performed: 2-3 days before SIRT, 10 days and 39-47 days after SIRT (in patients receiving SIRT with cycle 2 of chemotherapy) and between pCT scans performed : 2-17 days pre-SIRT and 26-40 days posts SIRT (in the patients who received SIRT with cycle 3 of chemotherapy) and compared these changes to those observed in patients having received chemotherapy alone at the same time points (control group). Since yttrium-90 SIR-spheres have a half-life of 64 hours and 97% of the dose is delivered within 2 weeks of SIRT, it was postulated specifically that there would be acute increase in perfusion 10 days after therapy [347, 348, 443] and a significant decrease in perfusion >2 weeks after therapy.

On analysis of the percentage change in perfusion parameters between scans 2 and 3 for the 4 patients who received SIRT on Day 3 cycle 2 of chemotherapy (scan 3, 10 days post SIRT), there was a reduction in mean BF and mean BV for all 4 patients (see figure 78); in the same patient group 39-47 days after SIRT, all 4 exhibited a reduction in mean BF, mean BV and HAF (see figure 79). In only one patient (P1053), who received SIRT on Day 4 cycle 3 was there an increase in tumour BF and BV (figure 79 a). A further one patient who received SIRT with cycle 3 of chemotherapy demonstrated a decrease in tumour BF and BV on sequential scans before and after SIRT, although the timing deviated from the intended scanning protocol (see figure 79c).

Figure 78 Percentage change in perfusion parameters between scan 2 and scan 3 (10 days after SIRT) in arm B patients receiving SIRT with cycle 2 of chemotherapy

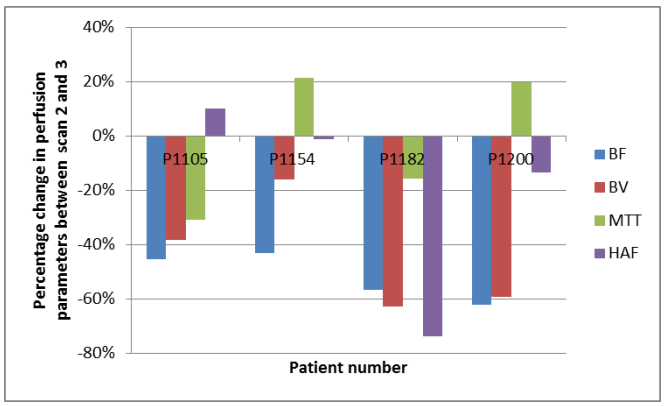

Figure 79 Percentage change in perfusion parameters (a) between scan 3 and 4 in patient P1053 who received SIRT on Day 3 of cycle 3 i.e. scan 4 26 days post SIRT and (b) between scan 2 and 4 in patients who received SIRT on Day 3 of cycle 2 i.e. scan 4 39-47 days post SIRT (c) between scan 2 (17 days pre-SIRT) and scan 4 (40 days post SIRT) in patient P1085 who received SIRT on Day 4 cycle 3

(a)

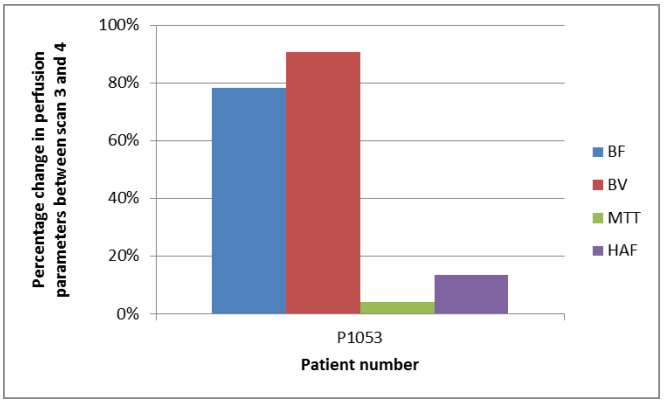

(b)

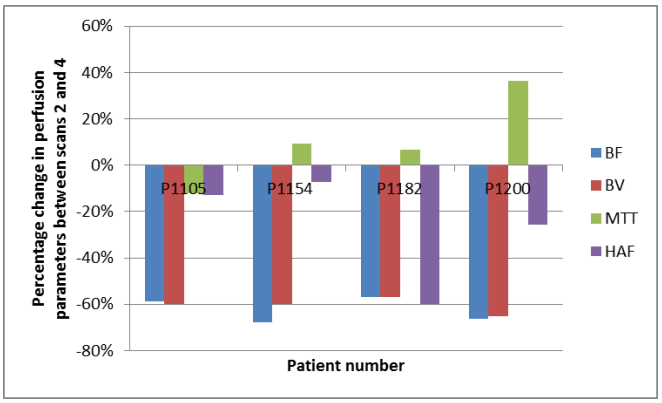

(c)

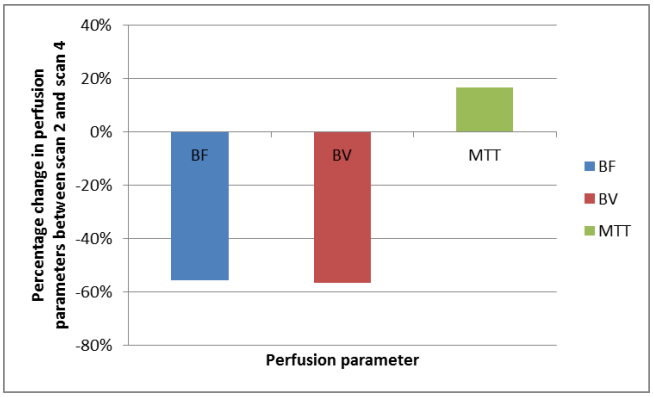

Overall, there was a mean 52% reduction in Blood Flow and 93% reduction in BV 10 days after SIRT and concurrent chemotherapy which did not quite reach statistical significance (see table 73) in comparison to a non-significant 8% reduction in BF and 16% reduction in BV in control patients having received chemotherapy only between the same time points.

Table 73 Summary of absolute and percentage change in perfusion parameters between scans 2 and 3 (a) in patients receiving SIRT on day 2 Cycle 2 of chemotherapy and (b) in control patients receiving chemotherapy alone in Arm A; statistical significance evaluated using paired t test for pairwise differences

(a)

Perfusion parameter	Mean difference in parameter between scan 2 (2 days before SIRT) and scan 3 (10 days post SIRT (n=4)	95 % confidence interval of the difference	Statistical significance Paired t test (2 – sided)
Blood Flow (ml/100ml/min)	-177.14 (-51.8%)	-267.32 to 86.97	P=0.08
Blood Volume (ml/100ml)	-9.73 (-93%)	-20.7 to +1.24	P=0.067
Mean Transit Time (seconds)	+0.05 (+0.43%)	-2.63 to +2.73	P=0.956
Hepatic Arterial Fraction (n=5)	-0.05 (-11.03%)	-0.25 to +0.14	P=0.42

(b)

Perfusion parameter	Mean difference in parameter between scan 2 (after 1 cycle chemo) and scan 3 (after 2 cycles chemo) (n=5)	95 % confidence interval of the difference	Statistical significance Paired t test (2 – sided)
Blood Flow (ml/100ml/min)	-4.05 (-8.02%)	-106.72 to + 98.63	P=0.918
Blood Volume (ml/100ml)	-1.15 (-16.36%)	-4.78 to + 2.48	P=0.429
Mean Transit Time (seconds)	+0.45 (+3.13%)	-2.36 to + 3.26	P=0.679
Hepatic Arterial Fraction (n=4)	-0.07 (-23.58%)	-0.21 to +0.06	P=0.18

Notably, at a scanning interval of 39-47 days after SIRT and chemotherapy there was a mean 62% reduction in tumour BF and 61% reduction in BV, which was statistically significant (see table 74); in comparison, a lower magnitude of mean change in these parameters was demonstrated in control patients, which was not statistically significant.

Table 74 Summary of absolute and percentage change in perfusion parameters between scans 2 and 4 (a) in patients receiving SIRT on day 2 Cycle 2 of chemotherapy and (b) in control patients receiving chemotherapy alone in Arm A; statistical significance evaluated using paired t test for pairwise differences

(a)

Perfusion parameter	Mean difference in parameter between scan 2 and scan 4 (39-47 days post SIRT (n=4)	95 % confidence interval of the difference	Statistical significance Paired t test (2 – sided)
Blood Flow (ml/100ml/min)	-214.33 (-62.4%)	103.43 to 325.33	**P=0.009**
Blood Volume (ml/100ml)	-12.44 (-60.59%)	-17.96 to -6.92	**P=0.006**
Mean Transit Time (seconds)	+0.89 (+10.07%)	-1.92 to +3.70	P=0.387
Hepatic Arterial Fraction (n=4)	-0.12 (-26.55%)	-0.35 to +0.11	P=0.194

(b)

Perfusion parameter	Mean difference in parameter between scan 2 (after 1 cycle chemo) and scan 3 (after 2 cycles chemo) (n=5)	95 % confidence interval of the difference	Statistical significance Paired t test (2 – sided)
Blood Flow (ml/100ml/min)	-54.85 (-24.88%)	-138.70 to 29.01	P=0.144
Blood Volume (ml/100ml)	-3.76 (-18.70%)	-9.90 to + 2.38	P=0.165
Mean Transit Time (seconds)	+1.85 (+27.1%)	-0.56 to + 4.25	P=0.100
Hepatic Arterial Fraction (n=5)	-0.04 (-19.57%)	-0.13 to 0.04	P=0.22

On qualitative analysis of perfusion parameter maps for patients who received SIRT, appreciable changes were observable 10 days post SIRT in all patients scanned at this time point but changes were more pronounced after 39-46 days after SIRT (see figure 80 for example of changes in BF maps). Specifically, there was a reduction in the proportion of voxels with high BF and BV in the tumour rim indicating reduced perfusion; there was also an increase in the proportion of voxels with low or no assigned parameter value in the core of a number of the metastases, suggestive of increased necrosis.

Figure 80 Blood Flow parameter maps for patient P1154 receiving SIRT in Arm B (a) 2 days prior to SIRT (b) 10 days after SIRT and cycle 2 of chemotherapy (c) 39-47 days post SIRT and 4 cycles chemotherapy

(a) **(b)** **(c)**

P1154

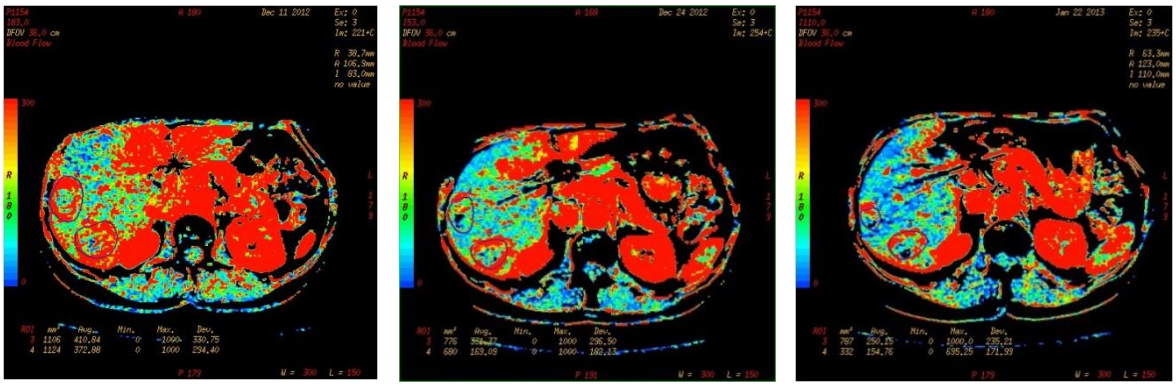

Figure 81 Blood Flow Parameter maps for patient P1053 after (a) 2 days prior to SIRT (b) 26 days after SIRT and 4 cycles chemotherapy

(a) **(b)**

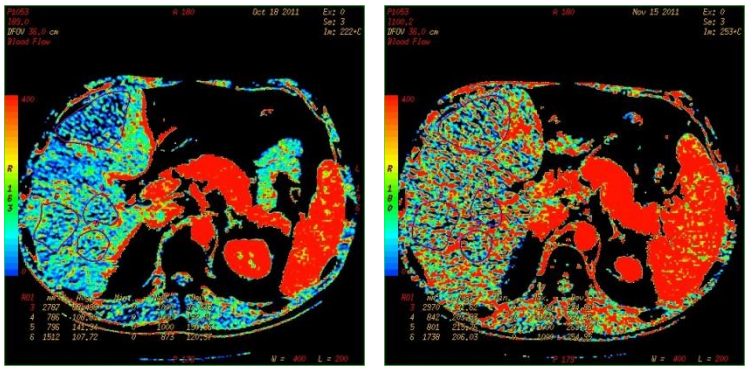

In patient P1053, who had SIRT with cycle 3 of chemotherapy, there appeared to be an increase in the proportion of higher blood flow and blood volume values in the metastases as well as in the adjacent liver (see figure 81).

E7 RECIST Response

Table 75 summarises the RECIST response in the liver of patients receiving chemotherapy in Arm A of the study 3 months after commencement of treatment. There was no apparent association between baseline tumour BF and RECIST response. Notably, patient P1131 was the only patient in

Arm A to have progressive disease on CT after 3 months of therapy. Although there was no apparent pattern of distinction between changes in perfusion parameters between this patient and responding patients after 1 or 2 cycles of chemotherapy, after 4 cycles of chemotherapy, substantial increases in BF and BV were demonstrated for patient P1131, whilst BF and BV decreased in responding patients at this time-point.

Table 75 Summary of RECIST response in liver on CT 3 months after commencement of therapy for patients in Arm A

PATIENT NUMBER	RECIST
P1056	Stable Disease
P1099	Partial Response
P1109	Partial Response
P1131	Progressive Disease
P1170	Complete Response
P1172	Partial Response
P1200	Partial Response

Table 76 summarises RECIST responses on CT after 3 months of therapy in patients who received SIRT as well as chemotherapy in Arm B of FOXFIRE. Of note, patient P1053 was one of 2 patient s who received SIRT to demonstrate progressive liver disease on standard contrast-enhanced CT scanning 12 weeks after the commencement of chemotherapy but the only patient who had progressive disease in the liver after SIRT. Although patient P1105 had an increase in the volume of liver disease between the baseline CT CAP and 3 month follow-up study, portal phase CT liver scans performed at the same time as the pCT scans and serial CEA measurements demonstrated that the disease progression occurred before the delivery of SIRT, with a reduction in the volume of liver metastases and reduction in CEA values between the scan 2-3 days before SIRT and 12 week contrast enhanced CT, indicative of a response to SIRT; all other patients demonstrated a partial response according to RECIST measurement of liver lesions. Patient P1053 was the only patient in Arm B, for whom BF and BV increased on pCT scans after SIRT, whilst for responding patients BF and BV decreased. The number of patients in this study is too small to adequately evaluate whether parameter values are prognostic or predictive but our data suggests that

further research is warranted to evaluate whether changes in pCT parameters can predict response to chemotherapy and SIRT, as well as to explore the best time-point for pCT response evaluation.

Table 76 Summary of RECIST response in liver on CT 3 months after commencement of therapy for patients in Arm B

Patient Number	RECIST Response
P1048	Partial Response
P1053	Progressive Disease
P1085	Partial Response
P1105	Progressive Disease
P1154	Partial Response
P1182	Partial Response
P1200	Partial Response

E8 Summary

In summary, we have demonstrated that it is feasible to perform sequential pCT scans in patients with colorectal liver metastases receiving oxaliplatin and modified de Gramont chemotherapy with and without the addition of SIRT using yttrium-90 SIR-spheres, in order to evaluate the vascular effects of treatment. This chapter highlights some of the technical challenges associated with liver perfusion CT acquisition and analysis in this patient cohort; we have presented details of pCT liver protocol development to facilitate the evaluation of Hepatic Arterial Fraction and minimise the impact of coil artefact on tumour perfusion estimation. We have evaluated the extent of intra-sequence motion and tested the hypothesis that inter-sequence motion correction reduces inter-observer variation in parameter estimation but found little data in support of this hypothesis in this small patient cohort. In this chapter, the hypothesis that multiple cycles of oxaliplatin and modified de Gramont chemotherapy result in changes in tumour perfusion which are unfavourable for subsequent SIRT; the data presented suggests that chemotherapy can reduce BF to liver metastases and reduce HAF, with the proportion of tumours demonstrating these changes increasing with increasing numbers of cycles. Statistically significant reductions in tumour perfusion and hepatic arterial fraction were only demonstrated after 4 cycles of

chemotherapy. In this chapter, the hypothesis that SIRT of colorectal liver metastases results in significant changes in perfusion consistent with the effects expected from radiotherapy was also tested. The data presented demonstrates that there are reductions in tumour perfusion 10 days after SIRT and chemotherapy. Substantial, statistically significant reductions in tumour perfusion parameters were also demonstrated 39-47 after SIRT and concurrent chemotherapy, in support of the specific hypothesis that SIRT results in decreases in tumour perfusion >2 weeks post SIRT, consistent with the delayed effects expected from radiotherapy.

4 Discussion

4A General discussion and Clinical Relevance

Colorectal cancer is a common disease and both systemic chemotherapy and radiotherapy play an important role in its treatment, in both the radical or palliative setting. Although there is evidence from clinical trials to support a range of different treatment schedules for locally advanced rectal cancer (concurrent long-course chemo-radiation, neo-adjuvant chemotherapy with selective pelvic radiation, a short course of pelvic radiation followed by chemotherapy), uncertainties exist regarding the optimal schedule from a biological perspective. In the context of metastatic colorectal cancer, systemic chemotherapy is a principal treatment modality; the integration of SIRT has potential to improve disease outcomes in patients with liver predominant metastases and may even increase the proportion of patients able to proceed to a curative resection.

Some of the greatest improvements in cancer outcomes have been achieved by combining systemic agents with radiation, although much of the research into radio-sensitising drugs has been largely empirical rather than representing a translation of scientific research. The published literature is inconclusive regarding which is the most clinically effective combination of radio-sensitising drug and radiation in colorectal cancer and particularly in regard to whether multiple cycles of chemotherapy before radiation are detrimental or beneficial for the efficacy of treatment. In this thesis, the biological importance of tumour perfusion for the efficacy of both chemotherapy and radiotherapy has been highlighted; it has been argued that research directed towards understanding the impact of pre-treatment tumour perfusion characteristics on treatment outcomes and the ways in which different treatments modulate tumour perfusion may inform the rational selection of new radio-sensitising drugs and biologically optimal sequencing of treatments as well as improved personalisation of therapy. In this thesis the general hypothesis is

tested that the evaluation of changes in tumour perfusion can guide the rational sequencing of drugs and radiation.

This is the first research evaluating the toxicity, efficacy and biological activity of the novel radiosensitising drug, nelfinavir, in combination with radiation, without the confounding effect of concurrent chemotherapy. We have tested the specific hypotheses that the combination of nelfinavir and hypo-fractionated pelvic radiotherapy in rectal cancer is tolerated with acceptable toxicity and that nelfinavir can improve blood flow to human rectal cancer. Additionally we have evaluated the feasibility of evaluating a novel tissue biomarker based on quantitative TCD analysis in rectal tumour biopsies before and after nelfinavir and radiation; we have tested the specific hypothesis that it is feasible to use TCD as an early endpoint for comparing the relative efficacy of radio-sensitisation in the context of an early phase clinical trial.

This research is the first to perform and evaluate dual modality perfusion imaging, using pCT and Dce-MRI, at multiple time-points to evaluate changes in perfusion in cancer patients receiving drug therapy before and concurrent with radiotherapy. Whether pCT or Dce-MRI represent equally valuable modalities for the evaluation of changes in tumour perfusion during and after cancer therapy is not established in the literature. Therefore, this research provides unique insights into the comparability of the actual data derived and technical challenges associated with each modality. This thesis has also considered the effect of oxaliplatin and 5FU chemotherapy on the perfusion of colorectal liver metastases, in particular the impact of this treatment on the subsequent delivery of SIRT. We have tested the specific hypothesis that multiple cycles of oxaliplatin and 5FU chemotherapy result in changes in tumour perfusion which are unfavourable for subsequent SIRT. This is the first study to evaluate the effect of SIRT on tumour perfusion in liver metastases; we have tested the hypothesis that SIRT results in changes in tumour perfusion that are consistent with the effects of radiation rather than significant embolization, thereby

adding insights to the mechanism of effect of this treatment and its sequencing with chemotherapy.

A fundamental requirement for the evaluation of changes in tumour perfusion is robust imaging modalities and analysis methods, which can accurately and reproducibly measure tumour perfusion. In this thesis, we have explored the limitations of existing methods of perfusion analysis using perfusion CT and Dce-MRI and we argue that changes in tumour perfusion using these tests need to be interpreted in the context of their limitations and that methods for acquisition and analysis need to be further developed and optimised.

4B Toxicity and activity of nelfinavir and hypo-fractionated radiotherapy for rectal cancer

B1 Baseline patient characteristics

In this project, the schedule of nelfinavir before and during radiotherapy was evaluated in patients with locally advanced rectal cancer and synchronous metastatic disease. An initial short course of radiotherapy followed by subsequent chemotherapy is one treatment option for such patients, many of whom have local tumour symptoms such as pain or bleeding. This patient population was selected since we wished to evaluate the effect of nelfinavir without the confounding effect of concurrent chemotherapy. Nevertheless, recruitment to this study was more challenging than anticipated because of other treatment approaches available to patients in this category, namely systemic chemotherapy or long-course chemo-radiotherapy.

B2 Toxicity of nelfinavir and hypo-fractionated radiotherapy

The data presented in chapter 3B support the hypothesis that the combination of nelfinavir and hypo-fractionated pelvic radiotherapy for rectal cancer is safe and tolerated with acceptable toxicity, since less than a third (20%) of patients developed dose limiting toxicity (necessitating

interruption of therapy). Compared to historical data from patients treated with SCRT alone, the rates of grade 3 non-haematological toxicity observed in patients treated with SCRT and nelfinavir were slightly higher but did not significantly exceed expected rates of toxicity based on qualitative judgement. Of the 5 grade 3 non-haematological toxicities observed in this research, 1 of these was likely to have been causally related to radiotherapy, 1 to have been causally related to nelfinavir and 1 to both. In the Stockholm III prospective randomised controlled trial, 5 (4.2%) of 113 patients who received SCRT and delayed surgery had severe side effects, defined as "symptoms demanding hospital admission corresponding to G3/4 toxicities according to RTOG criteria"[432, 444](named as vomiting, diarrhoea with dehydration, constipation, vaginal bleeding and lower back pain). The limitations of comparing our toxicity data with the data from the Stockholm III trial is that acute severe toxicity was defined according to the RTOG criteria for acute radiation toxicity[444] which is consistent with CTCAE version 3 rather than CTCAE version 4, as defined in our study protocol. Of specific note, Grade 3 diarrhoea is defined as "diarrhoea requiring parenteral support/severe mucous or bloody discharge requiring pads/ plain abdominal X Ray demonstrated distended bowel loops" according to the RTOG CTCAE version 3, whereas in version 4 it is defined as "an increase of>=7 stools per day over baseline, incontinence, hospitalisation, severe increase in stoma output; limiting ADL." The only other toxicity data from patients treated with SCRT and delayed surgery comes from 2 retrospective studies[33, 34], where Grade 3 and 4 diarrhoea were reported in a small proportion of patients. It is likely that these 2 studies under-represented the true levels of Grade 3/4 radiation toxicity in the treated patients, as severe acute toxicity was identified according to those patients admitted to hospital rather than prospective patient assessment. In this study, 3 patients were admitted to hospital within 28 days of receiving nelfinavir and radiotherapy, the first due to non-neutropenic fever, whilst receiving systemic chemotherapy, the second due to diarrhoea after completion of protocol therapy and the third due to vomiting, which was likely to have been disease-related.

In this project, we wished to investigate the safety of nelfinavir and RT without the confounding effect of concurrent chemotherapy. A previous study of nelfinavir and long course chemo-radiotherapy with capecitabine in rectal cancer resulted in unacceptable levels of Grade 3 hepatotoxicity [235, 236] , which may have been attributable to a drug interaction between chemotherapy and nelfinavir. Similarly, in a study of concurrent nelfinavir, temozolomide and radiotherapy for patients with glioma, 3 patients experienced dose-limiting Grade 3 transaminase elevation[234]. In our study, Grade 3 hepatotoxicity was not observed.

A limitation of our research is the absence of a control group receiving SCRT alone for direct comparison of rates of toxicity with those receiving SCRT and nelfinavir. However a large number of patients would have been required to adequately power such a randomised comparison, which was not feasible within the time constraints and resources available for this research. Nevertheless, we have demonstrated that the majority of adverse events occurring were those which might have been expected as a result of SCRT alone or due to chemotherapy administered after completion of radiotherapy and nelfinavir. Thus, the combination of nelfinavir and hypo fractionated radiotherapy for rectal cancer is safe.

B3 Clinical Efficacy of nelfinavir and radiotherapy

Similar to the published studies in other cancers combining radiotherapy and nelfinavir, we found a high radiological response rate. Compared to long-course chemo-radiotherapy for locally advanced rectal cancer, the rate of good mrTRG after hypo-fractionated radiotherapy and concurrent nelfinavir was favourable, which is promising given the high proportion with T4 disease and/or CRM margin threat involvement. In the MERCURY study, the rate of good mrTRG for LARC was 50% overall[123] and for ≥T3c tumours only 33%, in comparison to 56% in this small study, in which 60% patients had T4 tumours and 70% had a detectable *KRAS* mutation. It should be noted that 4 of the patients with good mrTRG score had 3-6 weeks of chemotherapy between

the end of radiotherapy and MRI assessment. Although systemic therapy may have contributed to some extent to the clinical response rates seen in this trial, this novel approach of being able to administer full-dose systemic therapy so soon after hypo-fractionated RT is a promising approach as suggested in a previous study[40]. The efficacy of using hypo-fractionated RT followed by systemic chemotherapy in comparison to standard chemo-radiation is currently being tested in the international, multi-centre, randomised trial, RAPIDO (NCT01558921)[445].

B4 Tumour Cell Density Analysis

A particular strength of this research is its incorporation of a reproducible, quantitative tissue biomarker, TCD, which has previously been shown in a retrospective study to have value in comparing the relative effects of different chemo-radiation schedules on tumour cell kill after RT[255]. TCD has previously been evaluated in pre-treatment rectal tumour biopsy specimens and resected tumours [254, 255]. In this project, we have demonstrated for the first time the feasibility of performing TCD measurement in pre- and post-RT samples obtained at endoscopy. Only one tissue sample (post-RT) was non-evaluable due to the absence of tumour cells, but this is likely to have been the result of sampling error rather than RT-induced necrosis. The data presented demonstrates that hypo-fractionated radiotherapy +/- nelfinavir results in a significant reduction in tumour cell density after 7 days of completing treatment.

A potential criticism of TCD analysis in tumour biopsy specimens and the evaluation of changes in TCD in individual patients is that TCD measurements may underestimate the TCD in the luminal surface of the tumour and dependent on the quality of the biopsies taken. We endeavoured to counter this by taking multiple large biopsies and calculating TCD within the area with the greatest apparent TCD. Nevertheless, our data suggest that sampling of necrotic regions of tumour may lead to proportionately lower TCD values for individual patients. Differences in the proportion of necrosis in tumour samples from the same patient before and after treatment are

liable to result in non-representative assessment of changes in TCD, unless the whole tumour has become necrotic in response to treatment.

Our TCD results demonstrate the feasibility of using TCD as an early endpoint of response to radiation combined with a radiosensitising drug. Furthermore, our data indicate that the addition of nelfinavir to hypo-fractionated RT may result in additional tumour cell kill compared to RT alone. Based on these findings, we propose that TCD merits further validation as a biomarker of radio sensitization for use in prospective clinical trials. Although in our limited study sample size, no statistically significant association was demonstrated between TCD and radiological response (mrTRG), we observed a statistical trend in 8 of the 10 patients, whereby a large reduction in TCD after treatment was associated with a good mrTRG score and a small reduction in TCD was associated with a poor TRG.

B5 Hypoxia and Vascular Markers

We explored changes in MVD after SCRT and nelfinavir. Consistent with previous research, we found CD105a to be a more specific marker for MVD than CD31. Our finding of a statistically significant increase in MVD after SCRT and nelfinavir (evaluated by CD105a) is contrary to the findings of a previous study which showed a trend towards a decrease in MVD (evaluated by CD34)in rectal tumour biopsies after SCRT alone[446]. It is possible that the contradictory results are due to the use of different micro vessel stains (particularly since we found no significant change in MVD as assessed by CD31). It would be anticipated that nelfinavir would result in a reduction rather than an increase in MVD, although our finding could be explained by an increase in tumour neovascularisation induced by radiation. However, since tumour micro vessel density in tumours is characteristically heterogeneous, it can be argued that the evaluation of MVD on small biopsy samples may be non -representative and the evaluation of changes in MVD on such biopsies unreliable in terms of evaluating the effect of radiotherapy with or without radiosensitising drugs.

Although based on pre-clinical research into the effects of nelfinavir [229], we would have expected a reduction in the expression of the tumour hypoxia markers CAIX and HIF- 1α after treatment with nelfinavir, no such pattern of change was observed on analysis of pre-treatment and post-treatment biopsy samples. However, it is well described that both CAIX and HIF- 1α expression tend to be heterogeneous in tumours and typically greatest in peri-necrotic areas; it is therefore possible that hypoxia marker expression on small biopsy samples is non-representative (as for MVD analysis) and has limited validity as a means of assessing the effect of novel radiosensitisers on hypoxia or accuracy in distinguishing which tumours are hypoxic. Nevertheless, the presence of positive hypoxia marker expression in several of the pre-treatment tumour biopsies supports the principle that these tumours could potentially benefit from hypoxia modulation prior to and during radiotherapy. The discordance between CAIX and HIF- 1α expression in contiguous sections from the same tumour samples can be explained by their differential half-lives and sensitivity for detecting chronic vs acute hypoxia [283, 284].

B6 Markers associated with activation of the RAS-PI3K-AKT signalling pathway

Pre-clinical research suggests that radio-sensitisation of tumour cells by nelfinavir is mediated through inhibition of Akt independent of *KRAS* status [447]. Our clinical results support this finding since no obvious association was observed between *KRAS* status of the tumour and radiological response to treatment.

A limitation of our research is that we did not evaluate the *EGFR*, *PIK-3CA* mutational status or *PTEN* expression of the tumours, which may have provided additional information about the activation of the RAS-PI3K-AKt signalling pathway; this was due to the lack of adequate tumour tissue remaining after our other analyses. *PIK-3CA* mutation status and *PTEN* immunohistochemical expression might have been useful in this research, since PIK-3CA mutation

(which occurs in approximately 8-10% rectal cancers[302, 304]) can result in altered tumour signalling through the PI3K-Akt pathway resulting in intrinsic radio resistance and *PTEN* is an inhibitor of PI3K; inactivating *PTEN* mutations (which occur in <5 % of all colorectal cancers[448]) or *PTEN* loss (which occurs in 20-40% of all colorectal cancers[449, 450]) result in activation of PI3K. *PIK-3CA* mutation and loss of *PTEN* expression results in phosphorylation of Akt and therefore *PIK-3CA* mutation status and absence of *PTEN* expression have potential as markers to indicate which human tumours might benefit from treatment with the Akt inhibitor nelfinavir, which has been demonstrated to reduce intrinsic radio resistance pre-clinically in tumours with activation of the PI3K-Akt signalling pathway [227].

Although phospho-Akt immunohistochemical expression has been suggested as a tissue biomarker for identifying tumours with activation of the RAS-PI3K-Akt signalling pathway (which are intrinsically radio resistant and may benefit from an Akt-inhibitor such as nelfinavir to improve radio sensitivity), it has not been formally validated as such the published literature. It has previously been demonstrated that not all commercially available antibodies directed against phospho-Akt have adequate sensitivity and specificity for use in immunohistochemical assays[317]. Using a commercially available antibody which has been demonstrated to have adequate sensitivity and specificity for use in immunohistochemical assays, positive phospho-Akt expression was observed in only one pre-treatment tumour biopsy in this research. Although tissue samples were analysed in one batch at the same time-point, due to the fact that the paraffin embedded tissue samples were diagnostic samples acquired in several different centres and of different ages, it seems likely that the presence of this potentially unstable phospho-protein may have been affected by tissue storage and preservation methods. In contrast, 3 of the post –treatment biopsies, which were all acquired and processed by the same laboratory, demonstrated phospho-Akt expression. Although nelfinavir would be expected to cause de-

phosphorylation of phospho-Akt, the presence of a greater proportion of tumours with positive phospho-Akt expression after treatment may be explained by the previous observation that radiation induces Akt phosphorylation[451].

To our knowledge, this is the first study to have evaluated phospho-PRAS40 expression in rectal cancer as a potential biomarker of Akt activation, since it is potentially more stable than phospho-Akt in fixed human tissue. [319] In the pre-treatment rectal biopsies, a higher number of biopsies were positive for phospho-PRAS than phospho-Akt, which could be due to its better stability in preserved tissue; immunohistochemical staining for phospho-PRAS40 was also considerably stronger than phospho-Akt. The low proportion of tumours with positive phospho-RAS expression before treatment (33%) might suggest that the majority of the tumours treated with nelfinavir would not have benefited from Akt-inhibition. A potential criticism of the analysis of phospho-Akt and phospho-PRAS40 immunohistochemical expression in this research is that cell lines known to express the phospho-proteins incubated with antibody diluent in the absence of the antibodies were used as negative controls; optimal negative controls would have been the same cell lines, in which phospho-Akt and phospho-PRAS40 had been knocked-down using si-RNA. A further limitation of our research is that we did not perform our own stability studies to evaluate the effect of tissue storage on phospho-PRAS40 expression, which would be essential for further development of phospho-PRAS40 as a potential biomarker. There is currently only limited published data on the short-term stability of phospho-PRAS 40 in human tissue samples [319]. Furthermore, since we evaluated rectal biopsy specimens rather that whole tumours, it is uncertain whether phospho-PRAS40 is homogeneously or heterogeneously expressed, the latter of which would influence the value of evaluating this marker in biopsy specimens. Although, this research has demonstrated the feasibility of evaluating phospho-PRAS40 immunohistochemical expression in formalin-fixed paraffin-embedded rectal tumour biopsies, further work is required to validate it fully and to define its clinical utility as a biomarker for predicting response to Akt-inhibition.

4C Perfusion CT imaging of Rectal Cancer

C1 Scans performed and evaluated

This study has demonstrated the feasibility of evaluating changes in tumour perfusion using sequential pCT scans during a "window of opportunity" for novel drug treatment before as well as during radiotherapy treatment in the context of an early phase clinical trial. All patients completed the scheduled pCT scans, although the scans from one patient had to be excluded for technical reasons and it was not possible to perform every post-treatment scan on the last day of radiotherapy for practical reasons since there were 4 patients in the study at one time. It is uncertain what impact the delay in performing the final pCT scan may have had on the parameters derived for the relevant tumours, since no previous studies have evaluated changes in tumour perfusion at different time-points within the week after radiotherapy.

C2 Technical factors influencing pCT analysis

Since previous research has demonstrated that a number of technical factors that can potentially influence the derivation of tumour perfusion parameters using pCT, we wished to analyse such factors in the scans studied in this project. With respect to intra-sequence motion on pCT analysis for rectal cancer, although a previous study in patients with colonic as well as rectal cancers has shown that this can be a major technical challenge[345], our data did not wholly support this finding. This may be because the rectal tumours in our study were locally advanced, with a high proportion of low tumours, which were relatively fixed. Nevertheless, some degree of intra-sequence motion, mostly due to peristalsis rather than respiration, was observed in the majority of patients; one study suggests that this could have been minimised by consistent use of buscopan prior to scanning[345]. The data presented illustrates that there can be significant changes in bowel and bladder filling between sequential pCT scans for individual patients, which can affect tumour position. Although this issue has been little described in previous studies, it is

argued that this could be potentially problematic when attempting to identify the same limited portion of tumour for pCT analysis on sequential scans to evaluate changes in perfusion in response to cancer therapy; it would be less relevant for single time-point pCT analysis or for pCT with extended coverage, where it would be possible to image the entire tumour on each scan.

C3 Method development

Previous research has advocated that rectal tumour perfusion parameters should be analysed on a single pCT slice rather than multiple pCT slices[337]. However, our data supports the argument that there can be heterogeneity in tumour perfusion parameters between different levels in tumours. Since different observers may be liable to select a different slice of the tumour for analysis when analysing pCT parameters on a single slice, such a method could result in derivation of non-representative tumour perfusion parameter measurements on sequential scans and be problematic for evaluating the effect of therapy. We have developed a method for evaluating tumour perfusion in multiple pCT slices (to account for tumour heterogeneity) and to evaluate perfusion in the same portion of tumours on sequential scans. Our data demonstrates improved inter-observer agreement in tumour perfusion measurements using this method in comparison to analysis of a single pCT slice. The comparison of 2-D analysis of multiple pCT slices (using a weighted mean) and 3-D volumetric analysis in Matlab suggests that both are acceptable methods, which correlate statistically. However, since there were significant differences in the perfusion parameters derived using the Matlab program and the GE software, the 2-D method was used for analysis of changes in perfusion in study patients, since this is a validated method. A problem with this method is that it needs to be performed manually and is labour-intensive. On the basis of this analysis, we would advocate the use of pCT techniques which improve tumour coverage and the development of analysis packages which perform volumetric analysis of perfusion CT data, such that it is feasible to reliably measure mean perfusion parameters for

whole tumours on sequential scans in the context of clinical trials investigating the effect of therapy.

C4. Quantitative and qualitative evaluation of changes in tumour perfusion parameters during nelfinavir and radiotherapy

In Chapter 3C, the results of quantitative and qualitative evaluation of pCT scans during nelfinavir and radiotherapy in patients with rectal cancer were presented to test the hypothesis that nelfinavir can improve blood flow to human rectal tumours. The magnitude of percentage change in perfusion parameters needs to be interpreted in light of published values for the reproducibility of these measurements [331, 452] [332]. A challenge in the interpretation of these data is uncertainty regarding the measurement error of the test using the technique and methods of analysis we used. A published study evaluating the measurement error and repeatability of perfusion CT in 10 primary colorectal tumours by evaluation of 2 perfusion CT scans performed 48 hours apart reported the within-subject coefficient of variation for blood flow, blood volume and mean transit time as 14%, 23% and 35% respectively [335]. Based on their analysis of the data the authors calculated that for a single patient undergoing therapy, a measurement change of at least +/- 38%, 65% and 97% were required to be significant at the 5% level for blood volume, blood flow and mean transit time, respectively. Another study demonstrated a coefficient of variation of 23% for BF and 14% for BV[337].

The data presented do not support the hypothesis that 7 days of nelfinavir treatment results in improved blood flow to human rectal cancer, since no statistically significant changes in blood flow were demonstrated at this time point overall and most of the individual changes in perfusion parameters demonstrated between the first two scans were within the limits of normal measurement variation. There are a number of possible explanations for this, which will be discussed in the next section in the context of the findings of the Dce-MRI analysis. However, our study demonstrated a statistically significant 40% increase in mean tumour blood flow after 7

days of nelfinavir in combination with hypo-fractionated radiotherapy. Since this change exceeds the coefficient of variation for BF reported in previous studies evaluating repeatability, this finding suggests a treatment effect rather than measurement variation.

A limitation of this analysis is the absence of a control group (i.e. no nelfinavir), which means that it is not possible to explicitly differentiate the effect of RT on blood flow from the effect of nelfinavir plus RT. This is the first study to have demonstrated acute increases in tumour blood flow during SCRT using pCT, although a previous study demonstrated significant increases in K^{trans} during SCRT for rectal cancers using pCT, which was interpreted to be due to increased permeability as a result of radiation.[350] The finding is consistent with previous studies having demonstrated acute increases in tumour perfusion parameters during the initial weeks of long-course chemo-radiotherapy for rectal cancer using Dce-MRI[368, 453] but the comparison complicated by the use of a different imaging modality and parameters as well as use of chemotherapy in these studies. The significance of the finding that SCRT results in acute increases in tumour perfusion is that this treatment could improve the delivery of sequential or concurrent systemic chemotherapy and provides evidence in support of this treatment strategy.

A limitation of evaluating changes in mean tumour perfusion parameters using pCT is that it does not demonstrate the heterogeneity of perfusion parameters within the tumour. It has been demonstrated that it is possible to evaluate tumour perfusion heterogeneity on perfusion parameter maps and to visually appreciate changes in of regional tumour perfusion on sequential scans. However this approach is open to criticism for being subjective, is time-consuming for evaluating large numbers of scans in the context of clinical trials and may also be susceptible to missing subtle changes in tumour perfusion. Nevertheless, our qualitative findings on the baseline scans were consistent with previous research which has demonstrated a statistically significant higher mean BV and BF parameter values in rectal tumour ROIs compared to normal rectum ROIs for the same individuals [347, 351]. We explored whether histogram analysis of perfusion CT

parameters within tumour volumes of interest might provide valuable information regarding changes in tumour perfusion heterogeneity during nelfinavir and radiotherapy, since histogram analysis of Dce-MRI data has been demonstrated to provide additional value in response assessment to therapy. We demonstrated distinctively shaped histograms for each of the perfusion parameters BF, BV, and MTT and this is the first study to have evaluated tumour BF, BV and MTT heterogeneity in rectal cancers using pCT parameter histograms. Although histograms were strikingly similar for the majority of tumours between the baseline pCT and a second pCT after 7 days of nelfinavir, after 7 days of nelfinavir concurrent with radiotherapy, a rightward shift in the distribution of BF values was observed, a flattening of the BV curve and reduction in the peak of high MTT values. These findings suggest that the combination of nelfinavir and radiation results in changes in tumour perfusion heterogeneity within tumours and more specifically improves tumour perfusion in those regions of the tumour with poor perfusion (low BF and high interstitial pressures or high MTT). The explanation for this is uncertain but may be explained by vascular endothelial damage, reduced cellular density or closing of AV shunts. We explored changes in the skewness and kurtosis of histogram distributions for the tumour VOI between successive pCT scans. In the context of our data analysis, this appeared to be of limited value for comparing histograms, with only non-significant findings of a trend towards a reduction in mean positive skewness of the BF histograms and a trend towards a reduction in mean positive skewness of the MTT histograms after radiotherapy and nelfinavir. It is likely that the values for skewness and kurtosis in our analysis were influenced by the noise within the histograms and possible that this could have been optimised by altering the histogram bin width.

Methods for evaluating the heterogeneity of tumour perfusion parameters within a tumour volume of interest are of biological significance because it is known that the vasculature of tumours are frequently non-uniform and the identification of sub-regions of tumour with low or high perfusion may be more important than the average perfusion of the whole tumour in determining response to therapy. In this research, it has been demonstrated that there is

significant heterogeneity in all of the pCT parameters evaluated in human rectal tumours. In the future, as pCT methodology and software is developed to more readily produce histograms of pCT parameters for whole tumour volume of interest and related statistics, further research is warranted to evaluate the utility of pCT histograms, as an indicator of tumour perfusion heterogeneity, to predict response to radiation therapy and to evaluate the effect of novel treatment strategies in colorectal cancer.

4D Dce-MRI Imaging of Rectal Cancer

D1 Dce-MRI scans and pCT scans performed and evaluated

A number of previous studies have utilised sequential Dce-MRI scans to evaluate changes in perfusion during or after cancer therapy but only one study has previously demonstrated the feasibility of performing both pCT and Dce-MRI scans at a single time point in patients with rectal cancer[434]. This project demonstrates the feasibility of performing dual modality perfusion imaging at multiple time points to evaluate the microvascular effects of a novel radio-sensitising drug given before and concurrent with radiotherapy.

D2 Technical factors influencing perfusion parameter analysis

Few published studies integrating Dce-MRI into the assessment of rectal cancer have described the technical challenges and limitations associated with analysis of this imaging modality, although these have been highlighted in recent guidelines.[428] Intra-sequence motion was a greater problem for Dce-MRI analysis than pCT analysis because the acquisition time of the dynamic sequence and inter-sequence time interval were considerably longer for Dce-MRI scans than pCT scans to allow pharmacokinetic modelling of delayed phase data. A strength of our Dce-MRI analysis is that data were motion corrected using an algorithm developed by our collaborators. We utilised a semi-quantitative scoring system to evaluate the severity of tumour

intra-sequence motion before and after motion correction, demonstrating improvements in motion scores after motion correction in the majority of studies. Nevertheless, for studies with severe intra-sequence motion there appeared to be a limit to the improvement achievable in intra-sequence motion scores, indicating that motion reduction strategies such as buscopan and improved breathing control techniques may have been beneficial. The evaluation of other technical challenges in our Dce-MRI analysis using proprietary software highlights that in comparison to pCT analysis using commercially available software, Dce-MRI analysis is far more complex, potentially error prone and less validated. A particular limitation of the analysis of our Dce-MRI analysis was the lack of T1 mapping (due to use of a protocol with sub-optimal flip angle sequences), which theoretically could have affected the accuracy of the pharmacokinetic parameters derived in this research.

D3 Quantitative and qualitative evaluation of changes in tumour perfusion during nelfinavir and radiation therapy for rectal cancer

In Chapter 3C, the results of quantitative and qualitative evaluation of Dce-MRI scans during nelfinavir and radiotherapy in patients with rectal cancer were presented to test the hypothesis that nelfinavir can improve blood flow to human rectal tumours. The magnitude of percentage change in perfusion parameters needs to be interpreted in light of published values for the reproducibility of these measurements. Galbraith et al.[367] demonstrated that the repeatability of mean K^{trans} measurements of the median pixel values of tumours in a series of 16 pelvic tumours was -45% to +83% (that is, the 95% confidence interval for significant change in an individual). The reproducibility of mean K^{rans} in a group of 16 patients was -14% to +16% (that is, the size of change needed for significance at the 95% level of confidence). Other studies suggest that the coefficient of variation for mean K^{trans} measurements in tumours using Dce-MRI is in the order of 20% [454, 455] and therefore a 40% change in K^{trans} is required to show clinical significance. In this context, the data presented do not support the hypothesis that 7 days of

nelfinavir treatment results in improved perfusion to human rectal cancer, since no statistically significant changes in K^{trans} was demonstrated at this time point overall and most of the individual changes in perfusion parameters demonstrated between the first two scans were within the limits of measurement variation. However, our study did demonstrate a statistically significant 42% increase in median K^{trans} after 7 days of nelfinavir in combination with hypo-fractionated radiotherapy, which suggests a clinical effect from the combination of nelfinavir and radiation rather than measurement variation. The consistency between the findings of pCT and Dce-MRI analyses adds substantial support to this conclusion. As for the pCT data, a limitation of this analysis is the lack of reproducibility data for Dce-MRI parameters in our own centre and the absence of a control group (i.e. no nelfinavir), which means that it is not possible to explicitly differentiate the effect of RT on blood flow from the effect of nelfinavir plus RT. However, the magnitude of change in median K^{trans} is broadly comparable to the increase in median K^{trans} between pCT scans at baseline and on the fifth day fraction of hypo-fractionated RT for locally advanced rectal cancer reported by Janssen et al, [350] which suggests that the changes in K^{trans} observed in our study are principally due the effects of radiation, rather than nelfinavir. The data from multi-modality imaging in our project, adds to the findings of Janssen et al.[350] in demonstrating that the increases in K^{trans} SCRT are related to improved blood flow, not just permeability.

As for the pCT data, we explored whether histogram analysis of Dce-MRI parameters within tumour volumes of interest might provide valuable information regarding changes in tumour perfusion heterogeneity during nelfinavir and radiotherapy, since histogram analysis of Dce-MRI data has been demonstrated to provide additional value in response assessment to therapy. In contrast to the pCT histogram analyses after 7 days of nelfinavir and a further 7 days of nelfinavir and radiation, there were changes in the shape of the pharmacokinetic parameter distributions for the majority of tumours but less of a consistent pattern and it is unclear whether this may have been due to tumour progression, treatment effect (improved perfusion) or technical reasons

relating to Dce-MRI analysis. Statistical analysis of changes in the skewness of the parameter distributions was more valuable than that for the pCT histograms, since the histograms were less noisy and there was a statistically significant difference in mean skewness for K^{trans} after 7 days of nelfinavir and concurrent radiation, showing significant changes in the pattern of heterogeneity of K^{trans} within the tumour volume of interests, from lower towards higher K^{trans} values.

There are several possible explanations why no significant change in blood flow or K^{trans} was observed after 7 days of nelfinavir. One possible explanation is that the vasculature of tumour xenografts in mice develop in a different way to the vasculature in spontaneous tumours in humans and its clinical effects are specific to xenografts. A second explanation for the failure of the pre-clinical findings to translate to human rectal cancers is that the xenograft tumours in pre-clinical studies were all derived from SQ2B (squamous cell carcinoma) and HT1080cell lines, with known activation of Akt[229], whereas we demonstrated activation of Akt using phospho-Akt or phospho-PRAS immunohistochemistry in a small minority of patients. Another possible explanation is that although 5-14 days of nelfinavir was shown to cause improvements in perfusion in mice xenografts, the duration of treatment required in human tumours is greater, potentially due to differences in tumour biology and metabolism of the drug. A limitation of our analysis is the lack of pharmacokinetic studies demonstrating adequacy of the serum drug levels and pharmacodynamic tests to demonstrate the adequacy of Akt de-phosphorylation by nelfinavir; the latter was planned using an assay in blood polymorpho-nuclear cells. [232].

Although Dce-MRI has a higher signal to noise ratio than pCT, which should mean that it is more sensitive for detecting treatment effects, the interpretation of changes in K^{trans} is more ambiguous than changes in blood flow on pCT. Since K^{trans} is dependent on both blood flow and permeability, but believed to equate to blood flow in untreated tumours, we made an assumption that nelfinavir would be expected to result in increases in k^{trans}. However, it is possible that nelfinavir, in normalising the vasculature results in simultaneous decreases in tumour permeability and

increases in blood flow which equates to largely unchanged K^{trans} values. For this reason, pCT has a potential advantage over Dce-MRI in providing a more direct insight into changes in tumour perfusion, although noise is still a significant challenge in pCT analysis.

4E Imaging of Colorectal Liver Metastases

E1 Scans performed and evaluated

This research has demonstrated the feasibility of evaluating changes in tumour perfusion using sequential pCT scans of the liver in patients with colorectal liver metastases receiving oxaliplatin chemotherapy +/-SIRT in the context of a clinical trial. Compliance with the study schedule was good, although 2 of the patients in the SIRT arm of the study had SIRT with cycle 3 rather than 2 of chemotherapy, meaning that the timing of the pCT scans was inconsistent with patients receiving SIRT with cycle 2 of chemotherapy and had to be analysed separately.

E2 Technical factors influencing perfusion parameter analysis

As for pCT rectal scans, we evaluated technical factors in the liver scans studied that can potentially influence the derivation of tumour perfusion parameters using pCT. One challenge was the ability to scan the portal vein as well as a suitable liver metastasis for dual vascular modelling in the context of limited z axis coverage; although we modified our scanning protocol to try and meet this challenge, dual vascular modelling was not possible for all scans.

As expected, intra-sequence motion was a greater problem in analysis of pCT scans of the liver than pCT scans of the rectum. In contrast with the majority of previous studies utilising perfusion imaging of the liver to evaluate changes in tumour perfusion in response to therapy, we evaluated and reported the extent of motion for individual scans. A semi-automated deformable image registration algorithm developed by our collaborators was applied to try and correct for intra-sequence motion prior to analysis of the pCT data using GE software. Although, improvements in intra-sequence motion were demonstrated in over half of scans, for studies with

severe intra-sequence motion, there appeared to be a limit to the improvement achievable in intra-sequence motion scores, suggesting that improved motion control techniques for pCT liver warrant development.

This is one of few studies to have evaluated tumour perfusion of colorectal liver metastases and the first to highlight that embolization coils can result in beam-hardening artefact, which could influence the validity of tumour perfusion parameters, if the studied metastasis is in proximity. In light of this, we recommend selecting a metastasis distant from the site of the embolization coil placement in the hepatic arterial system for pCT studies.

E3 Development of methods for analysis

As for pCT rectum, our data for pCT liver supports the argument that there may be heterogeneity in tumour perfusion parameters between different levels in tumours which could result in deriving non-representative tumour perfusion parameter measurements from different regions of a tumour on sequential scans and be problematic for evaluating the effect of therapy. Compared to pCT rectum scans evaluated in this project, it was more challenging to scan and evaluate the same region of tumour in each of the sequential scans because of the inherently greater motion of the liver compared to the rectum, less fixed anatomical landmarks for comparing the position of a liver tumour and in many cases, shrinkage of the liver metastases during treatment. This problem was a function of the limited z axis coverage which meant that it was not possible to study entire liver metastases in all scans. This challenge could be potentially mitigated in future by pCT scanning with greater z axis coverage, at the expense of increased radiation exposure. Our data support the hypothesis that deriving a weighted mean of tumour perfusion parameters in multiple pCT slices results in better inter-observer agreement in perfusion parameters compared to analysis of single slices. Our data did not support the hypothesis that motion correction reduces inter-observer variation in tumour perfusion parameter estimates; however a limitation of our analysis was the small number of patients and

inclusion of all baseline studies, whether intra-sequence motion was reduced after “motion correction” or not. Further investigation in a larger sample of pCT scans, accounting for the severity of motion and impact of motion correction is warranted.

E4 Quantitative and qualitative evaluation of perfusion parameters on baseline scans

The mean values for mean BF and mean BV determined on baseline scans in this study are higher than values reported for colorectal liver metastases in one other study having used the same software analysis package[392]. Published values for the HAF of other colorectal liver metastases are lacking but the study by Kim et al[392] reported values for Hepatic Perfusion Index of which were significantly higher than the mean HAF in this study of (0.38 +/- 0.08). Of note, the HAF values of liver metastases estimated by this method are substantially lower than the values expected from previous research using other methods to measure the relative proportion of tumour blood flow derived from the hepatic artery and portal vein[456, 457].Further research is required to validate HAF estimation using pCT scans.

Our analyses highlight that there is significant spatial variation of perfusion parameters within the majority of colorectal liver metastases and the way in which a tumour ROI is defined on pCT liver imaging can result in differences in the mean perfusion parameters derived. Our finding of higher BF and BV in the periphery of liver metastases on pCT parameter maps is consistent with the findings previously reported by Miles et al of a high arterial perfusion in the rim of tissue outside of liver metastases, defined using non-contrast images[419]. This research has provided additional insights into the spatial heterogeneity of perfusion parameters in colorectal liver metastases in demonstrating higher perfusion values in the rim of tissue inside as well as outside of a tumour boundary, as defined on contrast-enhanced CT.

E5 Quantitative and qualitative evaluation of changes in tumour perfusion parameters during oxaliplatin and modified de Gramont chemotherapy

This is the first study to have evaluated changes in the tumour perfusion of colorectal liver metastases in patients receiving a single schedule of systemic chemotherapy at multiple time points in the course of treatment. From the evaluation of sequential changes in tumour perfusion parameters in colorectal liver metastases in patients receiving oxaliplatin and modified de Gramont chemotherapy using pCT, we found some evidence to support the hypothesis that chemotherapy results in changes in the perfusion of colorectal liver metastases which are unfavourable for subsequent radioembolisation with yttrium-90 SIR-spheres. Mean BF decreased in 5/13 evaluable tumours after 1 cycle of chemotherapy, in 5/8 evaluable tumours after 2 cycles of chemotherapy and 4/5 evaluable tumours after 4 cycles of chemotherapy, changes which could reduce the therapeutic ratio of SIRT for those tumours with reductions in BF. No statistically significant change in tumour BF or BV was demonstrated after 1, 2 or 4 cycles of chemotherapy. However, a mean 28.43% statistically significant reduction in HAF was observed after 4 cycles of chemotherapy as well as an increase in mean MTT of 40.46%, which bordered on statistical significance, suggestive of reduced tumour perfusion. These data suggests that delaying SIRT until the fourth cycle of chemotherapy might be detrimental to the efficacy of treatment, since the technique depends on liver tumours having a high hepatic arterial perfusion. A limitation of this analysis is the uncertainty about the accuracy of HAF estimation using the GE perfusion software, since it has not been validated in the literature and also the technical limitations of our pCT method (namely presence of intra-sequence motion and inability to measure mean tumour perfusion values for the whole selected metastasis on sequential scans).

As for pCT rectal scans, we developed and tested a method for evaluating changes in the heterogeneity of perfusion within liver metastases using perfusion parameter histograms. In view of the spatial heterogeneity appreciable in perfusion within colorectal liver metastases, this method could be a valuable tool in evaluating response assessment over and above changes in mean parameter values, which warrants further research.

E6 Quantitative and qualitative evaluation of changes in tumour perfusion parameters after SIRT using yttrium-90 SIR-spheres and concurrent oxaliplatin and modified de Gramont chemotherapy

Although 2 previous studies have explored the use of pCT liver as a biomarker for response to SIRT in patients with liver metastases, this is the first study to have evaluated the effect of SIRT on tumour perfusion using sequential pCT scans [406, 407]. Our analysis of changes in tumour perfusion after SIRT using yttrium-90 SIR-spheres and concurrent chemotherapy does not support the specific hypothesis that SIRT results in acute increases in tumour perfusion up to 10 days after delivery of therapy but does support the hypothesis that SIRT results in significant reductions in perfusion >2 weeks post treatment. The finding of substantial reductions in mean BF and BV 10 days after SIRT can be explained in a number of ways. The first possible explanation is that contrary to previously held opinion[124], the effect of tumour embolism does predominate over the effects of radiation in SIRT of colorectal liver metastases using resin microspheres. An alternative explanation is that acute increases in tumour perfusion after radiation, as demonstrated in our study of patients with rectal cancer, are not sustained for 10 days after delivery of treatment; this is possible since no study has specifically evaluated when acute increases in perfusion subside and post-treatment reductions in perfusion develop. It is only known that increases in perfusion are seen during and at the end of radiotherapy and reductions in perfusion can be demonstrated 1-2 weeks after completion of treatment with external beam radiotherapy [347-349]. Since the delivery of SIRT using Yttrium-90 is a highly targeted form of

radiation which delivers a continuous dose over a period of time with the highest dose rate being delivered in the first few days after treatment, it may be that this form of radiation does not cause acute increases in tumour perfusion due to a lesser effect on vascular endothelium than fractionated external beam radiation, which is believed to mediate its acute effects via vessel endothelial cell damage. Our findings of significant reductions in tumour perfusion >2 weeks after SIRT are consistent with the known effects of chemo-radiation on tumour perfusion [347, 348, 379].

4F Summary of Findings and Future Directions

In this thesis, we have presented findings which support the hypothesis that perfusion imaging can guide the rational sequencing of drugs and radiation therapy. We have developed a paradigm for the evaluation of drugs which may improve tumour perfusion before and during radiation therapy using perfusion imaging and tissue markers, which could be adopted in future trials of radiosensitisers.

This is the first research to have evaluated the clinical effects of the Akt-inhibitor nelfinavir without the confounding effects of chemotherapy and we have demonstrated that the combination of nelfinavir and hypo-fractionated radiotherapy are tolerated with acceptable toxicity in patients with rectal cancer. Notably dose-limiting hepatotoxicity was not observed in this study, which suggests that hepatotoxicity observed in previous studies was due to a drug interaction between nelfinavir and chemotherapy. As in other studies of nelfinavir combined with radiation, radiological response rates were promising but randomised trial data are required to formally evaluate whether the addition of nelfinavir to radiotherapy improves patient outcomes. It is proposed that future research should incorporate tissue markers which identify the activation status of the RAS-PI3K-Akt signalling pathway, to permit further evaluation of their utility as biomarkers of response to signal transduction inhibitors such as nelfinavir and radiation. In concordance with a previous study, our research suggests that phospho-PRAS40 may be superior

to phospho-Akt as a marker of Akt activation but further stability studies and validation of this immunohistochemical marker is required in clinical samples to evaluate its clinical utility as a tissue biomarker.

This research demonstrates the feasibility of using TCD as an early endpoint of response to radiation combined with a radiosensitising drug. Furthermore, our data suggest that the addition of nelfinavir to hypo-fractionated RT results in additional tumour cell kill compared to RT alone. The prospective validation of TCD in rectal cancer has not yet been published but this research is ongoing in the context of a number of large randomised trials (personal communication-Nick West). Another focus for future research is the evaluation of the relationship between TCD and mrTRG in a larger patient group, without the confounding effect of inter-current chemotherapy; if TCD were demonstrated to have value in predicting individual patient response, this may allow treatment intensification for patients likely to have a poor radiological response.

This research does not support the hypothesis based on pre-clinical research that nelfinavir given for 7 days before radiotherapy improves blood flow to human rectal cancer. However, we have demonstrated significant increases in rectal tumour perfusion using both pCT and Dce-MRI during SCRT and concurrent nelfinavir, which is likely to be primarily explained by the acute biological effects of radiation. This finding provides some biological rationale for the strategy of administering SCRT followed by sequential chemotherapy in patients with metastatic rectal cancer, a schedule which was also found to be clinically efficacious in this study.

Following on from this research, a future multi-arm Phase II trial should be considered in rectal cancer, in which several novel radio-senistisers demonstrated to be safe in combination with radiation in the phase I setting, including nelfinavir, are evaluated. Following further validation of TCD, this tissue biomarker could be incorporated as an endpoint to evaluate the relative clinical efficacy of the radiosensitisers and help to identify which drugs warrant taking forward to the phase III setting. There is also scope for a trial which stratifies patients to be randomised to

receive a particular type of targeted radio-sensitiser combined with radiation or standard treatment, on the basis of molecular tests or other validated biomarkers, as a way of evaluating the feasibility of personalising radio-sensitising drugs in rectal cancer, in a similar way to which the NCRN FOCUS4 trial stratifies patients with metastatic colorectal cancer to receive different molecularly targeted agents. Since the combination of molecularly targeted drugs with long-course chemo radiotherapy (with capecitabine or 5FU) may be complicated by interactions between the investigational drug and the chemotherapy, it is proposed that short-course radiotherapy would be a preferable schedule for such trials.

This research indicates that 4 cycles of oxaliplatin and modified de Gramont chemotherapy can result in changes in tumour perfusion of colorectal liver metastases which would be detrimental to subsequent SIRT using yttrium-90 SIR-spheres. Specifically, significant reductions in HAF were observed after 4 cycles of chemotherapy which suggests that delaying SIRT until the fourth cycle of chemotherapy could be detrimental to the efficacy of treatment, since the technique depends on liver tumours having a high hepatic arterial perfusion. Furthermore, it has been demonstrated that SIRT results in substantial reductions in tumour perfusion, which are observed ≥10 days after treatment delivery and also evident >2 weeks after treatment delivery, which could be explained by the effects of radiation. The significance of this finding is that reductions in tumour perfusion may make subsequent chemotherapy less efficacious and potentially redundant. Future studies should observe pCT changes at longer time-points after SIRT and formally evaluate the ability of changes in pCT parameters after SIRT to predict outcomes such as RECIST response and PFS. There is also scope for future window studies, incorporating perfusion imaging, to evaluate the effect of drugs which have the potential to favourably modulate tumour perfusion prior to radiotherapy.

In this thesis, it has been demonstrated that there are a number of variables and technical issues which can potentially influence the validity of tumour perfusion parameters derived using pCT

and Dce-MRI. It has been argued that in order to robustly evaluate changes in tumour perfusion in colorectal cancers occurring as a result of cancer therapy, protocols which allow evaluation of the entire tumour are likely to be optimal. Further research is needed to develop perfusion analysis software to optimise motion correction algorithms, to develop automated techniques for tumour volume definition, which overcome inter-observer variation and to integrate perfusion parameter histograms. Specific to perfusion CT liver, a method has been developed for evaluating tumour perfusion parameters in the rim of colorectal liver metastases, which requires further optimisation for practical use. It is not fully understood whether the regions of high perfusion at the tumour rim represent regions of viable tumour, extending beyond the apparent tumour edge on CT as well as angiogenic tumour micro-vessels. Cross correlation between pCT imaging and pathological specimens is required in future research to clarify this uncertainty.

APPENDIX 1: pCT histograms for individual trial participants

Pre-Nelfinavir **After 7 days Nelfinavir**

ST1001

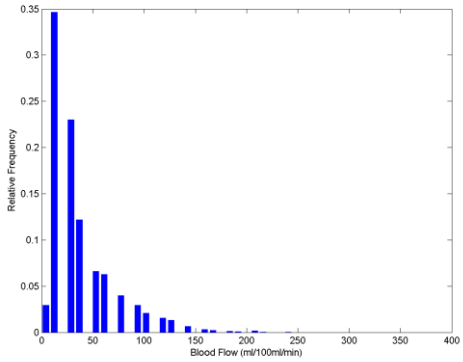

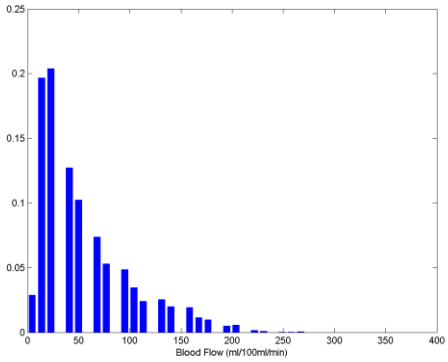

ST1002

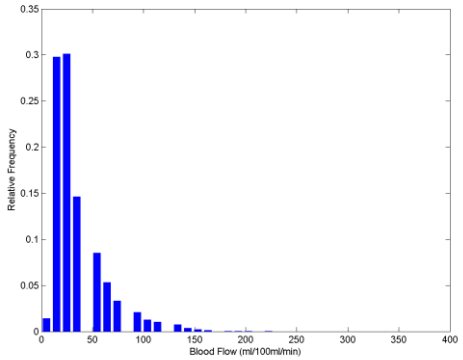

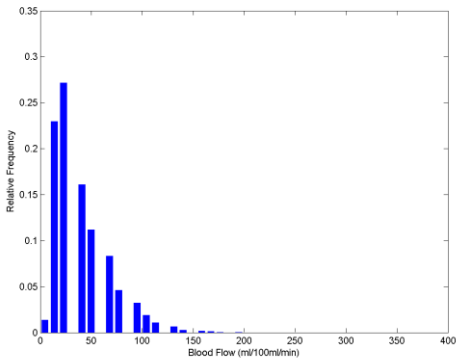

ST1003

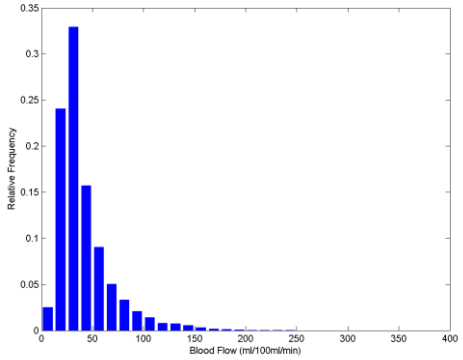

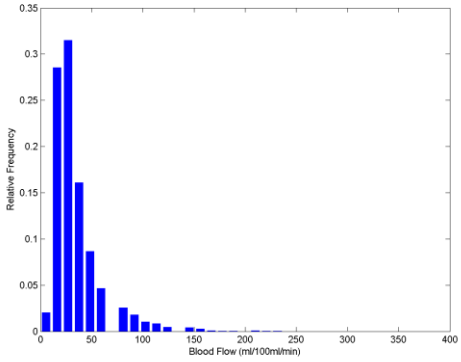

ST1004

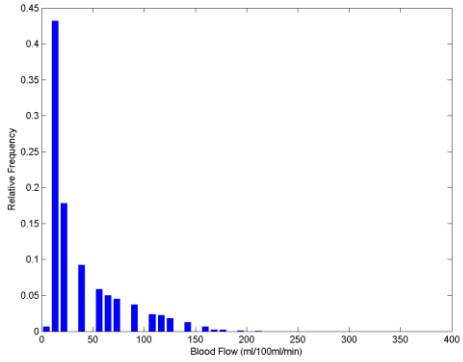

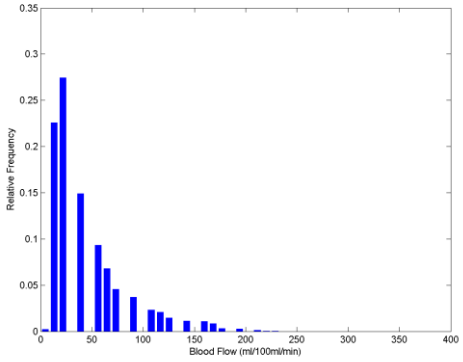

ST1005

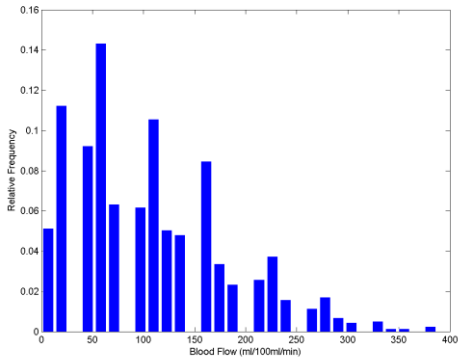

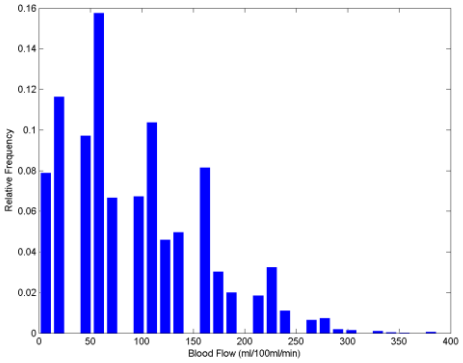

ST1006

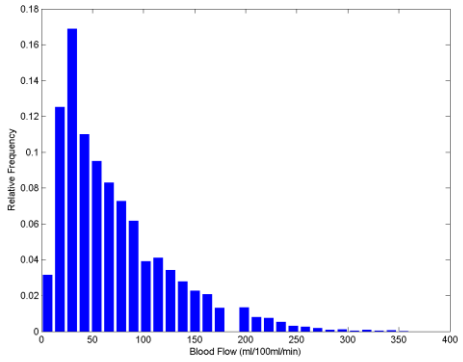

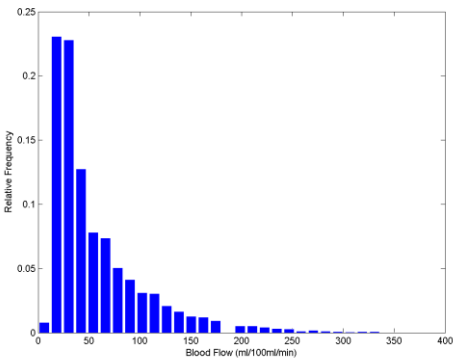

ST1008

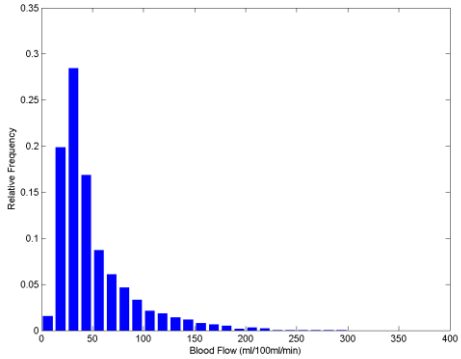

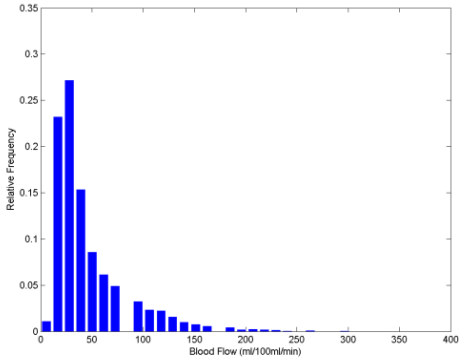

ST1009

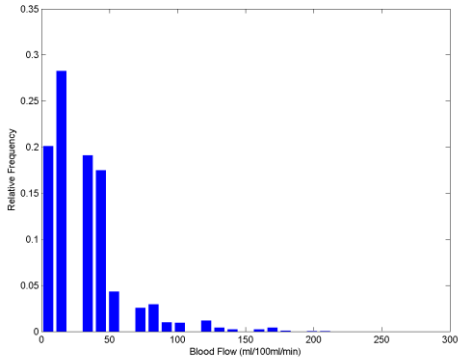

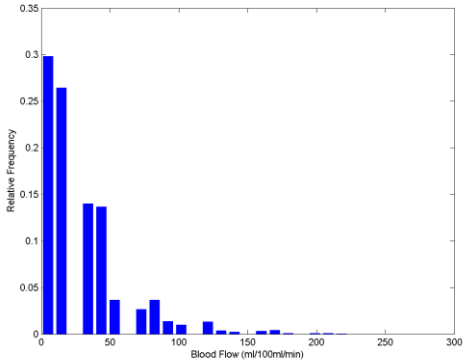

ST1010

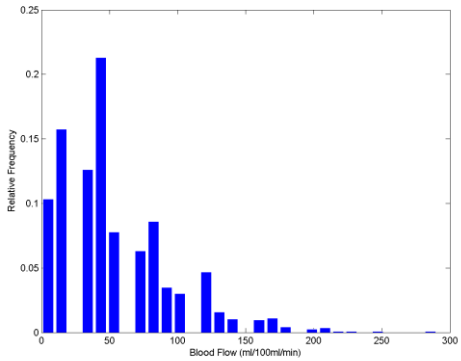

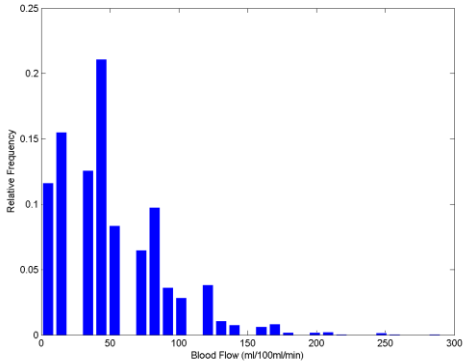

Blood Volume

Pre- Nelfinavir

After 7 days Nelfinavir

ST1001

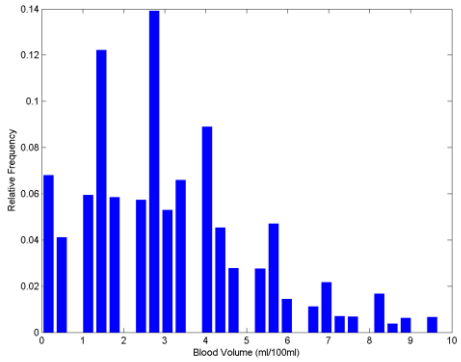

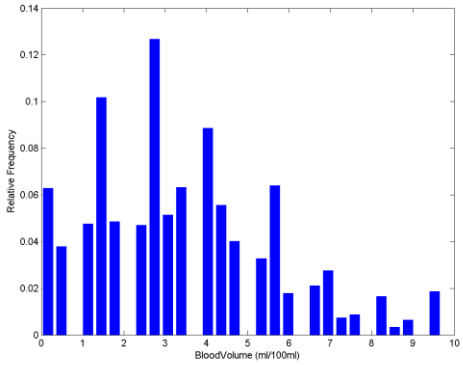

ST1002

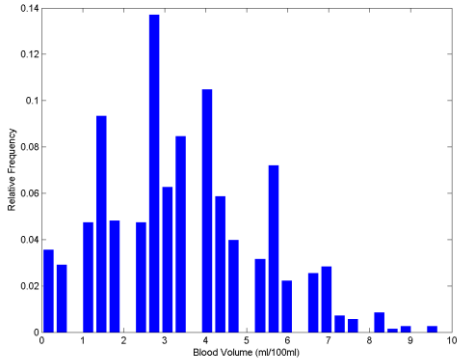

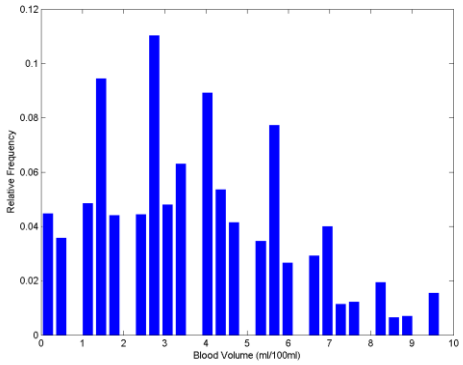

ST1003

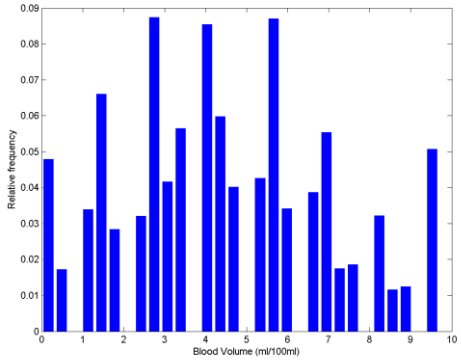

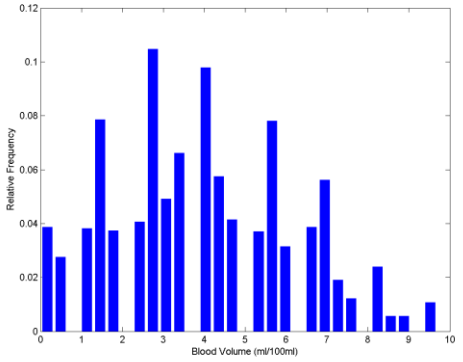

ST1004

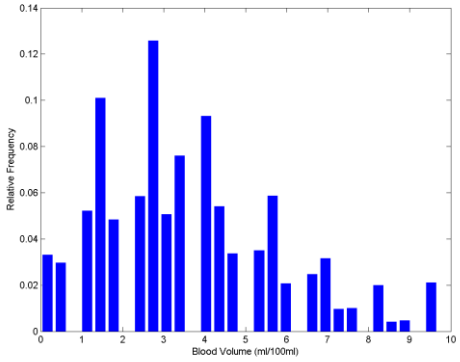

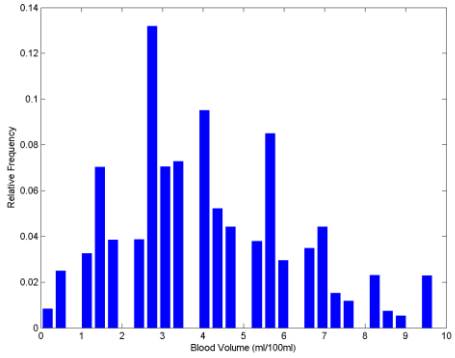

ST1005

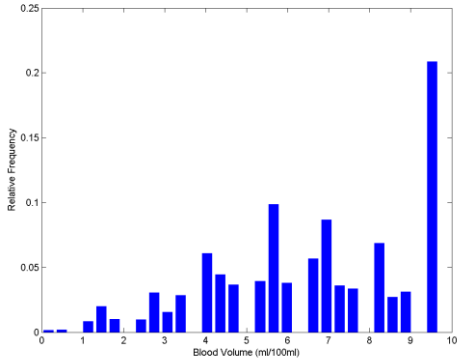

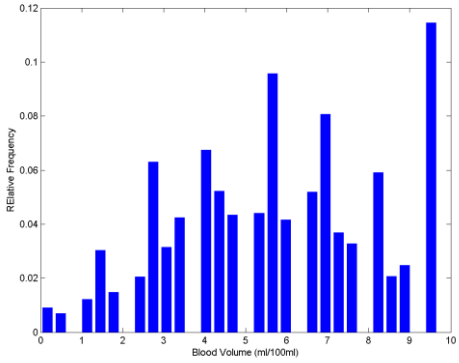

ST1006

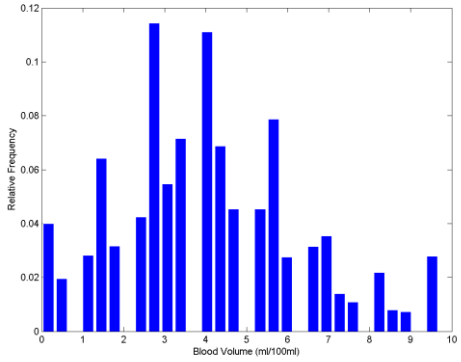

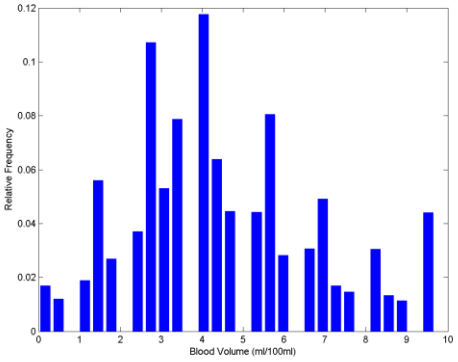

ST1008

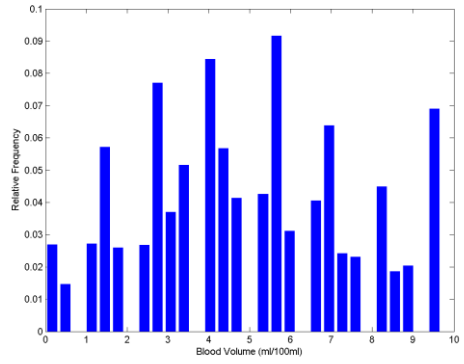

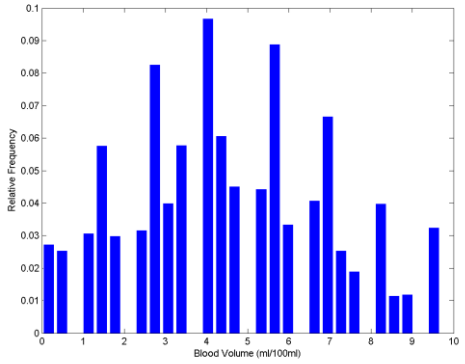

ST1009

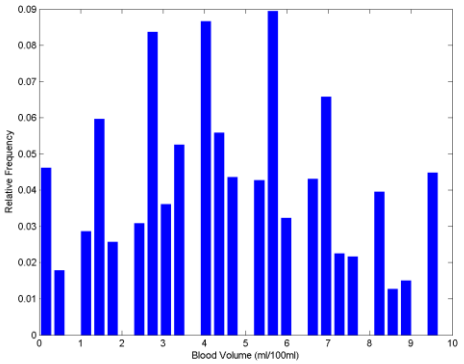

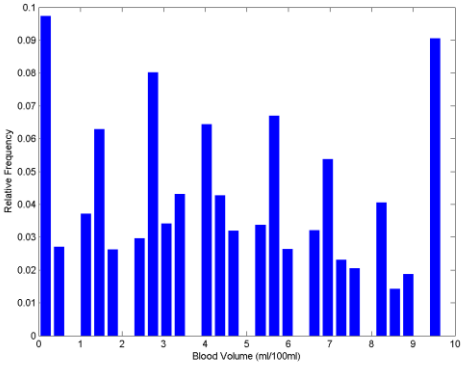

ST1010

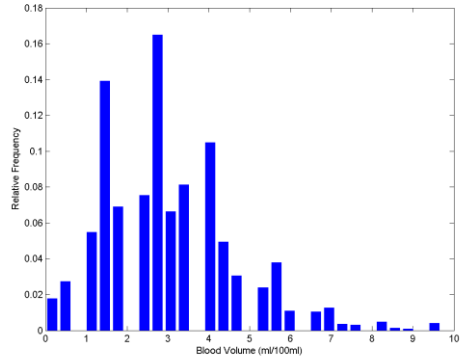

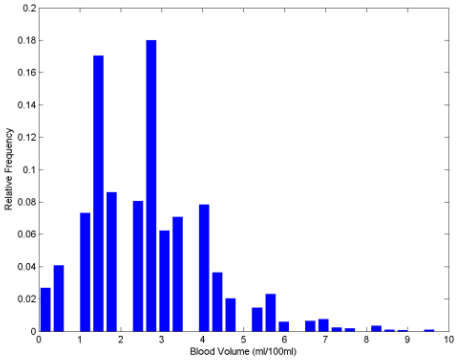

Mean Transit Time

Pre-treatment **After 7 days Nelfinavir and RT**

ST1001

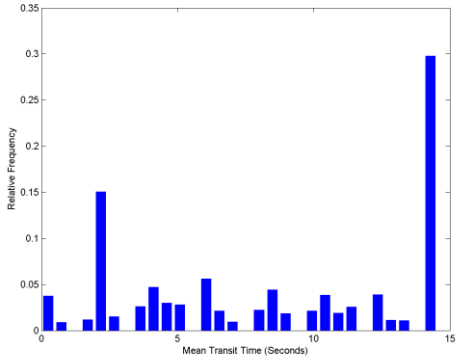

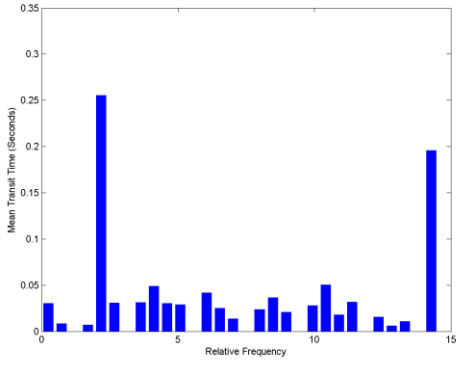

ST1002

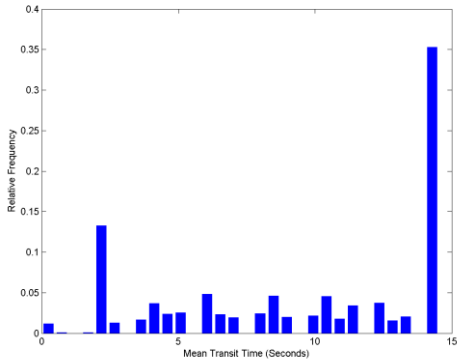

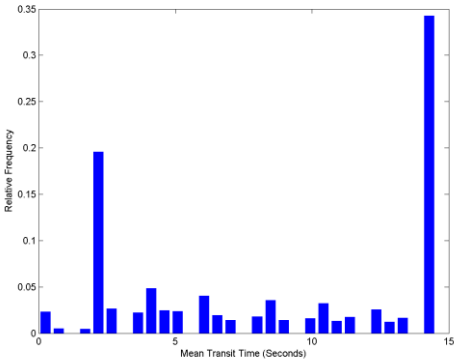

ST1003

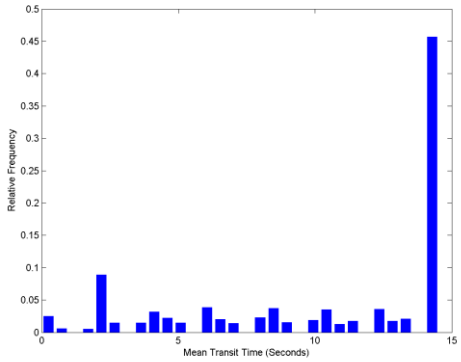

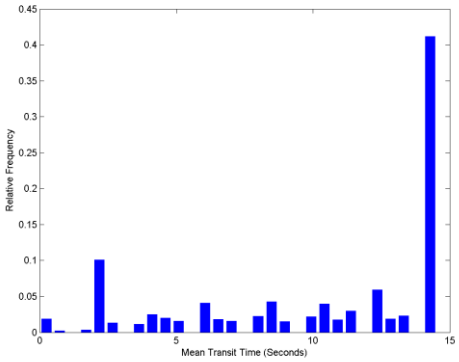

ST1004

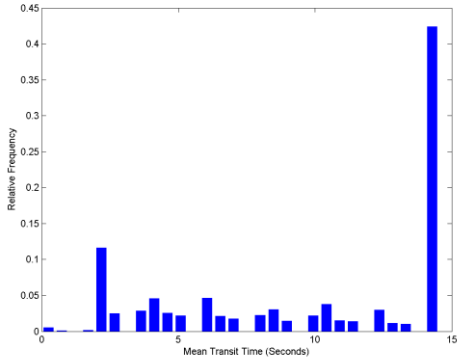

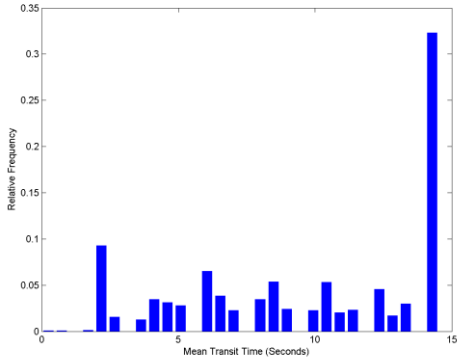

ST1005

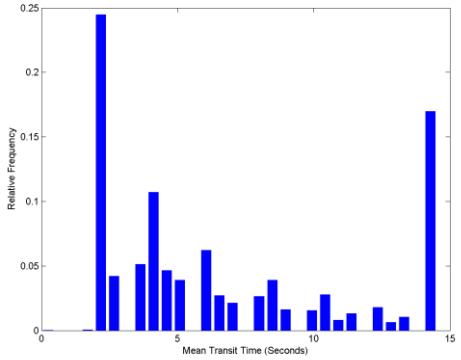

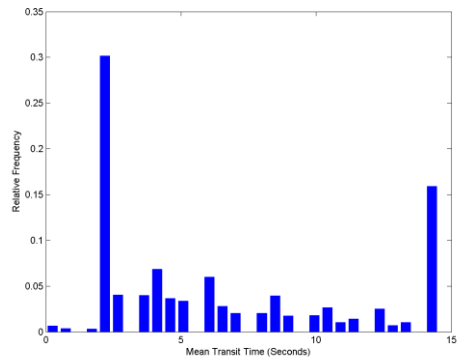

ST1006

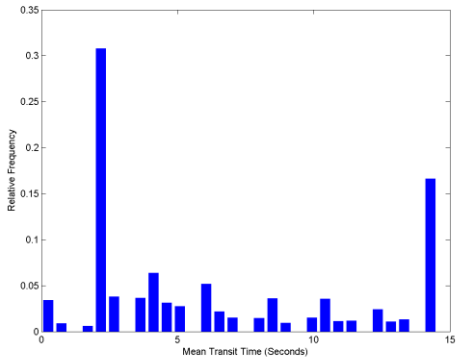

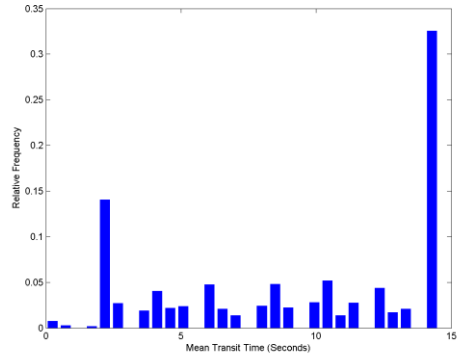

ST1008

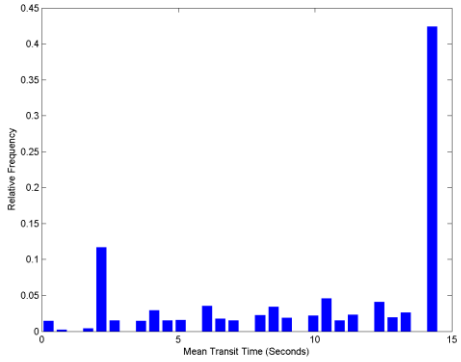

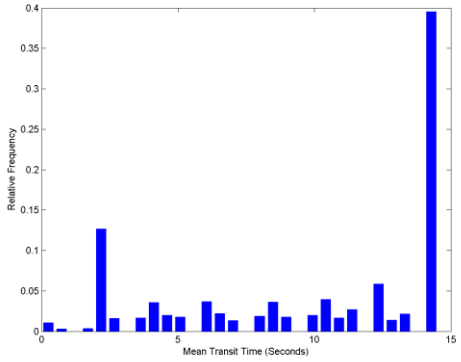

ST1009

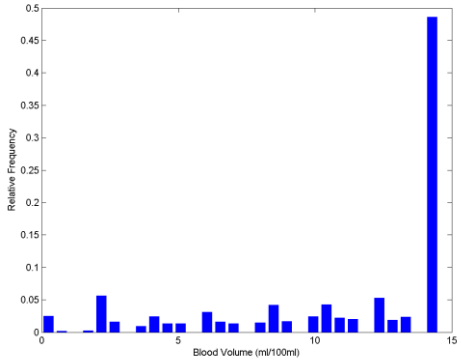

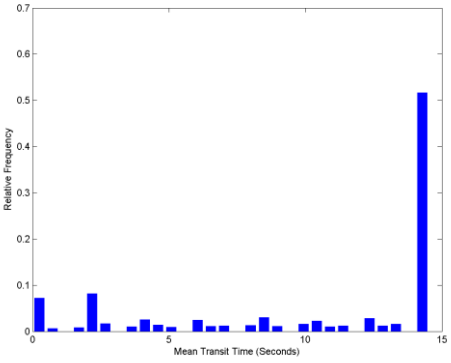

ST1010

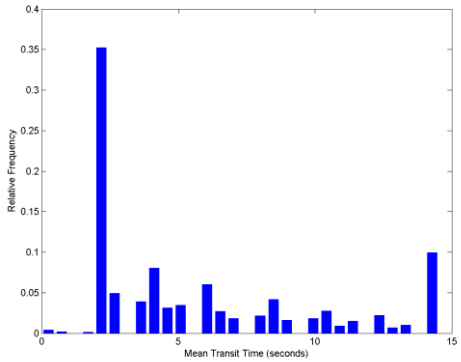

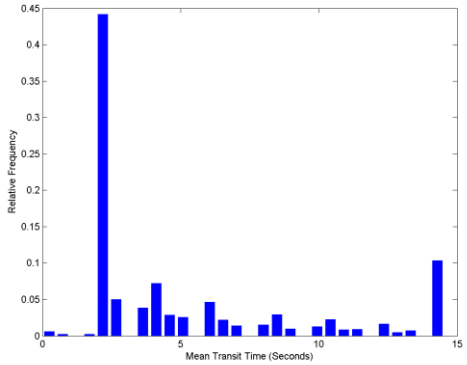

Histograms for tumour volume at comparable anatomical levels for Scan 2 (after 7 days of nelfinavir) and Scan 3 (after 14 days of nelfinavir and radiotherapy)

Blood Flow

After 7 days Nelfinavir **After 14 days Nelfinavir and RT**

ST1001

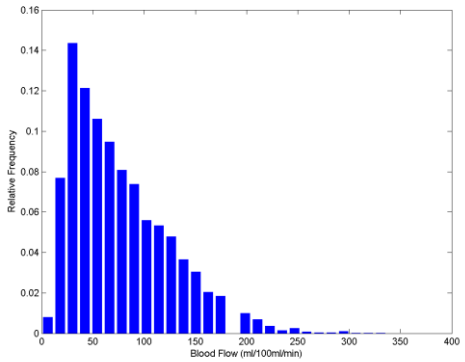

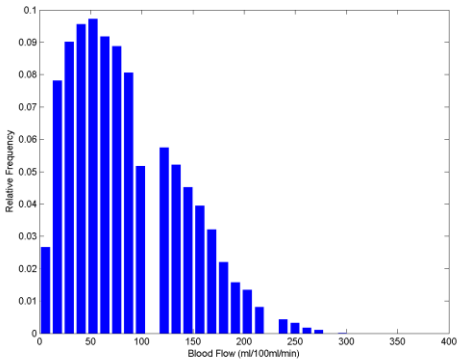

ST1002

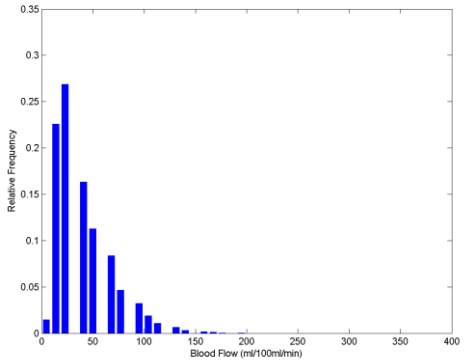

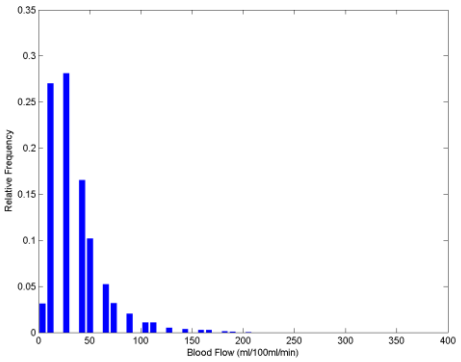

ST1003

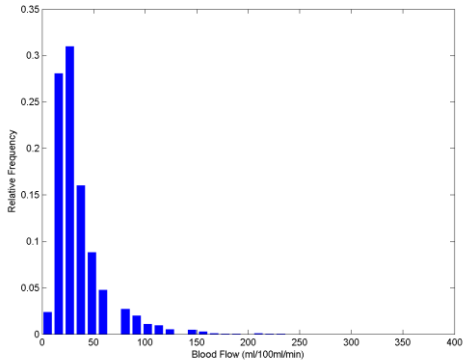

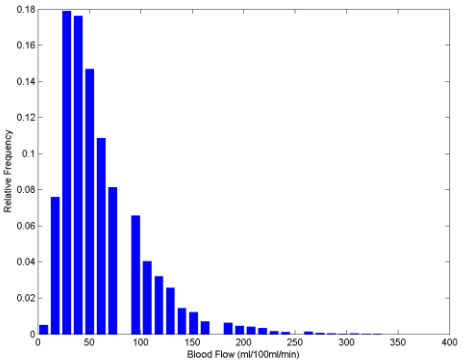

ST1004

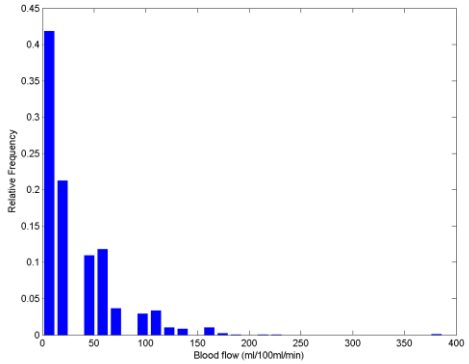

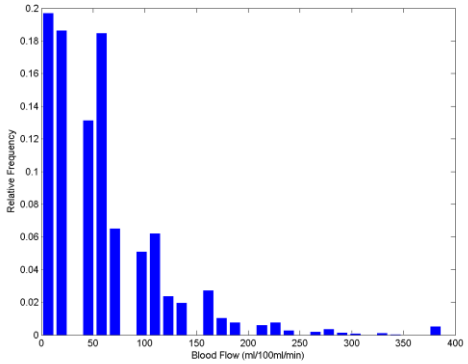

ST1005

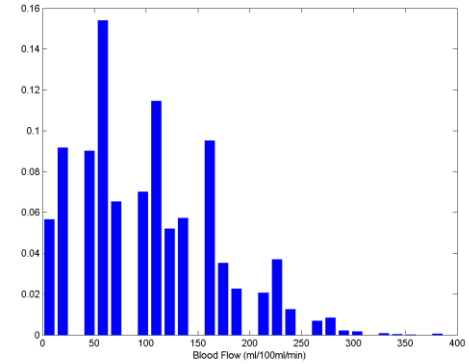

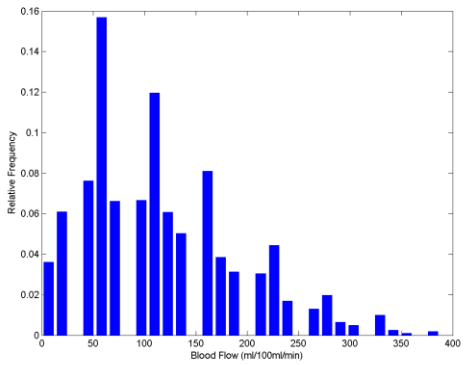

ST1006

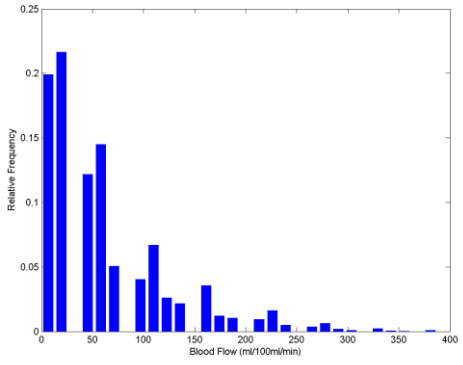

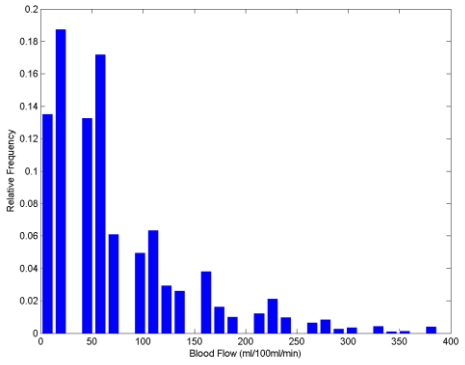

ST1008

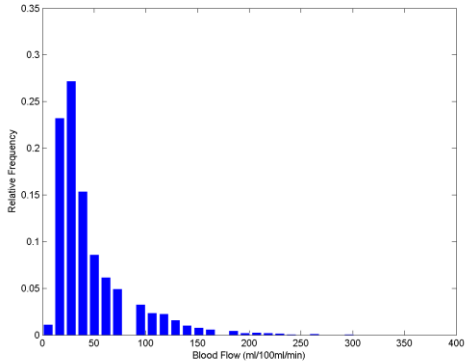

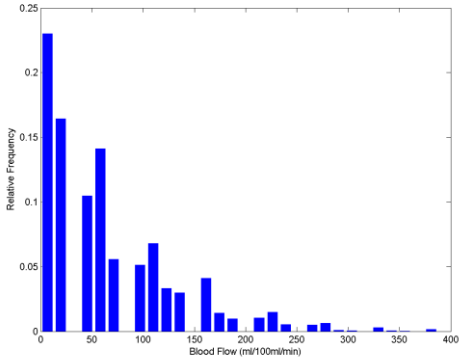

ST1009

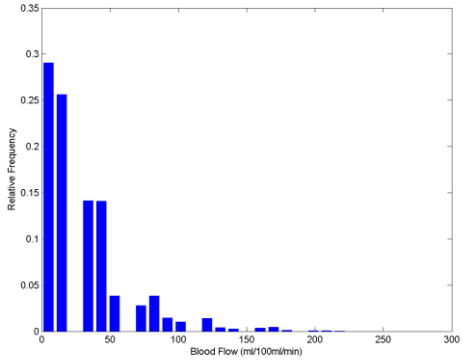

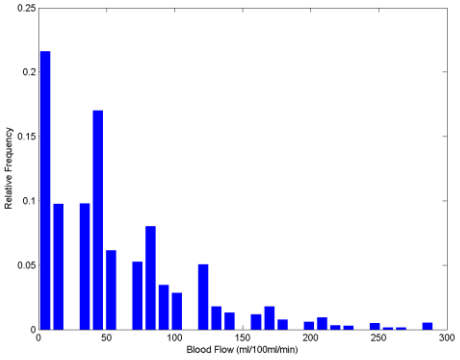

ST1010

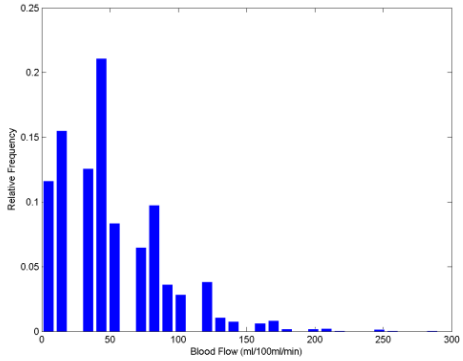

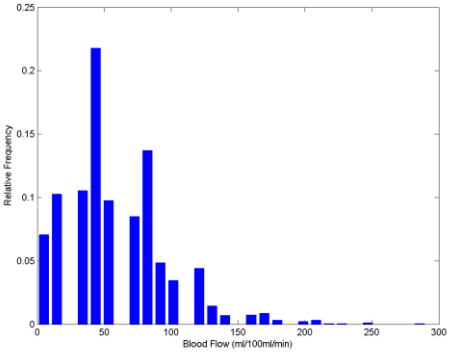

Blood Volume

After 7 days Nelfinavir

After 14 days Nelfinavir + RT

ST1001

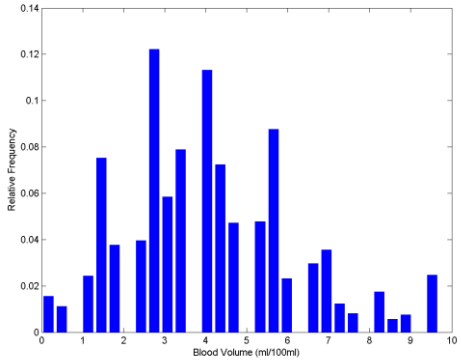

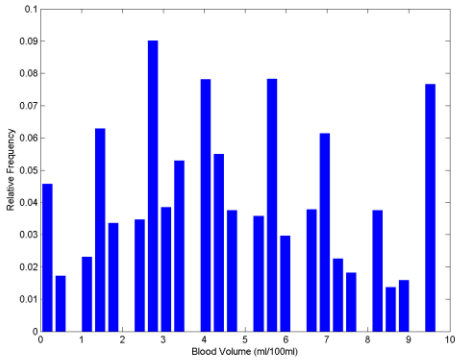

ST1002

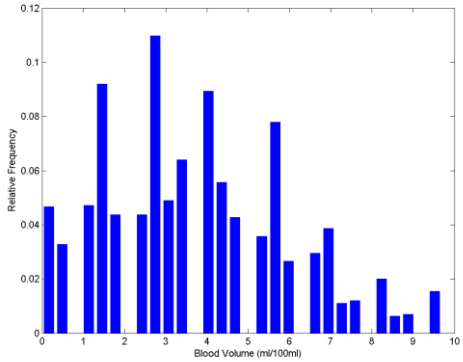

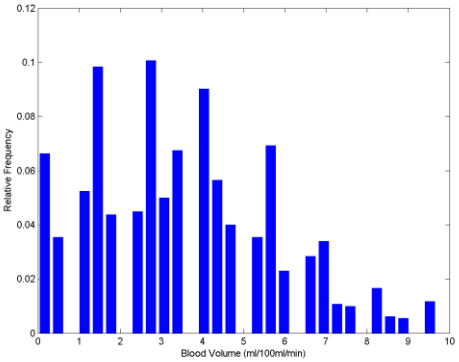

ST1003

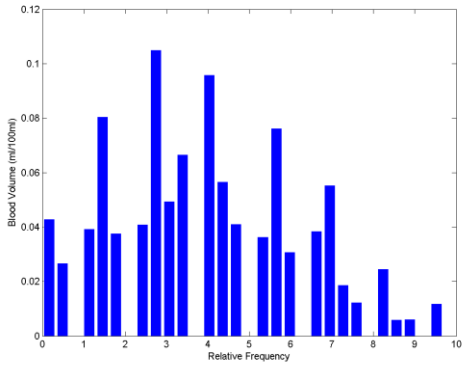

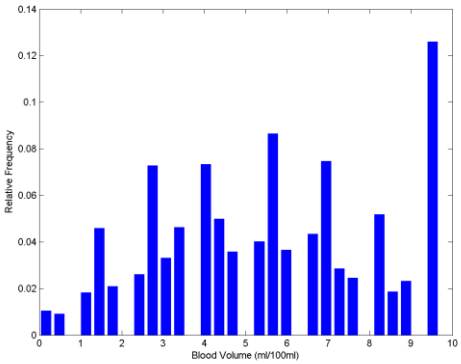

ST1004

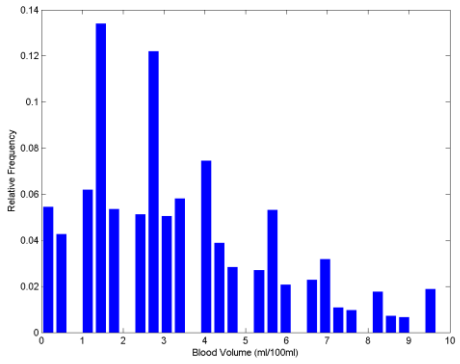

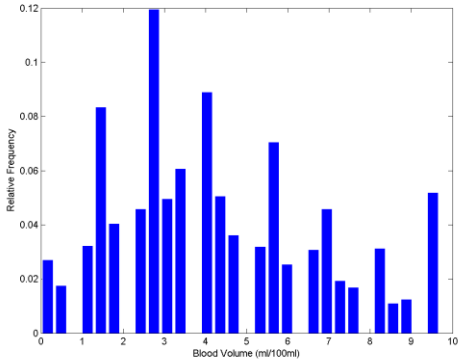

ST1005

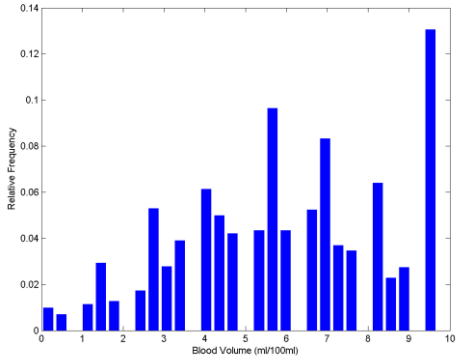

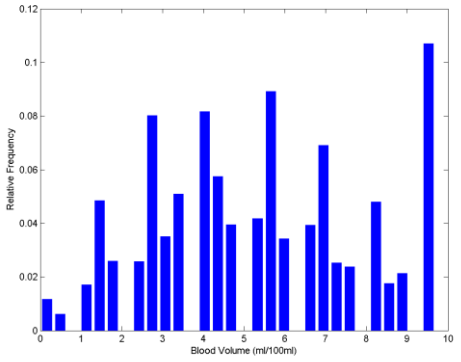

ST1006

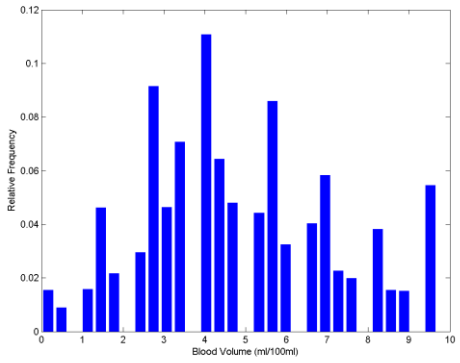

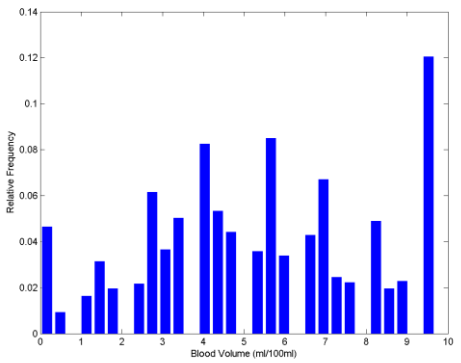

ST1008

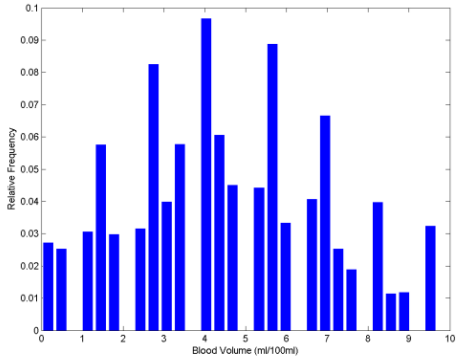

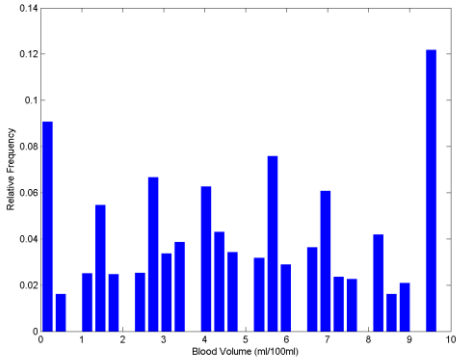

ST1009

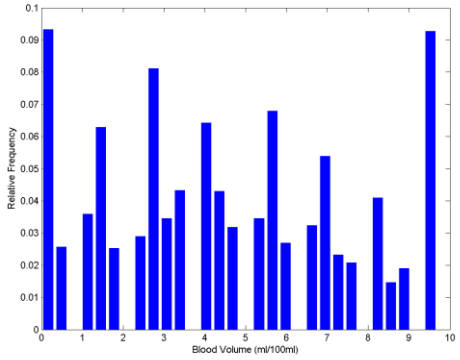

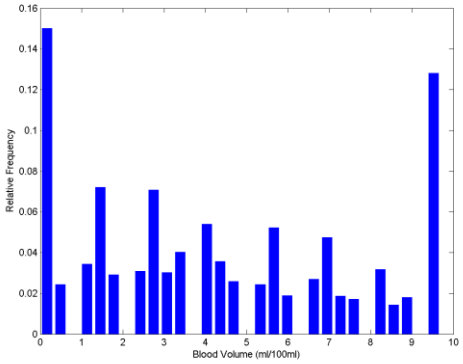

ST1010

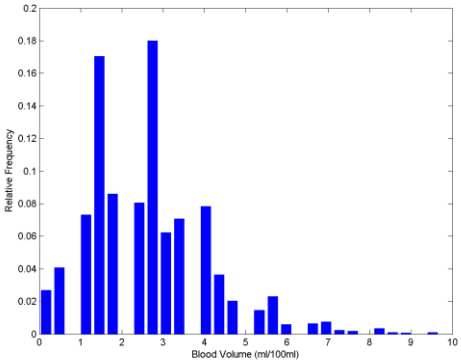

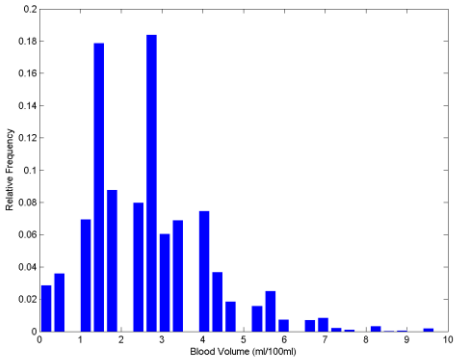

Mean Transit Time

After 7 days of Nelfinavir

After 14 days of Nelfinavir

ST1001

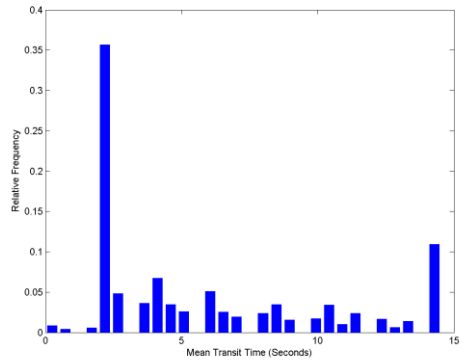

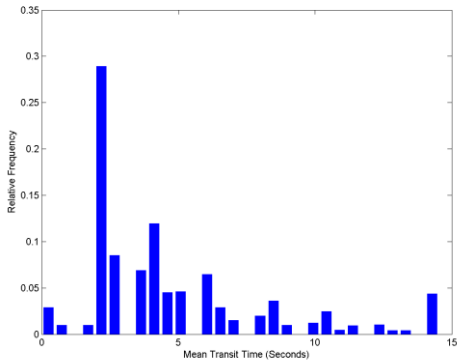

ST1002

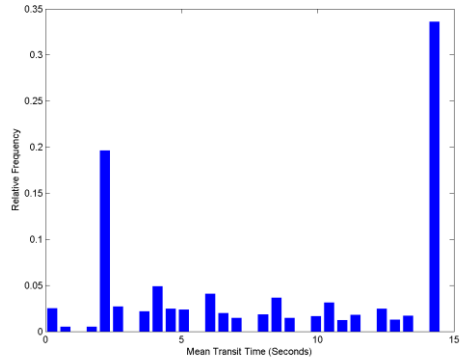

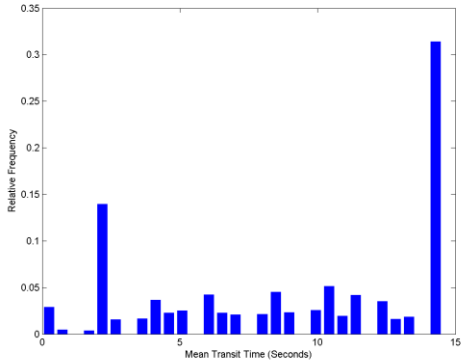

ST1003

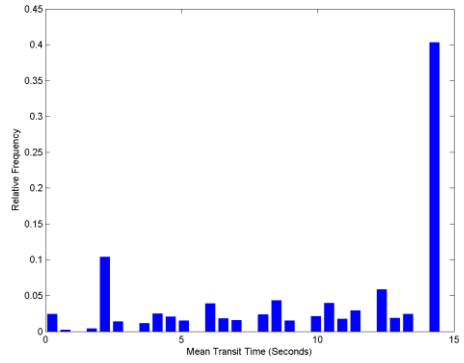

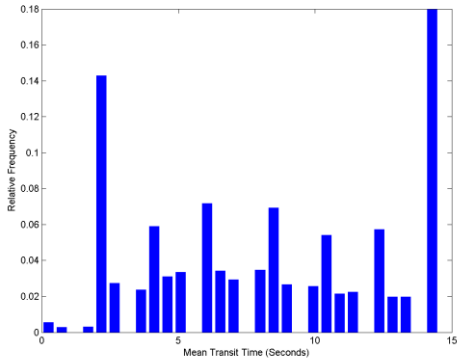

ST1004

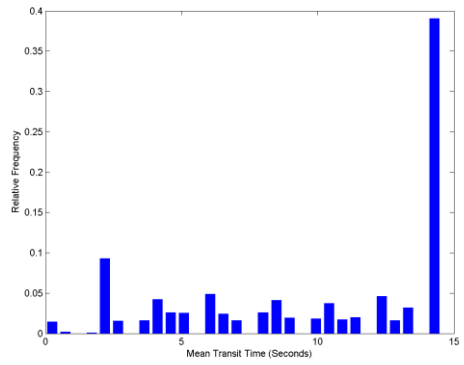

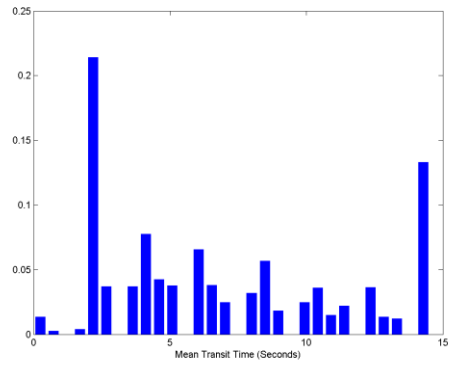

ST1005

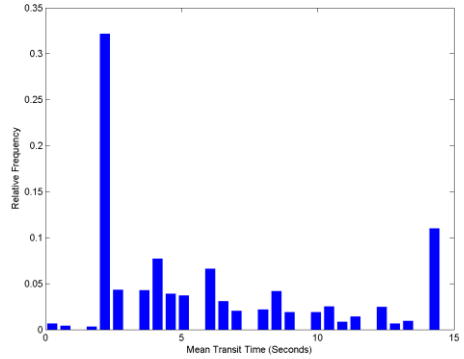

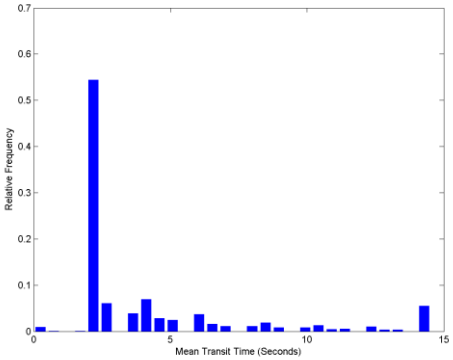

ST1006

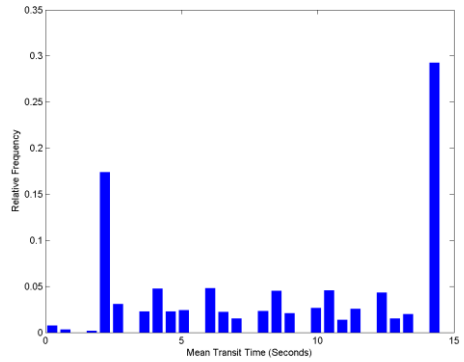

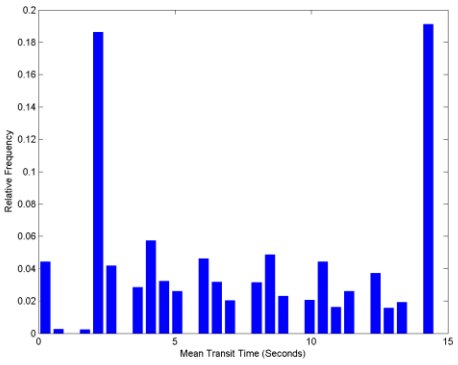

ST1008

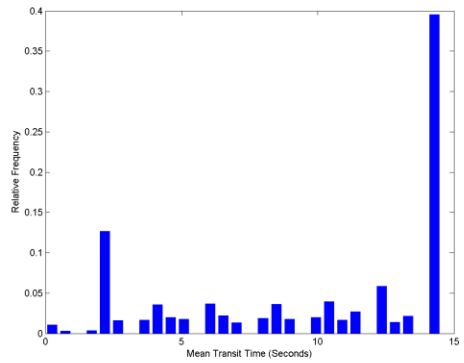

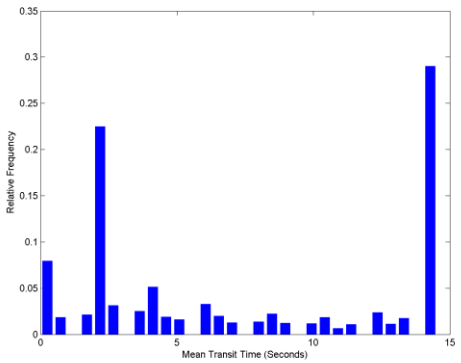

ST1009

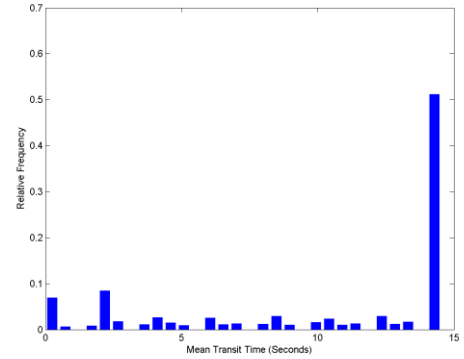

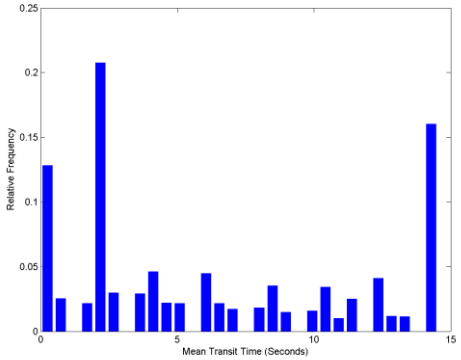

ST1010

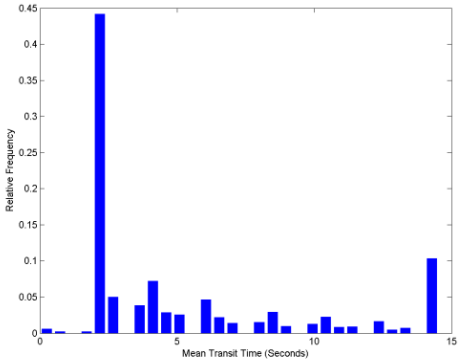

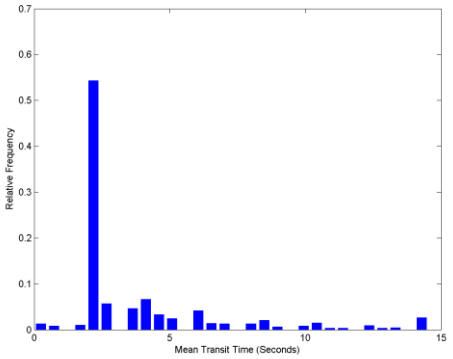

APPENDIX 2: Dce-MRI histograms for individual trial participants

K^{trans}

ST1001

Scan 1 **Scan 2** **Scan 3**

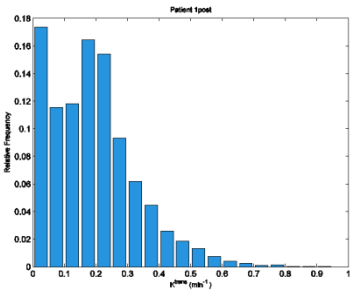

ST1002

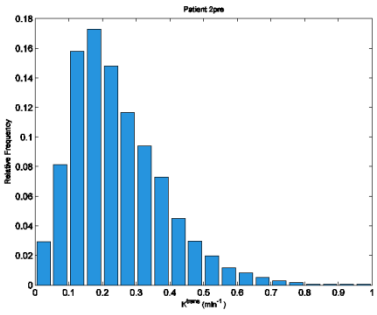

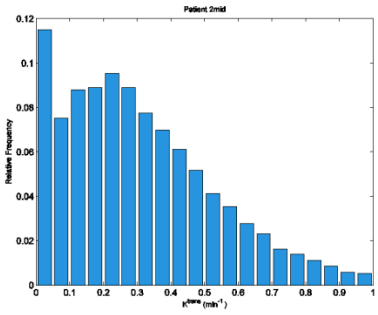

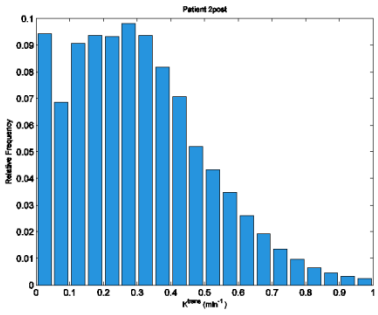

ST1003

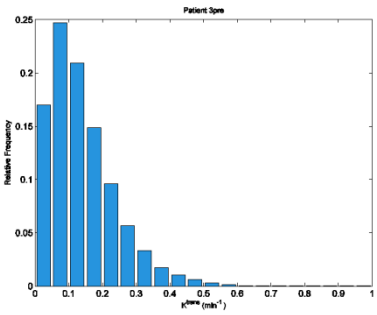

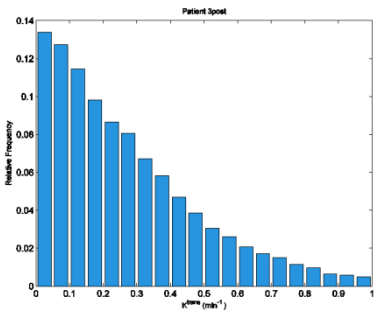

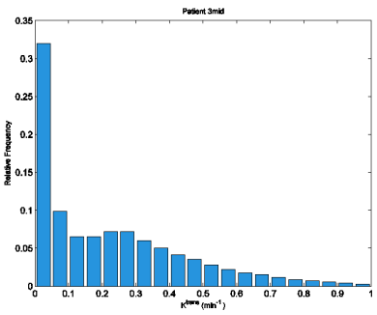

ST1004

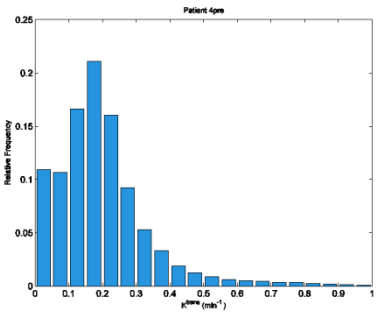

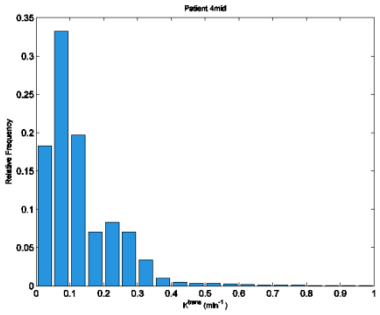

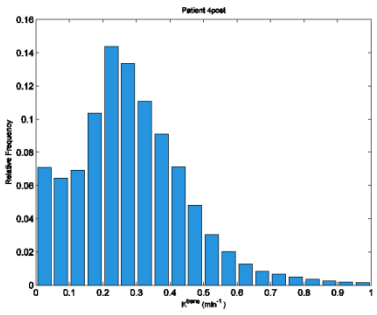

ST1005

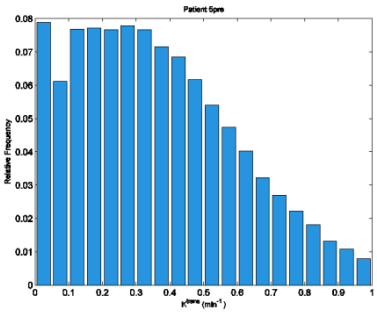

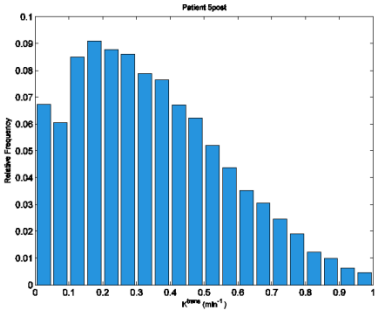

ST1006

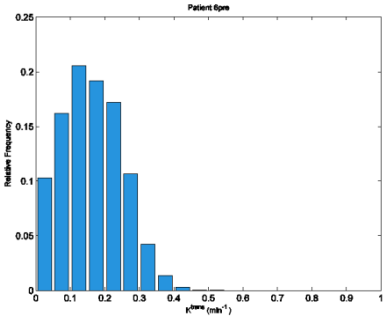

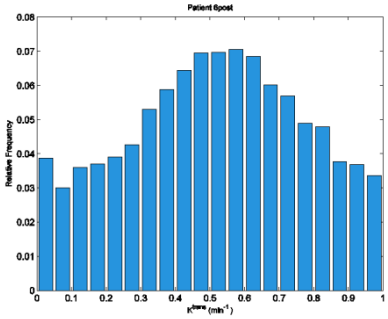

ST1007

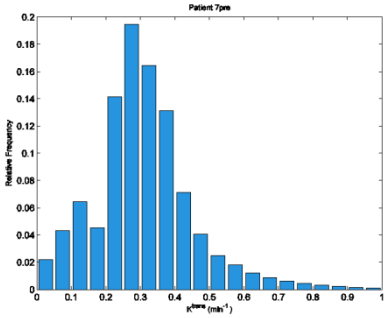

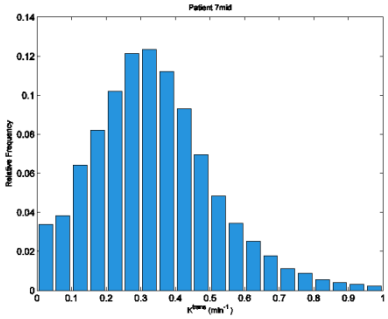

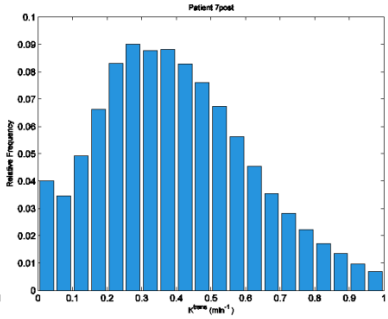

ST1008

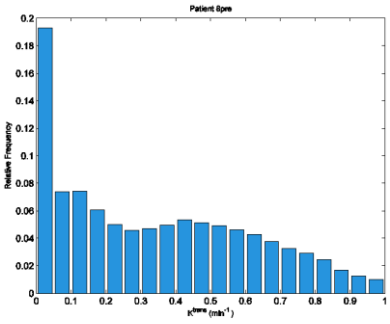

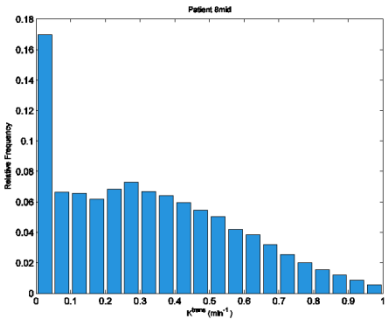

ST1009

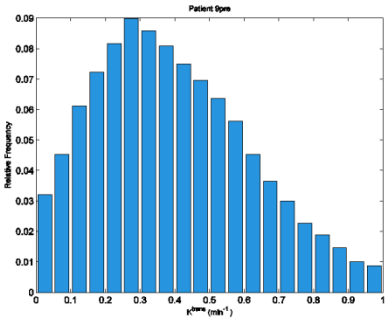

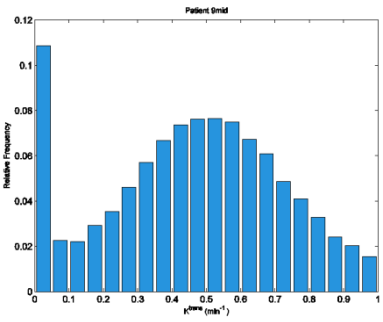

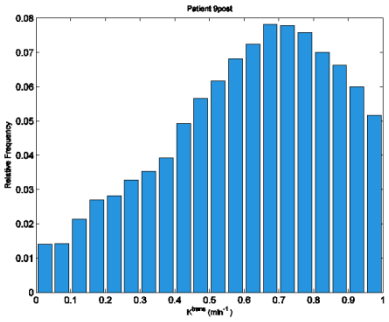

ST1010

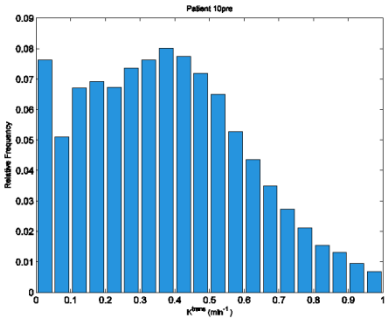

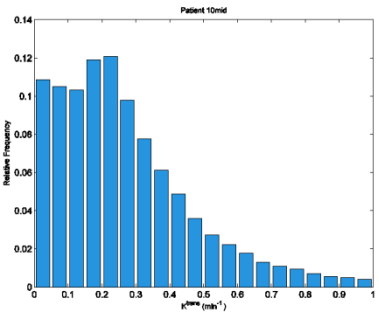

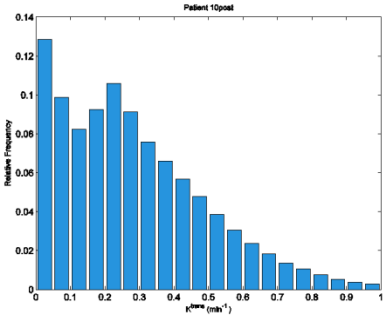

Kep

Scan 1 **Scan 2** **Scan 3**

ST1001

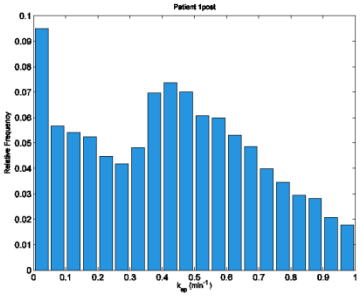

ST1002

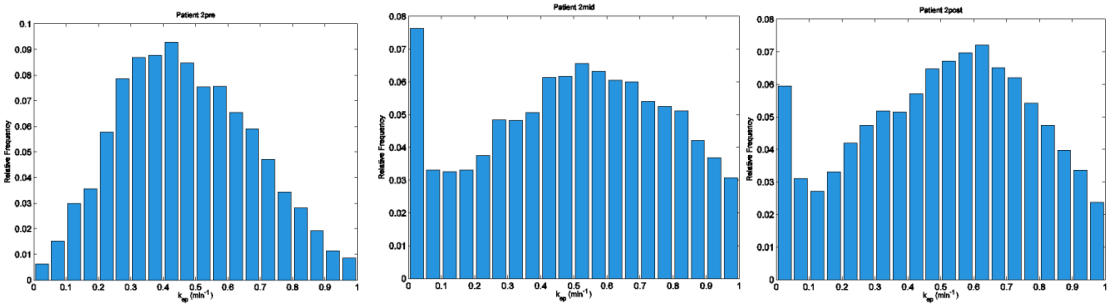

ST1003

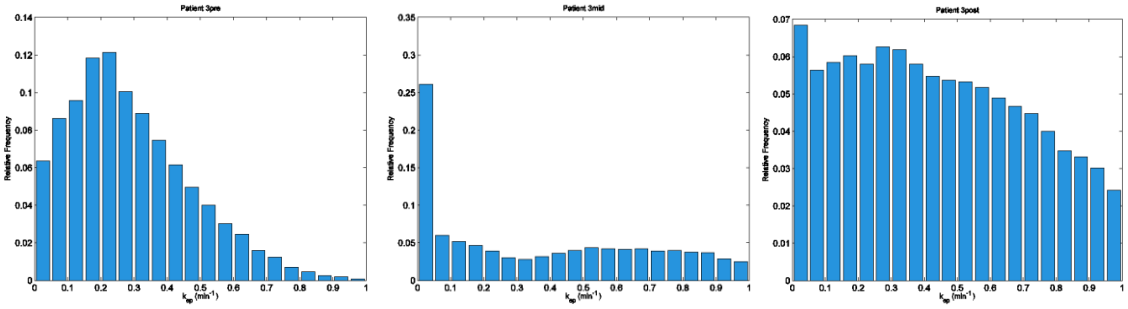

ST1004

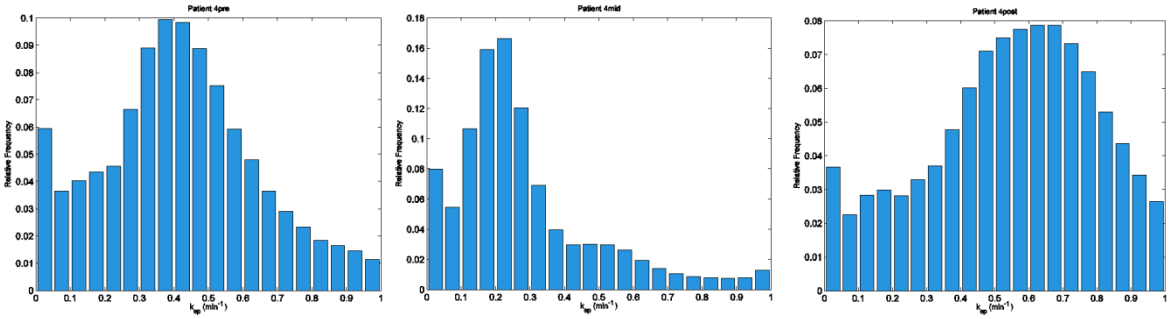

ST1005

ST1006

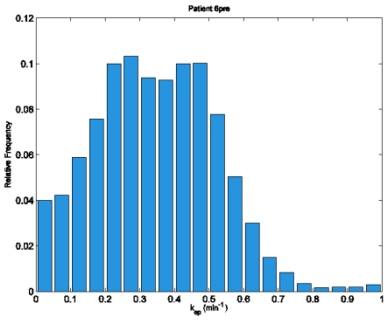

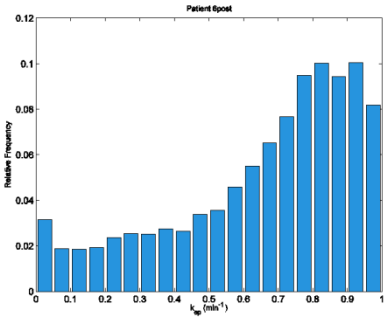

ST1007

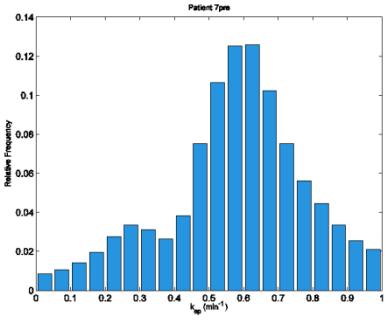

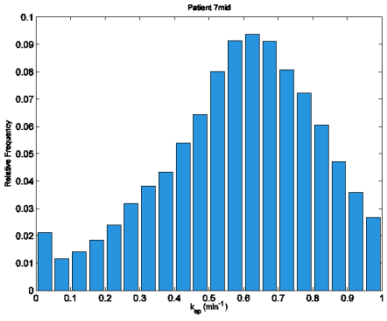

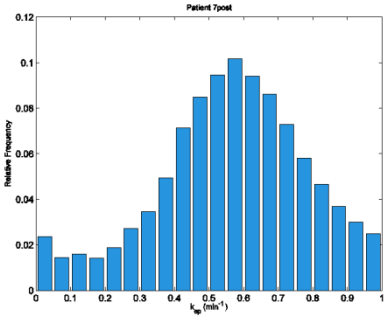

ST1008

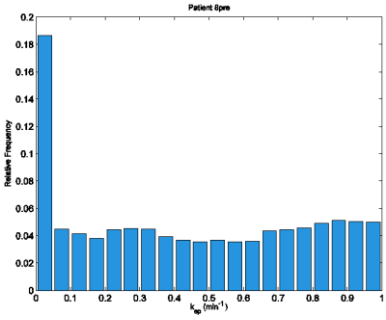

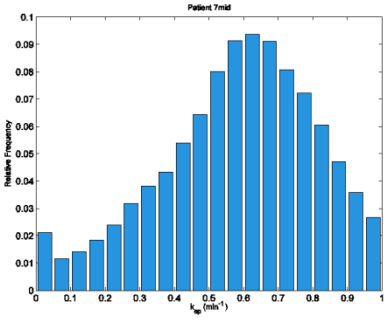

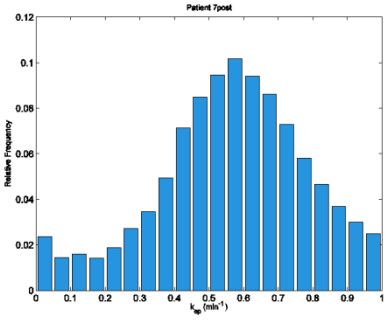

ST1009

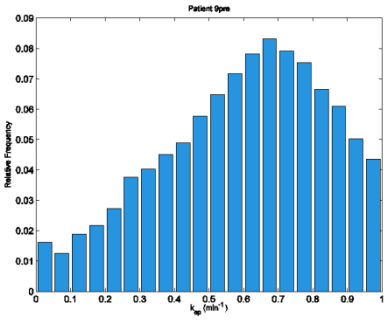

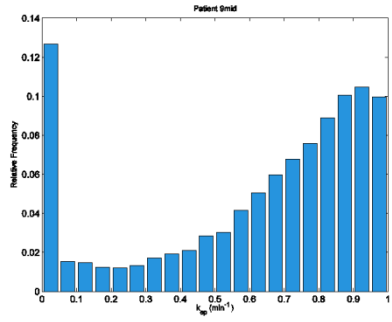

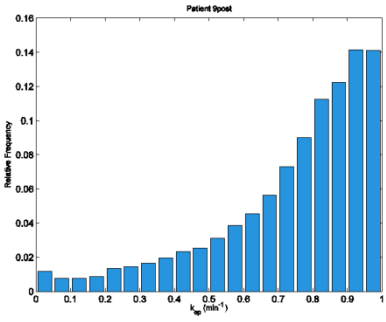

ST1010

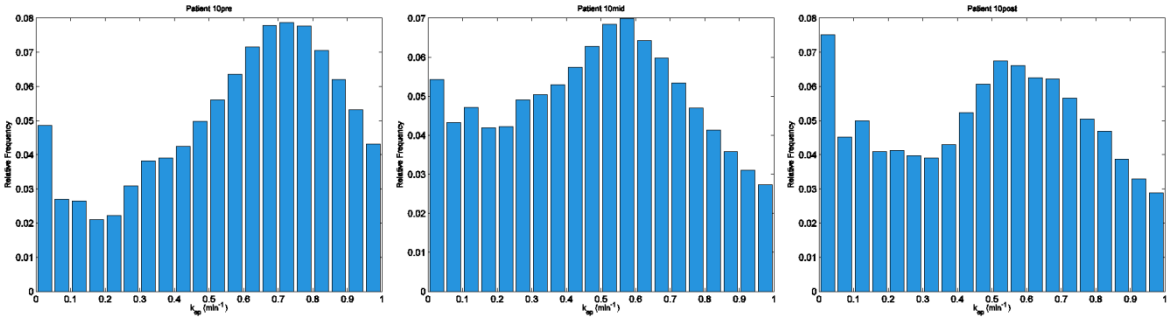

V_e

Scan 1 **Scan 2** **Scan 3**

ST1001

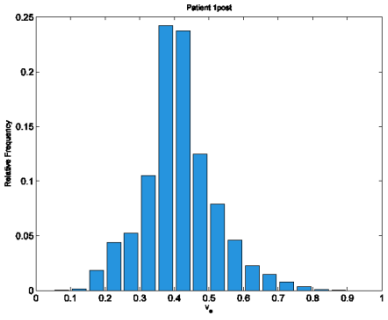

ST1002

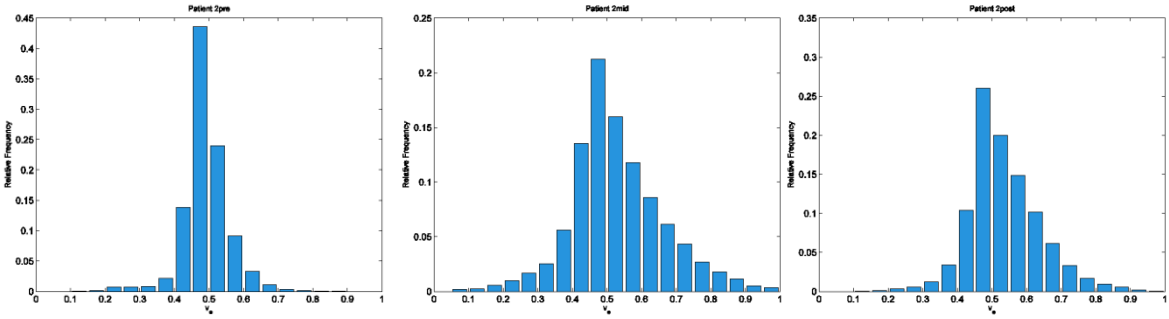

ST1003

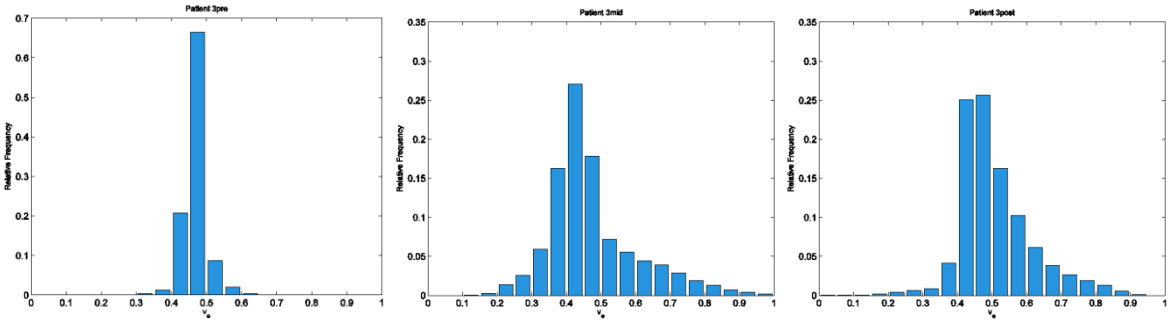

ST1004

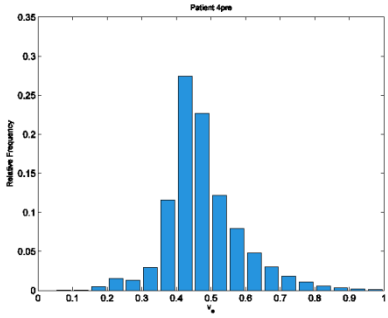

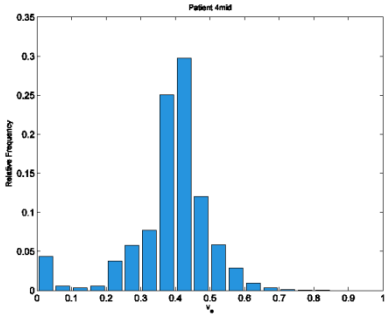

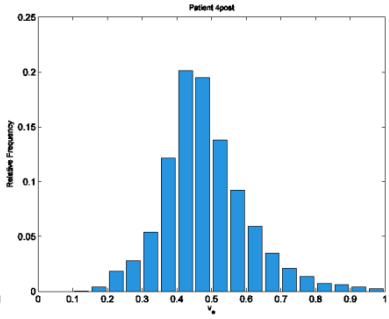

ST1005

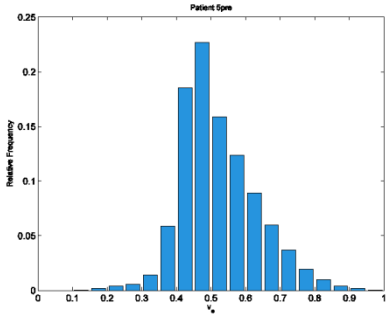

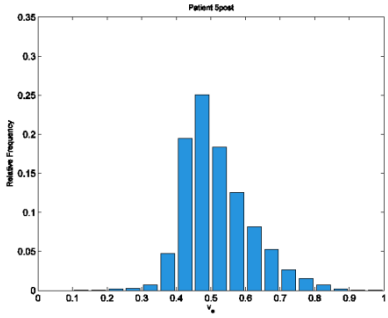

ST1006

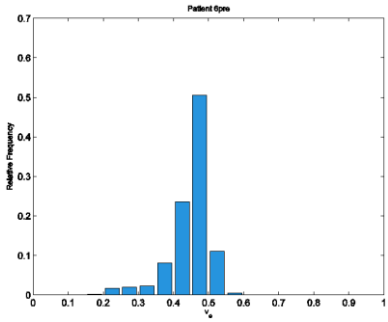

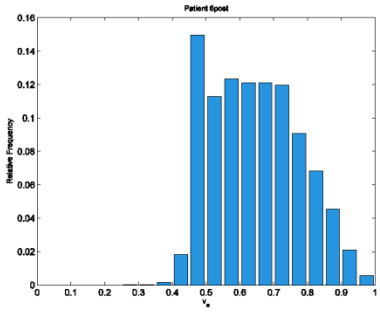

ST1007

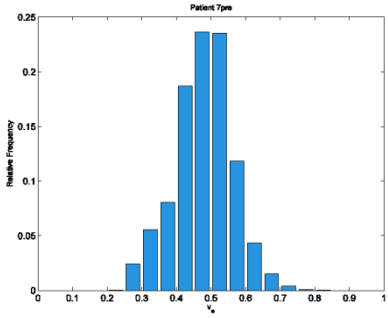

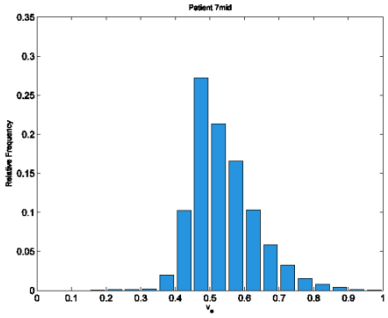

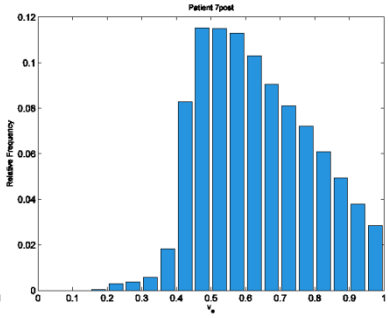

ST1008

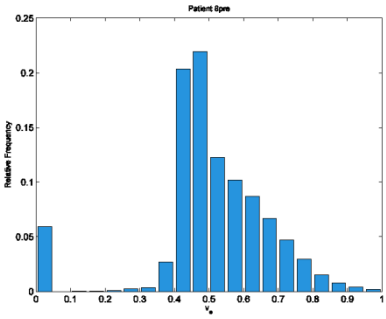

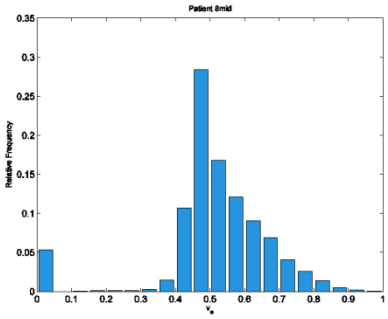

ST1009

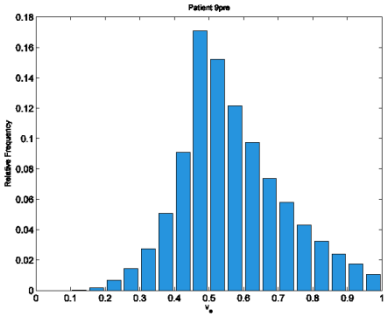

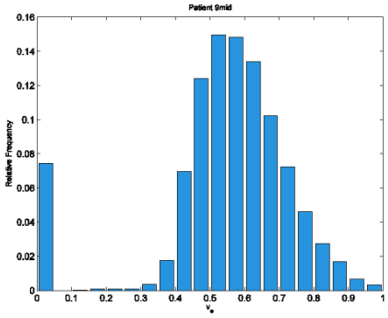

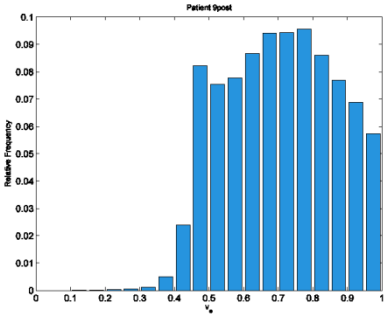

ST1010

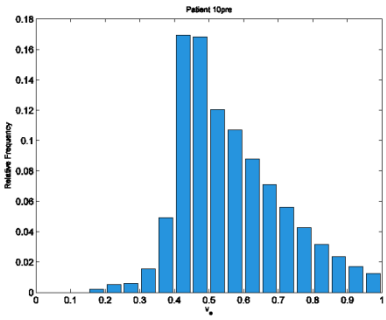

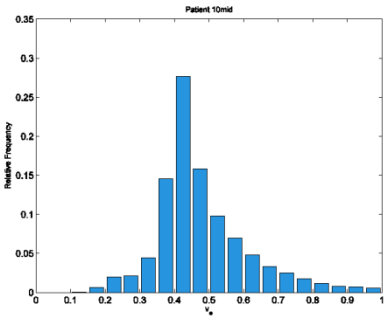

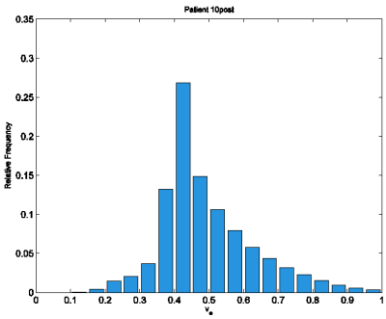

Bibliography

1. Edge, S., Byrd, DR, Compton CC et al., ed. *AJCC Cancer Staging Manual*. 7th Edition ed. 2010, Springer: New York.
2. O'Connell, J.B., M.A. Maggard, and C.Y. Ko, *Colon cancer survival rates with the new American Joint Committee on Cancer sixth edition staging.* J Natl Cancer Inst, 2004. 96(19): p. 1420-5.
3. Chapuis, P.H., et al., *A multivariate analysis of clinical and pathological variables in prognosis after resection of large bowel cancer.* Br J Surg, 1985. 72(9): p. 698-702.
4. Tominaga, T., et al., *Prognostic factors for patients with colon or rectal carcinoma treated with resection only. Five-year follow-up report.* Cancer, 1996. 78(3): p. 403-8.
5. Shepherd, N.A., K.J. Baxter, and S.B. Love, *The prognostic importance of peritoneal involvement in colonic cancer: a prospective evaluation.* Gastroenterology, 1997. 112(4): p. 1096-102.
6. Wolmark, N., B. Fisher, and H.S. Wieand, *The prognostic value of the modifications of the Dukes' C class of colorectal cancer. An analysis of the NSABP clinical trials.* Ann Surg, 1986. 203(2): p. 115-22.
7. Greene, F.L., A.K. Stewart, and H.J. Norton, *A new TNM staging strategy for node-positive (stage III) colon cancer: an analysis of 50,042 patients.* Ann Surg, 2002. 236(4): p. 416-21; discussion 421.
8. Stangl, R., et al., *Factors influencing the natural history of colorectal liver metastases.* Lancet, 1994. 343(8910): p. 1405-10.
9. Maughan, T.S., et al., *Addition of cetuximab to oxaliplatin-based first-line combination chemotherapy for treatment of advanced colorectal cancer: results of the randomised phase 3 MRC COIN trial.* Lancet, 2011. 377(9783): p. 2103-14.
10. Abdalla, E.K., et al., *Recurrence and outcomes following hepatic resection, radiofrequency ablation, and combined resection/ablation for colorectal liver metastases.* Ann Surg, 2004. 239(6): p. 818-25; discussion 825-7.
11. Hughes, K.S., et al., *Resection of the liver for colorectal carcinoma metastases: a multi-institutional study of patterns of recurrence.* Surgery, 1986. 100(2): p. 278-84.
12. Jamison, R.L., et al., *Hepatic resection for metastatic colorectal cancer results in cure for some patients.* Arch Surg, 1997. 132(5): p. 505-10; discussion 511.
13. Fong, Y., et al., *Clinical score for predicting recurrence after hepatic resection for metastatic colorectal cancer: analysis of 1001 consecutive cases.* Ann Surg, 1999. 230(3): p. 309-18; discussion 318-21.
14. Wei, A.C., et al., *Survival after hepatic resection for colorectal metastases: a 10-year experience.* Ann Surg Oncol, 2006. 13(5): p. 668-76.
15. Rees, M., et al., *Evaluation of long-term survival after hepatic resection for metastatic colorectal cancer: a multifactorial model of 929 patients.* Ann Surg, 2008. 247(1): p. 125-35.
16. de Jong, M.C., et al., *Rates and patterns of recurrence following curative intent surgery for colorectal liver metastasis: an international multi-institutional analysis of 1669 patients.* Ann Surg, 2009. 250(3): p. 440-8.
17. Simmonds, P.C., et al., *Surgical resection of hepatic metastases from colorectal cancer: a systematic review of published studies.* Br J Cancer, 2006. 94(7): p. 982-99.
18. Nordlinger, B., et al., *Surgical resection of colorectal carcinoma metastases to the liver. A prognostic scoring system to improve case selection, based on 1568 patients. Association Francaise de Chirurgie.* Cancer, 1996. 77(7): p. 1254-62.

19. Scheele, J., et al., *Resection of colorectal liver metastases.* World J Surg, 1995. 19(1): p. 59-71.
20. Nordlinger, B., et al., *Does chemotherapy prior to liver resection increase the potential for cure in patients with metastatic colorectal cancer? A report from the European Colorectal Metastases Treatment Group.* Eur J Cancer, 2007. 43(14): p. 2037-45.
21. Weiss, L., et al., *Haematogenous metastatic patterns in colonic carcinoma: an analysis of 1541 necropsies.* J Pathol, 1986. 150(3): p. 195-203.
22. Sugarbaker, P.H., *Surgical decision making for large bowel cancer metastatic to the liver.* Radiology, 1990. 174(3 Pt 1): p. 621-6.
23. Penna, C. and B. Nordlinger, *Surgery of liver metastases from colorectal cancer: new promises.* Br Med Bull, 2002. 64: p. 127-40.
24. *Adjuvant radiotherapy for rectal cancer: a systematic overview of 8,507 patients from 22 randomised trials.* Lancet, 2001. 358(9290): p. 1291-304.
25. Camma, C., et al., *Preoperative radiotherapy for resectable rectal cancer: A meta-analysis.* JAMA, 2000. 284(8): p. 1008-15.
26. Marijnen, C.A., et al., *Acute side effects and complications after short-term preoperative radiotherapy combined with total mesorectal excision in primary rectal cancer: report of a multicenter randomized trial.* J Clin Oncol, 2002. 20(3): p. 817-25.
27. Kapiteijn, E., et al., *Preoperative radiotherapy combined with total mesorectal excision for resectable rectal cancer.* N Engl J Med, 2001. 345(9): p. 638-46.
28. Sebag-Montefiore, D., et al., *Preoperative radiotherapy versus selective postoperative chemoradiotherapy in patients with rectal cancer (MRC CR07 and NCIC-CTG C016): a multicentre, randomised trial.* Lancet, 2009. 373(9666): p. 811-20.
29. Vironen, J., et al., *Tumour regression grading in the evaluation of tumour response after different preoperative radiotherapy treatments for rectal carcinoma.* Int J Colorectal Dis, 2005. 20(5): p. 440-5.
30. Theodoropoulos, G., et al., *T-level downstaging and complete pathologic response after preoperative chemoradiation for advanced rectal cancer result in decreased recurrence and improved disease-free survival.* Dis Colon Rectum, 2002. 45(7): p. 895-903.
31. Bouzourene, H., et al., *Importance of tumor regression assessment in predicting the outcome in patients with locally advanced rectal carcinoma who are treated with preoperative radiotherapy.* Cancer, 2002. 94(4): p. 1121-30.
32. Glimelius, B. and U. Isacsson, *Preoperative radiotherapy for rectal cancer--is 5 x 5 Gy a good or a bad schedule?* Acta Oncol, 2001. 40(8): p. 958-67.
33. Hatfield, P., et al., *Short-course radiotherapy, with elective delay prior to surgery, in patients with unresectable rectal cancer who have poor performance status or significant co-morbidity.* Radiother Oncol, 2009. 92(2): p. 210-4.
34. Radu, C., et al., *Short-course preoperative radiotherapy with delayed surgery in rectal cancer - a retrospective study.* Radiother Oncol, 2008. 87(3): p. 343-9.
35. Peeters, K.C., et al., *Late side effects of short-course preoperative radiotherapy combined with total mesorectal excision for rectal cancer: increased bowel dysfunction in irradiated patients--a Dutch colorectal cancer group study.* J Clin Oncol, 2005. 23(25): p. 6199-206.
36. Lange, M.M., et al., *Risk factors for faecal incontinence after rectal cancer treatment.* Br J Surg, 2007. 94(10): p. 1278-84.
37. *NICE Clinical Guideline 131: The diagnosis and management of colorectal cancer*. 2014 [cited 2014 18/12/2014]; Available from: guidance.nice.org.uk/cg131.
38. Siriwardena, A.K., et al., *Management of colorectal cancer presenting with synchronous liver metastases.* Nat Rev Clin Oncol, 2014. 11(8): p. 446-59.

39. **Schrag, D., et al.,** ***Neoadjuvant chemotherapy without routine use of radiation therapy for patients with locally advanced rectal cancer: a pilot trial.*** **J Clin Oncol, 2014. 32(6): p. 513-8.**
40. **van Dijk, T.H., et al.,** ***Evaluation of short-course radiotherapy followed by neoadjuvant bevacizumab, capecitabine, and oxaliplatin and subsequent radical surgical treatment in primary stage IV rectal cancer.*** **Ann Oncol, 2013. 24(7): p. 1762-9.**
41. ***Modulation of fluorouracil by leucovorin in patients with advanced colorectal cancer: evidence in terms of response rate. Advanced Colorectal Cancer Meta-Analysis Project.*** **J Clin Oncol, 1992. 10(6): p. 896-903.**
42. **Machover, D.,** ***A comprehensive review of 5-fluorouracil and leucovorin in patients with metastatic colorectal carcinoma.*** **Cancer, 1997. 80(7): p. 1179-87.**
43. **de Gramont, A., et al.,** ***Randomized trial comparing monthly low-dose leucovorin and fluorouracil bolus with bimonthly high-dose leucovorin and fluorouracil bolus plus continuous infusion for advanced colorectal cancer: a French intergroup study.*** **J Clin Oncol, 1997. 15(2): p. 808-15.**
44. **Hill, E.J., et al.,** ***Oxaliplatin as a radiosensitiser for upper and lower gastrointestinal tract malignancies: what have we learned from a decade of translational research?*** **Crit Rev Oncol Hematol, 2012. 83(3): p. 353-87.**
45. **de Gramont, A., et al.,** ***Leucovorin and fluorouracil with or without oxaliplatin as first-line treatment in advanced colorectal cancer.*** **J Clin Oncol, 2000. 18(16): p. 2938-47.**
46. **Saltz, L.B., et al.,** ***Irinotecan plus Fluorouracil and Leucovorin for Metastatic Colorectal Cancer.*** **New England Journal of Medicine, 2000. 343(13): p. 905-914.**
47. **Douillard, J.Y., et al.,** ***Irinotecan combined with fluorouracil compared with fluorouracil alone as first-line treatment for metastatic colorectal cancer: a multicentre randomised trial.*** **Lancet, 2000. 355(9209): p. 1041-7.**
48. **Louvet, C. and A. de Gramont,** ***Colorectal cancer: integrating oxaliplatin.*** **Curr Treat Options Oncol, 2003. 4(5): p. 405-11.**
49. **Ychou, M., et al.,** ***Tritherapy with fluorouracil/leucovorin, irinotecan and oxaliplatin (FOLFIRINOX): a phase II study in colorectal cancer patients with non-resectable liver metastases.*** **Cancer Chemother Pharmacol, 2008. 62(2): p. 195-201.**
50. **Masi, G., et al.,** ***Long-term outcome of initially unresectable metastatic colorectal cancer patients treated with 5-fluorouracil/leucovorin, oxaliplatin, and irinotecan (FOLFOXIRI) followed by radical surgery of metastases.*** **Ann Surg, 2009. 249(3): p. 420-5.**
51. **Bismuth, H. and R. Adam,** ***Reduction of nonresectable liver metastasis from colorectal cancer after oxaliplatin chemotherapy.*** **Semin Oncol, 1998. 25(2 Suppl 5): p. 40-6.**
52. **Adam, R., et al.,** ***Five-year survival following hepatic resection after neoadjuvant therapy for nonresectable colorectal.*** **Ann Surg Oncol, 2001. 8(4): p. 347-53.**
53. **Wein, A., et al.,** ***Impact of surgery on survival in palliative patients with metastatic colorectal cancer after first line treatment with weekly 24-hour infusion of high-dose 5-fluorouracil and folinic acid.*** **Ann Oncol, 2001. 12(12): p. 1721-7.**
54. **Alberts, S.R., et al.,** ***Oxaliplatin, fluorouracil, and leucovorin for patients with unresectable liver-only metastases from colorectal cancer: a North Central Cancer Treatment Group phase II study.*** **J Clin Oncol, 2005. 23(36): p. 9243-9.**
55. **Barone, C., et al.,** ***Final analysis of colorectal cancer patients treated with irinotecan and 5-fluorouracil plus folinic acid neoadjuvant chemotherapy for unresectable liver metastases.*** **Br J Cancer, 2007. 97(8): p. 1035-9.**
56. **Tournigand, C., et al.,** ***FOLFIRI followed by FOLFOX6 or the reverse sequence in advanced colorectal cancer: a randomized GERCOR study.*** **J Clin Oncol, 2004. 22(2): p. 229-37.**
57. **Folprecht, G., et al.,** ***Neoadjuvant treatment of unresectable colorectal liver metastases: correlation between tumour response and resection rates.*** **Ann Oncol, 2005. 16(8): p. 1311-9.**

58. *NICE Technology Guidance 176: Cetuximab for the first line treatment of metastatic colorectal cancer*. Available from: guidance.nice.org.uk/ta176.
59. Tveit, K.M., et al., *Phase III trial of cetuximab with continuous or intermittent fluorouracil, leucovorin, and oxaliplatin (Nordic FLOX) versus FLOX alone in first-line treatment of metastatic colorectal cancer: the NORDIC-VII study.* J Clin Oncol, 2012. 30(15): p. 1755-62.
60. Saltz, L.B., et al., *Bevacizumab in combination with oxaliplatin-based chemotherapy as first-line therapy in metastatic colorectal cancer: a randomized phase III study.* J Clin Oncol, 2008. 26(12): p. 2013-9.
61. Hurwitz, H., et al., *Bevacizumab plus irinotecan, fluorouracil, and leucovorin for metastatic colorectal cancer.* N Engl J Med, 2004. 350(23): p. 2335-42.
62. Ye, L.C., et al., *Randomized controlled trial of cetuximab plus chemotherapy for patients with KRAS wild-type unresectable colorectal liver-limited metastases.* J Clin Oncol, 2013. 31(16): p. 1931-8.
63. Van Cutsem, E., et al., *Cetuximab and chemotherapy as initial treatment for metastatic colorectal cancer.* N Engl J Med, 2009. 360(14): p. 1408-17.
64. Bokemeyer, C., et al., *Fluorouracil, leucovorin, and oxaliplatin with and without cetuximab in the first-line treatment of metastatic colorectal cancer.* J Clin Oncol, 2009. 27(5): p. 663-71.
65. Fernandez, F.G., et al., *Effect of steatohepatitis associated with irinotecan or oxaliplatin pretreatment on resectability of hepatic colorectal metastases.* J Am Coll Surg, 2005. 200(6): p. 845-53.
66. Rubbia-Brandt, L., et al., *Severe hepatic sinusoidal obstruction associated with oxaliplatin-based chemotherapy in patients with metastatic colorectal cancer.* Ann Oncol, 2004. 15(3): p. 460-6.
67. Vauthey, J.N., et al., *Chemotherapy regimen predicts steatohepatitis and an increase in 90-day mortality after surgery for hepatic colorectal metastases.* J Clin Oncol, 2006. 24(13): p. 2065-72.
68. Pawlik, T.M., et al., *Preoperative chemotherapy for colorectal liver metastases: impact on hepatic histology and postoperative outcome.* J Gastrointest Surg, 2007. 11(7): p. 860-8.
69. Nagorney, D.M. and J.F. Gigot, *Primary epithelial hepatic malignancies: etiology, epidemiology, and outcome after subtotal and total hepatic resection.* Surg Oncol Clin N Am, 1996. 5(2): p. 283-300.
70. Ho, S., et al., *Tumour-to-normal uptake ratio of 90Y microspheres in hepatic cancer assessed with 99Tcm macroaggregated albumin.* Br J Radiol, 1997. 70(836): p. 823-8.
71. Hill EJ, S.R., *Multi-modality therapy of hepatic metastases from colorectal carcinoma: optimal combination of systemic chemotherapy with radio-embolization.* Journal of Nuclear Medicine & Radiation Therapy, 2011. 2(108).
72. Seidensticker, R., et al., *Matched-pair comparison of radioembolization plus best supportive care versus best supportive care alone for chemotherapy refractory liver-dominant colorectal metastases.* Cardiovasc Intervent Radiol, 2011. 35(5): p. 1066-73.
73. Cosimelli, M., et al., *Multi-centre phase II clinical trial of yttrium-90 resin microspheres alone in unresectable, chemotherapy refractory colorectal liver metastases.* Br J Cancer, 2010. 103(3): p. 324-31.
74. Bester, L., et al., *Radioembolisation with Yttrium-90 microspheres: an effective treatment modality for unresectable liver metastases.* J Med Imaging Radiat Oncol, 2013. 57(1): p. 72-80.
75. Sofocleous, C.T., et al., *Phase I trial of selective internal radiation therapy for chemorefractory colorectal cancer liver metastases progressing after hepatic arterial pump and systemic chemotherapy.* Clin Colorectal Cancer, 2013. 13(1): p. 27-36.

76. **Kennedy, A.S., et al.,** ***Resin 90Y-microsphere brachytherapy for unresectable colorectal liver metastases: modern USA experience.*** **Int J Radiat Oncol Biol Phys, 2006. 65(2): p. 412-25.**
77. **Nace, G.W., et al.,** ***Yttrium-90 radioembolization for colorectal cancer liver metastases: a single institution experience.*** **Int J Surg Oncol. 2011: p. 571261.**
78. **Cianni, R., et al.,** ***Selective internal radiation therapy with SIR-spheres for the treatment of unresectable colorectal hepatic metastases.*** **Cardiovasc Intervent Radiol, 2009. 32(6): p. 1179-86.**
79. **Jakobs, T.F., et al.,** ***Hepatic yttrium-90 radioembolization of chemotherapy-refractory colorectal cancer liver metastases.*** **J Vasc Interv Radiol, 2008. 19(8): p. 1187-95.**
80. **Gray, B., et al.,** ***Randomised trial of SIR-Spheres plus chemotherapy vs. chemotherapy alone for treating patients with liver metastases from primary large bowel cancer.*** **Ann Oncol, 2001. 12(12): p. 1711-20.**
81. **Van Hazel, G., et al.,** ***Randomised phase 2 trial of SIR-Spheres plus fluorouracil/leucovorin chemotherapy versus fluorouracil/leucovorin chemotherapy alone in advanced colorectal cancer.*** **J Surg Oncol, 2004. 88(2): p. 78-85.**
82. **Sharma, R.A., et al.,** ***Radioembolization of liver metastases from colorectal cancer using yttrium-90 microspheres with concomitant systemic oxaliplatin, fluorouracil, and leucovorin chemotherapy.*** **J Clin Oncol, 2007. 25(9): p. 1099-106.**
83. **Lim, L., et al.,** ***A prospective evaluation of treatment with Selective Internal Radiation Therapy (SIR-spheres) in patients with unresectable liver metastases from colorectal cancer previously treated with 5-FU based chemotherapy.*** **BMC Cancer, 2005. 5: p. 132.**
84. **van Hazel, G.A., et al.,** ***Treatment of fluorouracil-refractory patients with liver metastases from colorectal cancer by using yttrium-90 resin microspheres plus concomitant systemic irinotecan chemotherapy.*** **J Clin Oncol, 2009. 27(25): p. 4089-95.**
85. **Hendlisz, A., et al.,** ***Phase III trial comparing protracted intravenous fluorouracil infusion alone or with yttrium-90 resin microspheres radioembolization for liver-limited metastatic colorectal cancer refractory to standard chemotherapy.*** **J Clin Oncol, 2010. 28(23): p. 3687-94.**
86. **Sharma, R.A., et al.,** ***Radioembolization of Liver Metastases From Colorectal Cancer Using Yttrium-90 Microspheres With Concomitant Systemic Oxaliplatin, Fluorouracil, and Leucovorin Chemotherapy.*** **Journal of Clinical Oncology, 2007. 25(9): p. 1099-1106.**
87. **Hanahan, D. and R.A. Weinberg,** ***The hallmarks of cancer.*** **Cell, 2000. 100(1): p. 57-70.**
88. **Hanahan, D. and R.A. Weinberg,** ***Hallmarks of cancer: the next generation.*** **Cell, 2011. 144(5): p. 646-74.**
89. **Hanahan, D. and J. Folkman,** ***Patterns and emerging mechanisms of the angiogenic switch during tumorigenesis.*** **Cell, 1996. 86(3): p. 353-64.**
90. **Gillies, R.J., et al.,** ***Causes and effects of heterogeneous perfusion in tumors.*** **Neoplasia, 1999. 1(3): p. 197-207.**
91. **Vaupel, P.,** ***Tumor microenvironmental physiology and its implications for radiation oncology.*** **Semin Radiat Oncol, 2004. 14(3): p. 198-206.**
92. **Koukourakis, M.I., et al.,** ***Cancer vascularization: implications in radiotherapy?*** **Int J Radiat Oncol Biol Phys, 2000. 48(2): p. 545-53.**
93. **Vaupel, P., et al.,** ***O(2) extraction is a key parameter determining the oxygenation status of malignant tumors and normal tissues.*** **Int J Oncol, 2003. 22(4): p. 795-8.**
94. **Vaupel, P., O. Thews, and M. Hoeckel,** ***Treatment resistance of solid tumors: role of hypoxia and anemia.*** **Med Oncol, 2001. 18(4): p. 243-59.**
95. **Ljungkvist, A.S., et al.,** ***Dynamics of tumor hypoxia measured with bioreductive hypoxic cell markers.*** **Radiat Res, 2007. 167(2): p. 127-45.**
96. **Thomlinson, R.H. and L.H. Gray,** ***The histological structure of some human lung cancers and the possible implications for radiotherapy.*** **Br J Cancer, 1955. 9(4): p. 539-49.**

97. Fyles, A.W., et al., *Oxygenation predicts radiation response and survival in patients with cervix cancer.* Radiother Oncol, 1998. 48(2): p. 149-56.
98. Brizel, D.M., et al., *Oxygenation of head and neck cancer: changes during radiotherapy and impact on treatment outcome.* Radiother Oncol, 1999. 53(2): p. 113-7.
99. Milosevic, M.F., et al., *Interstitial fluid pressure in cervical carcinoma: within tumor heterogeneity, and relation to oxygen tension.* Cancer, 1998. 82(12): p. 2418-26.
100. Nordsmark, M., et al., *Prognostic value of tumor oxygenation in 397 head and neck tumors after primary radiation therapy. An international multi-center study.* Radiother Oncol, 2005. 77(1): p. 18-24.
101. Palcic, B., J.W. Brosing, and L.D. Skarsgard, *Survival measurements at low doses: oxygen enhancement ratio.* Br J Cancer, 1982. 46(6): p. 980-4.
102. Palcic, B. and L.D. Skarsgard, *Reduced oxygen enhancement ratio at low doses of ionizing radiation.* Radiat Res, 1984. 100(2): p. 328-39.
103. Graeber, T.G., et al., *Hypoxia-mediated selection of cells with diminished apoptotic potential in solid tumours.* Nature, 1996. 379(6560): p. 88-91.
104. Hockel, M., et al., *Association between tumor hypoxia and malignant progression in advanced cancer of the uterine cervix.* Cancer Res, 1996. 56(19): p. 4509-15.
105. Vaupel, P., S. Briest, and M. Hockel, *Hypoxia in breast cancer: pathogenesis, characterization and biological/therapeutic implications.* Wien Med Wochenschr, 2002. 152(13-14): p. 334-42.
106. Evans, S.M. and C.J. Koch, *Prognostic significance of tumor oxygenation in humans.* Cancer Lett, 2003. 195(1): p. 1-16.
107. Lu, X. and Y. Kang, *Hypoxia and hypoxia-inducible factors: master regulators of metastasis.* Clin Cancer Res, 2010. 16(24): p. 5928-35.
108. Roberts, D.L., et al., *Contribution of HIF-1 and drug penetrance to oxaliplatin resistance in hypoxic colorectal cancer cells.* Br J Cancer, 2009. 101(8): p. 1290-7.
109. Jain, R.K., *Normalizing tumor vasculature with anti-angiogenic therapy: A new paradigm for combination therapy.* Nat Med, 2001. 7(9): p. 987-989.
110. Van der Veldt, A.A., et al., *Rapid decrease in delivery of chemotherapy to tumors after anti-VEGF therapy: implications for scheduling of anti-angiogenic drugs.* Cancer cell, 2012. 21(1): p. 82-91.
111. Willett, C.G., et al., *Direct evidence that the VEGF-specific antibody bevacizumab has antivascular effects in human rectal cancer.* Nat Med, 2004. 10(2): p. 145-7.
112. Rini, B.I. and M.B. Atkins, *Resistance to targeted therapy in renal-cell carcinoma.* Lancet Oncol, 2009. 10(10): p. 992-1000.
113. Bergers, G. and D. Hanahan, *Modes of resistance to anti-angiogenic therapy.* Nat Rev Cancer, 2008. 8(8): p. 592-603.
114. Ebos, J.M., et al., *Accelerated metastasis after short-term treatment with a potent inhibitor of tumor angiogenesis.* Cancer cell, 2009. 15(3): p. 232-9.
115. Conley, S.J., et al., *Antiangiogenic agents increase breast cancer stem cells via the generation of tumor hypoxia.* Proc Natl Acad Sci U S A, 2012. 109(8): p. 2784-9.
116. Casanovas, O., *Cancer: Limitations of therapies exposed.* Nature. 484(7392): p. 44-46.
117. Williams, M.P. and J.E. Husband, *CT scanning in carcinoma of the rectum: a review.* Journal of the Royal Society of Medicine, 1987. 80(11): p. 701-703.
118. Sica, G.T., H. Ji, and P.R. Ros, *CT and MR imaging of hepatic metastases.* AJR Am J Roentgenol, 2000. 174(3): p. 691-8.
119. Therasse, P., et al., *New guidelines to evaluate the response to treatment in solid tumors. European Organization for Research and Treatment of Cancer, National Cancer Institute of the United States, National Cancer Institute of Canada.* J Natl Cancer Inst, 2000. 92(3): p. 205-16.

120. Eisenhauer, E.A., et al., *New response evaluation criteria in solid tumours: revised RECIST guideline (version 1.1).* Eur J Cancer, 2009. 45(2): p. 228-47.
121. Bruix, J., et al., *Clinical Management of Hepatocellular Carcinoma. Conclusions of the Barcelona-2000 EASL Conference.* Journal of Hepatology, 2015. 35(3): p. 421-430.
122. *Diagnostic accuracy of preoperative magnetic resonance imaging in predicting curative resection of rectal cancer: prospective observational study.* BMJ, 2006. 333(7572): p. 779.
123. Patel, U.B., et al., *Magnetic resonance imaging-detected tumor response for locally advanced rectal cancer predicts survival outcomes: MERCURY experience.* J Clin Oncol, 2011. 29(28): p. 3753-60.
124. Morgan, B., et al., *Intra-arterial brachytherapy of hepatic malignancies: watch the flow.* Nat Rev Clin Oncol, 2010. 8(2): p. 115-20.
125. Padhani, A.R., *Functional MRI for anticancer therapy assessment.* Eur J Cancer, 2002. 38(16): p. 2116-27.
126. Steel, G.G., *Terminology in the description of drug-radiation interactions.* Int J Radiat Oncol Biol Phys, 1979. 5(8): p. 1145-50.
127. Gordon Steel, G. and M.J. Peckham, *Exploitable mechanisms in combined radiotherapy-chemotherapy: The concept of additivity.* International Journal of Radiation Oncology Biology Physics, 1979. 5(1): p. 85-91.
128. Steel, G., ed. *Basic Clinical Radiobiology*. 2002, Arnold: London.
129. Bentzen, S.M., P.M. Harari, and J. Bernier, *Exploitable mechanisms for combining drugs with radiation: concepts, achievements and future directions.* Nat Clin Pract Oncol, 2007. 4(3): p. 172-80.
130. Tozer, G.M., C. Kanthou, and B.C. Baguley, *Disrupting tumour blood vessels.* Nat Rev Cancer, 2005. 5(6): p. 423-35.
131. Harrington, K.J., et al., *Guidelines for preclinical and early phase clinical assessment of novel radiosensitisers.* Br J Cancer, 2011. 105(5): p. 628-39.
132. Hornsey, S. and S. Vatistas, *Some Characteristics of the Survival Curve of Crypt Cells of the Small Intestine of the Mouse deduced after Whole Body X Irradiation.* The British Journal of Radiology, 1963. 36(431): p. 795-800.
133. Hagemann, R.F. and S. Lesher, *Intestinal crypt survival and total and per crypt levels of proliferative cellularity following irradiation: age response and animal lethality.* Radiat Res, 1971. 47(1): p. 159-67.
134. Dorr, W., K. Spekl, and M. Martin, *Radiation-induced oral mucositis in mice: strain differences.* Cell Prolif, 2002. 35 Suppl 1: p. 60-7.
135. Steven, M., et al., *Assessment of Intestinal Stem Cell Survival Using the Microcolony Formation Assay*, in *Colorectal Cancer*. 2001, Humana Press. p. 267-273.
136. Bruso, C.E., D.S. Shewach, and T.S. Lawrence, *Fluorodeoxyuridine-induced radiosensitization and inhibition of DNA double strand break repair in human colon cancer cells.* Int J Radiat Oncol Biol Phys, 1990. 19(6): p. 1411-7.
137. Byfield, J.E., *5-Fluorouracil radiation sensitization--a brief review.* Invest New Drugs, 1989. 7(1): p. 111-6.
138. Sawada, N., et al., *X-ray irradiation induces thymidine phosphorylase and enhances the efficacy of capecitabine (Xeloda) in human cancer xenografts.* Clin Cancer Res, 1999. 5(10): p. 2948-53.
139. Blackstock, A.W., et al., *202 Oxaliplatin: In vitro evidence of its radiation sensitizing activity -- preclinical observations relevant to clinical trials.* International Journal of Radiation Oncology*Biology*Physics, 1999. 45(3, Supplement 1): p. 253-254.
140. Kjellstrom, J., E. Kjellen, and A. Johnsson, *In vitro radiosensitization by oxaliplatin and 5-fluorouracil in a human colon cancer cell line.* Acta Oncol, 2005. 44: p. 687 - 693.

141. Espinosa, M., et al., *Oxaliplatin activity in head and neck cancer cell lines.* Cancer Chemotherapy and Pharmacology, 2005. 55(3): p. 301-305.
142. Rave-FrÃ¤nk, M., et al., *Comparison of the combined action of oxaliplatin or cisplatin and radiation in cervical and lung cancer cells.* International Journal of Radiation Biology, 2007. 83(1): p. 41-47.
143. Benzina, S., et al., *High-LET radiation combined with oxaliplatin induce autophagy in U-87 glioblastoma cells.* Cancer Letters, 2008. 264(1): p. 63-70.
144. Chater, S., et al., *Differential effects of ionizing radiation and platinum-derivative chemotherapy on apoptotic pathways in testicular germ cells.* International Journal of Radiation Biology, 2007. 83(4): p. 269-278.
145. Folkvord, S., et al., *Inhibitory effects of oxaliplatin in experimental radiation treatment of colorectal carcinoma: does oxaliplatin improve 5-fluorouracil-dependent radiosensitivity?* Radiother Oncol, 2008. 86(3): p. 428-34.
146. Benzina, S., et al., *The cytotoxicity of high-linear energy transfer radiation is reinforced by oxaliplatin in human glioblastoma cells.* Cancer Letters, 2007. 254(1): p. 54-62.
147. Morgan, M.A., et al., *Radiotherapy combined with gemcitabine and oxaliplatin in pancreatic cancer cells.* Transl Oncol, 2008. 1(1): p. 36-43.
148. Khan, Z., et al., *Down-regulation of survivin by oxaliplatin diminishes radioresistance of head and neck squamous carcinoma cells.* Radiotherapy and Oncology, 2010. 96(2): p. 267-273.
149. Mattern, M.R., et al., *Synergistic cell killing by ionizing radiation and topoisomerase I inhibitor topotecan (SK&F 104864).* Cancer Res, 1991. 51(21): p. 5813-6.
150. Kim, J.H., et al., *Potentiation of radiation response in human carcinoma cells in vitro and murine fibrosarcoma in vivo by topotecan, an inhibitor of DNA topoisomerase I.* Int J Radiat Oncol Biol Phys, 1992. 22(3): p. 515-8.
151. Boothman, D.A., et al., *Posttreatment exposure to camptothecin enhances the lethal effects of x-rays on radioresistant human malignant melanoma cells.* Int J Radiat Oncol Biol Phys, 1992. 24(5): p. 939-48.
152. Roffler, S.R., J. Chan, and M.Y. Yeh, *Potentiation of radioimmunotherapy by inhibition of topoisomerase I.* Cancer Res, 1994. 54(5): p. 1276-85.
153. Hennequin, C., et al., *Interaction of ionizing radiation with the topoisomerase I poison camptothecin in growing V-79 and HeLa cells.* Cancer Res, 1994. 54(7): p. 1720-8.
154. Chen, A.Y., et al., *Mammalian DNA topoisomerase I mediates the enhancement of radiation cytotoxicity by camptothecin derivatives.* Cancer Res, 1997. 57(8): p. 1529-36.
155. Aschele, C., et al., *Primary Tumor Response to Preoperative Chemoradiation With or Without Oxaliplatin in Locally Advanced Rectal Cancer: Pathologic Results of the STAR-01 Randomized Phase III Trial.* Journal of Clinical Oncology, 2011. 29(20): p. 2773-2780.
156. Gerard, J., et al., *Randomized multicenter phase III trial comparing two neoadjuvant chemoradiotherapy (CT-RT) regimens (RT45-Cap versus RT50-Capox) in patients (pts) with locally advanced rectal cancer (LARC): Results of the ACCORD 12/0405 PRODIGE 2.* J Clin Oncol (Meeting Abstracts), 2009. 27(18S): p. LBA4007-.
157. Rodel, C., et al., *Preoperative chemoradiotherapy and postoperative chemotherapy with fluorouracil and oxaliplatin versus fluorouracil alone in locally advanced rectal cancer: initial results of the German CAO/ARO/AIO-04 randomised phase 3 trial.* Lancet Oncol, 2012. 13(7): p. 679-87.
158. O'Connell, M.J., et al., *Capecitabine and Oxaliplatin in the Preoperative Multimodality Treatment of Rectal Cancer: Surgical End Points From National Surgical Adjuvant Breast and Bowel Project Trial R-04.* Journal of Clinical Oncology, 2014. 32(18): p. 1927-1934.
159. Schmoll, H.-J., et al., *Preoperative chemoradiotherapy and postoperative chemotherapy with capecitabine and oxaliplatin versus capecitabine alone in locally advanced rectal*

cancer: Disease-free survival results at interim analysis. **ASCO Meeting Abstracts, 2014. 32(15_suppl): p. 3501.**

160. **Freyer, G., et al.,** ***Addition of Oxaliplatin to Continuous Fluorouracil, L-Folinic Acid, and Concomitant Radiotherapy in Rectal Cancer: The Lyon R 97-03 Phase I Trial.*** **J Clin Oncol, 2001. 19(9): p. 2433-2438.**
161. **Ryan, D.P., et al.,** ***Phase I/II Study of Preoperative Oxaliplatin, Fluorouracil, and External-Beam Radiation Therapy in Patients With Locally Advanced Rectal Cancer: Cancer and Leukemia Group B 89901.*** **J Clin Oncol, 2006. 24(16): p. 2557-2562.**
162. **Loi, S., et al.,** ***Oxaliplatin combined with infusional 5-fluorouracil and concomitant radiotherapy in inoperable and metastatic rectal cancer: a phase I trial.*** **Br J Cancer, 2005. 92(4): p. 655-661.**
163. **François, E., et al.,** ***Combined radiotherapy, 5-fluorouracil continuous infusion and weekly oxaliplatin in advanced rectal cancer: A phase I study.*** **European Journal of Cancer, 2005. 41(18): p. 2861-2867.**
164. **Rosenthal, D.I., et al.,** ***Phase I Study of Preoperative Radiation Therapy With Concurrent Infusional 5-Fluorouracil and Oxaliplatin Followed by Surgery and Postoperative 5-Fluorouracil Plus Leucovorin for T3/T4 Rectal Adenocarcinoma: ECOG E1297.*** **International Journal of Radiation Oncology Biology Physics, 2008. 72(1): p. 108-113.**
165. **Sebag-Montefiore, D., et al.,** ***A phase I//II study of oxaliplatin when added to 5-fluorouracil and leucovorin and pelvic radiation in locally advanced rectal cancer: a Colorectal Clinical Oncology Group (CCOG) study.*** **Br J Cancer, 2005. 93(9): p. 993-998.**
166. **Reerink, O., et al.,** ***Addition of oxaliplatin to neo-adjuvant radiochemotherapy for irresectable rectal cancer, a phase I study.*** **Anticancer Res, 2005. 25(1B): p. 629-33.**
167. **Fakih, M.G., et al.,** ***A Phase I study of weekly intravenous oxaliplatin in combination with oral daily capecitabine and radiation therapy in the neoadjuvant treatment of rectal adenocarcinoma.*** **International Journal of Radiation Oncology Biology Physics, 2006. 65(5): p. 1462-1470.**
168. **Glynne-Jones, R., et al.,** ***A phase I dose escalation study of continuous oral capecitabine in combination with oxaliplatin and pelvic radiation (XELOX-RT) in patients with locally advanced rectal cancer.*** **Ann Oncol, 2006. 17(1): p. 50-6.**
169. **Rodel, C., et al.,** ***Phase I/II Trial of Capecitabine, Oxaliplatin, and Radiation for Rectal Cancer.*** **J Clin Oncol, 2003. 21: p. 3098 - 3104.**
170. **Hospers, G.A., et al.,** ***Preoperative chemoradiotherapy with capecitabine and oxaliplatin in locally advanced rectal cancer. A phase I-II multicenter study of the Dutch Colorectal Cancer Group.*** **Ann Surg Oncol, 2007. 14(10): p. 2773-9.**
171. **Carraro, S., et al.,** ***Radiochemotherapy with short daily infusion of low-dose oxaliplatin, leucovorin, and 5-FU in T3-T4 unresectable rectal cancer: a phase II IATTGI study.*** **International Journal of Radiation Oncology*Biology*Physics, 2002. 54(2): p. 397-402.**
172. **Gerard, J.P., et al.,** ***Preoperative concurrent chemoradiotherapy in locally advanced rectal cancer with high-dose radiation and oxaliplatin-containing regimen: the Lyon R0-04 phase II trial.*** **J Clin Oncol, 2003. 21(6): p. 1119-24.**
173. **Aschele, C., et al.,** ***A phase I-II study of weekly oxaliplatin, 5-fluorouracil continuous infusion and preoperative radiotherapy in locally advanced rectal cancer.*** **Ann Oncol, 2005. 16(7): p. 1140-6.**
174. **Feng, H.Y., et al.,** ***[Preoperative chemoradiotherapy as neoadjuvant therapy for 35 patients with locally advanced lower rectal carcinoma].*** **Zhonghua Wei Chang Wai Ke Za Zhi, 2005. 8(2): p. 125-8.**
175. **Pucciarelli, S., et al.,** ***5-Fluorouracil and Weekly Oxaliplatin Combined with Radiotherapy for Locally Advanced Rectal Cancer: Surgical Complications and Long-term Results.*** **Archives of Medical Research, 2006. 37(7): p. 860-865.**

176. **Turitto, G., et al.,** ***Phase II study of neoadjuvant concurrent chemioradiotherapy with oxaliplatin-containing regimen in locally advanced rectal cancer.*** **Front Biosci, 2006. 11: p. 1275-9.**
177. **Djellali, L., et al.,** ***Preoperative concomitant chemoradiotherapy with oxaliplatin and 5-fluorouracil in locally advanced rectal carcinoma.*** **J Clin Oncol (Meeting Abstracts), 2009. 27(15S): p. e15108-.**
178. **Machiels, J.P., et al.,** ***Phase II study of preoperative oxaliplatin, capecitabine and external beam radiotherapy in patients with rectal cancer: the RadiOxCape study.*** **Ann Oncol, 2005. 16(12): p. 1898-905.**
179. **Glynne-Jones, R., et al.,** ***Socrates phase II study results: Capecitabine (CAP) combined with oxaliplatin (OX) and preoperative radiation (RT) in patients (pts) with locally advanced rectal cancer (LARC).*** **Journal of Clinical Oncology, 2005. 23(16): p. 252S-252S.**
180. **Rutten, H., et al.,** ***Capecitabine, oxaliplatin, radiotherapy, and excision (CORE) in patients with MRI-defined locally advanced rectal adenocarcinoma: Results of an international multicenter phase II study.*** **J Clin Oncol (Meeting Abstracts), 2006. 24(18_suppl): p. 3528-.**
181. **Rodel, C., et al.,** ***Multicenter Phase II Trial of Chemoradiation With Oxaliplatin for Rectal Cancer.*** **J Clin Oncol, 2007. 25(1): p. 110-117.**
182. **Alonso, V., et al.,** ***Preoperative chemoradiotherapy with capecitabine and oxaliplatin in locally advanced rectal carcinoma: A phase II trial.*** **J Clin Oncol (Meeting Abstracts), 2007. 25(18_suppl): p. 4044-.**
183. **Fakih, M.G., et al.,** ***Phase II Study of Weekly Intravenous Oxaliplatin Combined With Oral Daily Capecitabine and Radiotherapy With Biologic Correlates in Neoadjuvant Treatment of Rectal Adenocarcinoma.*** **International Journal of Radiation Oncology Biology Physics, 2008. 72(3): p. 650-657.**
184. **Majem, M.,** ***Phase II clinical trial of weekly oxaliplatin concurrent with capecitabine plus pre-operative radiotherapy in resectable locally advanced rectal cancer.*** **J Clin Oncol, 2008. 26(15S).**
185. **Carlomagno, C., et al.,** ***Neo-adjuvant treatment of rectal cancer with capecitabine and oxaliplatin in combination with radiotherapy: a phase II study.*** **Ann Oncol, 2009. 20(5): p. 906-12.**
186. **Lin, J.Z., et al.,** ***Phase II study of pre-operative radiotherapy with capecitabine and oxaliplatin for rectal cancer and carcinoembryonic antigen as a predictor of pathological tumour response.*** **J Int Med Res, 2010. 38(2): p. 645-54.**
187. **Wang, J.P., et al.,** ***[Preoperative chemoradiotherapy with FOLFOX in low rectal cancer: a multicenter study].*** **Zhonghua Wei Chang Wai Ke Za Zhi, 2008. 11(2): p. 116-9.**
188. **Koeberle, D., et al.,** ***Phase II study of capecitabine and oxaliplatin given prior to and concurrently with preoperative pelvic radiotherapy in patients with locally advanced rectal cancer.*** **Br J Cancer, 2008. 98(7): p. 1204-1209.**
189. **Gunnlaugsson, A., et al.,** ***Multicentre phase II trial of capecitabine and oxaliplatin in combination with radiotherapy for unresectable colorectal cancer: The CORGI-L study.*** **European Journal of Cancer, 2009. 45(5): p. 807-813.**
190. **Fernandez-Martos, C., et al.,** ***Phase II, Randomized Study of Concomitant Chemoradiotherapy Followed by Surgery and Adjuvant Capecitabine Plus Oxaliplatin (CAPOX) Compared With Induction CAPOX Followed by Concomitant Chemoradiotherapy and Surgery in Magnetic Resonance Imaging-Defined, Locally Advanced Rectal Cancer: Grupo Cancer de Recto 3 Study.*** **J Clin Oncol, 2010. 28(5): p. 859-865.**
191. **Aschele, C., et al.,** ***Preoperative fluorouracil (FU)-based chemoradiation with and without weekly oxaliplatin in locally advanced rectal cancer: Pathologic response***

analysis of the Studio Terapia Adiuvante Retto (STAR)-01 randomized phase III trial. J Clin Oncol (Meeting Abstracts), 2009. 27(18S): p. CRA4008-.

192. Roh, M.S., et al., *The impact of capecitabine and oxaliplatin in the preoperative multimodality treatment in patients with carcinoma of the rectum: NSABP R-04.* ASCO Meeting Abstracts, 2011. 29(15_suppl): p. 3503.
193. Gerard, J.P., et al., *Comparison of two neoadjuvant chemoradiotherapy regimens for locally advanced rectal cancer: results of the phase III trial ACCORD 12/0405-Prodige 2.* J Clin Oncol, 2010. 28(10): p. 1638-44.
194. Harrington, K., P. Jankowska, and M. Hingorani, *Molecular Biology for the Radiation Oncologist: the 5Rs of Radiobiology meet the Hallmarks of Cancer.* Clinical Oncology, 2007. 19(8): p. 561-571.
195. Huang, S.M., J.M. Bock, and P.M. Harari, *Epidermal growth factor receptor blockade with C225 modulates proliferation, apoptosis, and radiosensitivity in squamous cell carcinomas of the head and neck.* Cancer Research, 1999. 59(8): p. 1935-1940.
196. Huang, S.M. and P.M. Harari, *Modulation of radiation response after epidermal growth factor receptor blockade in squamous cell carcinomas: Inhibition of damage repair, cell cycle kinetics, and tumor angiogenesis.* Clinical Cancer Research, 2000. 6(6): p. 2166-2174.
197. Milas, L., et al., *In vivo enhancement of tumor radioresponse by C225 antiepidermal growth factor receptor antibody.* Clinical Cancer Research, 2000. 6(2): p. 701-708.
198. Bonner, J.A., et al., *Radiotherapy plus Cetuximab for Squamous-Cell Carcinoma of the Head and Neck.* New England Journal of Medicine, 2006. 354(6): p. 567-578.
199. Fokas, E., et al., *Preoperative chemoradiation therapy with capecitabine/oxaliplatin and cetuximab in rectal cancer: long-term results of a prospective phase 1/2 study.* Int J Radiat Oncol Biol Phys, 2013. 87(5): p. 992-9.
200. Machiels, J.P., et al., *Phase I/II study of preoperative cetuximab, capecitabine, and external beam radiotherapy in patients with rectal cancer.* Ann Oncol, 2007. 18(4): p. 738-44.
201. Debucquoy, A., et al., *Molecular response to cetuximab and efficacy of preoperative cetuximab-based chemoradiation in rectal cancer.* J Clin Oncol, 2009. 27(17): p. 2751-7.
202. Bertolini, F., et al., *Neoadjuvant Treatment With Single-Agent Cetuximab Followed by 5-FU, Cetuximab, and Pelvic Radiotherapy: A Phase II Study in Locally Advanced Rectal Cancer.* International Journal of Radiation Oncology Biology Physics, 2009. 73(2): p. 466-472.
203. Marquardt, F., et al., *Molecular targeted treatment and radiation therapy for rectal cancer.* Strahlentherapie und Onkologie, 2009. 185(6): p. 371-378.
204. Rodel, C., et al., *Phase I-II trial of cetuximab, capecitabine, oxaliplatin, and radiotherapy as preoperative treatment in rectal cancer.* International Journal of Radiation Oncology Biology Physics, 2008. 70(4): p. 1081-1086.
205. Horisberger, K., et al., *Cetuximab in Combination With Capecitabine, Irinotecan, and Radiotherapy for Patients With Locally Advanced Rectal Cancer: Results of a Phase II MARGIT Trial.* International Journal of Radiation Oncology BiologyPhysics, 2009. 74(5): p. 1487-1493.
206. Sun, P.L., B. Li, and Q.F. Ye, *Effect of neoadjuvant cetuximab, capecitabine, and radiotherapy for locally advanced rectal cancer: Results of a phase II study.* International Journal of Colorectal Disease, 2012. 27(10): p. 1325-1332.
207. Velenik, V., et al., *Cetuximab in preoperative treatment of rectal cancer-term outcome of the XERT trial.* Radiology and Oncology, 2012. 46(3): p. 252-257.
208. Weiss, C., et al., *Preoperative radiotherapy of advanced rectal cancer with capecitabine and oxaliplatin with or without cetuximab: A pooled analysis of three prospective phase I-II trials.* Int J Radiat Oncol Biol Phys, 2010. 78(2): p. 472-8.

209. Kim, S.Y., et al., *KRAS mutation status and clinical outcome of preoperative chemoradiation with cetuximab in locally advanced rectal cancer: a pooled analysis of 2 phase II trials.* Int J Radiat Oncol Biol Phys, 2012. 85(1): p. 201-7.
210. Gorski, D.H., et al., *Blockage of the vascular endothelial growth factor stress response increases the antitumor effects of ionizing radiation.* Cancer Res, 1999. 59(14): p. 3374-8.
211. Lee, C.G., et al., *Anti-Vascular endothelial growth factor treatment augments tumor radiation response under normoxic or hypoxic conditions.* Cancer Res, 2000. 60(19): p. 5565-70.
212. Duda, D.G., R.K. Jain, and C.G. Willett, *Antiangiogenics: The Potential Role of Integrating This Novel Treatment Modality With Chemoradiation for Solid Cancers.* Journal of Clinical Oncology, 2007. 25(26): p. 4033-4042.
213. Ansiaux, R.g., et al., *Thalidomide Radiosensitizes Tumors through Early Changes in the Tumor Microenvironment.* Clinical Cancer Research, 2005. 11(2): p. 743-750.
214. Kozin, S.V., et al., *Vascular Endothelial Growth Factor Receptor-2-blocking Antibody Potentiates Radiation-induced Long-Term Control of Human Tumor Xenografts.* Cancer Research, 2001. 61(1): p. 39-44.
215. Jain, R.K., *Normalizing tumor vasculature with anti-angiogenic therapy: a new paradigm for combination therapy.* Nat Med, 2001. 7(9): p. 987-9.
216. Jain, R.K., *Normalization of Tumor Vasculature: An Emerging Concept in Antiangiogenic Therapy.* Science, 2005. 307(5706): p. 58-62.
217. Good, J.S. and K.J. Harrington, *The Hallmarks of Cancer and the Radiation Oncologist: Updating the 5Rs of Radiobiology*, in *Advances in Clinical Radiobiology,* Clinical Oncology *2013*. p. 569-577.
218. Yuan, T.L. and L.C. Cantley, *PI3K pathway alterations in cancer: variations on a theme.* Oncogene, 2008. 27(41): p. 5497-510.
219. Gupta, A.K., et al., *Ras regulation of radioresistance in cell culture.* Methods Enzymol, 2001. 333: p. 284-90.
220. Grana, T.M., et al., *Ras mediates radioresistance through both phosphatidylinositol 3-kinase-dependent and Raf-dependent but mitogen-activated protein kinase/extracellular signal-regulated kinase kinase-independent signaling pathways.* Cancer Res, 2002. 62(14): p. 4142-50.
221. Nakamura, J.L., et al., *PKB/Akt mediates radiosensitization by the signaling inhibitor LY294002 in human malignant gliomas.* J Neurooncol, 2005. 71(3): p. 215-22.
222. Gupta, A.K., et al., *Radiation sensitization of human cancer cells in vivo by inhibiting the activity of PI3K using LY294002.* Int J Radiat Oncol Biol Phys, 2003. 56(3): p. 846-53.
223. Gupta, A.K., et al., *The HIV protease inhibitor nelfinavir downregulates Akt phosphorylation by inhibiting proteasomal activity and inducing the unfolded protein response.* Neoplasia, 2007. 9(4): p. 271-8.
224. Gupta, A.K., et al., *Local recurrence in head and neck cancer: relationship to radiation resistance and signal transduction.* Clin Cancer Res, 2002. 8(3): p. 885-92.
225. Kim, I.A., et al., *The influence of Ras pathway signaling on tumor radiosensitivity.* Cancer Metastasis Rev, 2004. 23(3-4): p. 227-36.
226. Pajonk, F., et al., *The human immunodeficiency virus (HIV)-1 protease inhibitor saquinavir inhibits proteasome function and causes apoptosis and radiosensitization in non-HIV-associated human cancer cells.* Cancer Res, 2002. 62(18): p. 5230-5.
227. Gupta, A.K., et al., *HIV protease inhibitors block Akt signaling and radiosensitize tumor cells both in vitro and in vivo.* Cancer Res, 2005. 65(18): p. 8256-65.
228. Pore, N., et al., *Nelfinavir Down-regulates Hypoxia-Inducible Factor 1Î± and VEGF Expression and Increases Tumor Oxygenation: Implications for Radiotherapy.* Cancer Research, 2006. 66(18): p. 9252-9259.

229. Qayum, N., et al., *Tumor vascular changes mediated by inhibition of oncogenic signaling.* Cancer Res, 2009. 69(15): p. 6347-54.
230. Saag, M.S., et al., *Randomized, double-blind comparison of two nelfinavir doses plus nucleosides in HIV-infected patients (Agouron study 511).* Aids, 2001. 15(15): p. 1971-8.
231. Oehler-Janne, C., et al., *Local tumor control and toxicity in HIV-associated anal carcinoma treated with radiotherapy in the era of antiretroviral therapy.* Radiat Oncol, 2006. 1: p. 29.
232. Brunner, T.B., et al., *Phase I trial of the human immunodeficiency virus protease inhibitor nelfinavir and chemoradiation for locally advanced pancreatic cancer.* J Clin Oncol, 2008. 26(16): p. 2699-706.
233. Rengan, R., et al., *A phase I trial of the HIV protease inhibitor nelfinavir with concurrent chemoradiotherapy for unresectable stage IIIA/IIIB non-small cell lung cancer: a report of toxicities and clinical response.* J Thorac Oncol, 2012. 7(4): p. 709-15.
234. Alonso-Basanta, M., et al., *A phase I study of nelfinavir concurrent with temozolomide and radiotherapy in patients with glioblastoma multiforme.* J Neurooncol, 2013. 116(2): p. 365-72.
235. Buijsen, J., et al., *Phase I Trial of the Combination of the AKT Inhibitor Nelfinavir and Chemoradiation for Locally Advanced Rectal Cancer.* International Journal of Radiation Oncology Biology Physics, 2011. 81(2): p. S97-S97.
236. Buijsen, J., et al., *Phase I trial of the combination of the Akt inhibitor nelfinavir and chemoradiation for locally advanced rectal cancer.* Radiother Oncol, 2011. 107(2): p. 184-8.
237. Midgley, R. and D. Kerr, *Colorectal cancer.* Lancet, 1999. 353(9150): p. 391-9.
238. Khambata-Ford, S., et al., *Expression of epiregulin and amphiregulin and K-ras mutation status predict disease control in metastatic colorectal cancer patients treated with cetuximab.* J Clin Oncol, 2007. 25(22): p. 3230-7.
239. O'Leary, B. and D.C. Gilbert, *Mismatch Repair as a Prognostic Marker for Adjuvant Therapy in Colorectal Cancer. How Soon is Now?* Clinical oncology (Royal College of Radiologists (Great Britain)), 2013. 25(11): p. 625-629.
240. Garcia-Aguilar, J., et al., *Identification of a biomarker profile associated with resistance to neoadjuvant chemoradiation therapy in rectal cancer.* Ann Surg, 2011. 254(3): p. 486-92; discussion 492-3.
241. Suzuki, T., et al., *Biopsy Specimens Obtained 7 Days After Starting Chemoradiotherapy (CRT) Provide Reliable Predictors of Response to CRT for Rectal Cancer.* International journal of radiation oncology, biology, physics, 2013. 85(5): p. 1232-1238.
242. Kuremsky, J.G., J.E. Tepper, and H.L. McLeod, *Biomarkers for Response to Neoadjuvant Chemoradiation for Rectal Cancer.* International Journal of Radiation Oncology*Biology*Physics, 2009. 74(3): p. 673-688.
243. Maas, M., et al., *Long-term outcome in patients with a pathological complete response after chemoradiation for rectal cancer: a pooled analysis of individual patient data.* The Lancet Oncology, 2010. 11(9): p. 835-844.
244. Hartley, A., et al., *Pathological complete response following pre-operative chemoradiotherapy in rectal cancer: analysis of phase II/III trials.* Br J Radiol, 2005. 78(934): p. 934-938.
245. Dworak, O., L. Keilholz, and A. Hoffmann, *Pathological features of rectal cancer after preoperative radiochemotherapy.* Int J Colorectal Dis, 1997. 12(1): p. 19-23.
246. Williams JT, Q.P., Shepherd NA and . *Dataset for Colorectal Cancer* 2007, The Royal College of Pathologists: London.
247. Chetty, R., et al., *A multi-centre pathologist survey on pathological processing and regression grading of colorectal cancer resection specimens treated by neoadjuvant chemoradiation.* Virchows Arch, 2012. 460(2): p. 151-5.

248. **Connolly JL, S.S., Wang HH, et al, *Tumor Structure and Tumor Stroma Generation*, in *Holland-Frei Cancer Medicine*, P.R. Kufe DW, Weichselbaum RR, et al., editors. , Editor. 2003, Hamilton (ON): BC Decker.**

249. **Neesse, A., et al., *Stromal biology and therapy in pancreatic cancer.* Gut. 60(6): p. 861-8.**

250. **Olson, P. and D. Hanahan, *Cancer. Breaching the cancer fortress.* Science, 2009. 324(5933): p. 1400-1.**

251. **Mesker, W.E., et al., *The carcinoma-stromal ratio of colon carcinoma is an independent factor for survival compared to lymph node status and tumor stage.* Cell Oncol, 2007. 29(5): p. 387-98.**

252. **Mesker, W.E., et al., *Presence of a high amount of stroma and downregulation of SMAD4 predict for worse survival for stage I-II colon cancer patients.* Cell Oncol, 2009. 31(3): p. 169-78.**

253. **Huijbers, A., et al., *The proportion of tumor-stroma as a strong prognosticator for stage II and III colon cancer patients: validation in the VICTOR trial.* Ann Oncol,2012. 24(1): p. 179-85.**

254. **West, N.P., et al., *The proportion of tumour cells is an independent predictor for survival in colorectal cancer patients.* Br J Cancer, 2010. 102(10): p. 1519-23.**

255. **West N, G.H., Treanor D, Sebag-Montefiore D, Thorpe H, Jayne D, Rutten H, Swellengrebel H, Nagtegaal I and Quirke P, *Quantitative assessment of tumour cell density in rectal cancer following three pre-operative therapies compared to surgery alone.* Journal of Clinical Oncology, 2010. 28(15(s)): p. 3651.**

256. **Srivastava, A., et al., *The prognostic significance of tumor vascularity in intermediate-thickness (0.76-4.0 mm thick) skin melanoma. A quantitative histologic study.* Am J Pathol, 1988. 133(2): p. 419-23.**

257. **Weidner, N., et al., *Tumor angiogenesis and metastasis--correlation in invasive breast carcinoma.* N Engl J Med, 1991. 324(1): p. 1-8.**

258. **Weidner, N., et al., *Tumor angiogenesis: a new significant and independent prognostic indicator in early-stage breast carcinoma.* J Natl Cancer Inst, 1992. 84(24): p. 1875-87.**

259. **Horak, E.R., et al., *Angiogenesis, assessed by platelet/endothelial cell adhesion molecule antibodies, as indicator of node metastases and survival in breast cancer.* Lancet, 1992. 340(8828): p. 1120-4.**

260. **Tanigawa, N., et al., *Association of tumour vasculature with tumour progression and overall survival of patients with non-early gastric carcinomas.* Br J Cancer, 1997. 75(4): p. 566-71.**

261. **Fox, S.B., et al., *Quantitation and prognostic value of breast cancer angiogenesis: comparison of microvessel density, Chalkley count, and computer image analysis.* J Pathol, 1995. 177(3): p. 275-83.**

262. **Vermeulen, P.B., et al., *Second international consensus on the methodology and criteria of evaluation of angiogenesis quantification in solid human tumours.* Eur J Cancer, 2002. 38(12): p. 1564-79.**

263. **Dallas, N.A., et al., *Endoglin (CD105): a marker of tumor vasculature and potential target for therapy.* Clin Cancer Res, 2008. 14(7): p. 1931-7.**

264. **Duff, S.E., et al., *CD105 is important for angiogenesis: evidence and potential applications.* FASEB J, 2003. 17(9): p. 984-92.**

265. **Rasheed, S., et al., *Hypoxia-inducible factor-1alpha and -2alpha are expressed in most rectal cancers but only hypoxia-inducible factor-1alpha is associated with prognosis.* Br J Cancer, 2009. 100(10): p. 1666-73.**

266. **Rasheed, S., et al., *Assessment of microvessel density and carbonic anhydrase-9 (CA-9) expression in rectal cancer.* Pathol Res Pract, 2009. 205(1): p. 1-9.**

267. Kikuchi, M., et al., *High Ki67, Bax, and thymidylate synthase expression well correlates with response to chemoradiation therapy in locally advanced rectal cancers: proposal of a logistic model for prediction.* Br J Cancer, 2009. 101(1): p. 116-123.
268. Svagzdys, S., et al., *Microvessel density as new prognostic marker after radiotherapy in rectal cancer.* BMC Cancer, 2009. 9: p. 95.
269. Baeten, C.I., et al., *Effects of radiotherapy and chemotherapy on angiogenesis and leukocyte infiltration in rectal cancer.* Int J Radiat Oncol Biol Phys, 2006. 66(4): p. 1219-27.
270. Robertson, N., C. Potter, and A.L. Harris, *Role of carbonic anhydrase IX in human tumor cell growth, survival, and invasion.* Cancer Res, 2004. 64(17): p. 6160-5.
271. Loncaster, J.A., et al., *Carbonic anhydrase (CA IX) expression, a potential new intrinsic marker of hypoxia: correlations with tumor oxygen measurements and prognosis in locally advanced carcinoma of the cervix.* Cancer Res, 2001. 61(17): p. 6394-9.
272. Iliopoulos, O. and W.G. Kaelin, Jr., *The molecular basis of von Hippel-Lindau disease.* Mol Med, 1997. 3(5): p. 289-93.
273. Kivela, A.J., et al., *Differential expression of cytoplasmic carbonic anhydrases, CA I and II, and membrane-associated isozymes, CA IX and XII, in normal mucosa of large intestine and in colorectal tumors.* Dig Dis Sci, 2001. 46(10): p. 2179-86.
274. Beasley, N.J., et al., *Carbonic anhydrase IX, an endogenous hypoxia marker, expression in head and neck squamous cell carcinoma and its relationship to hypoxia, necrosis, and microvessel density.* Cancer Res, 2001. 61(13): p. 5262-7.
275. Korkeila, E., et al., *Expression of carbonic anhydrase IX suggests poor outcome in rectal cancer.* Br J Cancer, 2009. 100(6): p. 874-80.
276. Bos, R., et al., *Levels of hypoxia-inducible factor-1alpha independently predict prognosis in patients with lymph node negative breast carcinoma.* Cancer, 2003. 97(6): p. 1573-81.
277. Dales, J.P., et al., *Overexpression of hypoxia-inducible factor HIF-1alpha predicts early relapse in breast cancer: retrospective study in a series of 745 patients.* Int J Cancer, 2005. 116(5): p. 734-9.
278. Vaupel, P. and A. Mayer, *Hypoxia in cancer: significance and impact on clinical outcome.* Cancer Metastasis Rev, 2007. 26(2): p. 225-39.
279. Theodoropoulos, G.E., et al., *Hypoxia, angiogenesis and apoptosis markers in locally advanced rectal cancer.* Int J Colorectal Dis, 2006. 21(3): p. 248-57.
280. Lu, X.G., et al., *Clinical significance of immunohistochemical expression of hypoxia-inducible factor-1alpha as a prognostic marker in rectal adenocarcinoma.* Clin Colorectal Cancer, 2006. 5(5): p. 350-3.
281. Korkeila, E., et al., *Preoperative radiotherapy downregulates the nuclear expression of hypoxia-inducible factor-1alpha in rectal cancer.* Scand J Gastroenterol, 2009. 45(3): p. 340-8.
282. Lee, J.W., et al., *Hypoxia-inducible factor (HIF-1)alpha: its protein stability and biological functions.* Exp Mol Med, 2004. 36(1): p. 1-12.
283. Jubb, A.M., F.M. Buffa, and A.L. Harris, *Assessment of tumour hypoxia for prediction of response to therapy and cancer prognosis.* J Cell Mol Med, 2009. 14(1-2): p. 18-29.
284. Sobhanifar, S., et al., *Reduced expression of hypoxia-inducible factor-1alpha in perinecrotic regions of solid tumors.* Cancer Res, 2005. 65(16): p. 7259-66.
285. Havelund, B.M., et al., *Immunohistological expression of HIF-1alpha, GLUT-1, Bcl-2 and Ki-67 in consecutive biopsies during chemoradiotherapy in patients with rectal cancer.* APMIS, 2012. 121(2): p. 127-38.
286. Vaughn, C.P., et al., *Frequency of KRAS, BRAF, and NRAS mutations in colorectal cancer.* Genes Chromosomes Cancer, 2011. 50(5): p. 307-12.
287. Andreyev, H.J., et al., *Kirsten ras mutations in patients with colorectal cancer: the 'RASCAL II' study.* Br J Cancer, 2001. 85(5): p. 692-6.

288. **Andreyev, H.J., et al.,** ***Kirsten ras mutations in patients with colorectal cancer: the multicenter "RASCAL" study.*** **J Natl Cancer Inst, 1998. 90(9): p. 675-84.**
289. **Guerrero, S., et al.,** ***Codon 12 and codon 13 mutations at the K-ras gene induce different soft tissue sarcoma types in nude mice.*** **FASEB J, 2002. 16(12): p. 1642-4.**
290. **Guerrero, S., et al.,** ***K-ras codon 12 mutation induces higher level of resistance to apoptosis and predisposition to anchorage-independent growth than codon 13 mutation or proto-oncogene overexpression.*** **Cancer Res, 2000. 60(23): p. 6750-6.**
291. **Keohavong, P., et al.,** ***Detection of K-ras mutations in lung carcinomas: relationship to prognosis.*** **Clin Cancer Res, 1996. 2(2): p. 411-8.**
292. **Gaedcke, J., et al.,** ***KRAS and BRAF mutations in patients with rectal cancer treated with preoperative chemoradiotherapy.*** **Radiother Oncol, 2009. 94(1): p. 76-81.**
293. **Davies, J.M., et al.,** ***Phospho-ERK and AKT status, but not KRAS mutation status, are associated with outcomes in rectal cancer treated with chemoradiotherapy.*** **Radiat Oncol, 2011. 6: p. 114.**
294. **Demes, M., et al.,** ***Signature of microsatellite instability, KRAS and BRAF gene mutations in German patients with locally advanced rectal adenocarcinoma before and after neoadjuvant 5-FU radiochemotherapy.*** **J Gastrointest Oncol, 2013. 4(2): p. 182-92.**
295. **Duldulao, M.P., et al.,** ***Mutations in specific codons of the KRAS oncogene are associated with variable resistance to neoadjuvant chemoradiation therapy in patients with rectal adenocarcinoma.*** **Ann Surg Oncol, 2013. 20(7): p. 2166-71.**
296. **Zauber, N.P., et al.,** ***Molecular Genetic Changes Associated With Colorectal Carcinogenesis Are Not Prognostic for Tumor Regression Following Preoperative Chemoradiation of Rectal Carcinoma.*** **International Journal of Radiation Oncology Biology Physics, 2009. 74(2): p. 472-476.**
297. **Grimminger, P.P., et al.,** ***Biomarkers for cetuximab-based neoadjuvant radiochemotherapy in locally advanced rectal cancer.*** **Clin Cancer Res, 2011. 17(10): p. 3469-77.**
298. **Erben, P., et al.,** ***KRAS and BRAF mutations and PTEN expression do not predict efficacy of cetuximab-based chemoradiotherapy in locally advanced rectal cancer.*** **Int J Radiat Oncol Biol Phys, 2010. 81(4): p. 1032-8.**
299. **Bengala, C., et al.,** ***Prognostic role of EGFR gene copy number and KRAS mutation in patients with locally advanced rectal cancer treated with preoperative chemoradiotherapy.*** **Br J Cancer, 2010. 103(7): p. 1019-24.**
300. **Sun, P.L., B. Li, and Q.F. Ye,** ***Effect of neoadjuvant cetuximab, capecitabine, and radiotherapy for locally advanced rectal cancer: results of a phase II study.*** **Int J Colorectal Dis, 2012. 27(10): p. 1325-32.**
301. **Clancy, C., J.P. Burke, and J.C. Coffey,** ***KRAS mutation does not predict the efficacy of neo-adjuvant chemoradiotherapy in rectal cancer: a systematic review and meta-analysis.*** **Surg Oncol, 2013. 22(2): p. 105-11.**
302. **Rosty, C., et al.,** ***PIK3CA activating mutation in colorectal carcinoma: associations with molecular features and survival.*** **PLoS One, 2013. 8(6): p. e65479.**
303. **Nosho, K., et al.,** ***PIK3CA mutation in colorectal cancer: relationship with genetic and epigenetic alterations.*** **Neoplasia, 2008. 10(6): p. 534-41.**
304. **He, Y., et al.,** ***PIK3CA mutations predict local recurrences in rectal cancer patients.*** **Clin Cancer Res, 2009. 15(22): p. 6956-62.**
305. **He, Y., et al.,** ***Do rectal cancer patients with PIK3CA mutations benefit from preoperative radiotherapy with regard to local recurrences?*** **Clin Cancer Res, 2009. 16(24): p. 6179.**
306. **Derbel, O., et al.,** ***Impact of KRAS, BRAF and PI3KCA mutations in rectal carcinomas treated with neoadjuvant radiochemotherapy and surgery.*** **BMC Cancer, 2013. 13: p. 200.**

307. Shtilbans, V., M. Wu, and D.E. Burstein, *Current overview of the role of Akt in cancer studies via applied immunohistochemistry.* Ann Diagn Pathol, 2008. 12(2): p. 153-60.
308. Roy, H.K., et al., *AKT proto-oncogene overexpression is an early event during sporadic colon carcinogenesis.* Carcinogenesis, 2002. 23(1): p. 201-5.
309. Saglam, O., et al., *Activation of the serine/threonine protein kinase AKT during the progression of colorectal neoplasia.* Clin Colorectal Cancer, 2007. 6(9): p. 652-6.
310. Lugli, A., et al., *Role of the mitogen-activated protein kinase and phosphoinositide 3-kinase/AKT pathways downstream molecules, phosphorylated extracellular signal-regulated kinase, and phosphorylated AKT in colorectal cancer-a tissue microarray-based approach.* Hum Pathol, 2006. 37(8): p. 1022-31.
311. Kato, S., et al., *PIK3CA mutation is predictive of poor survival in patients with colorectal cancer.* Int J Cancer, 2007. 121(8): p. 1771-8.
312. Schmitz, K.J., et al., *Activation of the ERK and AKT signalling pathway predicts poor prognosis in hepatocellular carcinoma and ERK activation in cancer tissue is associated with hepatitis C virus infection.* J Hepatol, 2008. 48(1): p. 83-90.
313. Colakoglu, T., et al., *Clinicopathological significance of PTEN loss and the phosphoinositide 3-kinase/Akt pathway in sporadic colorectal neoplasms: is PTEN loss predictor of local recurrence?* Am J Surg, 2008. 195(6): p. 719-25.
314. Baba, Y., et al., *Phosphorylated AKT expression is associated with PIK3CA mutation, low stage, and favorable outcome in 717 colorectal cancers.* Cancer, 2011. 117(7): p. 1399-408.
315. Plastaras, J.P., et al., *Validation and toxicity of PI3K/Akt pathway inhibition by HIV protease inhibitors in humans.* Cancer Biol Ther, 2008. 7(5): p. 628-35.
316. Farkas, R., et al., *Possible predictors of histopathological response to neoadjuvant chemoradiotherapy for rectal cancer.* J Cancer Res Clin Oncol, 2011. 138(3): p. 387-95.
317. Jeffers, M., *Comparison of commerically available phospho-AKT antibodies for Immunohistochemical Biomarker Analysis.* AACR, 2010.
318. Baker, A.F., et al., *Stability of phosphoprotein as a biological marker of tumor signaling.* Clin Cancer Res, 2005. 11(12): p. 4338-40.
319. Andersen, J.N., et al., *Pathway-based identification of biomarkers for targeted therapeutics: personalized oncology with PI3K pathway inhibitors.* Sci Transl Med, 2010. 2(43): p. 43ra55.
320. Yap, T.A., et al., *Preclinical pharmacology, antitumor activity, and development of pharmacodynamic markers for the novel, potent AKT inhibitor CCT128930.* Mol Cancer Ther, 2010. 10(2): p. 360-71.
321. Blake, J.F., et al., *Discovery of pyrrolopyrimidine inhibitors of Akt.* Bioorg Med Chem Lett, 2010. 20(19): p. 5607-12.
322. Garcia, J.A. and D. Danielpour, *Mammalian target of rapamycin inhibition as a therapeutic strategy in the management of urologic malignancies.* Mol Cancer Ther, 2008. 7(6): p. 1347-54.
323. Yan, Y., et al., *Evaluation and Clinical Analyses of Downstream Targets of the Akt Inhibitor GDC-0068.* Clinical Cancer Research, 2013. 19(24): p. 6976-6986.
324. Axel, L., *Cerebral blood flow determination by rapid-sequence computed tomography: theoretical analysis.* Radiology, 1980. 137(3): p. 679-86.
325. Schumann, P., et al., *Evaluation of the ratio of cerebral blood flow to cerebral blood volume as an index of local cerebral perfusion pressure.* Brain, 1998. 121 (Pt 7): p. 1369-79.
326. Goh, V. and R. Glynne-Jones, *Perfusion CT imaging of colorectal cancer.* Br J Radiol, 2014. 87(1034): p. 20130811.

327. **Kealey, S.M., et al.,** ***User-defined vascular input function curves: influence on mean perfusion parameter values and signal-to-noise ratio.*** **Radiology, 2004. 231(2): p. 587-93.**
328. **Meier, P. and K.L. Zierler,** ***On the theory of the indicator-dilution method for measurement of blood flow and volume.*** **J Appl Physiol, 1954. 6(12): p. 731-44.**
329. **Axel, L.,** ***Tissue mean transit time from dynamic computed tomography by a simple deconvolution technique.*** **Invest Radiol, 1983. 18(1): p. 94-9.**
330. **Nabavi, D.G., et al.,** ***CT assessment of cerebral perfusion: experimental validation and initial clinical experience.*** **Radiology, 1999. 213(1): p. 141-9.**
331. **Purdie, T.G., E. Henderson, and T.Y. Lee,** ***Functional CT imaging of angiogenesis in rabbit VX2 soft-tissue tumour.*** **Phys Med Biol, 2001. 46(12): p. 3161-75.**
332. **Cenic, A., et al.,** ***A CT method to measure hemodynamics in brain tumors: validation and application of cerebral blood flow maps.*** **AJNR Am J Neuroradiol, 2000. 21(3): p. 462-70.**
333. **Wintermark, M., et al.,** ***Simultaneous measurement of regional cerebral blood flow by perfusion CT and stable xenon CT: a validation study.*** **AJNR Am J Neuroradiol, 2001. 22(5): p. 905-14.**
334. **Kudo, K., et al.,** ***Quantitative cerebral blood flow measurement with dynamic perfusion CT using the vascular-pixel elimination method: comparison with H2(15)O positron emission tomography.*** **AJNR Am J Neuroradiol, 2003. 24(3): p. 419-26.**
335. **Goh, V., et al.,** ***Quantitative assessment of tissue perfusion using MDCT: comparison of colorectal cancer and skeletal muscle measurement reproducibility.*** **AJR Am J Roentgenol, 2006. 187(1): p. 164-9.**
336. **Goh, V., et al.,** ***Quantitative assessment of colorectal cancer perfusion using MDCT: inter- and intraobserver agreement.*** **AJR Am J Roentgenol, 2005. 185(1): p. 225-31.**
337. **Goh, V., et al.,** ***Quantitative colorectal cancer perfusion measurement by multidetector-row CT: does greater tumour coverage improve measurement reproducibility?*** **Br J Radiol, 2006. 79(943): p. 578-83.**
338. **Ng, Q.S., et al.,** ***Quantitative assessment of lung cancer perfusion using MDCT: does measurement reproducibility improve with greater tumor volume coverage?*** **AJR Am J Roentgenol, 2006. 187(4): p. 1079-84.**
339. **Ng, Q.S., et al.,** ***Lung cancer perfusion at multi-detector row CT: reproducibility of whole tumor quantitative measurements.*** **Radiology, 2006. 239(2): p. 547-53.**
340. **Goh, V., et al.,** ***Quantitative colorectal cancer perfusion measurement using dynamic contrast-enhanced multidetector-row computed tomography: effect of acquisition time and implications for protocols.*** **J Comput Assist Tomogr, 2005. 29(1): p. 59-63.**
341. **Goh, V., et al.,** ***Effect of temporal interval between scan acquisitions on quantitative vascular parameters in colorectal cancer: implications for helical volumetric perfusion CT techniques.*** **AJR Am J Roentgenol, 2008. 191(6): p. W288-92.**
342. **Zussman, B.M., et al.,** ***The relative effect of vendor variability in CT perfusion results: a method comparison study.*** **AJR Am J Roentgenol, 2011. 197(2): p. 468-73.**
343. **Goh, V., et al.,** ***Quantitative assessment of colorectal cancer tumor vascular parameters by using perfusion CT: influence of tumor region of interest.*** **Radiology, 2008. 247(3): p. 726-32.**
344. **Fiorella, D., et al.,** ***Assessment of the reproducibility of postprocessing dynamic CT perfusion data.*** **AJNR Am J Neuroradiol, 2004. 25(1): p. 97-107.**
345. **Dighe, S., et al.,** ***Perfusion CT to assess angiogenesis in colon cancer: technical limitations and practical challenges.*** **Br J Radiol, 2012. 85(1018): p. e814-25.**
346. **Miles, K.A., et al.,** ***Current status and guidelines for the assessment of tumour vascular support with dynamic contrast-enhanced computed tomography.*** **Eur Radiol, 2012. 22(7): p. 1430-41.**

347. **Bellomi, M., et al., *CT perfusion for the monitoring of neoadjuvant chemotherapy and radiation therapy in rectal carcinoma: initial experience.* Radiology, 2007. 244(2): p. 486-93.**
348. **Sahani, D.V., et al., *Assessing tumor perfusion and treatment response in rectal cancer with multisection CT: Initial observations.* Radiology, 2005. 234(3): p. 785-792.**
349. **Curvo-Semedo, L., et al., *Usefulness of Perfusion CT to Assess Response to Neoadjuvant Combined Chemoradiotherapy in Patients with Locally Advanced Rectal Cancer.* Academic Radiology, 2012. 19(2): p. 203-213.**
350. **Janssen, M.H.M., et al., *Tumor perfusion increases during hypofractionated short-course radiotherapy in rectal cancer: Sequential perfusion-CT findings.* Radiotherapy and Oncology, 2010. 94(2): p. 156-160.**
351. **Sahani, D.V., et al., *Assessing tumor perfusion and treatment response in rectal cancer with multisection CT: initial observations.* Radiology, 2005. 234(3): p. 785-92.**
352. **Falk, S.J., et al., *BW12C perturbs normal and tumour tissue oxygenation and blood flow in man.* Radiother Oncol, 1994. 32(3): p. 210-7.**
353. **Roberta Fusco, M.S., Mario Petrillo, Antonio Avallone, Paolo Delrio and Antonella Petrillo, ed. *Dynamic Contrast Enhanced Magnetic Resonance Imaging in Rectal Cancer, Rectal Cancer - A Multidisciplinary Approach to Management,*. ed. D.G.A. Santoro. 2011, InTech.**
354. **Kuhl, C.K., et al., *Dynamic breast MR imaging: are signal intensity time course data useful for differential diagnosis of enhancing lesions?* Radiology, 1999. 211(1): p. 101-10.**
355. **Jesberger, J.A., et al., *Model-free parameters from dynamic contrast-enhanced-MRI: sensitivity to EES volume fraction and bolus timing.* J Magn Reson Imaging, 2006. 24(3): p. 586-94.**
356. **Leach, M.O., et al., *The assessment of antiangiogenic and antivascular therapies in early-stage clinical trials using magnetic resonance imaging: issues and recommendations.* Br J Cancer, 2005. 92(9): p. 1599-610.**
357. **Tofts, P.S., et al., *Estimating kinetic parameters from dynamic contrast-enhanced T(1)-weighted MRI of a diffusable tracer: standardized quantities and symbols.* J Magn Reson Imaging, 1999. 10(3): p. 223-32.**
358. **Zweifel, M. and A.R. Padhani, *Perfusion MRI in the early clinical development of antivascular drugs: decorations or decision making tools?* Eur J Nucl Med Mol Imaging, 2010. 37 Suppl 1: p. S164-82.**
359. **Leach, M.O., et al., *Imaging vascular function for early stage clinical trials using dynamic contrast-enhanced magnetic resonance imaging.* Eur Radiol, 2012. 22(7): p. 1451-64.**
360. **Taylor NJ, T.N., Stirling JJ, et al. *Non-enhancing pixels: a specific additional DCE-MRI kinetic parameter for assessing antivascular effects of anti-angiogenic and vascular disruptive agents*. in *Proceedings of the joint meeting of International Society of Magnetic Resonance in Medicine, 16th Scientific Meeting and Exhibition*. 2009. Honolulu.**
361. **Hayes, C., A.R. Padhani, and M.O. Leach, *Assessing changes in tumour vascular function using dynamic contrast-enhanced magnetic resonance imaging.* NMR Biomed, 2002. 15(2): p. 154-63.**
362. **Johansen, R., et al., *Predicting survival and early clinical response to primary chemotherapy for patients with locally advanced breast cancer using DCE-MRI.* J Magn Reson Imaging, 2009. 29(6): p. 1300-7.**
363. **Mayr, N.A., et al., *Longitudinal changes in tumor perfusion pattern during the radiation therapy course and its clinical impact in cervical cancer.* Int J Radiat Oncol Biol Phys, 2009. 77(2): p. 502-8.**

364. **Padhani, A.R., et al.,** ***Prediction of clinicopathologic response of breast cancer to primary chemotherapy at contrast-enhanced MR imaging: initial clinical results.*** **Radiology, 2006. 239(2): p. 361-74.**
365. **Cron, G.O., et al.,** ***Arterial input functions determined from MR signal magnitude and phase for quantitative dynamic contrast-enhanced MRI in the human pelvis.*** **Magn Reson Med, 2011. 66(2): p. 498-504.**
366. **Patel, N., et al.,** ***Clinical imaging of tumor angiogenesis.*** **Future Oncol. 8(11): p. 1443-59.**
367. **Galbraith, S.M., et al.,** ***Reproducibility of dynamic contrast-enhanced MRI in human muscle and tumours: comparison of quantitative and semi-quantitative analysis.*** **NMR Biomed, 2002. 15(2): p. 132-42.**
368. **de Vries, A., et al.,** ***Monitoring of tumor microcirculation during fractionated radiation therapy in patients with rectal carcinoma: preliminary results and implications for therapy.*** **Radiology, 2000. 217(2): p. 385-91.**
369. **Lim, J.S., et al.,** ***Perfusion MRI for the prediction of treatment response after preoperative chemoradiotherapy in locally advanced rectal cancer.*** **Eur Radiol, 2012. 22(8): p. 1693-700.**
370. **Oberholzer, K., et al.,** ***Rectal cancer: assessment of response to neoadjuvant chemoradiation by dynamic contrast-enhanced MRI.*** **J Magn Reson Imaging, 2012. 38(1): p. 119-26.**
371. **Kim, S.H., et al.,** ***Dynamic contrast-enhanced MRI to evaluate the therapeutic response to neoadjuvant chemoradiation therapy in locally advanced rectal cancer.*** **J Magn Reson Imaging, 2013.**
372. **George, M.L., et al.,** ***Non-invasive methods of assessing angiogenesis and their value in predicting response to treatment in colorectal cancer.*** **Br J Surg, 2001. 88(12): p. 1628-36.**
373. **DeVries, A.F., et al.,** ***Tumor microcirculation and diffusion predict therapy outcome for primary rectal carcinoma.*** **International Journal of Radiation Oncology Biology Physics, 2003. 56(4): p. 958-965.**
374. **de Lussanet, Q.G., et al.,** ***Dynamic contrast-enhanced magnetic resonance imaging of radiation therapy-induced microcirculation changes in rectal cancer.*** **Int J Radiat Oncol Biol Phys, 2005. 63(5): p. 1309-15.**
375. **Kim, S.H., et al.,** ***Dynamic contrast-enhanced MRI to evaluate the therapeutic response to neoadjuvant chemoradiation therapy in locally advanced rectal cancer.*** **J Magn Reson Imaging, 2013. 40(3): p. 730-7.**
376. **Intven, M., O. Reerink, and M.E. Philippens,** ***Dynamic contrast enhanced MR imaging for rectal cancer response assessment after neo-adjuvant chemoradiation.*** **J Magn Reson Imaging, 2014.**
377. **DeVries, A.F., et al.,** ***Pretreatment evaluation of microcirculation by dynamic contrast-enhanced magnetic resonance imaging predicts survival in primary rectal cancer patients.*** **Int J Radiat Oncol Biol Phys, 2014. 90(5): p. 1161-7.**
378. **Martens, M.H., et al.,** ***Can perfusion MRI predict response to preoperative treatment in rectal cancer?*** **Radiother Oncol, 2014.**
379. **DeVries, A., et al.,** ***[Perfusion-index values evaluated by dynamic magnetic resonance imaging in advanced rectal carcinoma. A new predictor of response to preoperative radiochemotherapy?].*** **Strahlenther Onkol, 2000. 176(12): p. 567-72.**
380. **DeVries, A.F., et al.,** ***Tumor microcirculation and diffusion predict therapy outcome for primary rectal carcinoma.*** **Int J Radiat Oncol Biol Phys, 2003. 56(4): p. 958-65.**
381. **Wedam, S.B., et al.,** ***Antiangiogenic and antitumor effects of bevacizumab in patients with inflammatory and locally advanced breast cancer.*** **J Clin Oncol, 2006. 24(5): p. 769-77.**

382. **Liu, G., et al.,** ***Dynamic contrast-enhanced magnetic resonance imaging as a pharmacodynamic measure of response after acute dosing of AG-013736, an oral angiogenesis inhibitor, in patients with advanced solid tumors: results from a phase I study.*** **J Clin Oncol, 2005. 23(24): p. 5464-73.**

383. **O'Donnell, A., et al.,** ***A Phase I study of the angiogenesis inhibitor SU5416 (semaxanib) in solid tumours, incorporating dynamic contrast MR pharmacodynamic end points.*** **Br J Cancer, 2005. 93(8): p. 876-83.**

384. **Morgan, B., et al.,** ***Dynamic contrast-enhanced magnetic resonance imaging as a biomarker for the pharmacological response of PTK787/ZK 222584, an inhibitor of the vascular endothelial growth factor receptor tyrosine kinases, in patients with advanced colorectal cancer and liver metastases: results from two phase I studies.*** **J Clin Oncol, 2003. 21(21): p. 3955-64.**

385. **Mross, K., et al.,** ***Phase I clinical and pharmacokinetic study of PTK/ZK, a multiple VEGF receptor inhibitor, in patients with liver metastases from solid tumours.*** **Eur J Cancer, 2005. 41(9): p. 1291-9.**

386. **Gollub, M.J., et al.,** ***Dynamic contrast enhanced-MRI for the detection of pathological complete response to neoadjuvant chemotherapy for locally advanced rectal cancer.*** **Eur Radiol, 2011. 22(4): p. 821-31.**

387. **Kierkels, R.G., et al.,** ***Comparison between perfusion computed tomography and dynamic contrast-enhanced magnetic resonance imaging in rectal cancer.*** **Int J Radiat Oncol Biol Phys, 2009. 77(2): p. 400-8.**

388. **Kallehauge, J., et al.,** ***Voxelwise comparison of perfusion parameters estimated using dynamic contrast enhanced (DCE) computed tomography and DCE-magnetic resonance imaging in locally advanced cervical cancer.*** **Acta Oncol, 2013. 52(7): p. 1360-8.**

389. **Thomas, A.L., et al.,** ***Vascular endothelial growth factor receptor tyrosine kinase inhibitors: PTK787/ZK 222584.*** **Semin Oncol, 2003. 30(3 Suppl 6): p. 32-8.**

390. **Mross, K., et al.,** ***DCE-MRI assessment of the effect of vandetanib on tumor vasculature in patients with advanced colorectal cancer and liver metastases: a randomized phase I study.*** **J Angiogenes Res, 2009. 1: p. 5.**

391. **Ferl, G.Z., et al.,** ***Mixed-effects modeling of clinical DCE-MRI data: application to colorectal liver metastases treated with bevacizumab.*** **J Magn Reson Imaging, 2014. 41(1): p. 132-41.**

392. **Kim, D.H., et al.,** ***Intermodality comparison between 3D perfusion CT and 18F-FDG PET/CT imaging for predicting early tumor response in patients with liver metastasis after chemotherapy: Preliminary results of a prospective study.*** **Eur J Radiol, 2012.**

393. **Anzidei, M., et al.,** ***Liver metastases from colorectal cancer treated with conventional and antiangiogenetic chemotherapy: evaluation with liver computed tomography perfusion and magnetic resonance diffusion-weighted imaging.*** **J Comput Assist Tomogr, 2011. 35(6): p. 690-6.**

394. **Pauls, S., et al.,** ***Liver perfusion with dynamic multidetector-row computed tomography as an objective method to evaluate the efficacy of chemotherapy in patients with colorectal cancer.*** **Clin Imaging, 2009. 33(4): p. 289-94.**

395. **De Bruyne, S., et al.,** ***Value of DCE-MRI and FDG-PET/CT in the prediction of response to preoperative chemotherapy with bevacizumab for colorectal liver metastases.*** **Br J Cancer, 2012. 106(12): p. 1926-1933.**

396. **O'Connor, J.P., et al.,** ***DCE-MRI biomarkers of tumour heterogeneity predict CRC liver metastasis shrinkage following bevacizumab and FOLFOX-6.*** **Br J Cancer, 2011. 105(1): p. 139-45.**

397. **Hirashima, Y., et al.,** ***Pharmacokinetic parameters from 3-Tesla DCE-MRI as surrogate biomarkers of antitumor effects of bevacizumab plus FOLFIRI in colorectal cancer with liver metastasis.*** **International Journal of Cancer, 2012. 130(10): p. 2359-2365.**

398. **Vriens, D., et al.,** ***Chemotherapy response monitoring of colorectal liver metastases by dynamic Gd-DTPA-enhanced MRI perfusion parameters and 18F-FDG PET metabolic rate.*** **J Nucl Med, 2009. 50(11): p. 1777-84.**

399. **van Laarhoven, H.W., et al.,** ***Prediction of chemotherapeutic response of colorectal liver metastases with dynamic gadolinium-DTPA-enhanced MRI and localized 19F MRS pharmacokinetic studies of 5-fluorouracil.*** **NMR Biomed, 2007. 20(2): p. 128-40.**

400. **Ah-See, M.L., et al.,** ***Early changes in functional dynamic magnetic resonance imaging predict for pathologic response to neoadjuvant chemotherapy in primary breast cancer.*** **Clin Cancer Res, 2008. 14(20): p. 6580-9.**

401. **O'Connor, J.P.B., et al.,** ***DCE-MRI biomarkers of tumour heterogeneity predict CRC liver metastasis shrinkage following bevacizumab and FOLFOX-6.*** **Br J Cancer, 2011. 105(1): p. 139-145.**

402. **Kennedy, A.S., et al.,** ***Computer modeling of yttrium-90-microsphere transport in the hepatic arterial tree to improve clinical outcomes.*** **Int J Radiat Oncol Biol Phys, 2009. 76(2): p. 631-7.**

403. **Sato, K.T., et al.,** ***The role of tumor vascularity in predicting survival after yttrium-90 radioembolization for liver metastases.*** **J Vasc Interv Radiol, 2009. 20(12): p. 1564-9.**

404. **Dhabuwala, A., P. Lamerton, and R.S. Stubbs,** ***Relationship of 99mtechnetium labelled macroaggregated albumin (99mTc-MAA) uptake by colorectal liver metastases to response following Selective Internal Radiation Therapy (SIRT).*** **BMC Nucl Med, 2005. 5: p. 7.**

405. **Dancey, J.E., et al.,** ***Treatment of nonresectable hepatocellular carcinoma with intrahepatic 90Y-microspheres.*** **J Nucl Med, 2000. 41(10): p. 1673-81.**

406. **Morsbach, F., et al.,** ***Computed tomographic perfusion imaging for the prediction of response and survival to transarterial radioembolization of liver metastases.*** **Invest Radiol, 2013 . 48(11): p. 787-94.**

407. **Morsbach, F., et al.,** ***Perfusion CT best predicts outcome after radioembolization of liver metastases: a comparison of radionuclide and CT imaging techniques.*** **European Radiology, 2014. 24(7): p. 1455-1465.**

408. **Wang, L.M., et al.,** ***Anatomical basis and histopathological changes resulting from selective internal radiotherapy for liver metastases.*** **J Clin Pathol, 2012. 66(3): p. 205-11.**

409. **Pandharipande, P.V., et al.,** ***Perfusion imaging of the liver: current challenges and future goals.*** **Radiology, 2005. 234(3): p. 661-73.**

410. **Blomley, M.J., et al.,** ***Liver perfusion studied with ultrafast CT.*** **J Comput Assist Tomogr, 1995. 19(3): p. 424-33.**

411. **Kanda, T., et al.,** ***CT hepatic perfusion measurement: comparison of three analytic methods.*** **Eur J Radiol, 2011. 81(9): p. 2075-9.**

412. **Ng, C.S., et al.,** ***Effect of dual vascular input functions on CT perfusion parameter values and reproducibility in Liver Tumors and Normal liver.*** **Journal of Computer Assisted Tomography, 2012. 36(4): p. 388-393.**

413. **Yang, H.F., et al.,** ***Perfusion computed tomography evaluation of angiogenesis in liver cancer.*** **Eur Radiol, 2010. 20(6): p. 1424-30.**

414. **Meijerink, M.R., et al.,** ***Perfusion CT and US of colorectal cancer liver metastases: a correlative study of two dynamic imaging modalities.*** **Ultrasound Med Biol, 409. 36(10): p. 1626-36.**

415. **Veit-Haibach, P., et al.,** ***Feasibility of integrated CT-liver perfusion in routine FDG-PET/CT.*** **Abdom Imaging, 2009. 35(5): p. 528-36.**

416. **Ippolito, D., et al.,** ***Quantitative assessment of tumour associated neovascularisation in patients with liver cirrhosis and hepatocellular carcinoma: role of dynamic-CT perfusion imaging.*** **European Radiology, 2011. 22(4): p. 803-811.**

417. **Sahani, D.V., et al., *Advanced hepatocellular carcinoma: CT perfusion of liver and tumor tissue--initial experience.* Radiology, 2007. 243(3): p. 736-43.**

418. **Ng, C.S., et al., *Reproducibility of CT perfusion parameters in liver tumors and normal liver.* Radiology, 2011. 260(3): p. 762-70.**

419. **Miles, K.A., et al., *In vivo assessment of neovascularization of liver metastases using perfusion CT.* Br J Radiol, 1998. 71(843): p. 276-81.**

420. **Reiner, C.S., et al., *Liver Perfusion Imaging in Patients with Primary and Metastatic Liver Malignancy: Prospective Comparison between 99mTc-MAA SPECT and Dynamic CT Perfusion.* Academic Radiology, 2012. 19(5): p. 613-621.**

421. **Zhang, Q., et al., *Perfusion CT findings in liver of patients with tumor during chemotherapy.* World J Gastroenterol, 2010. 16(25): p. 3202-5.**

422. **Chandler, A., et al., *Validation of motion correction techniques for liver CT perfusion studies.* Br J Radiol, 2012. 85(1016): p. e514-22.**

423. **Oken, M.M., et al., *Toxicity and response criteria of the Eastern Cooperative Oncology Group.* Am J Clin Oncol, 1982. 5(6): p. 649-55.**

424. **Brown, G., et al., *Effectiveness of preoperative staging in rectal cancer: digital rectal examination, endoluminal ultrasound or magnetic resonance imaging?* Br J Cancer, 2004. 91(1): p. 23-9.**

425. **Petralia, G., et al., *CT perfusion in oncology: how to do it.* Cancer Imaging, 2010. 10: p. 8-19.**

426. **Orton, M.R., et al., *Computationally efficient vascular input function models for quantitative kinetic modelling using DCE-MRI.* Phys Med Biol, 2008. 53(5): p. 1225-39.**

427. **Bhushan, M., et al., *Motion correction and parameter estimation in dceMRI sequences: application to colorectal cancer.* Med Image Comput Comput Assist Interv, 2011. 14(Pt 1): p. 476-83.**

428. **DCE-MRI Technical Committee. *DCE MRI Quantification Profile, Quantitative Imaging Biomarkers Alliance.Version 1.0. Reviewed Draft.* 1 July, 2012; Available from: http://rsna.org/QIBA_.aspx.**

429. **Koukourakis, M.I., et al., *Endogenous markers of hypoxia/anaerobic metabolism and anemia in primary colorectal cancer.* Cancer Sci, 2006. 97(7): p. 582-8.**

430. **Weidner, N., *Intratumor microvessel density as a prognostic factor in cancer.* Am J Pathol, 1995. 147(1): p. 9-19.**

431. **Goh, V., et al., *Assessment of the metabolic flow phenotype of primary colorectal cancer: correlations with microvessel density are influenced by the histological scoring method.* Eur Radiol, 2012. 22(8): p. 1687-92.**

432. **Pettersson, D., et al., *Interim analysis of the Stockholm III trial of preoperative radiotherapy regimens for rectal cancer.* Br J Surg, 2010. 97(4): p. 580-7.**

433. **Caravatta, L., et al., *Clinical target volume delineation including elective nodal irradiation in preoperative and definitive radiotherapy of pancreatic cancer.* Radiat Oncol, 2012. 7(1): p. 86.**

434. **Kierkels, R.G.J., et al., *Comparison Between Perfusion Computed Tomography and Dynamic Contrast-Enhanced Magnetic Resonance Imaging in Rectal Cancer.* International journal of radiation oncology, biology, physics, 2009. 77(2): p. 400-408.**

435. **Nijkamp, J., et al., *Target volume shape variation during hypo-fractionated preoperative irradiation of rectal cancer patients.* Radiother Oncol, 2009. 92(2): p. 202-9.**

436. **Astner, S.T., et al., *Imaging of tumor physiology: impacts on clinical radiation oncology.* Exp Oncol, 2011. 32(3): p. 149-52.**

437. **Yeo, D.M., et al., *Correlation of dynamic contrast-enhanced MRI perfusion parameters with angiogenesis and biologic aggressiveness of rectal cancer: Preliminary results.* J Magn Reson Imaging, 2014.**

438. **Lollert, A., et al.,** ***Rectal cancer: Dynamic contrast-enhanced MRI correlates with lymph node status and epidermal growth factor receptor expression.*** **J Magn Reson Imaging, 2013.**
439. **Jackson, A., et al.,** ***Imaging Tumor Vascular Heterogeneity and Angiogenesis using Dynamic Contrast-Enhanced Magnetic Resonance Imaging.*** **Clinical Cancer Research, 2007. 13(12): p. 3449-3459.**
440. **Tanner, L.N.,** ***Functional Imaging for Tumour Characterisation*****. 2010, University of Oxford.**
441. **Treier R, S.A., Fried M, Schwizer W, Boesiger P.,** ***On the necessity of flip angle correction for fast T1 mapping using DESPOT 1.*** **Proc. Intl. Soc. Mag. Reson. Med., 2006. 14: p. 2264.**
442. **Yang, X. and M.V. Knopp,** ***Quantifying tumor vascular heterogeneity with dynamic contrast-enhanced magnetic resonance imaging: a review.*** **J Biomed Biotechnol. 2011: p. 732848.**
443. **Curvo-Semedo, L., et al.,** ***Usefulness of perfusion CT to assess response to neoadjuvant combined chemoradiotherapy in patients with locally advanced rectal cancer.*** **Acad Radiol, 2011. 19(2): p. 203-13.**
444. **Cox, J.D., J. Stetz, and T.F. Pajak,** ***Toxicity criteria of the Radiation Therapy Oncology Group (RTOG) and the European Organization for Research and Treatment of Cancer (EORTC).*** **Int J Radiat Oncol Biol Phys, 1995. 31(5): p. 1341-6.**
445. **Nilsson, P.J., et al.,** ***Short-course radiotherapy followed by neo-adjuvant chemotherapy in locally advanced rectal cancer--the RAPIDO trial.*** **BMC Cancer, 2013. 13: p. 279.**
446. **Baeten, C.I.M., et al.,** ***Effects of radiotherapy and chemotherapy on angiogenesis and leukocyte infiltration in rectal cancer.*** **International Journal of Radiation Oncology*Biology*Physics, 2006. 66(4): p. 1219-1227.**
447. **Kimple, R.J., et al.,** ***Radiosensitization of epidermal growth factor receptor/HER2-positive pancreatic cancer is mediated by inhibition of Akt independent of ras mutational status.*** **Clin Cancer Res, 2010. 16(3): p. 912-23.**
448. **Wang, Z.J., et al.,** ***Genetic pathways of colorectal carcinogenesis rarely involve the PTEN and LKB1 genes outside the inherited hamartoma syndromes.*** **Am J Pathol, 1998. 153(2): p. 363-6.**
449. **Frattini, M., et al.,** ***PTEN loss of expression predicts cetuximab efficacy in metastatic colorectal cancer patients.*** **Br J Cancer, 2007. 97(8): p. 1139-45.**
450. **Molinari, F., et al.,** ***Differing deregulation of EGFR and downstream proteins in primary colorectal cancer and related metastatic sites may be clinically relevant.*** **Br J Cancer, 2009. 100(7): p. 1087-94.**
451. **Albert, J.M., et al.,** ***Targeting the Akt/mammalian target of rapamycin pathway for radiosensitization of breast cancer.*** **Molecular Cancer Therapeutics, 2006. 5(5): p. 1183-1189.**
452. **Gillard, J.H., et al.,** ***Reproducibility of quantitative CT perfusion imaging.*** **Br J Radiol, 2001. 74(882): p. 552-5.**
453. **Kim, J.H., et al.,** ***Dynamic contrast-enhanced 3-T MR imaging in cervical cancer before and after concurrent chemoradiotherapy.*** **Eur Radiol, 2012. 22(11): p. 2533-9.**
454. **Morgan, B., et al.,** ***A simple, reproducible method for monitoring the treatment of tumours using dynamic contrast-enhanced MR imaging.*** **Br J Cancer, 2006. 94(10): p. 1420-7.**
455. **Lankester, K.J., et al.,** ***Dynamic MRI for imaging tumor microvasculature: comparison of susceptibility and relaxivity techniques in pelvic tumors.*** **J Magn Reson Imaging, 2007. 25(4): p. 796-805.**

456. **Chiandussi, L., et al.,** ***Estimation of hepatic arterial and portal venous blood flow by direct catheterization of the vena porta through the umbilical cord in man. Preliminary results.*** **Acta Hepatosplenol, 1968. 15(3): p. 166-71.**
457. **Schenk, W.G., Jr., et al.,** ***Direct measurement of hepatic blood flow in surgical patients: with related observations on hepatic flow dynamics in experimental animals.*** **Ann Surg, 1962. 156: p. 463-71.**